(51) International Patent Classification 6 : G06F 17/50	A2	(11) International Publication Number: **WO 98/06048**
		(43) International Publication Date: 12 February 1998 (12.02.98)

(21) International Application Number: PCT/CA97/00539

(22) International Filing Date: 31 July 1997 (31.07.97)

(30) Priority Data:
9616105.4   31 July 1996 (31.07.96)   GB

(71) Applicant (for all designated States except US): QUEEN'S UNIVERSITY AT KINGSTON [CA/CA]; Kingston, Ontario K7L 3N6 (CA).

(72) Inventors; and
(75) Inventors/Applicants (for US only): SHAMOVSKY, Igor, L. [RU/CA]; 6-202, 17 Van Order Drive, Kingston, Ontario K7M 1B5 (CA). ROSS, Gregory, M. [CA/CA]; 1090 Caitlin Crescent, Kingston, Ontario K7P 2S4 (CA). RIOPELLE, Richard, J. [CA/CA]; 32 Lakeshore Boulevard, Kingston, Ontario K7M 4J6 (CA). WEAVER, Donald, F. [CA/CA]; 27 Collegeview Crescent, Kingston, Ontario K7M 7J8 (CA).

(74) Agents: SCHUMACHER, Lynn, C. et al.; Hill & Schumacher, Suite 802, 335 Bay Street, Toronto, Ontario M5H 2R3 (CA).

(81) Designated States: AL, AM, AT, AU, AZ, BA, BB, BG, BR, BY, CA, CH, CN, CU, CZ, DE, DK, EE, ES, FI, GB, GE, GH, HU, IL, IS, JP, KE, KG, KP, KR, KZ, LC, LK, LR, LS, LT, LU, LV, MD, MG, MK, MN, MW, MX, NO, NZ, PL, PT, RO, RU, SD, SE, SG, SI, SK, SL, TJ, TM, TR, TT, UA, UG, US, UZ, VN, YU, ZW, ARIPO patent (GH, KE, LS, MW, SD, SZ, UG, ZW), Eurasian patent (AM, AZ, BY, KG, KZ, MD, RU, TJ, TM), European patent (AT, BE, CH, DE, DK, ES, FI, FR, GB, GR, IE, IT, LU, MC, NL, PT, SE), OAPI patent (BF, BJ, CF, CG, CI, CM, GA, GN, ML, MR, NE, SN, TD, TG).

Published
Without international search report and to be republished upon receipt of that report.

(54) Title: MOLECULAR MODELLING OF NEUROTROPHIN-RECEPTOR BINDING

(57) Abstract

The present invention relates to a computational method for identifying the bioactive conformations of peptide domains, in particular, the geometries of complexes of neurotrophins and their receptors. The bioactive conformation of the Nerve Growth Factor (NGF) amino and carboxyl termini (Trk binding domain) was determined. The complex of the NGF termini splits into two distinct regions: a rigid region (residues 9-11 and 112'-118') and a flexible loop (residues 1-8), the geometry of the rigid region, which is maintained by electrostatic interaction between Glu^{11} and $Arg^{118'}$, is conserved in active molecules only. The separation of the flexible loop from the rigid region is necessary in order to eliminate an influence of the loop on the biologically active conformation of the rigid region. The present invention also relates to a method for identifying and theoretically modelling specific receptor binding sites for Nerve Growth Factor (NGF) and Brain-Derived Neurotrophic Factor (BDNF) on their receptors, TrkA and TrkB, respectively. The present invention also relates to a method for identifying and theoretically modelling a receptor binding site for neurotrophins, such as NGF, BDNF, NT-3, and NT-4/5, of the common neurotrophin receptor $p75^{NTR}$.

MOLECULAR MODELLING OF NEUROTROPHIN-RECEPTOR BINDING

FIELD OF THE INVENTION

5   The present invention relates to a computational method for identifying minimum-
energy structures in molecular systems, and more particularly for determining the bioactive
conformations of peptide domains. The invention relates to determination of the bioactive
conformations of the amino and carboxyl termini of Nerve Growth Factor (NGF) and
analogues thereof, and the 3-dimensional structures of their complexes with the 24-amino
10   acid second leucine-rich motif (LRM) of TrkA which represents the binding site for NGF. The
invention further relates to the theoretically identified geometries of the TrkB and the $p75^{NTR}$
receptor binding sites and to the mechanisms of neurotrophin binding.

BACKGROUND OF THE INVENTION

15

         The neurotrophins are a family of structurally and functionally related proteins,
including Nerve Growth Factor (NGF), Brain-Derived Neurotrophic Factor (BDNF),
Neurotrophin-3 (NT-3), Neurotrophin-4/5 (NT-4/5) and Neurotrophin-6 (NT-6). These proteins
promote the survival and differentiation of diverse neuronal populations in both the peripheral
20   and central nervous systems (Hefti, 1986; Hefti and Weiner, 1986; Levi-Montalcini, 1987;
Barde, 1989; Leibrock et al., 1989; Maisonpierre et al., 1990; Rosenthal et al., 1990; Hohn et
al., 1990; Gotz et al., 1994; Maness et al., 1994) and are involved in the pathogenesis of
diverse neurological disorders. Neurotrophins exert certain of their biological effects through
specific interactions with a class of transmembrane receptor tyrosine kinases (TrkA, TrkB and
25   TrkC) (Kaplan et al., 1991; Klein et al., 1991, 1992; Soppet et al., 1991; Squinto et al., 1991;
Berkemeier et al., 1991; Escandon et al., 1993; Lamballe et al., 1991). Specificity of
neurotrophin action results from their selective interactions with Trk. That is, TrkA only binds
NGF (Kaplan et al., 1991; Klein et al., 1991); TrkB binds BDNF, NT-3 and NT-4/5 (Soppet et
al., 1991; Squinto et al., 1991; Berkemeier et al., 1991; Escandon et al., 1993; Lamballe et
30   al., 1991; Klein et al., 1992; Vale and Shooter, 1985; Barbacid, 1993); and TrkC exclusively
binds NT-3 (Lamballe et al., 1991; Vale and Shooter, 1985). This is particularly evident when
the Trk receptors are coexpressed with the common neurotrophin receptor $p75^{NTR}$ (For review
see Meakin and Shooter, 1992; Barbacid, 1993; Chao, 1994; Bradshaw et al., 1994; Ibáñez,
1995).
35   The common neurotrophin receptor $p75^{NTR}$ is a transmembrane glycoprotein
structurally related to the tumor necrosis factor and CD-40 receptors (Meakin and Shooter,

1992; Rydén and Ibáñez, 1996). As all neurotrophins bind to p75[NTR] with similar affinity (Rodriguez-Tébar *et al.*, 1990; Hallböök *et al.*, 1991; Rodriguez-Tébar *et al.*, 1992; Ibáñez, 1995), neurotrophin specificity is conventionally thought to be caused by the binding selectivity for Trk receptors which are differentially expressed in different neuronal populations (Ibáñez, 1995). However, accumulated experimental data on neurotrophin activity reveal important functional aspects of p75[NTR] (Heldin *et al.*, 1989; Jing *et al.*, 1992; Herrmann, 1993; Barker and Shooter, 1994; Dobrowsky *et al.*, 1994, Matsumoto *et al.*, 1995; Marchetti *et al.*, 1996; Washiyama *et al.*, 1996). The common neurotrophin receptor enhances functions and increases binding specificity of Trk receptors (Barker and Shooter, 1994; Mahadeo *et al.*, 1994; Chao and Hempstead, 1995; Rydén and Ibáñez, 1996). In addition, p75[NTR] possesses unique, Trk-independent signalling properties which involve ceramide production through activation of the sphingomyelin cycle (Dobrowsky *et al.*, 1994), apoptosis (cell death) (Van der Zee *et al.*, 1996; Cassacia-Bonnefil *et al.*, 1996; Frade *et al.*, 1996), and activation of the transcription factor NFκB (Carter *et al.*, 1996). Recently, p75[NTR] has been demonstrated to participate in human melanoma progression (Herrmann *et al.*, 1993; Marchetti *et al.*, 1996). Furthermore, NGF and NT-3 increase the production of heparin by 70W melanoma cells, which is associated with their metastatic potential (Marchetti *et al.*, 1996). Although this effect has been shown to be mediated by the common neurotrophin receptor, neither BDNF nor NT-4/5 appeared to be active. Explicit modelling of the various neurotrophin receptors will be critical to the rational design of neurotrophin-based drugs.

NGF displays high and low affinity binding sites in sensory and sympathetic neurons and in pheochromocytoma PC12 cells (Sutter *et al.*, 1979; Landreth and Shooter, 1980; Schechter and Bothwell, 1981). The coexpression of the common neurotrophin p75[NTR] receptor with TrkA is required to form the high affinity binding site (Hempstead *et al.*, 1991; Barker and Shooter, 1994; Mahadeo *et al.*, 1994; Chao and Hempstead, 1995). Several models of the TrkA-p75[NTR] interaction have been proposed to explain high affinity NGF binding (Bothwell, 1991; Chao, 1992b; Chao and Hempstead, 1995; Wolf *et al.*, 1995; Ross *et al.*, 1996; Ross *et al.*, 1997). These models differ with respect to direct (conformational model) or indirect (ligand-presentation model) interaction of p75[NTR] with TrkA. Direct TrkA-p75[NTR] interaction is consistent with much of the existing experimental data.

NGF, a 118 amino acid protein, is an extremely important neurotrophin, being implicated in the pathogenesis of Alzheimer's disease, epilepsy and pain (Ben and Represa, 1990; McKee *et al.*, 1991; Leven and Mendel, 1993; Woolf and Doubell, 1994; Rashid *et al.*, 1995; McMahon *et al.*, 1995). The binding of NGF to its receptors is determined by distinct sequences within its primary amino acid structure. While several regions of NGF participate in the NGF/TrkA interaction, mutation studies suggest that relatively few key residues, namely

those located in the NGF amino and carboxyl termini, are required for high affinity binding.

The hairpin loop at residues 29-35 is responsible for recognition by p75[NTR] (Ibáñez et al., 1992; Radziejewski et al., 1992), while the amino and carboxyl termini are important binding determinants for recognition by the TrkA receptor (Shih et al., 1994; Moore and

5   Shooter, 1975; Suter et al., 1992; Burton et al., 1992, 1995; Kahle et al., 1992; Luo and Neet, 1992; Drinkwater et al., 1993; Treanor et al., 1995; Taylor et al., 1991). Truncation of either the amino or carboxyl terminus of NGF produces less active NGF analogues; similarly most deletion or point mutations of the amino terminus also lead to NGF analogues with diminished activity (Shih et al., 1994; Burton et al., 1992, 1995; Kahle et al., 1992; Drinkwater et al.,

10   1993; Treanor et al., 1995; Taylor et al., 1991). On the other hand, the NGFΔ2-8 (NGF with residues 2-8 removed) and NGFΔ3-9 deletion mutants are almost as active as wild type NGF (Drinkwater et al., 1993). These NGF structure-activity relationships in combination with the considerable species variability (mouse, human, guinea pig and snake) of the amino acid sequence of the NGF termini (McDonald et al., 1991) are of potential value in understanding

15   the NGF/TrkA interaction.

NGF exerts its biological activity as a non-covalent dimer (Treanor et al., 1995; Burton et al., 1995; McDonald et al., 1991; Ibáñez et al., 1993; Bothwell and Shooter, 1977). Two 118 residue NGF monomers are dimerized by hydrophobic and van der Waals interactions between their three anti-parallel pairs of β-strands; consequently, the amino terminus of one

20   NGF monomer and the carboxyl terminus of the other are spatially juxtaposed (McDonald et al., 1991). Furthermore, although a dimer has 2 pairs of termini, only one pair of termini is required for TrkA receptor recognition (Treanor et al., 1995; Burton et al., 1995). Accordingly, solving the conformation of the complex formed by the amino terminus of one monomer and the carboxyl terminus of the other in dimeric NGF is of fundamental relevance to

25   understanding the interaction of NGF with TrkA.

The X-ray crystallographic 3-dimensional structure of a dimeric mouse NGF (mNGF) has been reported recently (McDonald et al., 1991). However, within this structure, the amino terminus (residues 1-11) and the carboxyl terminus (residues 112-118) remain unresolved for both pairs of termini. High flexibility of the NGF termini makes it difficult to experimentally

30   determine their bioactive conformations, particularly since transition metal ions commonly used in X-ray crystallography (McDonald et al., 1991) have high affinity for His residues (Gregory et al., 1993) which are present in the NGF amino terminus (Bradshaw et al., 1994). Indeed, conformational alterations in the receptor binding domains of NGF caused by Zn^{2+} cations leading to its inactivation have been described recently (Ross et al., 1997). Since the

35   amino and carboxyl termini are crucial for NGF bioactivity as mediated via TrkA and because of the significance of NGF in multiple neurologic disease processes, the determination of the

3

biologically active conformation of these termini is an important and challenging problem for computational chemistry.

In contrast with NGF, little is known about the BDNF binding determinant for TrkB activation. Although there were several attempts to identify structural elements of BDNF that determine its receptor specificity (Ibáñez et al., 1991, 1993, 1995; Suter et al., 1992; Ilag et al., 1994; Kullander and Ebendal, 1994; Urfer et al., 1994; Lai et al., 1996), the results of mutational experiments are still controversial. Thus, the reported importance of residues 40-49 (variable loop region II) for TrkB related activity of BDNF (Ibáñez et al., 1991; Ilag et al., 1994) has not been confirmed by recent studies (Lai et al., 1996), in which it has also been shown that the key residues of the TrkB receptor binding domain of BDNF are situated between residues 80 and 109. The latter result is consistent with earlier observations that the BDNF termini are not involved in TrkB binding and that the key residues of the BDNF binding epitope are Arg^{81} and Gln^{84} (Ibáñez et al., 1993). In addition, it has been found that receptor binding domains of BDNF and NT-3 are located in the same regions of the molecules, i.e. in their "waist" parts (Ibáñez et al., 1993; Urfer et al., 1994). As far as the NT-3 receptor binding domain is concerned, detailed mutational studies carried out by Urfer et al. (1994) revealed that it comprises a surface that includes major parts of the central β-strand stem, with the most important residues being Arg^{103}, Thr^{22}, Glu^{54}, Arg^{56}, Lys^{80} and Gln^{83}. These residues correspond to Arg^{104}, Thr^{21}, Glu^{55}, Lys^{57}, Arg^{81} and Gln^{84} of BDNF, respectively (McDonald et al., 1991).

The location of the neurotrophin binding sites within the Trk receptors is the subject of debate (MacDonald and Meakin, 1996). Published data indicate the existence of two putative neurotrophin binding sites of Trk proteins: the "second immunoglobulin-like domain" (residues Trp^{299t}-Asn^{365t}, denoted IgC2) and the "second leucine-rich motif" (LRM-2A and LRM-2B, residues Thr^{97}-Leu^{120} of TrkA and TrkB, respectively) (Schneider and Schweiger, 1991; Kullander and Ebendal, 1994; Pérez et al., 1995; Urfer et al., 1995; Windisch et al., 1995a, 1995b, 1995c; MacDonald and Meakin, 1996; Rydén and Ibáñez, 1996).

$p75^{NTR}$ belongs to a family of cell surface proteins that share a common pattern of four repeated cysteine-rich domains (CRDs) in the extracellular portion (Yan and Chao, 1991; Baldwin and Shooter, 1994). X-ray crystallographic studies on the extracellular portion of the related protein $p55^{TNFR}$ revealed that CRDs fold independently of each other, and three conserved disulfide bonds maintain a specific geometry of each CRD which consists of two loops (Banner et al., 1993) (loops A and B, Fig. 1a). Very little is known about the $p75^{NTR}$ receptor functional epitope and, particularly, about residues directly participating in molecular recognition processes. All four CRD repeats of $p75^{NTR}$ are found to be required for binding, with the second CRD being most important (Baldwin and Shooter, 1995). Residue Ser^{50} of

p75^{NTR} seems to be essential for NGF binding (Baldwin and Shooter, 1995).

The results of site-directed mutagenesis suggest that the p75^{NTR} receptor binding domains within neurotrophins are juxtaposed positively charged residues located in two adjacent hairpin loops which represent variable region I (residues 23-35) and V (residues 93-98) (Ibáñez et al., 1992; Rydén et al., 1995; Ibáñez, 1994; Ibáñez, 1995; Rydén and Ibáñez, 1996) (Fig. 1c). In NGF, residues Lys^{32}, Lys^{34}, and Lys^{95} have been found to be involved in p75^{NTR} receptor binding, with Lys^{32} making the strongest contact, followed by Lys^{34} and Lys^{95}. In addition, some role of Asp^{30}, Glu^{35}, Arg^{103}, Arg^{100}, Lys^{88}, and Ile^{31} in p75^{NTR} binding and biological activity has been demonstrated (Ibáñez et al., 1992; Ibáñez, 1994). Two residues of variable region I, namely Arg^{31} and His^{33}, have been demonstrated to be essential for binding of NT-3 to p75^{NTR}, whereas similarly located Arg^{34} and Arg^{36} mediate binding of NT-4/5 (Rydén et al., 1995). In contrast to NGF, a positively charged residue in variable region V is not critical for binding of NT-3 or NT-4/5 to p75^{NTR} (Rydén et al., 1995). In BDNF, however, only residues of variable region V, Lys^{95}, Lys^{96} and Arg^{97}, bind to p75^{NTR} and compensate for the lack of positively charged residues in variable loop region I (Rydén et al., 1995).

Therefore, it is an object of the invention to establish explicit atom-level models of the Trk and p75^{NTR} recognition sites for neurotrophins.

It is a further object of the invention to provide atom-level models of the mechanism of interaction of neurotrophins and their receptors.

SUMMARY OF THE INVENTION

The inventors describe a method of characterizing the interaction between non-contiguous domains of a ligand and its receptor. The specific examples of the method described in detail below concern the interaction of nerve growth factor (NGF) with its TrkA receptor binding site, brain-derived neurotrophic factor (BDNF) with its TrkB receptor binding site, and the interaction of the neurotrophins (e.g., NGF, BDNF, NT-3, and NT-4/5) with the neurotrophin binding site of the common neurotrophin receptor p75^{NTR}.

In one aspect of the invention there is provided a variable basis Monte-Carlo (VBMC) simulated annealing method for identifying an optimal structure in a molecular system. The method comprises:

(a)   providing a Markov chain with an initial basis set of N configurational variables which define a structure for said molecular system;

(b)   translating the N configurational variables simultaneously along a basis vector to produce a new structure for the molecular system, wherein magnitude of translation is chosen randomly within a preselected range;

(c)   calculating potential energy of the new state of the molecular system;

(d)   deciding whether to accept or reject the new structure using an effective temperature dependent transition function, and if the new structure is accepted, replacing the current structure with the accepted structure;

5

(e)   repeating steps (b) to (d), each repetition having a new basis vector, for a preselected first number of repetitions at a preselected upper temperature; then

(f)   decreasing temperature according to a preselected cooling schedule;

(g)   repeating steps (b) to (d) and (f), each repetition having a new basis vector, for a preselected second number of repetitions; then

10

(h)   storing current structure of the molecular system;

(I)   repeating steps (g) and (h) until a preselected number of stored structures have been accumulated; then

(j)   rotating the basis set of configurational variables according to an effective distribution of the accumulated structures so that basis vectors are directed along low-energy

15

valleys of a potential energy hypersurface thereby accelerating conformational motions and structural transitions of the molecular system, and erasing accumulated structures from steps (h) and (I);

(k)   repeating steps (I) and (j) until, after an effective third number of repetitions, a preselected lower temperature limit is reached, thereby producing an unrefined global

20

minimum structure; and

(l)   refining the global energy minimum structure so that at least one local minimum on the potential energy hypersurface is identified.

The present invention also provides a method of identifying structures of a peptide domain of a neurotrophin to bind with a binding site of a receptor. The method comprises

25

providing a plurality of neurotrophin analogues wherein at least one of neurotrophin analogue binds the receptor, identifying an optimal or near-optimal structure for respective peptide domains of the neurotrophin analogues that bind the receptor by applying a preselected number of the variable basis Monte-Carlo (VBMC) annealing simulations described above to each of the respective peptide domains to identify minimum or near-minimum energy

30

structures for the peptide domains, and comparing said minimum or near-minimum energy structures to identify common structural features shared by neurotrophin analogues exhibiting receptor mediated activity.

The step of providing neurotrophin analogues may include providing wild-type neurotrophin analogues or mutants thereof.

35

The present invention also provides a method of identifying structures of a domain of a ligand to bind with a binding site of a receptor, comprising providing a plurality of ligand

analogues wherein at least one ligand analogue binds the receptor, identifying an optimal or near-optimal structure for respective domains of the ligand analogues that bind the receptor by applying a preselected number of the variable basis Monte-Carlo (VBMC) annealing simulations described above to each of the respective domains to identify minimum or near-

5 minimum energy structures for the domains; and comparing said minimum or near-minimum energy structures to identify common structural features shared by ligands exhibiting receptor mediated activity.

As would be apparent to a person skilled in the art, methods of the present invention are not limited to neurotrophin-receptor interactions, but are applicable to the characterization

10 of other ligand-receptor interactions. That is, an array of ligands that are either known to interact with a specific receptor or are candidate ligands that may potentially interact with this receptor may be computationally analyzed to identify optimal or near-optimal structures that provide the desired interaction. In some embodiments of the invention, the ligand may have a peptide domain, e.g., the ligand may be a peptide hormone, such as insulin, prolactin, or

15 growth hormone. In some embodiments, the ligands or candidate ligands under study may be native ligands, mutants of native ligands, or isosteres of native ligands. They may be structurally different but have similar binding activity or functional effect(s). The optimal or near-optimal structure identified may act as an agonist or antagonist. "Isosteric" is an art-recognized term and, for purposes of this disclosure, a first moiety is "isosteric" to a

20 second when they have similar molecular topography and functionality. This term should not, therefore, be restricted to mere similarity in chemical bond configuration. Two compounds may have different chemical bond configurations but nonetheless be isosteric due their 3-dimensional similarity of form and chemical nature, e.g. relevant centers such as heteroatoms are located in the same position, charges and/or dipoles are comparable, and

25 the like.

The present invention provides a ligand for binding with TrkA, wherein TrkA comprises a leucine rich motif (LRM) comprising amino acid residues 93 to 117, the coordinates of the residues of said LRM given in Appendix 1, said LRM motif having five binding areas, area A comprising amino acid residue Phe^{105tA} capable of hydrophobic bonding, area B comprising

30 residues Phe^{111tA}, Phe^{113tA}, and Thr^{114tA} capable of hydrophobic bonding, area C comprising residues Asp^{109tA} and His^{112tA} capable of ionic interaction, area D comprising residue Lys^{100tA} capable of ionic interaction, and area E comprising residues Asn^{95tA} to Ile^{98tA} capable of multiple parallel β-strand type hydrogen bonding. The ligand includes at least three moieties each comprising effective atomic elements having spatial occupancy, relative atomic position,

35 bond type and charge to define a three dimensional conformation of said ligand so that a first moiety can bind with a first binding area, a second moiety can bind with a second binding

7

area, and a third moiety can bind with a third binding area.

      Put another way, the ligand comprises at least three moieties effectively spaced relative to each other so that a first moiety can bind with a first binding area, a second moiety can bind with a second binding area, and a third moiety can bind with a third binding

5   area.More specifically, the ligand comprises at least one moiety being capable of hydrophobic bonding and being present in an effective position in the ligand to hydrophobically bind to area A, at least one positively charged moiety being present in an effective position in said ligand to ionically bind to area C, and at least one negatively charged moiety being present in an effective position in said ligand to ionically bind to area D.

10   The present invention also provides a method of designing a ligand to bind with an LRM of TrkA. The method comprises providing a template of said LRM of TrkA, said LRM comprising amino acid residue sequence 93 to 117 inclusive, said amino acid residues having spatial Cartesian coordinates given in Appendix 1 wherein binding area A in the sequence comprises residue Phe^{105tA} capable of hydrophobic bonding, binding area B comprises

15   residues Phe^{111tA}, Phe^{113tA}, Thr^{114tA} capable of hydrophobic bonding, binding area C comprises residues Asp^{109tA} and His^{112tA} capable of ionic interaction, binding area D comprises Lys^{100tA} capable of ionic interactions, and binding area E comprises residues Asn^{95tA} to Ile^{98tA} capable of multiple parallel β-strand type hydrogen bonding and computationally evolving a chemical ligand using any effective algorithm with preselected spatial constraints so that said evolved

20   ligand comprises at least three effective moieties of suitable identity and spatially located relative to each other in the ligand so that a first of the moieties hydrophobically interacts with binding area A, a second of the moieties ionically interacts with binding area C, and a third of the moieties ionically interacts with binding area D of the LRM of TrkA. The algorithm may be a genetic algorithm and the LRM may be the second LRM of a plurality of LRMs.

25   The invention further provides a method of designing a ligand to bind with an LRM of TrkA, comprising providing a template of said LRM of TrkA, said LRM comprising amino acid residue sequence 93 to 117 inclusive, the amino acid residues having spatial Cartesian coordinates given in Appendix 1 wherein binding area A comprises Phe^{105tA} capable of hydrophobic bonding, binding area B comprises Phe^{111tA}, Phe^{113tA}, Thr^{114tA} capable of

30   hydrophobic bonding, binding area C comprises Asp^{109tA} and His^{112tA} capable of ionic interaction, binding area D comprises Lys^{100tA} capable of ionic interaction, and binding area E comprises Asn^{95tA} to Ile^{98tA} capable of hydrogen bonding. The method comprises computationally evolving a ligand using an effective algorithm so that said evolved ligand comprises at least three effective moieties located relative to each other in the ligand so that

35   a first moiety can bind with a first of the five binding areas, a second moiety can bind with a second of the five binding areas, and a third moiety can bind with a third of the binding areas.

In another aspect the invention provides a ligand for binding with TrkB, wherein TrkB comprises a leucine-rich motif (LRM) comprising amino acid residues 93 to 117, the coordinates of the residues of said LRM given in Appendix 2, said LRM having five binding areas, binding area F comprising amino acid residue Asp^{100tB} capable of ionic interaction,

5   binding area G comprising amino acid residue Lys^{109tB} capable of ionic interaction, binding area H comprising amino acid residues Lys^{113tB} capable of ionic interaction, binding area I comprising amino acid residue Arg^{94tB} capable of ionic interaction, and binding area K comprising amino acid residue Lys^{104tB} capable of hydrogen bonding or ionic interaction. The ligand comprises at least three moieties effectively spaced relative to each other so that a

10   first moiety can bind with a first binding area, a second moiety can bind with a second binding area, and a third moiety can bind with a third binding area.

The present invention provides a method of designing a ligand to bind with TrkB, wherein TrkB comprises a leucine-rich motif (LRM) comprising amino acid residues 93 to 117, the coordinates of the residues of said LRM given in Appendix 2, said LRM having five

15   binding areas, binding area F comprising amino acid residue Asp^{100tB} capable of ionic interaction, binding area G comprising amino acid residue Lys^{109tB} capable of ionic interaction, binding area H comprising amino acid residue Lys^{113tB} capable of ionic interaction, binding area I comprising amino acid residue Arg^{94tB} capable of ionic interaction, and binding area K comprising amino acid residue Lys^{104tB} capable of hydrogen bonding or ionic interaction. The

20   method comprises computationally evolving a ligand using an effective algorithm so that the evolved ligand comprises at least three effective moieties located relative to each other in the ligand so that a first moiety can bind with a first of said five binding areas, a second moiety can bind with a second of said five binding areas, and a third moiety can bind with a third of the binding areas. The algorithm may be a genetic algorithm.

25   The invention also provides a ligand for binding with the common neurotrophin receptor $p75^{NTR}$, wherein $p75^{NTR}$ comprises a binding site including amino acid residues Cys^{39p} to Cys^{94p} inclusive, said residues of said binding site having spatial coordinates given in Appendix 3, said binding site having three binding areas including binding loop 2A comprising region Cys^{39p} to Cys^{58p} capable of attractive electrostatic interactions, binding loop 2B

30   comprising region Cys^{58p} to Cys^{79p} capable of attractive electrostatic interactions, and binding loop 3A comprising region Cys^{79p} to Cys^{94p} capable of attractive electrostatic interactions. The ligand comprises at least two moieties effectively spaced relative to each other so that a first moiety can bind to a first loop and a second moiety can bind to a second loop.

The present invention also provides a method of designing a ligand for binding with

35   the common neurotrophin receptor $p75^{NTR}$, wherein $p75^{NTR}$ comprises a binding site including amino acid residues Cys^{39p} to Cys^{94p} inclusive. The residues of the binding site have spatial

9

coordinates given in Appendix 3. The binding site has three binding areas including binding loop 2A comprising region Cys^{39p} to Cys^{58p} capable of attractive electrostatic interaction, binding loop 2B comprising region Cys^{58p} to Cys^{79p} capable of attractive electrostatic interaction, and binding loop 3A comprising region Cys^{79p} to Cys^{94p} capable of attractive

5 electrostatic interaction. The method comprises computationally evolving a ligand using an effective algorithm so that the evolved ligand comprises at least two effective moieties located relative to each other in the ligand so that a first moiety can bind to a first of the three loops and a second moiety can bind to a second loop of the three loops.

The invention provides a method of identifying a ligand to bind with a leucine rich motif

10 (LRM) of TrkA. The method comprises providing a three dimensional conformation for the LRM. The LRM comprises amino acid residue sequence 93 to 117 inclusive, the amino acid residues having spatial Cartesian coordinates given in Appendix 1. The LRM has five binding areas, area A comprising amino acid residue Phe^{105tA} capable of hydrophobic interaction, area B comprising amino acid residues Phe^{111tA}, Phe^{113tA}, and Thr^{114tA} capable of hydrophobic

15 interaction, area C comprising amino acid residues Asp^{109tA} and His^{112tA} capable of ionic interaction, area D comprising amino acid residue Lys^{100tA} capable of ionic interaction, and area E comprising Asn^{95tA} to Ile^{98tA} capable of multiple parallel β-strand type hydrogen bonding. The method includes providing a data base containing molecules coded for spatial occupancy, relative atomic position, bond type and/or charge; and screening the data base to

20 select those molecules comprising moieties having a three dimensional conformation and effective charge that can bind with at least three of the five binding areas.

The invention provides a method of identifying a ligand to bind with a leucine rich motif (LRM) of TrkB. The method comprises providing a three dimensional conformation for the LRM. The LRM comprises amino acid residues 93 to 117, the coordinates of the residues of

25 the LRM are given in Appendix 2, the LRM having five binding areas, binding area F comprising amino acid residue Asp^{100tB} capable of ionic interaction, binding area G comprising amino acid residue Lys^{109tB} capable of ionic interaction, binding area H comprising amino acid residue Lys^{113tB} capable of ionic interaction, binding area I comprising amino acid residue Arg^{94tB} capable of ionic interaction, and binding area K comprising amino acid residue Lys^{104tB}

30 capable of hydrogen bonding or ionic interaction. The method includes providing a data base containing molecules coded for spatial occupancy, relative atomic position, bond type and/or charge; and screening the data base to select those molecules comprising moieties having a three dimensional conformation and effective charge that can bind with at least three of the five binding areas.

35 The present invention also provides a method of identifying a ligand to bind with common neurotrophin receptor $p75^{NTR}$. The method comprises providing a three dimensional

conformation for the common neurotrophin receptor p75^{NTR}, wherein p75^{NTR} comprises a binding site including amino acid residues Cys^{39p} to Cys^{94p} inclusive. The residues of the binding site have spatial coordinates given in Appendix 3, the binding site having three binding areas including binding loop 2A comprising region Cys^{39p} to Cys^{58p} capable of

5   attractive electrostatic interaction, binding loop 2B comprising region Cys^{58p} to Cys^{79p} capable of attractive electrostatic interaction, and binding loop 3A comprising region Cys^{79p} to Cys^{94p} capable of attractive electrostatic interaction. The method includes providing a data base containing molecules coded for spatial occupancy, relative atomic position, bond type and/or charge; and screening the data base to select those molecules comprising moieties that can

10   bind with at least two of the three binding loops.

        In one aspect of the invention, a ligand (e.g., small molecule) designed to interact with a receptor such as Trk or p75NTR may be bifunctional, such that a first portion of the ligand binds to one receptor monomer and a second portion of the ligand binds to a second receptor monomer. Thus, a receptor dimer is effectively cross-linked by the interaction of ligand with

15   both receptor monomers.

        According to the invention, detailed information is provided regarding those amino acid residues of neurotrophins and of neutrophin receptors which are involved in neurotrophin-receptor binding. Such information includes the bioactive conformations of the respective peptide domains of the neurotrophins and receptors. This in turn permits the

20   design of small molecules which interact with said amino acid residues or domains. Where such interaction block the residues or changes the conformation of the domain, the small molecule can inhibit neurotrophin-receptor binding, in certain cases abolishing it completely. As would be appreciated by a person skilled in the art, small molecule design according to this aspect of the invention is applicable to other ligand-receptor interactions in addition to

25   neurotrophins, according to the methods disclosed herein.

        As a person skilled in the art would appreciate, the invention not only provides molecules (ligands) that interact with receptors, but also molecules which, in their mimicry of a receptor's bioactive conformation, can bind to the receptor binding site of a ligand such as, for example, a neurotrophin. Such molecules, whether they interact with ligand or with

30   receptor, can block native ligand-receptor interaction. In some embodiments of the invention, a small molecule which binds to a receptor may even trigger signal transduction similar to that of the native ligand, i.e., act as an agonist.

35

BRIEF DESCRIPTION OF THE DRAWINGS

The invention will be described, by example only, reference being had to the accompanying drawings, in which:

5   Figure 1 shows the amino acid sequences of the conformationally variable termini of the dimeric NGF analogues under study. The residues are numbered from 1 to 118 for the first monomer, and from 1' to 118' for the second monomer. The fixed parts of the proteins simulated by the X-ray geometry of mouse NGF (McDonald et al., 1991) are underlined.

Figure 2 shows the structure of the complex of the amino and carboxyl termini of

10   (1-118)hNGF homodimer. The carboxyl terminus is shown in grey, the amino terminus in white, and the interacting conservative region His^{75}-Asn^{77} of the "south" part of the NGF dimer, in black.

Figure 3 shows the structure of the complex of the amino and carboxyl termini of (1-118)mNGF homodimer.

15   Figure 4 shows the structure of the complex of the amino and carboxyl termini of dimeric mNGFΔ3-9 molecule.

Figure 5 shows the structure of the complex of the amino and carboxyl termini of dimeric hNGF-H4D molecule.

Figure 6 shows the structure of the complex of the amino and carboxyl termini of

20   dimeric mNGFΔ1-8 molecule.

Figure 7 shows the structure of the complex of the amino and carboxyl termini of BDNF homodimer.

Figure 8 illustrates the TrkA leucine-rich motifs. Locations of parallel β-strands are illustrated by the shaded areas designated by symbol β. Fragments B1-B4 demonstrate NGF

25   binding affinity, while N1-N4 do not (Windisch et al., 1995a, 1995b).

Figure 9 shows sequences of the amino and carboxyl termini of fully active NGF analogues. Regions with rigid structures are underlined.

Figure 10 shows the predicted bioactive conformation of the NGF binding domain (a) and the structures of the NGF/LRM-2A complexes of hNGF (b), mNGF (c), mNGFΔ3-9 (d),

30   and hNGF:NT-4/5 (e). Only residues essential for discussion are designated. A, B, C, D and E represent specific NGF/LRM-2A binding areas. The LRM-2A is illustrated in grey, NGF in white.

Figure 11 shows the TrkB receptor binding site of BDNF (a), predicted features of the BDNF/LRM-2B complex (b), and geometry of the "improper" NGF/LRM-2B complex (c). Only

35   residues essential for discussion are designated. F, G, H, I and K represent specific BDNF/LRM-2B binding areas. The LRM-2B is illustrated in grey, BDNF and NGF in white.

Figure 12 is a detail of the LRM-2A conformation when bound to hNGF. The three groups of the β-strand involved in H-bonding with the parallel β-strand motif of the NGF analogues are designated by NH or CO. Hydrophobic residues are illustrated as light, polar uncharged as dark, charged as black.

5   Figure 13 presents principal residues of the NGF binding domain essential for TrkA receptor recognition. Conserved residues of NGF molecules among all characterized species (McDonald et al., 1991) are designated by X, whereas those which are substituted in NGF molecules derived from different species by similar amino acids and NGF residues maintaining the bioactive conformation or interacting with specific binding areas A-E of the

10   LRM-2A are indicated by X.

Figure 14 presents principal residues of the LRM-2A. The residues which are specific for TrkA (Windisch et al., 1995a, 1995b) and critical for the present model are designated by X and X, respectively.

Figure 15 is a schematic representation of the second leucine-rich motif of TrkA

15   (residues 93tA to 116tA) (a) and TrkB (residues 93tB to 116tB) (b) as specific binding sites for NGF and BDNF, respectively. General consensus residues are shaded. Arrows designate distinct positions essential for molecular recognition processes.

Figure 16 represents the X-ray crystallography-derived geometry of the α-carbon trace of the two loops (2A and 2B) of the second cysteine-rich domain (white bonds) and the first

20   loop (3A) of the third cysteine-rich domain (grey bonds) of p55^{TNFR} (Banner et al., 1993) (a), the preferred geometry of the α-carbon trace of the corresponding fragment of p75^{NTR} (b), and the predicted bioactive conformation of mouse NGF (McDonald et al., 1991); (c). White and grey bonds in panel (c) illustrate different protomers. The p75^{NTR} binding determinant of NGF (loops I and V) is denoted. Disulfide bonds are shown in black.

25   Figure 17 shows the sequence of a putative binding site for neurotrophins within p75^{NTR} aligned with the corresponding sequence of homologous p55^{TNFR}. Conserved pattern of disulfide bonds is illustrated. Abbreviation (h) stands for human (Johnson et al., 1986), (r) for rat (Radeke et al., 1987), and (c) for chicken (Large et al., 1989) p75^{NTR}.

Figure 18 illustrates the most stable geometries of the complexes of the neurotrophins

30   with the common neurotrophin receptor p75^{NTR}: with NGF (a); with BDNF (b); with NT-3 (c); with NT-4/5 (d). The α-carbon traces of the neurotrophins are shown in white, while that of the p75^{NTR} binding site is shown in grey. Disulfide bonds are illustrated in black. Only residues mentioned in the text are denoted.

Figure 19 demonstrates geometric compatibility of the van der Waals surfaces of

35   BDNF (light) and the p75^{NTR} binding site (dark).

Figure 20 illustrates conformational changes of the p75^{NTR} binding site upon BDNF

13

binding. Conformation of the p75^{NTR} receptor binding site before binding is illustrated in white, after binding in grey. The two conformations have been superimposed using the equilibrium positions of the reference α-carbon atoms located in loops 2A and 3A. Straight lines denote linear approximations of the conformations of the α-carbon traces of loop 2B in both

5   structures.

DETAILED DESCRIPTION OF THE INVENTION

PART A

10   THEORETICAL STUDIES OF THE BIOACTIVE CONFORMATION OF NERVE GROWTH
FACTOR USING VBMC - A NOVEL VARIABLE BASIS MONTE-CARLO SIMULATED
ANNEALING ALGORITHM FOR PEPTIDES

BACKGROUND TO THE VBMC ALGORITHM

15   The structural optimization of the peptide domains under study required a rigorous
search of conformational space. As with other theoretical peptide studies, such calculations
are plagued by a multiple-minima problem (Gibson and Scheraga, 1988) which traditionally is
addressed using either molecular dynamics, Monte Carlo approaches or other algorithms.
The Monte Carlo method, although exceedingly powerful, is limited by the excessive CPU

20   time requirements on existing computers. To remedy this problem, we have devised a novel
Variable Basis Monte Carlo simulated annealing algorithm for peptides (VBMC).

           The potential energy hypersurface of a peptide has an enormous number of local
minima (Gibson and Scheraga, 1988; Piela et al., 1989, 1994), but usually only the global
energy minimum structure is required. Despite efforts to elaborate an efficient method of

25   global energy minimization (Gibson and Scheraga, 1988; Judson et al., 1994), the
multiple-minima problem is far from being solved. Although simulated annealing (Kirkpatrick
et al., 1983; Vanderbilt et al., 1984) is mathematically correct and guarantees convergence to
the global minimum in principle, the suggested "cooling" schedule appears to be far too slow
for practical purposes, and faster "cooling" has to be used (Gidas, 1985; Kushner, 1987).

30   Within the simulated annealing approach, thermal molecular motion can be simulated either
by Monte Carlo (Kirkpatrick et al., 1983; Nayeem et al., 1991; Wilson et al., 1988; Snow,
1992; Shamovsky et al., 1992) or molecular dynamics (Lelj et al., 1991; Villani and Tamburro,
1994) methods.

           The major problem of the Monte Carlo technique is that motion of a molecular system

35   along a Markov chain is very slow (Piela et al., 1994; Scheraga, 1989; Nayeem et al., 1991).
On the other hand, the Monte Carlo technique has several considerable advantages over

molecular dynamics. First, it does not require calculating forces. Second, potential energy functions do not have to be continuous. Third, much larger steps in conformational space can be utilized (Li and Scheraga, 1988; Kincaid and Scheraga, 1982). Fourth, the additional iterative self-consistent SHAKE routine (Ryckaert et al., 1977), which is used in molecular

5   dynamics simulations to deal with holonomic constraints (Brooks III and Case, 1993), is not required in the Monte Carlo method. This has led to efforts to accelerate configurational motion within the Monte Carlo approach (Raj et al., 1994; Snow, 1992; Kincaid and Scheraga, 1982; Rao et al., 1979; Rossky et al., 1978). The main reason for inefficiency with the conventional Monte Carlo method (Metropolis et al., 1953) is a slow and cumbersome

10   sequential change of configurational variables.

To overcome these problems, lessons can be learned from molecular dynamics. In molecular dynamics (Allen and Tildesley, 1987) configurational variables move simultaneously, and the soft modes of the system explicitly direct these motions. Soft modes are defined as low-energy valleys on the potential energy hypersurface. Although there have

15   been attempts to direct Monte Carlo configurational motion along the soft modes (Raj et al., 1994; Rao et al., 1979; Rossky et al., 1978), these improvements require calculating forces and, consequently, result in losing the main advantages of the Monte Carlo approach. An algorithm which would retain the advantages of the Monte Carlo method and direct configurational changes along the soft modes is thus required. One possible solution has

20   recently been suggested (Szentpaly et al., 1994).

The classical Monte Carlo-Metropolis method (Metropolis et al., 1953) consists of modelling a Markov chain containing subsequent conformations of the molecule under study: $x_0, x_1, x_2, \ldots, x_i, \ldots,$ where x ($x_i = \{x_i^1 \ldots x_i^m \ldots x_i^N\}$) is the vector of independent structural parameters. Each vector x_{i+1} is derived from the preceding one, x_i, by means of a random

25   change of one randomly chosen variable:

$$x_{i+1}{}^m = x_i^m + \lambda_m \cdot \xi \qquad\qquad (1)$$

where ξ is a random quantity from the interval (-1,1) and λ_m is a maximal allowed increment of

30   the given variable. N moves of the Markov chain (where N is the number of independent parameters) represent a Monte Carlo step. Whether the new state x_{i+1} is accepted or rejected is decided according to a transition probability function. The following functional form of transition probability is used in the present expression (2) (Gunningham and Meijer, 1976):

35   $$W(x_i \Rightarrow x_{i+1}) = 1/[1 + \exp(\Delta E_i /kT)] \qquad\qquad (2)$$

where ΔE_i is the difference between conformational energies of the states x_{i+1} and x_i, k is the Boltzmann constant and T is absolute temperature.

Those skilled in the art will appreciate that other functional forms of transition functions may be used to screen state a new state x_{i+1}. For example, another effective temperature dependent transition function for screening a new state x_{i+1} derived from a previous state x_i is given by:

$$W(x_i \rightarrow x_{i+1}) = 1, \qquad\qquad \text{if } E(x_{i+1}) \leq E(W(x_i))$$
$$= \exp(-\Delta E_i / kT), \qquad \text{if } E(x_{i+1}) \geq E(W(x_i))$$

where ΔE_i is the difference between conformational energies of the states x_{i+1} and x_i, k is the Boltzmann constant and T is absolute temperature.

The direct application of this conventional Monte Carlo technique to the conformational space study of protein structure is not efficient because the conformational variables of peptide chains appear to be mutually dependent, i.e., low-energy conformational motions involve several conformational variables. When applied to molecular systems such as protein secondary, tertiary or quaternary structure, equation (1), in which structural parameters are sequentially changed one after another, results in very small values of ξ and, consequently, in a very slow conformational motion (Piela *et al.*, 1994; Scheraga, 1989; Nayeem *et al.*, 1991). In order to model a *simultaneous* change of the structural parameters, we have used Eq.(3) (instead of the conventional (1)),

$$x_{i+1} = x_i + \lambda_m \cdot \xi \cdot g^m \qquad\qquad\qquad (3)$$

where g^m is a randomly or sequentially chosen *basis vector* from a basis $G=\{g^m\}$, ξ is a random quantity from an interval (-1,1) and λ_m is a maximal acceptable move in direction g^m. In this study λ_m was constant and equal to $10°$.

A basis G is formed from linear combinations of independent conformational parameters x for their change to be realized *along the soft modes* of the molecule. These modes are revealed by dispersion analysis of the distribution of the sequential configurational points of the Markov chain. The soft modes of the molecular system are to be directed along the axes of the dispersion ellipsoid because they should correspond to the directions of maximal deviations made by the independent variables during a certain period of simulation. Initially, basis G coincides with a unit matrix, i.e., G = I, and Eq.(3) is equivalent to (1). The rotation of basis G is carried out after every 150 Monte Carlo steps based on the particular scattering of the previous 150 configurations x. Basis vectors g^m are made equal to the eigenvectors of the covariant matrix D which has the following elements:

$$d_{ij} = (1/M) \cdot \sum_{n=1}^{M} (x_n^i - (1/M) \cdot \sum_{n=1}^{M} x_n^i) \cdot (x_n^j - (1/M) \cdot \sum_{n=1}^{M} x_n^j) \qquad (4)$$

where M is the number of points in the distribution (M=150), and x_n^i is the i-th structural parameter at the n-th Monte Carlo step. Vectors g^m form the orthonormalized basis and are used in the Markov chain instead of independent conformational parameters. Periodic rotations of basis G in Monte Carlo simulations result in a simultaneous change of all the conformational variables along the valleys of a potential energy surface, which considerably accelerates conformational motions and transitions (Szentpaly et al., 1994).

The method disclosed herein is highly advantageous over known processes for several reasons. In the present process the preselected range from which the magnitude of translation is chosen is constant and does not depend on the basis set. Thus the present method is much more efficient than previous methods in part because the magnitude of translation along the basis vector is limited by a preselected range. The present method is also more efficient because rotation of the basis set of configurational variables is avoided at the upper temperatures and is implemented only at the lower temperatures.

IMPLEMENTATION OF THE VBMC ALGORITHM

VBMC was written in Fortran-77. The algorithm was then interfaced with the CHARMM force field (Brooks et al., 1983; The force field parameters are extracted from CHARMM release 23.1, Molecular Simulations, Inc., Waltham, MA). Torsional distortion, van der Waals and electrostatic interactions, and hydrogen bonding were thus explicitly considered. The united atom approach was used for all carbons with non-polar hydrogens. Point atomic charges of Weiner et al. (Weiner et al., 1984) were used. A dielectric constant equal to the interatomic separation in angstroms was utilized to implicitly simulate solvation effects (Weiner et al., 1984). All calculations were performed on an 8-node IBM Scalable POWERparallel 2 [SP2] high performance computer at Queen's University, Kingston, Canada. Each Monte Carlo simulated annealing computation required up to 120 hours of CPU time.

Appendix 4 is attached. Appendix 4 is a computer program written in Fortran-77 and is a non-limiting example of a program used to perform the VBMC simulated annealing method in accordance with the present invention.

Each run of the VBMC algorithm provides a unique final structure which would represent the global energy minimum structure, regardless of the initial geometry, if the "cooling" was performed infinitely slowly. However, since this is impossible, several Monte Carlo simulated annealing computations must be performed from different starting points x_0, using different initial temperatures T_0, "cooling" schedules and random sequences. An initial temperature of 1000° K is sufficient. The Markov chain is kept at a constant temperature T_0

for 10^4 Monte Carlo steps before the initiation of "cooling". The temperature T is then decreased at every Monte Carlo move (3) by a small increment such that after $2 \cdot 10^4$ Monte Carlo steps it reaches 120° K producing an unrefined global energy minimum structure.

5
The global energy minimum structure is then refined to identify the nearest local minimum or stationary point on the potential energy hypersurface. Refinement may be accomplished using any one of several non-linear minimization routines to identify the local minimum on the potential energy hypersurface. For example, gradient descent minimization and conjugate gradient minimization may be used. Quasi-Newton minimization methods such as the Newton-Raphson method may also be used. Other non-linear methods include the

10
Marquardt method, the Powell method and a variable metric method. Those skilled in the art will be aware of the various non-linear routines which may be used for refinement and those mentioned herein are more fully described in *Nonlinear Programming: Theory, Algorithms, and Applications.* 1983. New York: John Wiley & Sons.

APPLYING VBMC TO NGF

15
The aim of this computational study was to ascertain the biologically active conformation of the TrkA receptor binding determinant of NGF. A comprehensive review of the literature identified an initial study set of 17 proteins which have been assessed for TrkA mediated activity using comparable experimental methods. From these 17 analogues, a subset of six (three active and three inactive) which reflects the range of structural diversity

20
was selected for preliminary study. Accordingly, in the present invention the low-energy conformations of the amino and carboxyl termini of six NGF analogues were obtained by means of Monte Carlo simulated annealing calculations. Three of these analogues retain full TrkA mediated activity: human NGF (hNGF; Shih *et al.*, 1994; Burton *et al.*, 1992), mouse NGF (mNGF; Burton *et al.*, 1992; Drinkwater *et al.*, 1993), and mNGFΔ3-9 (deletion 3-9 of

25
mNGF; Drinkwater *et al.*, 1993). The other three analogues are biologically inactive: hNGF-H4D (a point mutation of hNGF in which His [H] in position 4 is replaced by Asp [D]; Shih *et al.*, 1994), mNGFΔ1-8 (Burton *et al.*, 1992; Drinkwater *et al.*, 1993; Taylor *et al.*, 1991) and BDNF (Suter *et al.*, 1992). The results and conclusions obtained from these six analogues were then validated by being applied to the remaining 11 analogues of the initial

30
study set.

The amino acid sequences of the termini of the neurotrophin molecules under study are presented in Figure 1. Residues are numbered from 1 to 118 for the first monomer, and from 1' to 118' for the second monomer. The mutual orientation of the termini of the different monomers is determined by the disulfide bonds $Cys^{15} - Cys^{80}$ and $Cys^{68'} - Cys^{110'}$ and

35
hydrophobic interactions $Val^{14} : Val^{14'}$ and $Val^{109} : Val^{109'}$, which are absolutely conserved in all neurotrophins (McDonald *et al.*, 1991). The conformational space of the peptide molecules

consists of flexible torsional angles determining geometry of the amino terminus of one monomer and the carboxyl terminus of the other, while keeping the rest of the dimer fixed in the known geometry of mNGF (McDonald *et al.*, 1991). Covalent bond lengths and bond angles of the termini are kept fixed. The geometry of each residue is determined only by

5   flexible torsional angles of the peptide backbone (ϕ and ψ) and the side chain (χ_1, χ_2,...). All torsional angles of amino acid Pro except for ψ are fixed. Torsional angles describing structural motifs with the essentially planar geometry (such as peptide bonds or conjugated regions in side chains) are kept fixed. Likewise, the configurations of the sp^3-carbons are fixed. With these constraints, the total conformational space of the flexible termini of hNGF,

10   mNGF and BDNF consists of 74, 73 and 67 variables, respectively.

RESULTS AND DISCUSSION

By diagonalizing the covariant matrix in the framework of the VBMC algorithm, rigid modes of a molecular system, which should slow down conformational changes, are supposed to be revealed simultaneously with soft modes of the system. To test the efficiency

15   of the VBMC algorithm, its performance was compared with the conventional Monte-Carlo method at the equilibrium parts of the Markov chains generated at different constant temperatures. These comparisons showed that at high temperatures (700^0-1000^0K) the basis variability results in decreasing acceptance rates. On the other hand, the temperature decrease reinforces the advantage of the VBMC approach, and at temperatures below 600^0

20   acceptance rates of the VBMC Markov chains were significantly higher. Thus, at T=300^0 K the acceptance rate of the conventional Markov chain was found to be 0.22, which is very close to that recommended by Kincaid and Scheraga (1982) as optimal (0.20). The acceptance rate of the VBMC algorithm obtained at the same conditions was 0.26, i.e. 18% higher. These evaluations are in agreement with what one would expect. Indeed, at low

25   temperatures only soft modes of molecules are involved in thermal motions, hence, they are especially populated in corresponding Monte-Carlo generated conformational ensembles and can be revealed from them. Higher acceptance rates of the low temperature VBMC Markov chains over conventional Markov chains mean that the average increase of the sizes of the Monte-Carlo moves along soft modes of the system are higher than their decrease along the

30   rigid modes. Thus, the VBMC disclosed herein for evaluating peptide conformations not only changes directions of the Monte-Carlo moves, but also accelerates conformational changes by directing them along the soft modes of the molecule. Consequently, the present VBMC algorithm is more efficient than conventional Monte-Carlo method only at moderate and low temperatures, when thermal motions tend to take place along the valleys of the potential

35   energy surface. This particular temperature region causes serious problems in known simulated annealing algorithms, and the VBMC method disclosed herein provides a solution

to these problems.

Seven independent VBMC simulations for each of the six molecular systems under study were performed. Simultaneously, local energy refinements were periodically carried out from a number of points generated during the "slow cooling" stage. All local minimizations resulted in higher energy stationary points on the potential energy surface than those produced by VBMC computations. This means that the VBMC technique as an approach to global minimization cannot be replaced by relatively inexpensive periodic energy refinements from the high-temperature conformational space; at high temperatures only high-energy conformers are sufficiently populated. Although VBMC runs did not converge to the same conformation, the final structures differed insignificantly; i.e., the peptide backbone conformation remained unchanged but there were limited differences in the side chain torsional angles. Multiple VBMC simulations identified rigid and flexible parts of the molecules. Minimum energy structures of all molecules are displayed in Figures 2-7 while Table 1 presents optimized conformational parameters of the amino and carboxyl termini of the considered NGF analogues.

GEOMETRIC SIMILARITY OF BIOACTIVE NGF CONFORMERS

Rigid regions of hNGF and mNGF which maintain the same conformation in all independent VBMC simulations are formed by residues 9-11 and 112'-118', creating a richly hydrogen bonded (H-bonded) 3-dimensional complex. Conformational variability within this rigid zone is primarily restricted to side chains and does not affect the geometry of the backbone. An interesting example of such side chain mobility occurs with $Arg^{114'}$, which is H-bonded to the carbonyl oxygen of the ninth amino acid of the amino terminus and which is therefore expected to have a fixed conformation. Nevertheless, $Arg^{114'}$ has two distinct conformers in which the H-bonding is realized by the hydrogen atoms attached to the different NH_2 groups, with the energy difference being about 1 kcal/mol. In addition to local conformational variability, hNGF and mNGF have a region of "cooperative" flexibility which is made up of residues 1-8. Several distinct conformations exist within this region, with its conformational variability being caused by a number of possibilities for the H-bond network formed by residues 1-3.

Comparison of the most stable conformers of hNGF (Figure 2) and mNGF (Figure 3) reveals striking conformational similarity between their rigid regions in spite of several differences in the primary structure of the amino and carboxyl termini (Figure 1). As shown in Table 1, both termini have the same conformation, except for the variable region consisting of residues 1-3. The most stable H-bond networks in this area differ considerably because of the mT3hS substitution.

The essential difference between the amino acid sequences of the termini of hNGF

and mNGF is the mM9hR substitution, which does not change the geometry of the rigid region. Residues Met and Arg have different side chain types, i.e., the former is non-polar while the latter is polar and positively charged under physiological conditions. It is surprising that this substitution does not affect geometry since it introduces the positive charge of Arg^9

5   which is located in an electrostatic field created by at least five neighbouring charged functional groups. Conformational stability of the rigid region of hNGF is maintained by the exact fit of the Arg^9 side chain into a "hollow" in the rigid region, which is occupied by the Met^9 side chain in mNGF. Furthermore, the Arg^9 side chain, being in this "hollow", forms two additional interchain H-bonds with carbonyl oxygens of residues $Val^{117'}$ and $Arg^{118'}$. This

10   further stabilizes the rigid region of hNGF.

The physical reason for the geometric similarity of the rigid regions of hNGF and mNGF is that the structural features of these two complexes are determined by similar H-bonding and electrostatic interactions. The major stabilizing factor is the H-bonding and electrostatic interaction of charged side chains of residues Glu^{11} and $Arg^{118'}$. In addition,

15   these side chains are involved in other H-bonding: the carboxyl oxygens of Glu^{11} are bonded to the δ-NH group of His^8 , the hydroxyl group of $Ser^{113'}$ and the backbone NH group of $Lys^{115'}$; the side chain NH and NH_2 groups of $Arg^{118'}$ are bonded to the backbone Phe^7 and $Lys^{115'}$ carbonyl groups. There are some other common interchain H-bonds in hNGF and mNGF. The ε-amino group of the $Lys^{115'}$ side chain forms a H-bond with the δ-carbonyl oxygen of the

20   $Asn^{77'}$ residue, situated at the "south" part of NGF structure (McDonald et al., 1991).

In addition to H-bonding, the particular geometry of the rigid region in both molecules is also maintained by electrostatic interactions of positively charged residues, specifically His^4, His^8, $Arg^{114'}$, $Arg^{118'}$ and $His^{75'}$. An electrostatic repulsion between His^4 and boundary residues His^8 and $Arg^{118'}$ of the rigid region forces His^4 to be located as far as possible from

25   the rigid region, separating the 1-8 loop from the rest of the structure. This tendency is further reinforced in hNGF by the presence of a third positively charged boundary residue Arg^9. The $His^{75'}$ amino acid located in the "south" part of NGF also participates in maintaining the structure of the rigid region. An electrostatic repulsion between $His^{75'}$ and $Arg^{114'}$ prevents H-bonding of the amino group of $Arg^{114'}$ with the $Asn^{77'}$ side chain and the $Ser^{113'}$ backbone:

30   indeed, removing the ε-proton from $His^{75'}$ results in two H-bond contacts which change the global energy minimum structure of the complex.

The separation of flexible loop 1-8 from the rigid region is also determined by residue Pro^5. This amino acid imposes restrictions on conformational motion of the loop, making it "bent" at this particular point, and thereby defining the location of the adjacent His^4 residue at

35   the most distant point from the rigid region. Thus, residues His^4 and Pro^5 are primarily responsible for the separation of the flexible loop from the rigid region.

Although mNGFΔ3-9 does not have the flexible loop, the energy optimized geometric features of its termini are very similar to those of the hNGF and mNGF rigid regions (Table 1, Figures 2-4). There are only two structural elements which are specific for the rigid region of mNGFΔ3-9. First, although $Arg^{118'}$ has a different conformation, the result is functionally the

5   same, namely both NH_2 groups of the $Arg^{118'}$ side chain are H-bonded to the Glu^{11} side chain. In addition, the ε-NH group of $Arg^{118'}$, which is H-bonded to the Phe^7 carbonyl group of the flexible loop in both hNGF and mNGF, faces the carbonyl terminus in mNGFΔ3-9. Second, the "hollow", which is occupied by the ninth amino acid side chain in hNGF and mNGF, is now filled with the protein backbone of the remainder of the loop, i.e., residues 1-2. Functionally,

10   the structure of the rigid region of mNGFΔ3-9 resembles that of hNGF because of the stabilizing interchain H-bond contacts of the moieties located in the "hollow".

GEOMETRIC DISTINCTION OF NGF ANALOGUES INACTIVE FOR TrkA BINDING

The energy minimum structures of the complexes formed by the amino and carboxyl termini of molecules, hNGF-H4D, mNGFΔ1-8 and BDNF, which are inactive with respect to

15   TrkA binding, do not possess the common structural features found in active molecules. Point mutation H4D in hNGF incorporates negative instead of positive charge into the 1-8 loop. As a result of this mutation, the loop is no longer separated from the rigid region, forming a united complex instead (Figure 5). In this complex the negatively charged carboxyl group of Asp^4 is surrounded by four positively charged NH_2 groups of Arg^9 and $Arg^{114'}$, and

20   residue His^8 is not H-bonded to the Glu^{11} carboxyl group. Thus, because of the H4D point mutation, the common structural features inherent in hNGF and mNGF are lost from hNGF-H4D.

Deletion 1-8 also changes dramatically the most stable structure of the rigid region of mNGF (Figure 6). The newly created positively charged amino terminus is located between

25   negatively charged carboxyl groups of Glu^{11} and $Arg^{118'}$, with charged side chains of $Arg^{114'}$, $Lys^{115'}$ and $Arg^{118'}$ being substantially shifted from their preferred positions in active molecules. Thus, the electrostatic field caused by the positive charge of the new amino terminus in mNGFΔ1-8, located in the vicinity of the carboxyl group of Glu^{11}, is responsible for the destruction of the geometry of the rigid region inherent in the active molecules.

30   The complex formed by the amino and carboxyl termini of BDNF is also significantly different from those formed by the molecules active for TrkA binding (Figure 7, Table 1). There are several reasons for the considerable conformational changes in BDNF. First, negatively charged residue Asp^5 eliminates the separation of the flexible loop from the rigid region, and interacts with the positively charged His^3, Arg^9 and amino terminus. Second,

35   because of its long tail, Arg^8 is unable to form the H-bond contact with the Glu^{11} side chain and forms bifurcated H-bonds with the carbonyl group of Gly^{10}. Third, $Arg^{116'}$ is H-bonded to

Glu$^{66'}$ located in the "south" part of the molecule, which imposes a specific restriction on conformational possibilities of the carboxyl terminus of BDNF.

EXPLANATION FOR THE OBSERVED STRUCTURE-ACTIVITY RELATIONSHIPS

The principal result of the molecular simulations presented is that the NGF molecules

5 with full TrkA mediated activity considered in this study have regions with similar 3-dimensional structure, whereas in all inactive analogues, the geometry of this region is altered, mainly by novel electrostatic interactions. It is therefore reasonable to attribute the TrkA mediated activity to a specific conformation of this particular region. The amino and carboxyl terminal regions therefore represent a "functional epitope" which contains relatively

10 few contact residues mediating high affinity binding. The ability of a small number of residues to cause high affinity binding has previously been demonstrated in other systems and may represent a general property of protein-protein interfaces. Some experimental data consistent with this concept are presented below.

The VBMC computations show that the following amino acids are critical in

15 determining the structure of the complex in wild type NGF dimers: His^4, Pro^5, His^8, Arg^9, Glu^{11}, His^{75}, Asn^{77}, Lys$^{115'}$ and Arg$^{118'}$. This is significant since residues His^4, Pro^5, Glu^{11}, His^{75}, Asn^{77} and Lys^{115} are conserved in NGF molecules across all species (McDonald et al., 1991). The overlap between these two sets reflects a tendency to maintain the particular geometry of the complex in natural NGF molecules. In addition, as demonstrated, the substitution of

20 the important residue Arg^9 by the essentially different Met^9 does not result in geometric changes of the complex, which is consistent with equivalent bioactivity of hNGF and mNGF (Burton et al., 1992). Thus, because of multiple physical factors maintaining the geometry of the complex, some species variability observed in NGF termini (McDonald et al., 1991) is acceptable and does not cause geometric changes in the rigid region.

25 It is shown that each NGF terminus has several important residues, which determine the particular structure of the complex. This is consistent with high sensitivity of biological activity of NGF to the primary structure of both the amino and carboxyl termini (Klein et al., 1991; Shih et al., 1994; Burton et al., 1992, 1995; Kahle et al., 1992; Drinkwater et al., 1993; Treanor et al., 1995; Taylor et al., 1991). The lack of the TrkA mediated activity of the

30 mNGFΔ3-11, mNGFΔ3-12, mNGFΔ3-13, mNGFΔ3-14, mNGFΔ9-14 and mNGFΔ112-118 deletion mutants (Drinkwater et al., 1993) is thus explained by the absence of the key residues Glu^{11} and Arg$^{118'}$.

The separation of the flexible loop from the rest of the complex is crucial in permitting the rigid region to exist with definite geometric features. Residues His^4 and Pro^5 which cause

35 this separation are absolutely conserved elements of the wild type NGF molecules derived from different species (McDonald et al., 1991), and their compulsory location in the middle of

the flexible loop is well suited for facilitating the maximal separation. Point mutation P5A or H4D weakens or destroys the tendency of the loop to separate from the rigid region; accordingly, these mutations result in dramatic loss of TrkA related activity (Shih et al., 1994).

The flexible loop is not an essential structural element for TrkA activation since the

5   mNGFΔ3-9 deletion mutant, which does not contain the loop (Figure 4), is as active as wild type mNGF (Drinkwater et al., 1993). However, complete elimination of all loop residues results in almost inactive mutants mNGFΔ1-8 (Burton et al., 1992; Drinkwater et al., 1993; Taylor et al., 1991) and hNGFΔ1-9 (Shih et al., 1994; Burton et al., 1992, 1995; Kahle et al., 1992; Luo and Neet, 1992). Our molecular simulation studies enable the explanation for this

10   apparent contradiction. It is demonstrated that the backbone of residues Ser^8-Ser^9 in the mNGFΔ3-9 mutant is naturally incorporated into the structure of the rigid region because it matches the geometry of the "hollow" occupied by either Met^9 or Arg^9 side chain in wild type NGF dimers. On the contrary, total truncation of the flexible loop in the mNGFΔ1-8 deletion mutant results in placing the positively charged amino end in the vicinity of the key H-bonded

15   Glu^{11} and Arg^{118} charged side chains (Figure 3), which abolishes the desired geometry of the rigid region (Figure 6). The same applies to the hNGFΔ1-9 deletion mutant which has neither the 1-8 loop nor the stabilizing Arg^9 residue (Figure 2). This being the case, biological activity of amino terminus deletions of NGF should be determined by the length of the remainder of the terminus rather than its particular sequence. Indeed, available experimental data confirm

20   this point. Deletion mutant mNGFΔ2-8 which has exactly the same number of residues in the amino terminus as the highly active mNGFΔ3-9 mutant is also very active (Drinkwater et al., 1993). Some decrease in biological activity of mNGFΔ2-8 is likely to be caused by unfavorable directing of the Met^9 hydrophobic side chain away from the complex whereas in the mNGFΔ3-9 deletion mutant this side chain is replaced by the hydrophilic hydroxyl group

25   (Figure 4). Deletion mutants mNGFΔ3-8 (Drinkwater et al., 1993) and hNGFΔ1-5 (Shih et al., 1994), which contain a greater number of amino terminus residues, are remarkably less active than wild type NGF because the remainder of the loop is too long to occupy the "hollow" but too short to separate from the rigid region. The present explanations for the observed structure-activity relationships enable the prediction that, for example, a S2G

30   mutation in the mNGFΔ3-9 deletion mutant would retain high biological activity.

Although the bioactive conformation of the NGF binding determinant has been disclosed above, the question of which NGF residues are involved in NGF/TrkA recognition was not yet addressed. One would reason, most probably, those residues which are primarily responsible for maintaining the particular structure of the NGF termini do not directly interact

35   with the receptor. Thus, side chains of His^4, Pro^5, His^8, Met^9, Arg^9, Glu^{11} and Arg^{118} are not expected to play a crucial role in molecular recognition. On the other hand, charged residues

Arg[114'] and Lys[115'] which are conserved in NGF molecules across all species (McDonald *et al.*,
1991) but not involved in principal intramolecular electrostatic interactions are candidates for
the centres of intramolecular electrostatic recognition. Although both Arg[114'] and Lys[115']
participate in stabilizing intramolecular H-bonding within the bioactive conformations of the

5   NGF termini, their electrostatic properties as charged residues are not utilized for this
purpose.

The other structural element of the termini with potential for stereochemical fit to the
TrkA receptor is a short exposed β-sheet motif located between the α-carbons of residues 7
and 9 (Figures 2,3). On the one hand, H-bonding between β-pleated sheets is rather

10   common for protein-protein interactions (Kobe and Deisenhofer, 1993, 1994, 1995; Yoder *et
al.*, 1993; Baumann *et al.*, 1993). On the other hand, a short exposed β-sheet motif is
generally inherent in the structure of a leucine-rich repeat (Kobe and Deisenhofer, 1993,
1994, 1995) which has been recently identified as the TrkA recognition site for NGF
(Windisch *et al.*, 1995a, 1995b). Other regions of NGF might also be involved in the

15   NGF/TrkA recognition (Shih *et al.*, 1994; Ibáñez *et al.*, 1993). This will be discussed in depth
below.

CONCLUSIONS

The Variable Basis Monte Carlo simulated annealing technique disclosed herein
enables analysis of the low-energy conformational space of peptide molecules. Although

20   multiple VBMC calculations do not consistently converge to the global energy minimum
structure, they do permit the biologically active conformation to be evaluated. Definite
physical factors maintain and distinguish the bioactive conformation of a molecule, and these
factors can be understood by analyzing the low-energy conformational space. The precisely
defined global energy minimum structure is unnecessary, especially considering that any

25   empirical force field functions are not ideal. In biologically relevant molecular modelling,
exploring the bioactive conformation is more important than determining the global energy
minimum. VBMC is a useful tool for facilitating this exploration.

The present VBMC simulations predict that the amino (1-11) and carboxyl (112'-118')
termini of dimeric (1-118)NGF form a complex comprised of a rigid region and a

30   conformationally variable loop. The rigid region is formed by residues 9-11 and 112'-118'
while the variable loop is formed by residues 1-8. The major stabilizing factor of the rigid
region is the ionic contact of the Glu[11] and Arg[118'] side chains. The separation of the loop
from the rigid region arises from the electrostatic repulsion between His[4] and boundary
residues of the rigid region His[8], Arg[9] (in hNGF) and Arg[118']. The geometry of the complex

35   explains observed structure-activity relationships. Accordingly, it is the conformation of the
rigid region which is recognized by the TrkA receptor, defining the biologically active

conformation of NGF for TrkA activation.

The split of the complex of the NGF termini into two distinct moieties could have important biological implications. Although only the structure of the rigid region is recognized by the TrkA receptor, the flexible loop is able to control conformational stability of the

5   biologically active conformation of the rigid region and, consequently, NGF-induced TrkA phosphorylation.

PART B

THEORETICAL MODELLING OF Trk-RECEPTOR RECOGNITION SITES FOR NGF AND

10   BDNF

INTRODUCTION

As mentioned above, the location of the neurotrophin binding sites within the Trk receptors is the subject of debate (MacDonald and Meakin, 1996). Based upon published data, there is reason to believe that Trk proteins have two putative neurotrophin binding sites:

15   the "second immunoglobulin-like domain" (IgC2, residues Trp^{299}-Asn^{365}) and the "second leucine-rich motif" (LRM-2A and LRM-2B, residues Thr^{97}-Leu^{120} of TrkA and TrkB, respectively) (Schneider and Schweiger, 1991; Kullander and Ebendal, 1994; Pérez et al., 1995; Urfer et al., 1995; Windisch et al., 1995a, 1995b, 1995c; MacDonald and Meakin, 1996; Rydén and Ibáñez, 1996). LRM containing proteins are a diverse group with different

20   functions and cellular locations, and are known to mediate strong and selective protein-protein interactions (Kobe and Deisenhofer, 1993, 1994, 1995). The amino acid sequence of an LRM is characterized by conserved hydrophobic consensus residues (Schneider et al., 1988; Schneider and Schweiger, 1991; Kobe and Deisenhofer, 1993, 1994, 1995). Typically, LRMs exist as repetitive cassettes, with an individual LRM representing a

25   right-handed β-α hairpin unit (Kobe and Deisenhofer, 1993, 1994, 1995). Recent crystallographic studies on porcine ribonuclease inhibitor indicate that the side chains of the consensus residues form the hydrophobic core of the LRM modules, thereby determining their geometric features (Kobe and Deisenhofer, 1993).

According to the invention, the inventors report explicit atom-level models of the

30   receptor sites for NGF and BDNF based on the structures of the second LRMs of TrkA (LRM-2A) and of TrkB (LRM-2B), respectively. To deduce these models, we have investigated the interaction of the bioactive conformation of the NGF amino and carboxyl termini region with the LRM-2A and of the "waist" region of BDNF with the LRM-2B. A series of four active NGF analogues, namely human NGF (hNGF) (Burton et al., 1992; Shih et al., 1994), mouse NGF

35   (mNGF) (Burton et al., 1992; Drinkwater et al., 1993), the 3-9 deletion of mNGF (mNGFΔ3-9) (Drinkwater et al., 1993) and the hNGF:NT-4/5 heterodimer (Treanor et al., 1995), have been

docked to the LRM-2A of rat TrkA. For all four NGF molecules studied, a stereochemical fit of the LRM-2A to the amino and carboxyl region was achieved. These results indicate that the bioactive conformation of the NGF termini is a functional epitope which mediates high affinity binding via an interaction with the LRM-2A. This approach has also been applied to

5   BDNF/LRM-2B docking, and their stereochemical fit, based mainly on electrostatic complementarity, has been identified and is described below.

METHODS

A sequence of three logical steps has been used to deduce the models of the interactions of NGF and BDNF with their respective Trk receptor binding sites: *Step 1:* The

10   bioactive conformations of the amino and carboxyl termini of NGF analogues were determined. *Step 2:* The residues of the Trk proteins which form potential binding sites for NGF and BDNF were identified. *Step 3:* The interaction of the bioactive conformation of the NGF amino and carboxyl termini with the TrkA binding site and the BDNF β-strand stem region with the TrkB binding site were modeled computationally. Finally, the predicted

15   features of the NGF/TrkA and BDNF/TrkB interaction models were validated against available experimental data. Residues of the first monomer of a neurotrophin are designated 1 to 118, those of the second monomer are designated 1' to 118'. Residues of the TrkA LRM-2A and the TrkB LRM-2B binding sites are designated by abbreviations tA and tB, respectively. Residues of the BDNF monomer are designated 1 to 119.

20   *Step 1:* REVEALING THE BIOACTIVE CONFORMATION OF THE NGF TERMINI

The most energetically favored conformations of the amino and carboxyl termini of NGF analogues have been obtained by VBMC computations and are described above. Since the 3-dimensional structures of the termini of fully active NGF molecules were found to be different from those of TrkA-inactive analogues, the former conformations were predicted to

25   be "bioactive" for TrkA-mediated activity of NGF. That is, those geometric features that are exclusively inherent to active NGF molecules are expected to be compatible with the structure of the TrkA binding site for NGF. Since the geometry of the central β-strand stem of BDNF is rigid and has been established by X-ray crystallography (Radziejewski and Robinson, 1993), this logical step is bypassed for BDNF. Instead, it is assumed that the X-ray crystallography

30   deduced conformation of the amino acid backbone of the TrkB binding determinant of BDNF represents its "bioactive" conformation.

Step 2: SELECTION OF THE LRM-2 BOUNDARIES WITHIN THE TRK RECEPTORS

Since there is controversy in the literature regarding the actual boundaries of LRMs (Schneider *et al.*, 1988; Schneider and Schweiger, 1991; Kobe and Deisenhofer, 1993, 1994,

35   1995; Windisch *et al.*, 1995a, 1995b), the following experimental background (Figure 8) was used to define boundaries for this computational study. According to Schneider and

colleagues (1988, 1991), the LRM domains of TrkA begin with Leu[68tA], Leu[93tA] and Leu[117tA], whereas those boundaries are slightly shifted in the crystallographic studies of Kobe and Deisenhofer (1993). Furthermore, the boundaries of the "minimal" LRM module of TrkA (designated B4 in Figure 8), which demonstrates the same NGF binding affinity as wild type

5   TrkA, are substantially shifted towards the carboxyl terminus (Windisch et al., 1995a, 1995b) with respect to those suggested by Schneider and colleagues (1988, 1991). The same boundary shift has been suggested for the LRM-2B module (Windisch et al., 1995a, 1995b, 1995c). However, a comparison of active (B1 and B4) and inactive (N4) LRM domains indicates that the presence of the "minimal" amino acid sequence (B4) does not ensure NGF

10   binding. Understanding those factors which maintain the essential features of the LRM geometry in segments B1 and B4, and those factors which destroy them in N4, is of fundamental relevance to the correct assignment of the LRM boundaries.

β-Strand motifs exist in proteins only if hydrogen bonded (H-bonded) to other β-strands; otherwise their structure is unstable (Kobe and Deisenhofer, 1994). Tandem

15   repeats of LRMs represent a prominent example of H-bonded parallel β-strand motifs. The general location of the β-strand motifs in the LRM, according to X-ray data, is illustrated in Figure 8; however, in a single LRM their particular geometry is destroyed (Kobe and Deisenhofer, 1993, 1994, 1995). Consequently, the only possibe way to exclude dramatic conformational changes in a protein domain upon disruption of the inter-strand H-bonding

20   between β-strand motifs is to avoid those motifs. Accordingly, both boundaries of segment B4 are located in the middle of the β-strand regions of the adjacent LRMs such that this segment appears to be free of any β-strand. Nevertheless, the β-strand motif is a characteristic structural unit of LRMs, and thus it is likely that this unit is involved in the NGF/TrkA recognition process. Additionally, a short exposed β-strand motif has been

25   detected in the bioactive conformation of the NGF termini, as described above. The incorporation of the β-strand regions at both sides of the B4 segment (as in N4) results in cooperative H-bonding between these β-strands and a complete loss of NGF binding, which indicates that accessibility of the β-strand motif for intermolecular contacts is essential. On the other hand, the separation of the entire LRM segment from the adjacent LRMs within the

30   B1 molecule as a result of conformational kinking is likely to be energetically more favorable, since the entire LRM module has the internal stabilizing factors. Moreover, kinking between adjacent LRMs does not disrupt the structure of their β-strand motifs (since they remain H-bonded with their opposite sides), but makes them accessible for molecular recognition processes.

35   Accordingly, in the modelling of the present invention we used the conventional boundaries of the LRMs of TrkA and TrkB (Schneider et al., 1988; Schneider and Schweiger,

1991), which keep the β-strand motif in the LRM, and we explicitly arranged H-bonding of this unit with the parallel β-strand motif of the NGF amino terminus to preserve it from conformational reorganizations. Thus, the segments between residues Leu^{93tA} and Leu^{117tA} in TrkA, and Leu^{93tB} and Leu^{117tB} in TrkB, were respectively designated the LRM-2A and the LRM-2B.

Step 3: COMPUTATIONAL SIMULATION OF THE NEUROTROPHIN/RECEPTOR INTERACTIONS

Docking interactions NGF/LRM-2A and BDNF/LRM-2B were simulated using a combined VBMC/CHARMM approach. As described above, the VBMC algorithm permits conformational space search; CHARMM (Brooks *et al.*, 1983) is a force field which defines conformational energy. The same approach was also used to study improper docking interactions of the central β-strand stem region of NGF with the LRM-2B, as a negative control.

The VBMC algorithm performs conformational and orientational space searches of a complicated molecular system with the aim of finding the structure which corresponds to the global minimum on the potential energy E_{tot} surface.

$$E_{tot} = E_t + E_w + E_e + E_{hb} + E_{qq} + E_{hy} + E_c \qquad (4)$$

The following potential energy terms have been considered in the framework of the united atom CHARMM force field (Brooks *et al.*, 1983; The force field parameters are extracted from CHARMM version 23.1, Molecular Simulations, Inc., Waltham, MA): torsional distortion E_t, van der Waals interactions E_w, electrostatic interactions E_e, and hydrogen bonding E_{hb}. Since the united atom approach is not appropriate to treat rigorously the quadrupole-quadrupole interactions of benzene rings (which are important for determining their mutual orientations in proteins (Hunter and Sanders, 1990; Hunter *et al.*, 1991), single quadrupoles have been placed at the centers of the benzene rings of phenylalanine, tryptophan and tyrosine, and the energy of the quadrupole-quadrupole interactions, E_{qq}, has been calculated as suggested by Schauer and Bernstein (1985). (The potential energy function of two interacting benzene molecules, comprising E_{qq} and E_w terms, has stationary points corresponding to both known electrostatically favorable "edge-to-face" and "offset stacked" orientations, with the dimerization energy of 1.94 kcal/mol agreeing well with *ab initio* quantum mechanical calculations (Hobza *et al.*, 1994).) In addition, the conformationally dependent free energy of hydration, E_{hy}, has been calculated according to the hydration shell model including both nonspecific and specific hydration terms (Hopfinger, 1973; Hodes *et al.*, 1979). Point atomic charges of Weiner and colleagues (1984) have been used. A dielectric constant equal to the interatomic separation in angstroms has been used to implicitly simulate solvation effects (Weiner *et al.*, 1984).

The E_c term is used only for the NGF/LRM-2A complex and represents the distance constraints which restrain the H-bonding of residues Glu[11] and Arg[118'] within the bioactive conformation of the NGF termini, as described above. In addition, two intermolecular H-bonds, arising from the alignment of complementary parallel β-strand motifs of NGF and LRM-2A, are also constrained and contribute to E_c. In the Monte Carlo conformational space search, E_c is defined as follows:

$$E_c = 10 \times \sum (d_{AB} - 1.8)^2 , \qquad (5)$$

where d_{AB} is the distance in angstroms between atoms A and B which are to be H-bonded. The E_c term is neglected when performing final energy minimization following the VBMC simulated annealing. In addition, this term has not been utilized when studying the mNGFΔ3-9/LRM-2A complex. Since, as described above, the mNGFΔ3-9 deletion mutant does not have a β-strand region, the geometry of its LRM-2A counterpart, namely Leu[93tA]-Ile[98tA], has been kept fixed in the crystallographic conformation (Kobe and Deisenhofer, 1993) during Monte Carlo simulations. The E_c term, being "soft", does not preclude conformational and orientational changes to occur during Monte Carlo simulations. This term increases rigidity of the bioactive conformation of the ligand, which allows us to utilize the knowledge obtained at *Step 1*, instead of explicit considerations of inactive NGF analogues, in *Step 3*. In addition, this term keeps conformations of the β-strands of both ligand and binding site from destruction, and thereby allows us to avoid an explicit consideration of the adjacent first LRM of TrkA. Furthermore, this term maintains the known orientation of the parallel β-strand motifs in the NGF/LRM-2A complex.

The amino acid sequences of the binding determinants of the NGF molecules studied are presented in Figure 9. The conformational space of the NGF analogues consists of torsional angles determining geometry of the amino terminus of one monomer (residues 1-11) and the carboxyl terminus of the other (residues 112'-118'), while keeping the rest of the dimer in the experimental geometry of mNGF (McDonald *et al.*, 1991). The conformational spaces of the LRM domains of TrkA and TrkB consist of torsional angles representing fragments Arg[94tA]-Leu[117tA] and Arg[94tB]-Leu[117tB], respectively. Covalent bond lengths and bond angles have been kept fixed. The geometry of each i-th residue is determined only by flexible torsional angles of the backbone (ϕ_i and ψ_i) and the side chain ($\chi_i 1$, $\chi_i 2$,...). All torsional angles for prolines, except ψ_i have been fixed. Torsional angles describing structural motifs with planar geometries (such as peptide bonds or conjugated regions in side chains) were fixed. Likewise, the configurations of the sp³-carbons were fixed. The conformational space of BDNF consists only of torsional angles determining side-chain geometries of those residues which are located in the vicinity of its central β-strand stem and define a molecular surface (Table 2). In addition to the conformational variables of each complex, the six

30

orientational variables (three Euler angles and three translations along the coordinate axes) were used to describe the ligand-receptor orientations.

In accordance generally with the simulated annealing approach (Kirkpatrick *et al.*, 1983; Vanderbilt and Louie, 1984; Brünger, 1998; Nilges *et al.*, 1988; Wilson *et al.*, 1988;

5   Wilson and Doniach, 1989), the molecular systems were kept at a constant temperature of $800^\circ K$ for 2×10^6 Monte Carlo moves before the initiation of "cooling". The temperature was then decreased at every Monte Carlo move by a small increment such that after 2×10^6 Monte Carlo moves it reached $120^\circ K$. At this time, a local energy refinement was performed to identify the nearest stationary point on the potential energy surface. According to the VBMC

10   algorithm described above, the basis of independent structural parameters was recalculated after every 7×10^4 Monte Carlo moves to direct them along the valleys of the potential energy surface, thereby accelerating conformational and orientational changes.

All calculations were performed on an Indigo-2 Silicon Graphics Workstation and an 8-node IBM Scalable POWER parallel 2 [SP2] high performance computer.

15   **RESULTS AND DISCUSSION**

CONFORMATIONAL FLEXIBILITY WITHIN RECEPTOR ENVIRONMENTS

Five independent VBMC simulations from different initial configurations were performed for each of the six molecular complexes under study. The elimination of the distance constraints E_c in the complexes with the LRM-2A did not result in any noticeable

20   conformational changes within the complexes. Although independent VBMC simulations did not always converge to the same geometry for the same molecule, the final structures differed insignificantly; i.e., the conformations of the peptide backbones remained unchanged with the exception of residues 1-3 of the NGF amino terminus and the terminal residue Leu[117tA] of the LRM-2A. The differences between the VBMC generated structures were

25   located in side-chain conformations of a limited number of residues, specifically Ser[1], Val[117'] (Thr[117'] in mNGF), Thr[97tA] and Ser[101tA]. These residues are not involved in intermolecular or intramolecular interactions, and do not affect the overall structures of the complexes. No considerable differences were identified in the independent VBMC-generated conformations of the BDNF/LRM-2B and the NGF/LRM-2B complexes.

30   A grid search of the internal space of the complexes using the water molecule radius 1.4 Å as a probe (Ponnuswamy and Manavalan, 1976) (as incorporated into the QUANTA program, Version 4.1, Molecular Simulations, Inc., Waltham, MA) showed that there is no internal cavity available for a solvent molecule in the hNGF/LRM-2A complex. This explains the rigidity of the complex and demonstrates the "perfect" stereochemical fit of the hNGF

35   amino-carboxyl termini complex to the LRM-2A. Other complexes have some internal cavities, especially with the LRM-2B binding site.

SPECIFIC BINDING AREAS WITHIN RECEPTOR ENVIRONMENTS

The TrkA Receptor Binding Site

Comparison of the most stable structures of the different complexes with the LRM-2A binding site (Figure 10) shows their striking conformational similarity. In all molecules,

5 ligand-receptor binding is caused by similar hydrophobic, ionic, H-bonding and van der Waals interactions. There are five distinct areas (A-E) within the NGF/LRM-2A fit: areas A and B have hydrophobic interactions, areas C and D have ionic H-bonding, and area E has cooperative H-bonding between parallel β-strand motifs.

Area A represents the hydrophobic region at which residue Phe^{105tA} interacts with

10 Trp$^{76'}$, which in turn forms hydrophobic contacts with Phe^{12} and Leu$^{112'}$. The aromatic rings of Phe^{12}, Trp$^{76'}$ and Phe^{105tA} are approximately perpendicular to each other, which is energetically favorable (Hunter and Sanders, 1990; Hunter $et\ al.$, 1991; Hobza $et\ al.$, 1994). This particular geometry would create a hole within the complex, if it was not filled by hydrophobic residue Leu$^{112'}$.

15 In area B, Phe^{7} of NGF is placed within the hydrophobic core of the LRM-2A created by the consensus residues (Schneider $et\ al.$, 1988; Schneider and Schweiger, 1991; Kobe and Deisenhofer, 1993, 1994, 1995). Similar to the favorable orientation of the aromatic residues in area A, the aromatic rings of Phe^{111tA} and Phe^{113tA} are perpendicular to that of Phe^{7}. On the other hand, residues Phe^{111tA} and Phe^{113tA} are not perpendicular to each other;

20 their orientation instead resembles the favorable "offset stacked" geometry described by Hunter and others (Hunter and Sanders, 1990; Hunter $et\ al.$, 1991; Hobza $et\ al.$, 1994). As in area A, a hole created by the three neighboring favorably oriented aromatic rings is filled by a fourth residue, Thr^{114tA}. Interactions between aromatic rings in proteins is very common and represent an important conformational driving force (Warme and Morgan, 1978; Hunter $et\ al.$,

25 1991). Consequently, the fact that all three phenylalanine residues of the LRM-2A find their counterparts within the NGF binding domain supports the calculated structure of the NGF/LRM-2A complex.

In ionic binding area C, the negatively charged residue Asp^{109tA} exerts a central role. It is surrounded by the three positively charged amino acids His^{112tA}, Arg$^{114'}$ and Lys^{115} in hNGF,

30 mNGF and mNGFΔ3-9, and by His^{112tA}, Arg$^{115'}$ and Arg^{9} in hNGF:NT-4/5. Residue His^{112tA} plays a secondary role: it creates the electrostatic dipole Asp^{109tA}→His^{112tA} in the LRM-2A, which imposes constraints on the spatial positions of the recognized positively charged residues of NGF, thereby reinforcing geometric selectivity in this area. Although the hNGF:NT-4/5 heterodimer has two substitutions in the C-area segment of the NT-4/5 carboxyl

35 terminus, namely R114S and K115R, the geometry of the C area remains qualitatively the same, since residues Arg^{9} and Arg$^{115'}$ of hNGF:NT-4/5 functionally replace the absent Lys$^{115'}$

32

and Arg^{114} amino acids, respectively. Although Arg^9 also exists in the hNGF homodimer, it is not involved in the ionic binding in this molecule, since it is separated from area C due to electrostatic repulsions. Similarly, the charged amino end of mNGFΔ3-9, which functionally replaces Arg^9, is also separated from area C. There is no place for the fourth positively charged residue in area C. Thus, in all molecules studied, the two positively charged amino acids of the ligand saturate the coordination possibilities of the receptor residue Asp^{109tA}.

Area C is partially isolated from its surrounding environment by flanking hydrophobic residues Val^{106tA} and Pro^{115tA}. Similarly, the principal charged residues of NGF, namely His^8, Glu^{11} and Arg^{118}, are located between hydrophobic residues Ile^6 (Val^6 in mNGF), Val^{111} (Leu^{113} in hNGF:NT-4/5) and Val^{99tA} within the complexes. Thus, residues Val^{99tA}, Val^{106tA} and Pro^{115tA} of the LRM-2A participate in "compartmentalization" of the principal ionic interactions of the complexes, thereby shielding them from the conformation destructive influence of solvation. .

The organization of ionic binding area D is similar to that of area C. Positively charged residues Arg^{59} and Arg^{69} are located in the vicinity of negatively charged Asp^{16} within the NGF structure (McDonald et al., 1991; Bradshaw et al., 1994), such that the coordination of the latter is not full. The third positively charged residue, Lys^{100tA}, comes from the LRM-2A to complete the Asp^{16} coordination. In addition to the ionic binding, residue Lys^{100tA} forms an H-bond with the Ser^{13} side chain.

Area E consists of the H-bonded parallel β-strand motifs of the LRM-2A and NGF (Figure 10b, 10c and 10e), each of the β-strands having three peptide bonds. The LRM-2A β-strand motif is located between the α-carbon atoms of Asn^{95tA} and Ile^{98tA}, whereas the NGF β-strand is located between the α-carbons of the sixth and ninth residues. The locations of the β-strand regions in the uncomplexed LRM (Kobe and Deisenhofer, 1993) and NGF (see above) resemble those in the complexes considered. In the complexed LRM-2A, the β-strand motif is shortened by one peptide bond at its amino end to accommodate the His^4 side chain of NGF. On the other hand, the two peptide bond β-strand of the uncomplexed NGF is lengthened by one peptide bond at its amino end in the complexes.

The TrkB Receptor Binding Site

Figure 11a illustrates the central β-strand stem region of BDNF, and Figure 11b presents the VBMC-generated structure of the BDNF/LRM-2B complex. In this complex, ligand-receptor binding is based mainly on intermolecular electrostatic interactions of either ionic or hydrogen bonding origin. There are five distinct binding areas (F-K) within the TrkB receptor environment: four salt bridges (areas F, G, H and I) and one H-bonding area K. In contrast with the NGF/LRM-2A binding pattern, there is no participation of the LRM-2B β-strand motif in cooperative H-bonding with the BDNF binding epitope.

In area F, the primary positively charged residue (Ibáñez et al., 1993) of the BDNF

binding domain, Arg[81], is bound to Asp[100tB], the only negatively charged residue of the LRM-2B. It should be noted that Arg[81] is exclusively inherent in BDNF molecules while being substituted by electrostatically neutral Thr in NGF or by Lys in NT-3 or NT-4/5 molecules (Bradshaw *et al.*, 1994), which indicates the importance of this area in neurotrophin

5   recognition processes (see also Urfer *et al.*, 1994). On the contrary, residue Gln[84], identified by Ibáñez and co-workers (1993) as important, is not directly involved in specific intermolecular interactions within the LRM-2B domain.

In binding area G, the negatively charged residue Glu[55], which is absolutely conserved in all neurotrophins (Bradshaw *et al.*, 1994), exerts a central role. It is surrounded by the

10   three positively charged amino acids, Lys[25], Lys[57] and Lys[109tB]. Two of them, belonging to the neurotrophin, are also highly conserved (Bradshaw *et al.*, 1994). The third one, Lys[109tB], is specific for the TrkB receptor site (Windisch *et al.*, 1995a, 1995b, 1995c). All BDNF residues of the G binding area, namely Lys[25], Lys[57] and Glu[55], have been shown to be essential in NT-3 structure for TrkC receptor activation (Urfer *et al.*, 1994), which is in agreement with

15   observations that the TrkB and TrkC binding domains are located in the same region of these neurotrophins. This particular arrangement of the three positively charged residues around one with a negative charge seems to be very common in neurotrophin-receptor recognition processes, since the NGF/LRM-2A interaction also includes two binding areas of this type (C and D). Existence of the absolutely conserved negatively charged residue Asp[106] in direct

20   proximity to area G increases binding affinity of Lys[109tB], thereby highlighting some importance of this area in the BDNF/TrkB recognition processes. Although detailed mutational experiments did not demonstrate importance of the equivalent residue Asp[105] in NT-3 for TrkC related activities (Urfer *et al.*, 1994), its direct involvement in the Zn^{2+} mediated regulation of neurotrophin bioactivities has been recently proven by multidisciplinary studies (Ross *et al.*,

25   1997), and, therefore, its location within the binding determinants of BDNF and NT-3 is consistent with these observations.

In area H, conserved residue Asp[24] of BDNF forms a salt bridge with specific TrkB residue Lys[113tB]. Although Asp[24] has not been demonstrated to be involved in direct neurotrophin-receptor interactions, either for TrkB or TrkC related activities, it is highly

30   conserved in neurotrophins (Bradshaw *et al.*, 1994) and located in direct proximity to Thr[22] in NT-3, which has been shown to be included in the TrkC receptor binding domain (Urfer *et al.*, 1994). These observations are consistent with the present model of BDNF/TrkB binding, since substitution of the equivalent residue of BDNF, Thr[21], by bulky Gln (Urfer *et al.*, 1994) would sterically hinder proper location of the LRM-2B domain (Figure 11b), whereas mutation

35   D24A, although lacking one specific ligand-receptor interaction, would not significantly alter the BDNF/LRM-2B orientation resulting from multiple-point electrostatic complementarity. In

addition, the absence of negatively charged residue Asp[24] is shown to induce salt bridge interaction of Lys[113tB] with neighboring Glu[18], with only minor conformational alterations of the LRM-2B.

In area I, Glu[18], a specific residue of BDNF (Bradshaw *et al.*, 1994), forms a salt bridge with the LRM-2B amino acid Arg[94tB]. Residue Glu[18] is also involved in intramolecular electrostatic interactions with Lys[57].

Area K is the only region of the distinct BDNF/LRM-2B interactions which is not of ionic nature. The positively charged residue Lys[104tB] forms multiple H-bond contacts with the BDNF loop I backbone carbonyl groups and the neutral Thr[35] side chain. The energy of such H-bonding is much lower than that of salt bridge contact, and, therefore, a substitution of the uncharged amino acid Thr[35] by a negatively charged residue would stabilize the particular structure of the BDNF/LRM-2B complex. In accordance with the present model, the experimental substitution of BDNF residues 34-41 by the corresponding segment of NGF, which includes the substitution of negatively charged residue Glu[35] for Thr[35], resulted in a significant increase in bioactivity of the resulting chimeric molecule relative to wild type BDNF in TrkB mediated survival (Lai *et al.*, 1996).

In addition to these five distinct binding areas of the BDNF/LRM-2B complex, there is one more area which reinforce binding specificity. The side chain of Pro[60], a specific residue of BDNF (Bradshaw *et al.*, 1994), demonstrates a perfect geometric fit into the hollow in the "zigzag"-shaped β-strand region of the LRM-2B (Figure 11b). This geometric complementarity indicates that Pro[60] "recognizes" the β-strand motif of the receptor binding site. This interaction, obviously, does not significantly contribute to the total energy of the complex in the case of a perfect fit, but does represent a steric hindrance when this fit cannot be readily achieved. Accordingly, BDNF is very selective and does not bind non-cognate Trk receptors.

Figure 11c illustrates the VBMC-generated geometry of the "improper" NGF/LRM-2B complex. In this complex, specific binding areas F and I are absent due to lack of properly charged residues at positions 20 and 81, which would correspond to BDNF residues Glu[18] and Arg[81], respectively. In addition, residue Pro[60], determining the proper BDNF/LRM-2B orientation, is substituted in NGF molecules (Bradshaw *et al.*, 1994). These substitutions cause dramatic conformational and orientational alterations in the complexed LRM-2B domain (compare Figure 11b and 11c). Predicted Cartesian 3-dimensional coordinates of atoms of the TrkB LRM-2B binding site in the complex with BDNF are presented in Appendix 2.

LIGAND-RECEPTOR INTERACTION ENERGY

NGF/TrkA Interactions

Table 3 presents the components of the intermolecular energies of the NGF/TrkA

complexes. Stability of the NGF/LRM-2A complexes results primarily from attractive electrostatic and van der Waals interactions, with intermolecular H-bonding playing a secondary role. It should be noted, however, that in the framework of the molecular mechanical approach, the H-bonding energy is partially incorporated into the electrostatic

5   interaction energy term, so the tabulated E_{hb} values reflect only part of the H-bonding energy. Accordingly, intermolecular H-bonding is more important for the NGF/LRM-2A interaction than it appears in Table 3. On the other hand, the intermolecular component of the E_{qq} term seems to be insignificant. The reason for the latter is that the aromatic moieties of Phe[7], Trp[76], Phe[105tA], Phe[111tA] and Phe[113tA] are "preorganized" for intermolecular contacts with their

10   counterparts in the complexes in electrostatically attractive geometry in which the quadrupole-quadrupole interaction energy term is not significant. In addition, hydrophobic ligand-receptor interaction energy is presumably extremely important for NGF/LRM-2A complex formation, but rigorous quantitative evaluation is currently not possible.

Since neither electrostatic interactions nor hydrogen bonding can significantly stabilize

15   a ligand-receptor complex in a water environment, the stability of the complex generally results from van der Waals and hydrophobic interactions (Clackson and Wells, 1995). Considerable contribution of intermolecular van der Waals interaction energy E_w (Table 3) arises from the geometric complementarity of the NGF binding domain and the TrkA recognition site, such that the high value of the E_w term is due to a large number of

20   intermolecular van der Waals contacts. This complementarity is a consequence of the right-handed twists of both the NGF amino-carboxyl termini complex and the LRM-2A, this geometric feature being characteristic of each of these domains in both uncomplexed (Kobe and Deisenhofer, 1993; Shamovsky et al., 1996) and complexed conformations. Thus, purely geometric ligand-receptor compatibility together with distinct hydrophobic contacts play a

25   crucial role in NGF/TrkA recognition, while attractive electrostatic interactions and H-bonding further reinforce specificity of binding, which is in agreement with generalizations made by Clackson and Wells (1995).

BDNF/TrkB and NGF/TrkB Interactions

Table 4 presents the components of the potential energies of the complexes of BDNF

30   and NGF with the LRM-2B in their minimum-energy conformations. Data presented in section A of Table 4 indicate that the difference in total energies (92.0 kcal/mol) is almost exclusively a consequence of more favorable electrostatic interactions in the BDNF/LRM-2B complex than in the NGF/LRM-2B complex (negative control). Section B of Table 4 illustrates that the BDNF complex is also more favorable in terms of intermolecular electrostatic energy by 77.2

35   kcal/mol (85% of the difference in total electrostatic energies). On the contrary, intermolecular van der Waals interactions are more favorable in the "improper" NGF/LRM-2B complex.

Furthermore, the value of intermolecular van der Waals energy is significantly lower for NGF/LRM-2B than for the NGF/LRM-2A complex, whereas electrostatic contribution is more than twice as high. Consequently, in contrast to the NGF/TrkA binding pattern, molecular recognition of BDNF by the TrkB receptor binding site is almost exclusively based on electrostatic complementarity, whereas the roles of van der Waals and hydrophobic interactions are insignificant. At the same time, such a perfect electrostatic fit could not be achieved without a purely geometric compatibility of the BDNF and the LRM-2B binding domains in size and shape (Figure 11b).

INDUCED CONFORMATIONAL CHANGES

The NGF Amino and Carboxyl Termini

Conformations of the NGF amino and carboxyl termini remain almost the same after complexation with the LRM-2A (Table 5; compare Figure 10a with 10b, 10c, 10d and 10e). A few local conformational changes occur in the $Arg^{114'}$ and the $Lys^{115'}$ side chains, and in the backbones of residues Ser^2 and Phe^7. As predicted above, conserved charged residues $Arg^{114'}$ and $Lys^{115'}$ do not participate in principal intermolecular interactions within the NGF termini but are expected to form ionic intermolecular contacts with the TrkA binding site. Indeed, these are the intermolecular ionic NGF/LRM-2A interactions in area C, which change considerably the side-chain conformations of $Arg^{114'}$ and $Lys^{115'}$ while keeping their backbone geometry intact. The LRM-2A-induced conformational changes in residue Phe^7 are caused by the intermolecular H-bonding in area E while the geometry of Ser^2 is slightly changed to accommodate the LRM-2A residue Thr^{114tA}. The rest of the structure of the LRM-2A-complexed NGF termini retains the energy minimum conformation of the uncomplexed molecules because it is controlled by multiple intramolecular H-bonds. Consequently, the geometry of the NGF termini is "preorganized" for complexation with the LRM-2A, and only local conformational changes, primarily in residues $Arg^{114'}$ and $Lys^{115'}$, occur upon complexation. Geometric "preorganization" of the NGF termini as a ligand for binding to a leucine-rich motif is consistent with X-ray studies of Kobe and Deisenhofer (1995), who have demonstrated that ribonuclease A maintains a fixed geometry upon binding to the LRMs of ribonuclease inhibitor.

The LRM-2A Domain

Figure 12 illustrates the isolated structure of the LRM-2A from the hNGF/LRM-2A complex. Table 6 presents the equilibrium torsional angles of the hNGF-bound LRM-2A. As seen, the side chains of the general consensus residues, Leu^{93tA}, Leu^{96tA}, Ile^{98tA}, Leu^{103tA} and Phe^{111tA} (Schneider et al., 1988; Schneider and Schweiger, 1991), form the hydrophobic core, similarly to their conformations in intact leucine-rich repeats (Kobe and Deisenhofer, 1993). Terminal consensus residue Leu^{117tA} is solvent-exposed due to a boundary effect. Amino

acids Ala^{107tA}, Pro^{108tA}, Ala^{110tA} and Phe^{113tA} are also incorporated into the LRM-2A hydrophobic core. On the other hand, residues Val^{99tA}, Phe^{105tA}, Val^{106tA} and Pro^{115tA} are not involved in hydrophobic interaction within the core, and apparently have specific roles in the recognition site of TrkA. The most hydrophilic residues of the LRM-2A, namely Arg^{94tA}, Lys^{100tA}, Arg^{104tA},

5   Asp^{109tA}, His^{112tA} and Arg^{116tA} are exposed from the hydrophobic core in the complexes. Amino acids Lys^{100tA}, Asp^{109tA} and His^{112tA} participate in specific intermolecular interactions, while the other three are solvent-exposed. The reasonable locations of the hydrophobic and hydrophilic residues of the LRM-2A within the NGF/LRM-2A complexes with respect to water environment supports the calculated structures.

10   NGF/LRM-2A binding spans almost the whole LRM-2A domain, i.e., an interval between residues Leu^{93tA} and Pro^{115tA} comprising three distinct regions: β-strand, α-helix, and loop connecting the carboxyl terminus of the β-strand and the amino terminus of the α-helix. This is in agreement with recent crystallographic studies on the ribonuclease A - porcine ribonuclease inhibitor complex (Kobe and Deisenhofer, 1995), in which these particular

15   regions of leucine-rich repeats of ribonuclease inhibitor are also involved in the molecular recognition process. While the β-strand structure exists in the complexed LRM-2A, the α-helix motif is destroyed by intermolecular interactions with NGF. Accordingly, the LRM-2A β-strand determines the proper orientation of the ligand with respect to the recognition site of TrkA, but does not undergo noticeable conformational changes. Consequently, the

20   cooperative ligand-receptor H-bonding in area E cannot directly mediate those changes in receptor conformation which trigger receptor phosphorylation processes. Available experimental data confirm this point. First, the mNGFΔ3-9 deletion mutant, which does not have the β-strand motif and, consequently, cannot specifically bind area E, is as active as wild type mNGF (Drinkwater et al., 1993). Second, the 24-residue LRM fragment

25   Thr^{97tA}-Leu^{120tA} lacking the β-strand region (Kobe and Deisenhofer, 1993), demonstrates the same kinetics of binding to NGF as wild type TrkA (Windisch et al., 1995a, 1995b).

The LRM-2B Domain

              Table 7 presents the equilibrium torsional angles of the LRM-2B in the complex with BDNF. Side chains of all general consensus residues of the LRM-2B, except for Phe^{111tB} and

30   terminal amino acid Leu^{117tB}, form the hydrophobic core and thereby stabilize the characteristic hairpin shape of the LRM (Figure 11b). In contrast with the LRM-2A, aromatic residues of the LRM-2B, namely Phe^{105tB}, Tyr^{108tB} and Phe^{111tB}, do not seem to have any specific roles in BDNF/LRM-2B molecular recognition. They form a cluster in which their aromatic rings interact with each other and are about mutually perpendicular (Figure 11b). On

35   the contrary, all charged residues of the LRM-2B, namely Arg^{94tB}, Asp^{100tB}, Lys^{104tB}, Lys^{109tB} and Lys^{113tB}, are involved in specific electrostatic interactions with BDNF.

Similar to the NGF/LRM-2A complex, almost the whole LRM-2B domain, from Leu^{93tB} to Lys^{113tB}, fits to the BDNF binding determinant (Figure 11b). On the other hand, there are significant differences of the neurotrophin-induced conformational alterations in the two LRM domains. First, since the BDNF binding domain does not have a β-strand motif which would fit to the β-strand of the LRM-2B, the characteristic geometric features of the latter are lost. Second, region Tyr^{108tB} to Asn^{116tB} retains its α-helical structure in the BDNF-bound LRM-2B domain. The reason of this conformational stability is that the spacer between the two BDNF-bound residues, Lys^{109tB} and Lys^{113tB} (3 residues), is consistent with the period of an α-helix (3.5 residues).

PRINCIPAL AMINO ACIDS INVOLVED IN MOLECULAR RECOGNITION

Principal NGF Residues

The amino acids of NGF which are primarily responsible for maintaining bioactive conformations (McDonald et al., 1991; Shamovsky et al., 1996) or which directly participate in NGF/TrkA recognition are specified in Figure 13. Almost all residues of the amino and carboxyl termini of NGF as well as the $His^{75'}$-$Asn^{77'}$ region are involved in specific intra- or intermolecular interactions. Only five amino acids of the 30-residue binding domain of NGF do not seem to be essential for either maintaining its bioactive conformation or binding to the recognition site of TrkA. These include Ser^1, Ser^2, Ser^3, $Ala^{116'}$ and $Val^{117'}$.

The observation that the important amino acids of the NGF binding domain are conserved across all species while the apparently unimportant five residues are variable (Figure 13) (McDonald et al., 1991) supports the particular structural features of the NGF/LRM-2A complexes calculated herein. There are, however, exceptions which require explanation. In most cases, principal amino acids of NGF molecules derived from different species appear to be substituted by similar residues, e.g. I6V, F7L, L112I, S113T or R114K. In some special cases, the substituted amino acid is quite different but the particular substitution is still consistent with the present model, e.g. R9M, R9L or R118Q (McDonald et al., 1991; Shamovsky et al., 1996); in the case of the H8N substitution (McDonald et al., 1991), histidine and asparagine have the same topology with respect to H-bonding to the Glu^{11} carboxyl oxygen. The structure of snake NGF (sNGF) requires special consideration. Principal hydrophobic residues Phe^7 and Phe^{12} are replaced by histidine residues in sNGF. Although these mutations could be accompanied by structural differences in snake TrkA, they are consistent with the present model. According to the survey of Warme and Morgan (1978), side-chain interactions of histidine with tryptophan or threonine are very common in natural proteins, which implies the existence of specific inter-residue affinities. This being the case, attractive interactions His^7...Thr^{114tA} and His^{12}...$Trp^{76'}$ in areas B and A, respectively, may replace corresponding hydrophobic interactions with Phe^7 and Phe^{12}.

Principal LRM-2A Residues

         The principal residues of the LRM-2A are shown in Figure 14. The general consensus residues (Schneider et al., 1988; Schneider and Schweiger, 1991) maintain the specific geometry of the LRM (Kobe and Deisenhofer, 1993, 1994, 1995). The amino acids which

5   form the distinct binding areas are involved in specific intermolecular interactions with the NGF binding domain. Since NGF does not activate the TrkB receptor, those residues which are specific for the TrkA receptor have been postulated to be directly involved in NGF/LRM-2A recognition (Windisch et al., 1995a, 1995b). As shown, the LRM-2A segment has nine specific residues, seven of them directly participating in NGF/LRM-2A recognition in the

10   framework of the present model. Thus, Lys^{100tA} binds Asp^{16} in area D, Pro^{108tA} is completely buried inside the NGF/LRM-2A complex, residues Asp^{109tA}, His^{112tA} and Pro^{115tA} form binding area C, and residues Phe^{113tA} and Thr^{114tA} are involved in forming area B. The other specific residues, Arg^{104tA} and Arg^{116tA}, do not seem to be required for specific NGF/LRM-2A interactions. It is seen, furthermore, that binding areas A and E are not specific for the

15   recognition site of TrkA, indicating that binding specificity of the LRM-2A is determined by Lys^{100tA}, Asp^{109tA} and Phe^{113tA}. The fact that these particular amino acids are replaced in the recognition site of TrkB by residues of a different chemical nature, namely Asp^{100tA}, Lys^{109tA} and Lys^{113tA}, respectively (Windisch et al., 1995a, 1995b), making NGF/TrkB binding impossible, supports the herein predicted details of NGF/LRM-2A recognition. Principal

20   residue Phe^{105tA}, although common to both the TrkA and TrkB recognition sites (Windisch et al., 1995a, 1995b), is also important for the NGF/TrkA recognition process, since oxidation of its counterpart, Trp^{76}, results in a complete loss of receptor binding (Merrell et al., 1975).

Principal BDNF residues

         Since BDNF/TrkB molecular recognition is predicted to be primarily based on

25   electrostatic complementarity, principal BDNF and LRM-2B residues are identified by analysing their contribution to the intermolecular electrostatic energy. Table 8 presents a comparison of individual contributions of residues of BDNF, NGF and the LRM-2B to the intermolecular electrostatic energy for the BDNF/LRM-2B and the NGF/LRM-2B complexes, with cutoff being ±10 kcal/mol. BDNF/TrkB molecular recognition is achieved by those

30   residues that make significantly more favourable contacts with their counterparts than do corresponding residues in the "improper" NGF/LRM-2B interaction. Accordingly, in section A of Table 8, residues of BDNF that make more favourable contacts with the LRM-2B than do those of NGF by at least 10 kcal/mol, are highlighted. They are: Glu^{18}, Asp^{24}, Glu^{55}, Arg^{81} and Gln^{84}. These residues make up the BDNF binding epitope for TrkB activation. Only two of

35   them, Arg^{81} and Gln^{84}, have been previously identified (Ibáñez et al., 1993). The most unusual case is residue Gln^{84}, which does not markedly participate in electrostatic interactions

with the LRM-2B; however, its substitution by His[84] results in considerable repulsive interactions with positively charged residues of the receptor site. Therefore, Gln[84] cannot be referred to as a principal residue by itself in terms of the TrkB receptor binding, and its apparent importance (Ibáñez *et al.*, 1993) comes from unfavorable substitution by a positively charged His[84]. The only residue of NGF which binds to the TrkB receptor site significantly more strongly than does the corresponding residue of BDNF is Glu[35], in agreement with observations (Lai *et al.*, 1996).

Principal LRM-2B residues

Section B of Table 8 identifies the LRM-2B residues which significantly contribute to specificity of binding. Amino acids Arg[94tB], Asp[100tB], Ser[101tB], Lys[109tB] and Lys[113tB] make significantly more favorable contacts with their counterparts in BDNF than with those in NGF. Additionally, these residues are responsible for specific binding in areas F-K. The only residue of the LRM-2B that favours the NGF counterpart is Lys[104tB], which is caused by the abovementioned effect of Glu[35].

Figure 15 illustrates schematically the geometry of the LRM-2A and the LRM-2B receptor sites. Those residues which are predicted to form specific bonds with their preferred ligand are shown by arrows. The similarity of the binding patterns of the two LRMs is striking, especially bearing in mind the differences pointed out in the nature of the intermolecular interactions, and that the binding patterns were identified in independent computations. Thus, binding specificity of TrkA and TrkB is determined by the residues located in distinct positions of their second LRMs, with their respective binding patterns being incompatible with each other.

It is shown that van der Waals and hydrophobic interactions play a more important role in TrkA than in TrkB recognition. As a part of this phenomenon, we have demonstrated that NGF/LRM-2A binding is characterized by greater geometric complementarity, such that the ligand-receptor complex does not contain marked internal cavities. A plausible explanation for these particular features of Trk receptor recognition is that the NGF binding determinant is flexible and, because of that, more is required to stabilize its bioactive conformation in solution. Accordingly, TrkA receptor binding involves physical factors that are more effective in an aqueous environment, namely van der Waals and hydrophobic interactions.

EXPLANATION FOR STRUCTURE-ACTIVITY RELATIONSHIPS

TrkA mediated activity has been evaluated for 27 point and deletion mutants of the TrkA binding domain of NGF: hNGF (Burton *et al.*, 1992; Shih *et al.*, 1994), mNGF (Burton *et al.*, 1992; Drinkwater *et al.*, 1993), mNGFΔ3-9 (Drinkwater *et al.*, 1993), (1-120)hNGF (Schmelzer *et al.*, 1992), (1-120)mNGF (Luo and Neet, 1992), (1-117)hNGF (Schmelzer *et al.*,

1992) and hNGF:NT-4/5 (Treanor *et al.*, 1995) retain full activity; mNGFΔ2-8, mNGFΔ61-66
(Drinkwater *et al.*, 1993), hNGF-R9A, hNGFΔ1-5 and hNGF-P5A (Shih *et al.*, 1994)
demonstrate intermediate potency; hNGFΔ1-9 (Burton *et al.*, 1992; Kahle *et al.*, 1992; Luo
and Neet, 1992; Drinkwater *et al.*, 1993; Shih *et al.*, 1994; Burton *et al.*, 1995), mNGFΔ1-8

5   (Taylor *et al.*, 1991; Burton *et al.*, 1992), mNGFΔ1-9, mNGFΔ9-13 (Woo *et al.*, 1995),
mNGFΔ3-8, mNGFΔ3-11, mNGFΔ3-12, mNGFΔ3-13, mNGFΔ3-14, mNGFΔ9-14,
mNGFΔ112-118 (Drinkwater *et al.*, 1993), hNGF-H4A, hNGF-H4D (Shih *et al.*, 1994), BDNF
(Suter *et al.*, 1992), and NT-4/5 (Treanor *et al.*, 1995) are almost or completely inactive. The
present model of NGF/LRM-2A recognition enables a comprehensive explanation for the

10   structure-activity relationships.

As demonstrated, fully active hNGF, mNGF and hNGF:NT-4/5 fit to the five binding
areas A-E of the recognition site of TrkA, while the mNGFΔ3-9 deletion mutant fits only to A,
C and D, without any specific binding taking place in areas B or E. Therefore, there are three
common geometric features of the four fully active molecules which distinguish them from the

15   less active analogues. First, conformations of the amino and carboxyl termini of these NGF
analogues are "preorganized" for binding to the principal LRM-2A binding areas A, C and D.
Second, there is no stereochemical incompatibility in the binding areas B and E. Third, there
is no hole inside the NGF/LRM-2A complexes.

The structures of the other three fully active NGF analogues, (1-120)hNGF,

20   (1-120)mNGF and (1-117)hNGF, are consistent with the above criteria. Indeed, since the
NGF carboxyl end is located on the surface of the NGF/LRM-2A complexes (Figure 10) and
does not directly participate in principal intermolecular interactions, the lengthening of the
NGF carboxyl terminus by two amino acids does not explicitly affect NGF/LRM-2A
compatibility. As far as the (1-117)hNGF molecule is concerned, terminal residue Arg[118'] of

25   NGF has been shown to form inter-chain ionic H-bonds with Glu[11] (see above) and, hence,
seems to be important in maintaining the structure of the NGF bioactive conformation. On
the other hand, there is a second factor stabilizing the bioactive conformation of the hNGF
termini, namely inter-chain H-bonding of residue Arg[9]. Because of the latter binding, the
above criteria are still fulfilled for (1-117)hNGF.

30   The deletion of principal residue Phe[12], which participates in hydrophobic interactions
in area A, results in a substantial loss of TrkA mediated activity of the mNGFΔ3-12,
mNGFΔ3-13, mNGFΔ3-14 and mNGFΔ9-14 deletion mutants (Drinkwater *et al.*, 1993).
Likewise, the absence of principal residues Arg[114'] and Lys[115'], essential for the ionic binding in
area C, results in dramatic loss of bioactivity of mNGFΔ112-118 (Drinkwater *et al.*, 1993).

35   Similarly, geometric perturbations of the essential residues Arg[59] and Arg[69] in the
mNGFΔ61-66 deletion mutant result in incomplete NGF/LRM-2A compatibility in area D and,

accordingly, a considerable loss of activity.

The specific location of the NGF ninth amino acid side chain in the "hollow" existing on the surface of the NGF rigid region has been predicted herein to be critical for high TrkA mediated activity. The present invention provides a detailed explanation for this prediction.

5   That is, the "hollow" is buried inside the NGF/LRM-2A complex, and a moiety located in this "hollow" fills the cavity which otherwise would exist inside the complex and destroy NGF/LRM-2A compatibility. Since this moiety is located in the internal cavity of the complex (Figure 10), severe limitations are imposed on its size. A short side chain does not fill this cavity; therefore, the hNGF-R9A mutant demonstrates noticeably diminished activity (Shih *et al.*,

10   1994). The cavity preferably is filled either by a bulky amino acid side chain, such as arginine (e.g. hNGF), methionine (e.g. mNGF) or leucine (sNGF), or by the two residue peptide backbone (mNGFΔ3-9 or mNGFΔ2-8). A longer amino terminus tail (e.g. in mNGFΔ3-8, mNGFΔ9-13 or mNGFΔ1-5) cannot be accommodated in the internal cavity of the NGF/LRM-2A complex and, hence, interferes with binding areas B and E.

15   Most deletion or point mutations of the NGF amino terminus destroy the exposed β-strand motif Phe^7-Arg^9 and change the proper orientation of the Phe^7 side chain, thereby affecting NGF/LRM-2A compatibility in areas B and E. Thus, incorporation of a negatively charged residue into the relatively long NGF amino terminus, as in hNGF-H4D, BDNF, NT-3 and NT-4/5, or substitution H8R, which is characteristic for BDNF and NT-4/5, has each been

20   demonstrated to cause dramatic conformational changes in the complex of the neurotrophin amino-carboxyl termini, making it incompatible with the LRM-2A. This stereochemical incompatibility of the geometry of the NGF amino terminus with binding areas B and E of the LRM-2A is the reason for the partial or complete loss of TrkA-related activity of mNGFΔ3-8, mNGFΔ1-5, hNGF-P5A, hNGF-H4A, hNGF-H4D, mNGFΔ1-8, hNGFΔ1-9, mNGFΔ1-9,

25   mNGFΔ9-13, mNGFΔ3-11, BDNF and NT-4/5.

As demonstrated, both NGF monomers are directly involved in specific ligand-receptor interactions, i.e., the first monomer binds areas B, D and E, whereas the second one binds areas A and C. Consequently, the dimeric structure of NGF is necessary to retain high biological activity, which is also consistent with experimental data (Maness *et al.*, 1994). On

30   the contrary, only one BDNF protomer is essential for TrkB binding (Figure 11a, 11b).

In addition, recent reports of experiments have demonstrated the importance of residues Phe^7 (Kullander and Ebendal, 1996), Leu^{112}, Arg^{114} and Lys^{115} (Krüttgen *et al.*, 1996) for TrkA mediated activity of NGF. This is consistent with their participation in the specific NGF/LRM-2A binding in the framework of the present model.

35   **CONCLUSIONS**

The complexes of the amino and carboxyl termini of the four fully active NGF

analogues with the second leucine-rich motif of TrkA were obtained using Variable Basis
Monte Carlo simulated annealing calculations. The same methodology was utilized to define
the structure of the complex of the second leucine-rich motif of TrkB with the BDNF receptor
binding determinant. The structural features of the resulting NGF/TrkA and BDNF/TrkB

5   binding predictions are supported by the following: (i) geometric and electrostatic
complementarity of the binding domains of NGF and BDNF to binding sites of TrkA and TrkB,
respectively, without considerable conformational changes of the ligands; (ii) appropriate
environments for hydrophobic and hydrophilic residues within the complexes; (iii) analysis of
structural variability of both binding domains; and (iv) comprehensive explanation of currently

10   published structure-activity relationships. Within these complexes, NGF/TrkA molecular
recognition is based upon multiple-point intermolecular interactions of hydrophobic, van der
Waals, ionic and hydrogen bonding type. Extensive intermolecular van der Waals contacts
arise from complementarity of the NGF binding domain and the TrkA recognition site in size
and shape. In addition, there are five specific binding areas within the receptor model:

15   hydrophobic A and B, ionic C and D and cooperative hydrogen bonding E. The NGF/TrkA
stereochemical compatibility in areas A, C and D is required for TrkA receptor activation,
whereas areas B and E reinforce binding specificity, making the NGF molecule a very
sophisticated key triggering the chain of biological events following receptor phosphorylation.
The 3-dimensional structures of the binding domains of the fully active NGF analogues are

20   "preorganized" for stereochemical fit to the second leucine-rich motif of TrkA. Five distinct
binding areas F-K were also identified in the BDNF/TrkB complex, although, in contrast with
NGF/TrkA binding, BDNF/TrkB recognition is based primarily on ionic and hydrogen bonding
interactions. In spite of significant differences in the nature of ligand-receptor interactions
involved in TrkA and TrkB recognition processes, binding patterns of their receptor binding

25   sites for NGF and BDNF are almost identical. The predicted mechanism of high affinity
NGF/TrkA and BDNF/TrkB binding is consistent with the conformational model of TrkA-p75^{NTR}
interactions (Chao and Hempstead, 1995).

PART C

30   ## THEORETICAL MODELLING OF THE P75^{NTR} RECEPTOR RECOGNITION SITE FOR
NEUROTROPHINS

INTRODUCTION

As summarized above, the neurotrophins represent a family of structurally and
35   functionally related proteins which play a crucial role in the development, survival and
maintenance of the sympathetic and sensory neurons (Purves, 1988; Snider and Johnson,

1989; Barde, 1989; Thoenen, 1991; Korsching, 1993; Persson and Ibáñez, 1993; Davies, 1994; Ibáñez, 1995). The neurotrophin family consists of nerve growth factor (NGF), brain-derived neurotrophic factor (BDNF), neurotrophin-3 (NT-3), neurotrophin-4/5 (NT-4/5), and more recently discovered neurotrophin-6 (NT-6) (Berkmeier et al., 1991; Barde, 1991;

5   Barbacid, 1993; Bradshaw et al., 1994; Chao, 1994; Gotz et al., 1994). Each neurotrophin is capable of binding independently with the common neurotrophin receptor p75^{NTR}, as opposed to specific Trk receptor interactions.

METHODS

The geometric features of complexes of monomeric neurotrophins with the p75^{NTR}

10   receptor binding site have been obtained by multiple molecular dynamics runs of 200-300 ps at constant temperatures between 300 and 400°K, followed by local energy refinements. The QUANTA V4.1 molecular modelling program (Molecular Simulations Inc., Waltham, MA) with the united atom CHARMM potential energy terms (Brooks et al., 1983) has been used. Residues of p75^{NTR} are designated by abbreviation p.

15   According to the invention, we superimposed the binding domains of NGF, BDNF, NT-3 and NT-4/5 with a putative binding site of p75^{NTR} and carried out multiple molecular dynamics computations of the ligand-receptor complexes. These calculations revealed the 3-dimensional structures of the binding domains of the neurotrophins and p75^{NTR}, demonstrated their geometric and electrostatic complementarity, and identified principal residues involved in

20   receptor recognition. All neurotrophins are believed to induce similar conformational changes in the p75^{NTR} binding site, generally located in the orientation of the sequential loops within the cysteine-rich repeats.

Initial geometries of individual components of the complexes were based upon the X-ray crystallographic coordinates of neurotrophins NGF (McDonald et al., 1991), BDNF and

25   NT-3 (Robinson et al., 1995) and the p55^{TNFR} receptor extracellular domain (Banner et al., 1993) which is homologous to p75^{NTR}. Geometry of the NT-4/5 monomer was constructed from the X-ray derived structure of NT-3 (Robinson et al., 1995). Since NGF and other neurotrophins fold in similar rigid conformations, their molecular motions were restricted by imposing the following atom constraints. First, peptide backbones of the neurotrophins were

30   fixed at their crystallographic coordinates. Further, conformations of the amino acid side chains of the neurotrophins were also fixed except for those located within and in the vicinity of the variable loop regions I and V (the p75^{NTR} binding determinant). Thus, amino acid side-chain motions were allowed for residues 23-35 and 93-98 (NGF numbering) as well as for eight additional neighboring residues, namely His^{84} (Gln in other neurotrophins), Phe^{86} (Tyr in

35   other neurotrophins), Lys^{88} (Arg in other neurotrophins), Trp^{99}, Arg^{100}, Phe^{101} (Trp in NT-3 and NT-4/5), Arg^{103}, and Asp^{105}. The flexible amino and carboxyl termini of the neurotrophins were

excluded to avoid artefactual spacial hindrances for the receptor binding.

Fig. 16a represents a fragment of the crystallographically resolved structure of the p55[TNFR] extracellular domain (Banner et al., 1993), corresponding to the second CRD (loops 2A and 2B) and the first loop of the third CRD (loop 3A). Fig. 17 illustrates the sequence of

5   this fragment and its alignment with the three known p75[NTR] peptides (Johnson et al., 1986; Radeke et al., 1987; Large et al., 1989). Fig. 16b presents the minimum energy conformation of the corresponding fragment of human p75[NTR]. As is apparent, its size and shape are complementary to the exposed p75[NTR] binding determinant of NGF (Fig. 16c). Accordingly, this 58-amino acid fragment of p75[NTR], including the second and the beginning of the third

10   CRDs (Fig. 17), has been considered as a putative binding site for neurotrophins. The artefactual charges on the terminal amino and carboxyl groups of the peptide representing the p75[NTR] binding site were neglected.

Once the most stable equilibrium 3-dimensional structures of the complexes being studied were obtained, the residues contributing the most to the energy of intermolecular

15   interactions were identified. Point atomic charges of Weiner et al. (1984) and a dielectric constant equal to the interatomic separation in angstroms (to implicitly simulate solvation effects) (Weiner et al., 1984) were utilized to calculate the electrostatic intermolecular terms. The van der Waals intermolecular terms were evaluated by the united atom CHARMM force field (Brooks et al., 1983). The calculations were performed on a 200 MHz Indigo-2

20   SiliconGraphics Workstation.

RESULTS AND DISCUSSION

The most stable structures of the complexes of the neurotrophins with the putative p75[NTR] receptor binding site obtained by the molecular dynamics computations described herein are illustrated in Fig. 18. Table 9 presents net values of the electrostatic and van der

25   Waals terms of the ligand-receptor interaction energy. Tables 9 and 10 list individual residues of the neurotrophins and the p75[NTR] receptor which significantly contribute to the intermolecular electrostatic interaction energy. The highlighted residues represent the functional epitopes of the ligands (Table 9) and the receptor (Table 10), whereas the other listed residues, although being located within the binding interfaces, apparently do not

30   participate in major ligand-receptor electrostatic interactions in the particular complex. Predicted Cartesian 3-dimensional coordinates of atoms of the p75[NTR] binding sites in the complexes with NGF and BDNF are presented in Appendix 3.

Significant contributions of electrostatic interactions to the ligand-receptor interaction energy (Table 9) result from opposite net charges of the binding domains of neurotrophins

35   (positively charged) and the common neurotrophin receptor (negatively charged), which effect is consistent with published predictions (Rydén et al., 1995). Data presented in Tables 9 and

10 demonstrate that, on the average, the interaction between the functional epitopes is responsible for 94% of intermolecular electrostatic energy, but only 43% of van der Waals interaction energy. Consequently, residues participating in strong and specific ligand-receptor interactions represent only a part of a bigger binding interface in which significant van der

5   Waals contribution is accumulated from a large number of weak contacts, which is possible only as a consequence of geometric complementarity of the binding domains. Fig. 19 presents the structure of the $BDNF/p75^{NTR}$ complex as atomic van der Waals spheres and demonstrates the geometric fit of the binding domains. The van der Waals energy and, therefore, geometric complementarity of the binding interfaces in the $NGF/p75^{NTR}$ complex is

10   significantly lower than in the other $neurotrophin/p75^{NTR}$ complexes (Table 9), which is consistent with its fastest rate of dissociation (Ibáñez, 1995). However, the pure geometric factor cannot explain the slowest rate of dissociation observed for the $BDNF/p75^{NTR}$ complex (Ibáñez, 1995). Thus, stability of the complex arises from a combination of geometric and electrostatic complementarities of the binding interfaces, consistent with the generalizations

15   of Clackson and Wells (1995). A specific feature of the $neurotrophin/p75^{NTR}$ binding interfaces is that they do not include substantially hydrophobic residues, so they do not have a hydrophobic core, which has been found in many other protein-protein complexes (Clackson and Wells, 1995; Livnah et al., 1996). The predominant interactions within the binding domains of the complexes under study are of the salt-bridge type.

20   Specificity of binding of the neurotrophins to the $p75^{NTR}$ receptor is determined by charged residues within the binding domains (Rydén et al., 1995). As seen in Fig. 18, they create 3-dimensional networks in which most of them are in contact with more than one residue of the opposite charge. Therefore, any missing charge would destroy more than just one bond, but a significant portion of, if not the whole, network. That is, the electrostatic

25   complementarity of the binding interfaces would be altered, which is consistent with the experimentally observed sensitivity of binding to mutations of charged residues (Ibáñez et al., 1992; Rydén et al., 1995; Rydén and Ibáñez, 1996). Both ligand and receptor provide the network with positive and negative charges (Table 9 and 10, Fig. 18), even though negative charges dominate in the receptor, and positive in the ligands. This particular spatial

30   arrangement of the charges increases specificity of binding and prevents electrostatic repulsions within the same binding domains. For example, in all the complexes, positively charged residue Lys^{56p} of the receptor forms salt-bridges with negatively charged residues Asp^{75p} and Asp^{76p} of the receptor, thereby occupying one site of their coordination, such that only the opposite sides of the latter residues remain available for intermolecular ionic

35   interactions (Fig. 18). Negatively charged residue Asp^{93} of BDNF holds together positively charged residues Arg^{97} and Arg^{101} of BDNF, such that they are both able to interact with

juxtaposed amino acids Asp^{75p} and Asp^{76p} of the receptor (Fig. 18b). Similarly, negatively
charged residue Asp^{30} of the neurotrophins forms a salt-bridge interaction with Arg^{100}, which
directly interacts with p75^{NTR}.

5   In spite of the differences in the binding interfaces of the respective complexes,
binding patterns of the p75^{NTR} receptor are similar. All three loops of the receptor binding site
(2A, 2B and 3A) are involved in binding (Fig. 18). The principal residues of loop 2A are Asp^{47p}
and Lys^{56p}; those of loop 2B are Asp^{75p} and Asp^{76p}; and those of loop 3A are Asp^{88p} and Glu^{89p}.
As is seen in Table 10, loop 2B forms the strongest contacts. In addition to the principal
binding pattern, the p75^{NTR} binding domain comprises specific residues for ionic interactions
10   with particular neurotrophins (Table 10, Fig. 18). Thus, Arg^{80p} interacts only with Glu^{35} of
NGF; residue Glu^{53p} interacts only with Lys^{96} of BDNF, and Glu^{60p} and Glu^{73p} interact only with
residues of NT-3 and NT-4/5.

Site-directed mutagenesis studies of the p75^{NTR} binding site have suggested that
mutation of any one of the residues Asp^{75p}, Asp^{76p} or Glu^{89p} to Ala does not affect NGF
15   binding, whereas mutation of Ser^{50p}, which does not participate in major ionic interactions,
results in the complete abolishment of binding (Baldwin and Shooter, 1995). The apparent
discrepancy with the present theoretical studies can be explained, since the cited
experimental observations are still controversial. Indeed, although both Asp^{75p} and Asp^{76p} are
involved in ionic interactions in the loop 2B region with positively charged residues of
20   neurotrophins, one of them might be enough to maintain binding to NGF. Likewise, the
functional role of the missing residue Glu^{89p} in loop 3A might be fulfilled by adjacent Asp^{88p}.
Residue Ser^{50p} of p75^{NTR} is predicted to be hydrogen bonded to Gln^{96} of NGF (Fig. 18a), and
its mutation to Asn, Ala or Thr, which abolishes receptor binding (Baldwin and Shooter,
1995), may create steric hindrances in the NGF/p75^{NTR} interface. The present molecular
25   modelling studies suggest that Ser^{50p} is not important for binding of any other neurotrophin
(Fig. 18, b-d).

In contrast to the p75^{NTR} receptor binding pattern, there are only two common
residues of the binding interfaces of neurotrophins which directly interact with the receptor
site, Arg^{100} and Arg^{103}. Contribution of Arg^{103} is significant in all the complexes, while Arg^{100}
30   seems to be less important for the NGF/p75^{NTR} binding.

As is seen in Table 9, most important residues of the NGF binding domain are (in
order of decreasing significance) Lys^{32}, Lys^{34}, Arg^{103}, Lys^{95}, and His^{84}, all of them forming
specific ionic contacts with negatively charged residues of p75^{NTR} (Fig. 18a). Involvement of
Lys^{32}, Lys^{34}, and Lys^{95} in p75^{NTR} binding has been very well established experimentally, with
35   the same order of significance being observed (Ibáñez, 1994). The most important residues
of NGF, Lys^{32} and Lys^{34}, bind to the loop 2B residues of p75^{NTR} (Fig. 18a). Here we

demonstrate that residue Lys[88] is not critical for p75[NTR] binding, whereas residues Arg[103] and His[84] make direct ionic contacts with the receptor binding site. Importance of the latter residue has not been previously reported in the context of p75[NTR] binding. The roles of Asp[30], Glu[35] and Arg[100] seem to be secondary, since their contributions are relatively small.

5   Hydrophobic residue Ile[31] is not directly involved in ligand-receptor interactions.

In BDNF, all three positively charged residues of variable region V, Lys[95], Lys[96] and Arg[97] (Rydén et al., 1995), bind to negatively charged residues of the p75[NTR] binding site, namely Asp[47p], Glu[53p] and Asp[75p], respectively (Fig. 18b). In addition, the residues Arg[88] and Arg[101] play a more important role than in the NGF case (Table 9); they bind to the loop 2B

10   residues Asp[75p] and Asp[76p] of p75[NTR], thereby fulfilling the function of missing positively charged residues of loop I. The increased importance of residue Arg[88] in BDNF and other neurotrophins relative to that of Lys[88] in NGF (Table 9) is permitted by a longer side chain of Arg, which results in a decrease of the separation between opposite charges (Fig. 18). Because of missing residue His[84], only the positively charged residue Arg[104] binds to the loop

15   3A residues Asp[88p] and Glu[89p] of p75[NTR].

In NT-3, the loop 2B residues of the receptor Glu[73p], Asp[75p], and Asp[76p] bind to Arg[31], His[33], Arg[100], and Arg[87]. Residue Asp[47p] of loop 2A of the receptor also binds to Arg[100]. Residue Lys[95] of variable region V does not form any salt-bridge contact with the receptor, consistent with its reported insignificance for NT-3 binding (Rydén et al., 1995). Thus, the

20   present results agree well with the established roles of Arg[31] and His[33] of NT-3 (Rydén et al., 1995; Rydén and Ibáñez, 1996) and predict the increased importance of residue Arg[100] in NT-3 for p75[NTR] binding (Table 9). The binding pattern of NT-4/5 is similar to that of NT-3 (Fig. 18, c,d). The increased electrostatic contribution of Arg[36] with respect to corresponding NT-3 residue His[33] (Table 9) is caused by the longer side chain of the former, which results in

25   formation of a salt-bridge contact with residue Glu[60p] of the receptor (Fig. 18d).

Binding of a neurotrophin induces conformational changes in the p75[NTR] binding site. The conformational space of the three loops (2A, 2B and 3A) is limited by eight disulfide bonds; therefore, the most significant changes occur in the junction areas of those loops. Fig. 20 illustrates the superimposed equilibrium geometries of the free and the BDNF-

30   complexed p75[NTR] binding site. The superimposition is performed by a least-square minimization technique using the α-carbon reference atoms of loops 2A and 3A. As is apparent, the orientation of loop 2B with respect to the two flanking loops is considerably changed upon binding. Because of striking similarities between the binding patterns of the p75[NTR] receptor with the different neurotrophins, a similar conformational change takes place

35   in all four complexes under investigation. The driving force behind this particular conformational transition is ionic interactions of the principal residues of loop 2B, Asp[75p] and

Asp^{76p}, with positively charged residues of the neurotrophins, taking into account that spacial

positions of the flanking loops 2A and 3A are fixed by ionic interactions of residues Asp^{47p},

Lys^{56p}, Asp^{88p}, and Glu^{89p} with corresponding residues of the neurotrophins (Fig. 18). Thus,

structural variability between the neurotrophins does not preclude them from inducing similar

5 conformational change in the common neurotrophin receptor.

The binding pattern of neurotrophins to the p75^{NTR} receptor predicted by the present

molecular modelling studies can be additionally verified by checking conservation of the

identified principal residues. The sequences of the binding site of the p75^{NTR} receptor from

different species (Fig. 17) demonstrate that principal residues forming its common binding

10 pattern, namely Asp^{47p}, Lys^{56p}, Asp^{75p}, Asp^{76p}, Asp^{88p}, and Glu^{89p}, are conserved in p75^{NTR}. The

known variability of regions I and V among neurotrophins (Rydén et al., 1995) implies that

conservation of the principal residues of the p75^{NTR} binding determinants may be checked

only within the same neurotrophin derived from different species. Study of a recent sequence

alignment of neurotrophins (Bradshaw et al., 1994) allowed us to conclude that the functional

15 epitope of the neurotrophins (Table 9) is generally conserved within the same neurotrophin

even though there are some exceptions, often represented by the substitution by a similar

amino acid. Arg^{100} and Arg^{103} are the only two residues of the binding epitopes which are

conserved throughout all neurotrophins (Bradshaw et al., 1994). Other residues within the

functional epitopes maintain specificity of binding of different neurotrophins.

20 The present model also represents a key to understanding the conservation of

residues which do not directly participate in receptor binding. For example, Gly^{33} is absolutely

conserved in all neurotrophins, yet is not involved in any specific interactions with the receptor

binding site. However, within the present model, its conservation can be understood, since it

is located very close to loop 3A of the receptor and forms van der Waals contacts with it (Fig.

25 18), such that any other residue would impose steric hindrance which would alter or destroy

the ligand-receptor geometric complementarity.

The principal NGF/TrkA binding areas necessary to trigger TrkA phosphorylation and

subsequent biological events have been discovered by the inventors. Specifically, the

inventors have discovered that essentially the full binding site of the second leucine rich motif

30 (LRM) of TrkA, amino acid residues 93 to 117, forms the binding site for NGF, and comprises

five distinct binding areas, A, B, C, D and E. Appendix 1 provides the Cartesian coordinates

of the LRM-2A residues defining the areas A to E in PDB format. Binding areas A and B bind

hydrophobically to ligands, areas C and D form ionic bonds with charged portions on ligands

and area E forms hydrogen bonds with ligands.

35 The stereochemical fit to at least three of these binding sites, A, C and D by a ligand

is necessary to activate TrkA receptor. Binding areas B and E reinforce stereoselectivity of

the TrkA binding site by selecting an NGF analogue with a stereochemically compatible amino terminus.

Binding area A of the second LRM comprises hydrophobic interaction of residue Phe[105tA]. Binding area B comprises hydrophobic interaction of residues Phe[111tA], Phe[113tA] and

5   Thr[114tA]. Binding area C comprises attractive ionic interaction between a suitable portion on the ligand and Asp[109tA]. Binding area D comprises attractive ionic interaction between a suitable portion on the ligand and residue Lys[100tA]. Binding area E comprises multiple parallel β-strand type hydrogen bonding with region Asn[95tA]-Ile[98tA].

Main structural features of the bioactive conformation of NGF include: 1) ionic

10   hydrogen bonding between Glu[11] in the amino terminus and Arg[118'] in the carboxyl terminus; 2) separation of the flexible loop 1-8 from the rigid region (9-11 and 112' to 118') because of electrostatic repulsions caused by His[4] and conformational restrictions imposed by Pro[5]; 3) packing the side chain of Arg[9] or Met[9] in the "hollow" of the rigid region, this "hollow" being an indentation in the protein structure by residues Lys[115']-Arg[118']; and 4) an embryonic β-sheet

15   structure present between the α-carbons of the 7th and 9th residues.

Within NGF, residues Trp[76'], Arg[114'], Lys[115'] and Asp[16] comprise the pharmacophore which binds TrkA. Any synthetic molecule, whether peptide or non-peptide, which fits into binding areas A, C and D is contemplated to elicit a biological response (agonist) or block biological response (antagonist).

20   The present invention provides a ligand for binding with TrkA, wherein TrkA comprises a second leucine rich motif (LRM) region comprising amino acid residues 93 to 117, the coordinates of the residues of said LRM given in Appendix 1, said LRM motif having five binding areas, area A comprising hydrophobic interaction of amino acid residue Phe[105tA], area B comprising hydrophobic interaction of amino acid residues Phe[111tA], Phe[113tA], and Thr[114tA],

25   area C comprising ionic interaction of amino acid residues Asp[109tA] and His[112tA], area D comprising ionic interaction of amino acid residue Lys[100tA], and area E comprising multiple parallel β-strand type hydrogen bonding of region Asn[95tA] to Ile[98tA]. The ligand comprises at least one functional group being capable of hydrophobic bonding and being present in an effective position in the ligand to hydrophobically bind to area A, at least one positively

30   charged functional group being present in an effective position in the ligand to ionically bind to area C, and at least one negatively charged functional group being present in an effective position in the ligand to ionically bind to area D.

Secondary features of the ligand include at least one effective functional group present in a position in the ligand to hydrophobically bind to area B of TrkA, and a functional

35   group present in an effective position in the ligand to hydrogen bind to area E of TrkA.

The invention further provides the ligand comprising amino acid residues, at least one

of the residues being capable of hydrophobic bonding and being present in an effective position in the ligand to hydrophobically bind to Phe[105tA] in area A on the TrkA receptor, at least one of the residues being a positively charged residue present in an effective position in the ligand to ionically interact with Asp[109tA] and His[112tA] forming area C on the TrkA receptor,

5   and one of the residues being a negatively charged residue present in an effective position in the ligand to ionically bind to Lys[100tA] in area D on the TrkA receptor.

The present invention also provides a method of designing a ligand to bind with an LRM binding site on TrkA. The method includes computationally evolving a chemical ligand using an effective genetic algorithm with preselected spatial constraints so that the evolved

10   ligand comprises at least three effective functional groups of suitable identity and spatially located relative to each other in the ligand so that a first of the functional groups hydrophobically interacts with binding area A, a second of the functional groups ionically interacts with binding area C, and a third one of the functional groups ionically interacts with binding area D of the second LRM of TrkA. Those skilled in the art will be aware of the

15   various techniques which may be used for *de novo* ligand design. For example, packages such as Quanta, Discover and Insight provide computational methodologies for generating ligands.

Some ligands according to the present invention may be peptides or peptidomimetics. Morgan and co-workers (Morgan *et al.*, 1989) define peptide mimetics as "structures which

20   serve as appropriate substitutes for peptides in interactions with receptors and enzymes". The mimetic must possess not only affinity but also efficacy and substrate function. For purposes of this disclosure, the terms "peptide mimetic" and "peptidomimetic" are used interchangeably according to the above excerpted definition. That is, a peptidomimetic exhibits function(s) of a particular peptide, without restriction of structure. Peptidomimetics of

25   the invention, e.g., analogues of the neurotrophin and receptor binding sites described herein, may include amino acid residues or other chemical moieties which provide functional characteristics described herein.

Known compounds may also be screened to determine if they satisfy the spatial and functional requirements for binding with the second LRM of TrkA. The molecules in the data

30   bases are screened to determine if they contain effective moieties spaced relative to each other so that a first moiety hydrophobically interacts with binding area A, a second of moiety ionically interacts with binding area C, and a third moiety ionically interacts with binding area D of the second LRM of TrkA.

The contents of all references and appendices (see Appendices 1, 2, 3, and 4) cited

35   throughout this application are hereby expressly incorporated by reference.

EQUIVALENTS

Those skilled in the art will recognize, or be able to ascertain using no more than routine experimentation, many equivalents to the specific embodiments of the invention described herein. Such equivalents are intended to be encompassed by the following claims.

Table 1. Equilibrium variable torsional angles (in degrees) of the amino and carboxyl termini of the most stable conformations of the NGF dimers and analogues.*

No.			Active structures							Inactive structures				
			hNGF		mNGF		mNGFD3-9		hNGF-H4D		mNGFD1-8		BDNF	
							Amino terminus							
11	ψ	E	82.9	E	85.9	E	89.2	E	80.9	E	63.7	E	68.2
	φ		55.7		56.3		57.8		57.2		47.9		56.3
	χ1		-69.8		-72.0		-72.1		-75.0		-66.2		-76.9
	χ2		72.7		71.7		66.0		72.6		71.2		70.1
	χ3		-120.4		-111.7		-107.0		-104.8		-102.8		-97.7
10	ψ	G	-89.1	G	-95.1	G	-88.0	G	-129.5	G	-81.6	G	-134.1
	φ		-172.5		-178.6		-177.5		104.7		-80.8		155.0
9	ψ	R	-36.1	M	-21.1	S	146.5	R	-46.5	M	-66.6	R	71.4
	φ		-92.8		-91.4		-103.6		-80.9		157.5		-128.5
	χ1		-77.2		-75.2		-66.7		-115.0		-142.4		-73.5
	χ2		-173.9		-179.7		64.0		69.5		-69.7		-179.8
	χ3		-175.5		179.9		-		-141.9		178.3		-71.4
	χ4		134.3		-		-		98.1		-		-109.8
8	ψ	H	118.6	H	110.4	S	106.1	H	151.6		-	R	105.2
	φ		-116.5		-110.4		52.8		-53.7		-		-100.1
	χ1		-89.7		-90.9		-45.9		-62.0		-		179.6
	χ2		-73.8		-71.5		-172.3		-72.5		-		-105.5
	χ3		-		-		-		-		-		162.1
	χ4		-		-		-		-		-		133.7
7	ψ	F	135.7	F	129.4		-	F	142.3		-	A	161.6
	φ		-68.8		-89.0		-		-114.8		-		-166.6
	χ1		-171.6		-163.9		-		-170.7		-		-
	χ2		-96.3		-91.5		-		-100.2		-		-
6	ψ	I	40.3	V	61.7		-	I	40.0		-	P	114.4
	φ		40.4		47.7		-		39.9		-		-
	χ1		-159.7		-177.3		-		-159.7		-		-
	χ2		87.1		-		-		88.6		-		-

5	ψ	P 156.0	P 149.8	-	P 105.5	-	D 82.8	
	φ	-	-	-	-	-	56.5	
	χ1	-	-	-	-	-	-176.9	
	χ2	-	-	-	-	-	-112.8	
4	ψ	H 121.4	H 122.1	-	D 117.9	-	S 136.2	
	φ	-129.2	-129.8	-	-102.8	-	-53.4	
	χ1	-162.5	-163.3	-	-66.4	-	-172.9	
	χ2	-69.1	-69.2	-	-97.5	-	-178.3	
3	ψ	S 2.1	T -1.9	-	S -25.0	-	H 153.8	
	φ	-91.9	-84.5	-	-68.2	-	48.2	
	χ1	-171.8	-174.9	-	39.3	-	82.1	
	χ2	-53.2	-51.2	-	-120.5	-	69.8	
2	ψ	S 138.5	S 139.4	-	S 38.5	-	-	
	φ	-128.9	-114.1	-	50.8	-	-	
	χ1	173.3	169.7	-	-173.2	-	-	
	χ2	-141.9	-139.8	-	-120.6	-	-	
1	ψ	S 133.0	S 127.9	-	S 131.9	-	-	
	φ	48.6	49.4	-	-133.8	-	-	
	χ1	-43.2	-44.1	-	-43.5	-	-	
	χ2	-171.5	-172.4	-	-173.6	-	-	

Carboxyl terminus

112'	φ	L -113.3	L -113.0	L -112.4	L -112.0	L -111.5	L -110.6
	ψ	98.8	98.7	99.2	97.7	89.9	100.1
	χ1	-72.3	-71.6	-71.6	-71.7	-71.8	-72.1
	χ2	163.7	163.0	162.6	162.2	161.9	161.1
113'	φ	S -83.4	S -77.2	S -77.4	S -76.8	S -91.9	T -89.5
	ψ	136.1	146.0	143.5	141.7	149.4	134.0
	χ1	177.0	179.4	176.3	175.6	169.6	57.4
	χ2	65.2	60.6	59.0	57.5	73.2	-179.7
114'	φ	R -66.7	R -71.5	R -78.0	R -75.1	R -117.0	I -57.9
	ψ	-47.0	-53.7	-59.3	-57.1	-31.9	-32.2
	χ1	-99.1	-145.6	-93.4	177.5	-168.1	-162.1
	χ2	-173.1	-179.8	-171.5	-159.7	86.5	87.9
	χ3	170.4	-173.6	-172.9	58.1	-73.8	-

	χ4		138.4		140.3		141.5		124.7		173.4		-
115'	φ	K	-163.2	K	-162.1	K	-167.1	K	-163.0	K	-133.4	K	-167.7
	ψ		110.6		132.0		153.3		157.6		141.7		126.1
	χ1		-139.8		-143.3		-140.1		-137.8		-164.0		-142.2
5	χ2		78.7		81.7		85.0		79.3		172.4		83.5
	χ3		-96.4		-97.9		-95.8		-97.4		133.9		-100.4
	χ4		129.5		120.9		131.0		133.6		-73.6		109.2
	χ5		-39.1		-35.6		-47.7		-44.1		9.6		-9.5
116'	φ	A	-60.5	A	-69.6	A	-58.2	A	-63.9	A	-51.6	R	-61.4
10	ψ		-47.5		-40.7		-47.5		-42.4		-45.3		-39.3
	χ1		-		-		-		-		-		-80.9
	χ2		-		-		-		-		-		-173.4
	χ3		-		-		-		-		-		174.3
	χ4		-		-		-		-		-		129.6
15	117'	φ	V -71.8	T	-85.5	T	-64.6	V	-41.0	T	-114.6	G	-73.3
	ψ		112.0		116.4		108.2		130.2		168.4		77.3
	χ1		-74.3		53.4		50.9		-66.2		57.2		-
	χ2		-		60.5		58.0		-		-170.5		-
118'	φ	R	-93.8	R	-118.2	R	-58.5	R	-125.2	R	-51.5	R	-49.0
20	ψ		-57.9		-48.4		-37.6		141.3		-56.3		-40.3
	χ1		-104.3		-80.9		-109.5		-126.2		-153.8		-125.9
	χ2		79.1		109.1		73.3		106.7		88.0		98.0
	χ3		147.7		116.1		-76.3		-78.8		-74.9		-76.6
	χ4		147.0		116.1		-87.2		-98.5		-125.9		-111.5

25 *Torsional angles are designated according to the IUPAC-IUB rules (1970).

Table 2. Residues of BDNF and NGF defining the surfaces of their central β-strand stems, the side-chain thermal motion of which is taken into account when optimizing the structures of the complexes with the LRM-2B.

5

BDNF		NGF	
Ile[16]	Lys[57]	-	Lys[57]
Glu[18]	Asn[59]	Val[18]	Arg[59]
Val[20]	Met[61]	Val[20]	Ser[61]
Thr[21]	Lys[65]	Val[22]	-
Asp[24]	Gln[79]	Asp[24]	Tyr[79]
Lys[25]	Arg[81]	Lys[25]	Thr[81]
Lys[26]	Thr[82]	Thr[26]	Thr[82]
Thr[27]	Gln[84]	Thr[27]	His[84]
Val[29]	Tyr[86]	Thr[29]	Phe[86]
Thr[35]	Arg[104]	Glu[35]	Arg[103]
Glu[55]	Asp[106]	Glu[55]	Asp[105]

20

Table 3. Components of the molecular mechanical potential energy of the intermolecular NGF/LRM-2A interactions (in kcal/mol)

25

Term	hNGF	mNGF		mNGFΔ3-9	hNGF:NT-4/5
E_w	-61.2	-57.9		-39.3	-65.1
E_e	-96.2	-87.9		-99.0	-65.2
E_{hb}	-7.4	-5.9	-3.1	-4.6	
E_{qq}	-0.3	-0.3	-0.1	-0.1	
Total	-165.1	-152.0		-141.5	-135.1

35

Table 4. Components of the molecular mechanical potential energy of the BDNF/LRM-2B
and the NGF/LRM-2B complexes (in kcal/mol)

A. Components of the potential energy

	BDNF/LRM-2B	NGF/LRM-2B	Difference*
E_w	89.3	82.3	-7.0
E_{el}	-183.8	-93.1	**90.7**
E_{hb}	-31.0	-21.5	9.5
Et	114.9	114.0	-0.9
E_{qq}	0.4	0.0	-0.4
Total	-10.2	81.8	**92.0**

B. Components of the intermolecular interactions energy

	BDNF/LRM-2B	NGF/LRM-2B	Difference*
E_w	-48.0	-64.9	-16.9
E_{el}	-221.4	-144.2	**77.2**
E_{hb}	-5.6	-4.3	1.3
Total	-275.0	-213.5	61.5

*Difference of the energy terms within the minimum-energy structures of the NGF/LRM-2B
and the BDNF/LRM-2B complexes. Underlined values demonstrate that the difference in
intermolecular electrostatic interactions dominates in the differences in potential energies of
the complexes.

Table 5. Equilibrium variable torsional angles (in degrees) of the amino and carboxyl termini of the most stable conformations of the uncomplexed (UC) and complexed (C) NGF analogues.*

No.			hNGF UC	C		mNGF UC	C		mNGFΔ3-9 UC	C
					Amino terminus					
11	ψ	E	82.9	78.2	E	85.9	85.4	E	89.2	96.6
	ϕ		55.7	60.3		56.3	56.3		57.8	60.3
	$\chi 1$		-69.8	-69.3		-72.0	-69.4		-72.1	-73.7
	$\chi 2$		72.7	70.2		71.7	71.3		66.0	67.0
	$\chi 3$		-120.4	-117.6		-111.7	-117.1		-107.0	-109.2
10	ψ	G	-89.1	-122.1	G	-95.1	-103.2	G	-88.0	-94.8
	ϕ		-172.5	-166.5		-178.6	174.1		-177.5	168.7
9	ψ	R	-36.1	-25.7	M	-21.1	-14.3	S	146.5	166.1
	ϕ		-92.8	-84.2		-91.4	-77.3		-103.6	-132.1
	$\chi 1$		-77.2	-92.9		-75.2	-84.9		**-66.7**	**-179.1**
	$\chi 2$		-173.9	-174.1		-179.7	179.0		**64.0**	**122.2**
	$\chi 3$		-175.5	158.1		179.9	171.5		-	-
	$\chi 4$		134.3	136.4		-	-		-	-
8	ψ	H	118.6	98.3	H	110.4	96.1	S	**106.1**	**156.1**
	ϕ		-116.5	-127.3		-110.4	-121.8		52.8	46.0
	$\chi 1$		-89.7	-108.0		-90.9	-104.1		-45.9	-35.5
	$\chi 2$		-73.8	-87.9		-71.5	-65.8		-172.3	-174.1
7	ψ	F	135.7	113.6	F	129.4	106.7		-	-
	ϕ		**-68.8**	**-122.4**		**-89.0**	**-130.8**		-	-
	$\chi 1$		-171.6	-147.2		-163.9	-143.9		-	-
	$\chi 2$		-96.3	-85.8		-91.5	-87.5		-	-
6	ψ	I	40.3	57.9	V	61.7	67.9		-	-
	ϕ		40.4	38.5		47.7	48.3		-	-
	$\chi 1$		-159.7	-165.7		-177.3	-177.3		-	-
	$\chi 2$		87.1	88.3		-	-		-	-
5	ψ	P	156.0	164.8	P	149.8	153.3		-	-

4		ψ	H	121.4	125.4	H	122.1	122.9	-	-	
		φ		-129.2	-133.8		-129.8	-125.9	-	-	
		χ1		-162.5	-163.2		-163.3	-161.8	-	-	
		χ2		-69.1	-71.9		-69.2	-69.9	-	-	
5	3	ψ	S	2.1	-4.9	T	-1.9	-5.1	-	-	
		φ		-91.9	-78.9		-84.5	-82.3	-	-	
		χ1		-171.8	-172.3		-174.9	-171.4	-	-	
		χ2		-53.2	-51.2		-51.2	-52.3	-	-	
	2	ψ	S	138.5	135.7	S	139.4	139.4	-	-	
10		φ		**-128.9**	**-157.5**		**-114.1**	**-160.3**	-	-	
		χ1		173.3	173.4		169.7	170.3	-	-	
		χ2		-141.9	-133.0		-139.8	-134.5	-	-	
	1	ψ	S	133.0	129.5	S	127.9	128.6	-	-	
		φ		48.6	46.6		49.4	53.8	-	-	
15		χ1		-43.2	-41.9		-44.1	-44.0	-	-	
		χ2		-171.5	-171.0		-172.4	-170.9	-	-	

Carboxyl terminus

20	112'	φ	L	-113.3	-113.1	L	-113.0	-114.1	L	-112.4	-113.7
		ψ		98.8	95.5		98.7	99.3		99.2	103.9
		χ1		-72.3	-72.1		-71.6	-72.1		-71.6	-72.1
		χ2		163.7	163.2		163.0	164.1		162.6	163.8
	113'	φ	S	-83.4	-72.5	S	-77.2	-70.5	S	-77.4	-63.0
25		ψ		136.1	147.9		146.0	148.6		143.5	145.8
		χ1		177.0	179.1		179.4	-177.9		176.3	-177.0
		χ2		65.2	56.0		60.6	56.3		59.0	52.4
	114'	φ	R	-66.7	-101.6	R	-71.5	-92.5	R	-78.0	-92.3
		ψ		-47.0	-41.9		-53.7	-43.8		-59.3	-50.4
30		χ1		-99.1	-175.3		-145.6	-173.2		-93.4	-167.4
		χ2		-173.1	-130.0		-179.8	-114.8		-171.5	-101.4
		χ3		170.4	159.9		-173.6	151.4		-172.9	172.3
		χ4		**138.4**	**-117.4**		**140.3**	**-139.0**		**141.5**	**-130.9**
	115'	φ	K	-163.2	-155.3	K	-162.1	-152.2	K	-167.1	-161.4
35		ψ		110.6	111.2		132.0	111.0		153.3	132.6

	χ^1		-139.8	-150.7		-143.3	-156.2		-140.1	-144.6
	χ^2		**78.7**	**-170.9**		**81.7**	**-170.0**		**85.0**	**-177.7**
	χ^3		**-96.4**	**177.2**		**-97.9**	**-174.3**		**-95.8**	**-169.3**
	χ^4		**129.5**	**-165.4**		**120.9**	**-173.7**		**131.0**	**175.4**
5	χ^5		-39.1	-63.2		-35.6	-61.4		-47.7	-53.3
116'	ϕ	A	-60.5	-62.3	A	-69.6	-61.7	A	-58.2	-67.9
	ψ		-47.5	-43.9		-40.7	-47.8		-47.5	-40.4
117'	ϕ	V	-71.8	-106.1	T	-85.5	-106.0	T	-64.6	-74.3
	ψ		112.0	107.0		116.4	98.5		108.2	107.7
10	χ^1		-74.3	-75.0		53.4	55.1		50.9	56.6
	χ^2		-	-		60.5	63.2		58.0	54.0
118'	ϕ	R	-93.8	-58.0	R	**-118.2**	**-58.4**	R	-58.5	-79.4
	ψ		-57.9	-53.7		-48.4	-59.7		-37.6	-49.6
	χ^1		-104.3	-88.5		-80.9	-84.7		-109.5	-135.3
15	χ^2		79.1	74.4		109.1	79.7		73.3	108.0
	χ^3		147.7	161.4		116.1	147.5		-76.3	-70.1
	χ^4		147.0	119.7		116.1	118.7		-87.2	-135.3

20　　*Torsional angles are designated according to the IUPAC-IUB rules (1970). Torsional angles undergoing considerable changes upon LRM-2A binding are shown in bold.

Table 6. Optimized conformational variables (in degrees) of hNGF-complexed LRM-2A.*

No.	Type	ϕ	ψ	$\chi 1$	$\chi 2$	$\chi 3$	$\chi 4$	$\chi 5$
94tA	Arg	-161.6	-62.5	-169.2	-164.9	66.8	172.2	
95tA	Asn	-114.1	132.0	33.0	-111.6			
96tA	Leu	-131.9	114.2	-161.2	141.1			
97tA	Thr	-145.0	125.0	-179.9	-176.6			
98tA	Ile	-123.1	21.6	61.3	105.7			
99tA	Val	-61.2	107.3	175.7				
100tA	Lys	54.4	40.8	-75.6	161.7	-174.8	166.2	-41.3
101tA	Ser	-97.4	-40.0	-176.4	167.7			
102tA	Gly	144.4	46.5					
103tA	Leu	-135.6	155.5	-85.0	90.0			
104tA	Arg	-81.7	179.3	-33.6	165.0	-52.8	-144.7	
105tA	Phe	-68.6	-40.8	-159.4	93.3			
106tA	Val	-106.1	94.3	176.1				
107tA	Ala	-173.5	-54.8					
108tA	Pro		-26.2					
109tA	Asp	-85.5	64.7	-116.1	102.8			
110tA	Ala	-117.5	-57.2					
111tA	Phe	-79.4	135.3	38.4	89.8			
112tA	His	-132.1	78.5	-67.1	89.9			
113tA	Phe	-120.8	-29.0	54.6	95.4			
114tA	Thr	-59.9	-56.0	-23.4	-176.5			
115tA	Pro		-47.9					
116tA	Arg	-150.8	142.7	46.8	98.5	-100.4	155.7	
117tA	Leu	-76.3	-39.4	57.0	117.9			

*Torsional angles are designated according to the IUPAC-IUB rules (1970).

Table 7.   Optimized conformational variables (in degrees) of BDNF-complexed LRM-2B.*

No.	Type	ϕ	ψ	χ^1	χ^2	χ^3	χ^4	χ^5
94tB	Arg	-109.3	-54.2	-69.7	169.4	-171.6	119.4	
95tB	Asn	-163.6	141.0	-129.4	-109.4			
96tB	Leu	-81.9	86.5	-92.9	-58.2			
97tB	Thr	-138.3	143.5	-177.9	169.6			
98tB	Ile	-136.4	136.6	-164.6	86.9			
99tB	Val	-107.6	151.8	-70.1				
100tB	Asp	-68.8	-72.8	23.6	95.2			
101tB	Ser	36.4	36.0	-156.1	157.6			
102tB	Gly	42.0	44.4					
103tB	Leu	-118.2	149.0	49.9	87.1			
104tB	Lys	-92.9	68.5	-147.2	173.5	91.3	-169.5	45.1
105tB	Phe	73.7	-78.5	-160.5	-111.0			
106tB	Val	52.6	19.9	-174.2				
107tB	Ala	-113.9	26.4					
108tB	Tyr	-58.7	-20.3	-46.5	102.7	-74.2		
109tB	Lys	-71.4	-27.6	62.1	-113.2	176.6	176.6	-55.9
110tB	Ala	-91.7	-32.6					
111tB	Phe	-63.5	-37.4	-168.3	83.6			
112tB	Leu	-60.3	-43.2	-169.7	91.0			
113tB	Lys	-61.5	-48.0	-78.9	152.7	-167.9	63.2	22.9
114tB	Asn	-59.4	-36.6	-70.9	-107.4			
115tB	Ser	-68.6	-32.9	-60.0	68.6			
116tB	Asn	-80.7	-45.4	-83.4	-96.8			
117tB	Leu	-127.8	-58.8	-75.6	105.5			

*Torsional angles are designated according to the IUPAC-IUB rules (1970).

Table 8.　　Contributions of individual residues to intermolecular electrostatic interaction energies of the complexes BDNF/LRM-2B and NGF/LRM-2B (in kcal/mol)*.

A. Binding epitopes of neurotrophins

BDNF/LRM-2B		NGF/LRM-2B		Difference‡
Glu[18]	-61.6	Val[18]	0.3	61.9
Asp[24]	-65.1	Asp[24]	-44.9	20.2
Lys[25]	25.3	Lys25	15.5	-9.8
Gly[33]	-11.9	Gly[33]	-13.4	-1.5
Thr[35]	-11.4	Glu[35]	-50.5	-39.1
Glu[55]	-50.2	Glu[55]	-18.9	31.3
Lys[57]	27.1	Lys[57]	22.5	-4.6
Arg[81]	-32.2	Thr[81]	0.1	32.3
Gln[84]	1.2	His[84]	11.5	10.3
Arg[104]	-14.3	Arg[103]	-9.5	4.8
Asp[106]	-39.7	Asp[105]	-46.4	-6.7

Total	-232.8		-133.7	99.1

B. Binding epitopes of the LRM-2B

BDNF/LRM-2B		NGF/LRM-2B	Difference‡
Arg[94tB]	-40.9	4.2	45.1
Asn[95tB]	0.2	-12.8	-13.0
Asp[100tB]	-42.1	-9.3	32.8
Ser[101tB]	-17.9	-0.1	17.8
Gly[102tB]	-1.3	-12.0	-10.7
Lys[104tB]	-18.5	-48.1	-29.6
Lys[109tB]	-46.4	-21.5	24.9
Lys[113tB]	-54.6	-37.2	17.4

Total	-221.5	-136.8	84.7

*The ±10 kcal/mol cutoff of intermolecular electrostatic interaction energy has been used to identify binding epitopes within the complexes. ‡Difference of the intermolecular electrostatic interaction energies of the given residue within the minimum-energy structures of the NGF/LRM-2B and the BDNF/LRM-2B complexes. Residues within the binding epitopes of BDNF and the LRM-2B which cause their binding specificity are bolded.

Table 9. Contributions of individual residues of the neurotrophins to the intermolecular interaction energy of their complexes with the common neurotrophin receptor p75^{NTR} (kcal/mol)*

NGF			BDNF			NT-3			NT-4/5		
Res.	EL	VDW	Res.	EL	VDW	Res.	EL	VDW	Res.	EL	VDW
D-30	17.9	-0.9	D-30	25.0	-1.8	D-29	24.6	-2.6	D-32	19.8	-1.8
K-32	-94.9	-6.0	S-32	0.5	-4.5	R-31	-48.2	-8.0	R-34	-42.6	-9.3
K-34	-88.8	-3.3	G-34	-1.8	-3.1	H-33	-35.0	-7.1	R-36	-57.2	-7.7
E-35	-10.0	-2.2	T-35	1.7	-1.4	Q-34	0.5	-2.3	D-37	-0.8	-1.7
H-84	-30.9	-1.0	Q-84	1.19	-2.4	Q-83	0.8	-0.7	Q-83	0.6	-1.0
F-86	-0.2	-0.3	Y-86	-0.5	-0.5	Y-85	-13.4	0.3	Y-96	-9.2	-0.3
K-88	-8.5	-0.1	R-88	-12.7	-0.2	R-87	-20.0	-0.3	R-98	-16.2	-0.2
D-93	-9.0	-1.3	D-93	13.7	-2.2	E-92	24.1	-2.8	D-103	9.0	-2.1
K-95	-63.7	-5.6	K-95	-82.9	-7.6	N-94	-0.1	-0.2	Q-105	-0.3	-0.2
Q-96	-0.3	-3.7	K-96	-58.2	2.0	K-95	-49.6	-2.6	G-106	-0.6	-0.6
A-97	0.2	-0.2	R-97	-79.3	-5.7	L-96	-0.5	-6.7	R-107	-28.0	-11.2
R-100	-11.8	-0.7	R-101	-59.2	-1.1	R-100	-79.3	1.7	R-111	-57.8	-1.9
R-103	-64.5	0.0	R-104	-64.2	-1.6	R-103	-51.5	0.6	R-114	-55.3	-2.9
D-105	10.6	-0.2	D-106	8.3	-0.2	D-105	5.5	-0.1	D-116	4.8	-0.1
Total	-336.1	-15.6		-317.8	-18.2		-248.3	-15.6		-237.3	-35.0
	100%	55%		99%	39%		97%	32%		102%	61%
Net	-337.3	-32.3		-321.4	-46.7		-254.8	-48.9		-233.0	-57.5

*EL and VDW denote electrostatic and van der Waals terms of the ligand-receptor interaction energy, respectively. The ±10 kcal/mol cutoff of the intermolecular electrostatic interaction energy has been used to identify the functional epitopes (bolded). "Total" electrostatic and van der Waals contributions of the functional epitopes to the "net" values of the intermolecular interaction energy calculated over the whole binding interface are presented. Residue numbering corresponds to the general alignment of neurotrophins (Bradshaw et al., 1994).

Table 10. Contributions of individual residues of p75[NTR] to the intermolecular interaction energy of their complexes with neurotrophins (kcal/mol)*.

NGF			BDNF			NT-3			NT-4/5		
Res.	EL	VDW	Res.	EL	VDW	Res.	EL	VDW	Res.	EL	VDW
D-47	-46.0	0.2	D-47	-67.1	0.1	D-47	-50.5	-0.3	D-47	-26.7	-4.1
E-53	-2.6	-0.2	E-53	-55.4	1.6	E-53	-6.6	-0.2	E-53	-3.6	-0.1
P-54	-12.4	-2.8	P-54	-13.5	-2.5	P-54	-15.1	0.2	P-54	-5.3	-0.8
C-55	-1.4	-0.9	C-55	-8.4	-1.3	C-55	-14.9	-1.0	C-55	-3.0	-1.2
K-56	21.8	-4.5	K-56	13.2	-4.8	K-56	32.9	-5.0	K-56	14.8	-5.8
E-60	-6.2	-0.3	E-60	-3.0	-0.1	E-60	-10.0	-0.2	E-60	-10.4	-0.4
E-73	-4.2	0.0	E-73	-9.7	-0.2	E-73	-12.5	-0.3	E-73	-11.2	-0.3
D-75	-56.5	0.6	D-75	-77.1	0.4	D-75	-65.5	-1.1	D-75	-59.4	-2.7
D-76	-91.6	-2.0	D-76	-22.3	-8.4	D-76	-39.9	-3.7	D-76	-39.3	-5.1
R-80	-18.5	-3.9	R-80	2.9	-2.1	R-80	5.3	-4.0	R-80	3.1	-4.3
D-88	-49.1	0.4	D-88	-39.8	-0.4	D-88	-34.4	0.4	D-88	-33.1	-1.2
E-89	-32.5	-1.6	E-89	-25.2	-6.2	E-89	-33.8	-3.8	E-89	-33.0	-5.9
Total	-285.4	-13.6		-287.2	-20.2		-243.7	-14.8		-198.3	-25.5
	84%	42%		89%	43%		96%	30%		85%	44%

*See footnote to Table 9.

Appendix 1. Geometry of the LRM-2A in PDB format.*

REMARK   1 The bioactive conformation of the second LRM of TrkA.

REMARK   2   HSC stands for charged HIS

5   REMARK   3

ATOM   1 N   LEU S 93   19.399 -23.034 -15.306 1.00 -0.45

ATOM   2 CA LEU S 93   18.757 -22.140 -14.332 1.00 -0.07

ATOM   3 C   LEU S 93   19.555 -20.869 -14.130 1.00 0.53

ATOM   4 O   LEU S 93   20.777 -20.864 -14.044 1.00 -0.50

10   ATOM   5 CB LEU S 93   18.635 -22.886 -13.002 1.00 0.02

ATOM   6 CG LEU S 93   17.661 -22.206 -12.037 1.00 0.05

ATOM   7 CD1 LEU S 93   16.251 -22.083 -12.617 1.00 -0.01

ATOM   8 CD2 LEU S 93   . 17.517 -22.968 -10.718 1.00 -0.01

ATOM   9 1H LEU S 93   19.651 -23.930 -14.841 1.00 0.15

15   ATOM   10 2H LEU S 93   18.742 -23.223 -16.089 1.00 0.15

ATOM   11 3H LEU S 93   20.260 -22.582 -15.677 1.00 0.15

ATOM   12 N   ARG S 94   18.551 -20.159 -13.624 1.00 -0.52

ATOM   13 CA ARG S 94   18.777 -19.044 -12.708 1.00 0.24

ATOM   14 C   ARG S 94   17.460 -18.800 -12.010 1.00 0.53

20   ATOM   15 O   ARG S 94   17.364 -18.941 -10.781 1.00 -0.50

ATOM   16 CB ARG S 94   19.316 -17.812 -13.451 1.00 0.05

ATOM   17 CG ARG S 94   19.818 -16.700 -12.515 1.00 0.06

ATOM   18 CD ARG S 94   . 20.009 -15.345 -13.215 1.00 0.11

ATOM   19 NE ARG S 94   18.720 -14.803 -13.642 1.00 -0.49

25   ATOM   20 CZ ARG S 94   18.631 -13.550 -14.138 1.00 0.81

ATOM   21 NH1 ARG S 94   19.703 -12.767 -14.256 1.00 -0.63

ATOM   22 NH2 ARG S 94   17.444 -13.087 -14.518 1.00 -0.63

ATOM   23 H   ARG S 94   17.611 -20.389 -13.873 1.00 0.25

ATOM   24 HE ARG S 94   17.892 -15.358 -13.571 1.00 0.29

30   ATOM   25 1HH1 ARG S 94   19.604 -11.843 -14.627 1.00 0.36

ATOM   26 2HH1 ARG S 94   20.606 -13.094 -13.977 1.00 0.36

ATOM   27 1HH2 ARG S 94   17.363 -12.161 -14.887 1.00 0.36

ATOM   28 2HH2 ARG S 94   16.633 -13.666 -14.434 1.00 0.36

ATOM   29 N   ASN S 95   16.446 -18.435 -12.789 1.00 -0.52

35   ATOM   30 CA ASN S 95   15.116 -18.165 -12.251 1.00 0.22

ATOM   31 C   ASN S 95   14.111 -19.178 -12.745 1.00 0.53

67

	ATOM	32 O ASN S 95	14.047 -19.466 -13.950 1.00 -0.50
	ATOM	33 CB ASN S 95	14.629 -16.742 -12.566 1.00 0.00
	ATOM	34 CG ASN S 95	15.171 -16.300 -13.911 1.00 0.68
	ATOM	35 OD1 ASN S 95	16.007 -15.410 -13.997 1.00 -0.47
5	ATOM	36 ND2 ASN S 95	14.657 -16.965 -14.959 1.00 -0.87
	ATOM	37 H ASN S 95	16.591 -18.340 -13.774 1.00 0.25
	ATOM	38 1HD2 ASN S 95	14.948 -16.750 -15.892 1.00 0.34
	ATOM	39 2HD2 ASN S 95	13.976 -17.684 -14.820 1.00 0.34
	ATOM	40 N LEU S 96	13.325 -19.720 -11.819 1.00 -0.52
10	ATOM	41 CA LEU S 96	12.308 -20.713 -12.151 1.00 0.20
	ATOM	42 C LEU S 96	11.023 -20.296 -11.479 1.00 0.53
	ATOM	43 O LEU S 96	10.934 -20.287 -10.242 1.00 -0.50
	ATOM	44 CB LEU S 96	12.767 -22.109 -11.701 1.00 0.02
	ATOM	45 CG LEU S 96	12.022 -23.268 -12.383 1.00 0.05
15	ATOM	46 CD1 LEU S 96	12.921 -24.464 -12.732 1.00 -0.01
	ATOM	47 CD2 LEU S 96	10.797 -23.704 -11.562 1.00 -0.01
	ATOM	48 H LEU S 96	13.428 -19.444 -10.863 1.00 0.25
	ATOM	49 N THR S 97	10.026 -19.951 -12.289 1.00 -0.52
	ATOM	50 CA THR S 97	8.726 -19.526 -11.778 1.00 0.27
20	ATOM	51 C THR S 97	7.604 -19.988 -12.678 1.00 0.53
	ATOM	52 O THR S 97	7.607 -19.702 -13.884 1.00 -0.50
	ATOM	53 CB THR S 97	8.692 -18.000 -11.598 1.00 0.21
	ATOM	54 OG1 THR S 97	7.420 -17.594 -11.097 1.00 -0.55
	ATOM	55 CG2 THR S 97	9.014 -17.248 -12.899 1.00 0.01
25	ATOM	56 H THR S 97	10.163 -19.980 -13.279 1.00 0.25
	ATOM	57 HG1 THR S 97	7.431 -16.635 -11.053 1.00 0.31
	ATOM	58 N ILE S 98	6.645 -20.701 -12.095 1.00 -0.52
	ATOM	59 CA ILE S 98	5.499 -21.213 -12.841 1.00 0.20
	ATOM	60 C ILE S 98	4.166 -20.765 -12.292 1.00 0.53
30	ATOM	61 O ILE S 98	3.134 -21.406 -12.544 1.00 -0.50
	ATOM	62 CB ILE S 98	5.633 -22.735 -13.006 1.00 0.03
	ATOM	63 CG1 ILE S 98	5.655 -23.480 -11.662 1.00 0.02
	ATOM	64 CG2 ILE S 98	6.841 -23.109 -13.880 1.00 0.00
	ATOM	65 CD1 ILE S 98	4.338 -24.216 -11.369 1.00 0.00
35	ATOM	66 H ILE S 98	6.703 -20.897 -11.116 1.00 0.25
	ATOM	67 N VAL S 99	4.183 -19.667 -11.541 1.00 -0.52

68

SUBSTITUTE SHEET (RULE 26)

	ATOM	68	CA	VAL S 99	2.969 -19.119 -10.945 1.00 0.20
	ATOM	69	C	VAL S 99	1.976 -18.727 -12.013 1.00 0.53
	ATOM	70	O	VAL S 99	2.172 -17.725 -12.717 1.00 -0.50
	ATOM	71	CB	VAL S 99	3.389 -17.945 -10.045 1.00 0.03
5	ATOM	72	CG1	VAL S 99	2.188 -17.207 -9.432 1.00 0.01
	ATOM	73	CG2	VAL S 99	4.444 -18.324 -8.993 1.00 0.01
	ATOM	74	H	VAL S 99	5.050 -19.197 -11.376 1.00 0.25
	ATOM	75	N	LYS S 100	0.911 -19.514 -12.136 1.00 -0.52
	ATOM	76	CA	LYS S 100	-0.131 -19.257 -13.126 1.00 0.23
10	ATOM	77	C	LYS S 100	0.517 -19.154 -14.486 1.00 0.53
	ATOM	78	O	LYS S 100	0.146 -18.291 -15.296 1.00 -0.50
	ATOM	79	CB	LYS S 100	-0.916 -17.989 -12.753 1.00 0.04
	ATOM	80	CG	LYS S 100	-1.911 -18.178 -11.597 1.00 0.05
	ATOM	81	CD	LYS S 100	-2.337 -16.845 -10.961 1.00 0.05
15	ATOM	82	CE	LYS S 100	-3.230 -17.043 -9.726 1.00 0.22
	ATOM	83	NZ	LYS S 100	-3.328 -15.780 -8.983 1.00 -0.27
	ATOM	84	H	LYS S 100	0.814 -20.308 -11.536 1.00 0.25
	ATOM	85	1HZ	LYS S 100	-2.395 -15.321 -8.953 1.00 0.31
	ATOM	86	2HZ	LYS S 100	-3.649 -15.972 -8.012 1.00 0.31
20	ATOM	87	3HZ	LYS S 100	-4.008 -15.150 -9.454 1.00 0.31
	ATOM	88	N	SER S 101	1.485 -20.030 -14.739 1.00 -0.52
	ATOM	89	CA	SER S 101	2.199 -20.048 -16.012 1.00 0.36
	ATOM	90	C	SER S 101	1.652 -21.075 -16.974 1.00 0.53
	ATOM	91	O	SER S 101	1.546 -20.813 -18.182 1.00 -0.50
25	ATOM	92	CB	SER S 101	3.695 -20.297 -15.758 1.00 0.19
	ATOM	93	OG	SER S 101	4.426 -20.237 -16.981 1.00 -0.55
	ATOM	94	H	SER S 101	1.736 -20.701 -14.041 1.00 0.25
	ATOM	95	HG	SER S 101	5.354 -20.203 -16.738 1.00 0.31
	ATOM	96	N	GLY S 102	1.302 -22.243 -16.444 1.00 -0.52
30	ATOM	97	CA	GLY S 102	0.758 -23.329 -17.254 1.00 0.25
	ATOM	98	C	GLY S 102	1.148 -24.732 -16.854 1.00 0.53
	ATOM	99	O	GLY S 102	1.526 -25.548 -17.708 1.00 -0.50
	ATOM	100	H	GLY S 102	1.413 -22.390 -15.461 1.00 0.25
	ATOM	101	N	LEU S 103	1.058 -25.015 -15.558 1.00 -0.52
35	ATOM	102	CA	LEU S 103	1.402 -26.331 -15.027 1.00 0.20
	ATOM	103	C	LEU S 103	0.326 -26.726 -14.045 1.00 0.53

69

ATOM	104	O	LEU S 103	-0.356 -25.860 -13.476	1.00 -0.50
ATOM	105	CB	LEU S 103	2.792 -26.289 -14.372	1.00 0.02
ATOM	106	CG	LEU S 103	3.957 -26.492 -15.354	1.00 0.05
ATOM	107	CD1	LEU S 103	4.502 -25.183 -15.949	1.00 -0.01
ATOM	108	CD2	LEU S 103	5.078 -27.333 -14.723	1.00 -0.01
ATOM	109	H	LEU S 103	0.745 -24.311 -14.920	1.00 0.25
ATOM	110	N	ARG S 104	0.170 -28.031 -13.843	1.00 -0.52
ATOM	111	CA	ARG S 104	-0.832 -28.558 -12.921	1.00 0.24
ATOM	112	C	ARG S 104	-0.225 -28.464 -11.541	1.00 0.53
ATOM	113	O	ARG S 104	0.920 -28.016 -11.387	1.00 -0.50
ATOM	114	CB	ARG S 104	-1.253 -29.984 -13.311	1.00 0.05
ATOM	115	CG	ARG S 104	-1.250 -30.233 -14.827	1.00 0.06
ATOM	116	CD	ARG S 104	-1.308 -31.721 -15.207	1.00 0.11
ATOM	117	NE	ARG S 104	-0.254 -32.467 -14.521	1.00 -0.49
ATOM	118	CZ	ARG S 104	0.365 -33.502 -15.129	1.00 0.81
ATOM	119	NH1	ARG S 104	0.042 -33.880 -16.366	1.00 -0.63
ATOM	120	NH2	ARG S 104	1.319 -34.159 -14.478	1.00 -0.63
ATOM	121	H	ARG S 104	0.754 -28.678 -14.334	1.00 0.25
ATOM	122	HE	ARG S 104	0.018 -32.215 -13.592	1.00 0.29
ATOM	123	1HH1	ARG S 104	0.519 -34.651 -16.789	1.00 0.36
ATOM	124	2HH1	ARG S 104	-0.672 -33.401 -16.875	1.00 0.36
ATOM	125	1HH2	ARG S 104	1.786 -34.927 -14.915	1.00 0.36
ATOM	126	2HH2	ARG S 104	1.569 -33.884 -13.549	1.00 0.36
ATOM	127	N	PHE S 105	-0.990 -28.886 -10.538	1.00 -0.52
ATOM	128	CA	PHE S 105	-0.535 -28.854 -9.152	1.00 0.21
ATOM	129	C	PHE S 105	0.558 -29.894 -9.090	1.00 0.53
ATOM	130	O	PHE S 105	1.596 -29.679 -8.447	1.00 -0.50
ATOM	131	CB	PHE S 105	-1.656 -29.230 -8.170	1.00 0.04
ATOM	132	CG	PHE S 105	-1.354 -28.726 -6.778	1.00 0.01
ATOM	133	CD1	PHE S 105	-1.851 -27.471 -6.366	1.00 -0.01
ATOM	134	CD2	PHE S 105	-0.575 -29.526 -5.913	1.00 -0.01
ATOM	135	CE1	PHE S 105	-1.566 -27.007 -5.067	1.00 0.00
ATOM	136	CE2	PHE S 105	-0.290 -29.063 -4.616	1.00 0.00
ATOM	137	CZ	PHE S 105	-0.788 -27.809 -4.206	1.00 0.00
ATOM	138	H	PHE S 105	-1.906 -29.236 -10.732	1.00 0.25
ATOM	139	N	VAL S 106	0.329 -31.021 -9.758	1.00 -0.52

70

	ATOM	140	CA	VAL	S	106	1.297 -32.114 -9.787	1.00 0.20
	ATOM	141	C	VAL	S	106	1.984 -32.186 -11.130	1.00 0.53
	ATOM	142	O	VAL	S	106	1.469 -32.815 -12.067	1.00 -0.50
	ATOM	143	CB	VAL	S	106	0.545 -33.403 -9.418	1.00 0.03
5	ATOM	144	CG1	VAL	S	106	1.433 -34.654 -9.506	1.00 0.01
	ATOM	145	CG2	VAL	S	106	-0.212 -33.313 -8.084	1.00 0.01
	ATOM	146	H	VAL	S	106	-0.530 -31.131 -10.258	1.00 0.25
	ATOM	147	N	ALA	S	107	3.145 -31.545 -11.226	1.00 -0.52
	ATOM	148	CA	ALA	S	107	3.920 -31.529 -12.463	1.00 0.22
10	ATOM	149	C	ALA	S	107	5.237 -30.854 -12.163	1.00 0.53
	ATOM	150	O	ALA	S	107	6.308 -31.425 -12.415	1.00 -0.50
	ATOM	151	CB	ALA	S	107	3.199 -30.751 -13.576	1.00 0.03
	ATOM	152	H	ALA	S	107	3.504 -31.056 -10.432	1.00 0.25
	ATOM	153	N	PRO	S	108	5.161 -29.640 -11.625	1.00 -0.26
15	ATOM	154	CA	PRO	S	108	6.351 -28.871 -11.283	1.00 0.11
	ATOM	155	C	PRO	S	108	7.264 -29.638 -10.357	1.00 0.53
	ATOM	156	O	PRO	S	108	8.481 -29.403 -10.336	1.00 -0.50
	ATOM	157	CB	PRO	S	108	5.782 -27.574 -10.686	1.00 0.00
	ATOM	158	CG	PRO	S	108	4.356 -27.900 -10.256	1.00 0.04
20	ATOM	159	CD	PRO	S	108	3.932 -28.917 -11.305	1.00 0.08
	ATOM	160	N	ASP	S	109	6.680 -30.556 -9.591	1.00 -0.52
	ATOM	161	CA	ASP	S	109	7.439 -31.374 -8.649	1.00 0.25
	ATOM	162	C	ASP	S	109	7.956 -32.544 -9.451	1.00 0.53
	ATOM	163	O	ASP	S	109	7.574 -33.697 -9.200	1.00 -0.50
25	ATOM	164	CB	ASP	S	109	6.510 -31.884 -7.536	1.00 -0.21
	ATOM	165	CG	ASP	S	109	6.933 -31.318 -6.195	1.00 0.62
	ATOM	166	OD1	ASP	S	109	6.290 -30.391 -5.711	1.00 -0.71
	ATOM	167	OD2	ASP	S	109	7.907 -31.800 -5.626	1.00 -0.71
	ATOM	168	H	ASP	S	109	5.692 -30.697 -9.657	1.00 0.25
30	ATOM	169	N	ALA	S	110	8.824 -32.252 -10.416	1.00 -0.52
	ATOM	170	CA	ALA	S	110	9.406 -33.282 -11.270	1.00 0.22
	ATOM	171	C	ALA	S	110	10.898 -33.275 -11.034	1.00 0.53
	ATOM	172	O	ALA	S	110	11.481 -34.304 -10.662	1.00 -0.50
	ATOM	173	CB	ALA	S	110	9.132 -33.009 -12.758	1.00 0.03
35	ATOM	174	H	ALA	S	110	9.090 -31.300 -10.566	1.00 0.25
	ATOM	175	N	PHE	S	111	11.517 -32.118 -11.249	1.00 -0.52

71

	ATOM	176	CA	PHE S 111	12.956	-31.964	-11.061	1.00	0.21
	ATOM	177	C	PHE S 111	13.127	-31.810	-9.568	1.00	0.53
	ATOM	178	O	PHE S 111	12.376	-31.064	-8.923	1.00	-0.50
	ATOM	179	CB	PHE S 111	13.497	-30.712	-11.770	1.00	0.04
5	ATOM	180	CG	PHE S 111	12.526	-29.559	-11.656	1.00	0.01
	ATOM	181	CD1	PHE S 111	12.618	-28.673	-10.561	1.00	-0.01
	ATOM	182	CD2	PHE S 111	11.542	-29.391	-12.654	1.00	-0.01
	ATOM	183	CE1	PHE S 111	11.710	-27.601	-10.462	1.00	0.00
	ATOM	184	CE2	PHE S 111	10.634	-28.321	-12.556	1.00	0.00
10	ATOM	185	CZ	PHE S 111	10.727	-27.436	-11.461	1.00	0.00
	ATOM	186	H	PHE S 111	10.987	-31.324	-11.549	1.00	0.25
	ATOM	187	N	HSC S 112	14.112	-32.515	-9.019	1.00	-0.52
	ATOM	188	H	HSC S 112	14.681	-33.099	-9.597	1.00	0.25
	ATOM	189	CA	HSC S 112	14.393	-32.465	-7.587	1.00	0.19
15	ATOM	190	CB	HSC S 112	13.775	-33.685	-6.885	1.00	0.21
	ATOM	191	CG	HSC S 112	12.263	-33.637	-6.920	1.00	0.10
	ATOM	192	CD2	HSC S 112	11.396	-33.062	-5.986	1.00	0.35
	ATOM	193	ND1	HSC S 112	11.533	-34.176	-7.915	1.00	-0.61
	ATOM	194	HD1	HSC S 112	11.881	-34.643	-8.703	1.00	0.48
20	ATOM	195	CE1	HSC S 112	10.215	-33.947	-7.619	1.00	0.72
	ATOM	196	NE2	HSC S 112	10.132	-33.262	-6.434	1.00	-0.69
	ATOM	197	HE2	HSC S 112	9.308	-32.971	-5.991	1.00	0.49
	ATOM	198	C	HSC S 112	15.841	-32.262	-7.208	1.00	0.53
	ATOM	199	O	HSC S 112	16.534	-33.221	-6.836	1.00	-0.50
25	ATOM	200	N	PHE S 113	16.299	-31.017	-7.301	1.00	-0.52
	ATOM	201	CA	PHE S 113	17.678	-30.673	-6.967	1.00	0.21
	ATOM	202	C	PHE S 113	17.554	-29.654	-5.860	1.00	0.53
	ATOM	203	O	PHE S 113	18.444	-29.545	-5.003	1.00	-0.50
	ATOM	204	CB	PHE S 113	18.418	-30.047	-8.160	1.00	0.04
30	ATOM	205	CG	PHE S 113	17.666	-28.854	-8.702	1.00	0.01
	ATOM	206	CD1	PHE S 113	18.011	-27.554	-8.270	1.00	-0.01
	ATOM	207	CD2	PHE S 113	16.627	-29.064	-9.635	1.00	-0.01
	ATOM	208	CE1	PHE S 113	17.306	-26.447	-8.780	1.00	0.00
	ATOM	209	CE2	PHE S 113	15.922	-27.959	-10.145	1.00	0.00
35	ATOM	210	CZ	PHE S 113	16.268	-26.661	-9.712	1.00	0.00

72

```
        ATOM  211 H   PHE S 113    15.686 -30.289 -7.608 1.00 0.25
        ATOM  212 N   THR S 114    16.454 -28.908 -5.874 1.00 -0.52
        ATOM  213 CA  THR S 114    16.200 -27.883 -4.866 1.00 0.27
        ATOM  214 C   THR S 114    16.150 -28.477 -3.478 1.00 0.53
  5     ATOM  215 O   THR S 114    16.898 -28.053 -2.585 1.00 -0.50
        ATOM  216 CB  THR S 114    14.903 -27.124 -5.185 1.00 0.21
        ATOM  217 OG1 THR S 114    14.606 -27.224 -6.576 1.00 -0.55
        ATOM  218 CG2 THR S 114    14.967 -25.648 -4.762 1.00 0.01
        ATOM  219 H   THR S 114    15.774 -29.046 -6.595 1.00 0.25
  10    ATOM  220 HG1 THR S 114    13.824 -26.691 -6.734 1.00 0.31
        ATOM  221 N   PRO S 115    15.270 -29.457 -3.296 1.00 -0.26
        ATOM  222 CA  PRO S 115    15.113 -30.124 -2.008 1.00 0.11
        ATOM  223 C   PRO S 115    16.420 -30.691 -1.510 1.00 0.53
        ATOM  224 O   PRO S 115    16.789 -30.490 -0.343 1.00 -0.50
  15    ATOM  225 CB  PRO S 115    14.024 -31.174 -2.277 1.00 0.00
        ATOM  226 CG  PRO S 115    14.008 -31.384 -3.788 1.00 0.04
        ATOM  227 CD  PRO S 115    14.364 -29.999 -4.305 1.00 0.08
        ATOM  228 N   ARG S 116    17.122 -31.399 -2.390 1.00 -0.52
        ATOM  229 CA  ARG S 116    18.405 -32.006 -2.048 1.00 0.24
  20    ATOM  230 C   ARG S 116    19.201 -32.059 -3.330 1.00 0.53
        ATOM  231 O   ARG S 116    18.642 -32.307 -4.408 1.00 -0.50
        ATOM  232 CB  ARG S 116    18.212 -33.381 -1.388 1.00 0.05
        ATOM  233 CG  ARG S 116    17.213 -34.284 -2.128 1.00 0.06
        ATOM  234 CD  ARG S 116    17.881 -35.312 -3.055 1.00 0.11
  25    ATOM  235 NE  ARG S 116    17.832 -34.856 -4.444 1.00 -0.49
        ATOM  236 CZ  ARG S 116    18.735 -35.300 -5.346 1.00 0.81
        ATOM  237 NH1 ARG S 116    19.694 -36.161 -5.009 1.00 -0.63
        ATOM  238 NH2 ARG S 116    18.663 -34.866 -6.600 1.00 -0.63
        ATOM  239 H   ARG S 116    16.767 -31.523 -3.317 1.00 0.25
  30    ATOM  240 HE  ARG S 116    17.128 -34.209 -4.737 1.00 0.29
        ATOM  241 1HH1 ARG S 116   20.347 -36.471 -5.701 1.00 0.36
        ATOM  242 2HH1 ARG S 116   19.767 -36.501 -4.072 1.00 0.36
        ATOM  243 1HH2 ARG S 116   19.324 -35.186 -7.279 1.00 0.36
        ATOM  244 2HH2 ARG S 116   17.947 -34.219 -6.864 1.00 0.36
  35    ATOM  245 N   LEU S 117    20.506 -31.828 -3.216 1.00 -0.52
        ATOM  246 CA  LEU S 117    21.399 -31.846 -4.370 1.00 0.23
```

73

SUBSTITUTE SHEET (RULE 26)

```
       ATOM   247 C   LEU S 117      21.643 -33.299  -4.741  1.00  0.50
       ATOM   248 O   LEU S 117      21.687 -33.594  -5.933  1.00 -0.25
       ATOM   249 CB  LEU S 117      22.706 -31.110  -4.038  1.00  0.02
       ATOM   250 CG  LEU S 117      23.454 -31.672  -2.818  1.00  0.05
   5   ATOM   251 CD1 LEU S 117      24.851 -32.222  -3.147  1.00 -0.01
       ATOM   252 CD2 LEU S 117      23.506 -30.647  -1.674  1.00 -0.01
       ATOM   253 OXT LEU S 117      21.785 -34.114  -3.834  1.00 -0.25
       ATOM   254 H   LEU S 117      20.894 -31.634  -2.315  1.00  0.25
       END
  10
```

*Principal residues are bolded.

Appendix 2. Geometry of the LRM-2B in PDB format.*

REMARK 1 The bioactive conformation of the second LRM of TrkB.

REMARK 2

	ATOM	1 N	LEU S 93	-32.287 14.723 17.944 1.00 -0.45
5	ATOM	2 CA	LEU S 93	-33.186 15.831 17.679 1.00 -0.07
	ATOM	3 C	LEU S 93	-32.411 17.027 17.215 1.00 0.53
	ATOM	4 O	LEU S 93	-31.203 17.150 17.385 1.00 -0.50
	ATOM	5 CB	LEU S 93	-33.996 16.167 18.941 1.00 0.02
	ATOM	6 CG	LEU S 93	-35.339 15.426 19.042 1.00 0.05
10	ATOM	7 CD1	LEU S 93	-36.286 15.694 17.861 1.00 -0.01
	ATOM	8 CD2	LEU S 93	-35.131 13.920 19.266 1.00 -0.01
	ATOM	9 1H	LEU S 93	-31.777 14.490 17.116 1.00 0.15
	ATOM	10 2H	LEU S 93	-32.810 13.922 18.239 1.00 0.15
	ATOM	11 3H	LEU S 93	-31.641 14.971 18.665 1.00 0.15
15	ATOM	12 N	ARG S 94	-33.510 17.650 16.801 1.00 -0.52
	ATOM	13 CA	ARG S 94	-33.484 19.028 16.320 1.00 0.24
	ATOM	14 C	ARG S 94	-34.175 19.857 17.377 1.00 0.53
	ATOM	15 O	ARG S 94	-33.609 20.841 17.874 1.00 -0.50
	ATOM	16 CB	ARG S 94	-34.128 19.146 14.929 1.00 0.05
20	ATOM	17 CG	ARG S 94	-33.300 18.494 13.811 1.00 0.06
	ATOM	18 CD	ARG S 94	-34.051 18.379 12.475 1.00 0.11
	ATOM	19 NE	ARG S 94	-33.282 17.579 11.523 1.00 -0.49
	ATOM	20 CZ	ARG S 94	-33.792 16.435 11.016 1.00 0.81
	ATOM	21 NH1	ARG S 94	-35.003 15.996 11.360 1.00 -0.63
25	ATOM	22 NH2	ARG S 94	-33.068 15.730 10.153 1.00 -0.63
	ATOM	23 H	ARG S 94	-34.386 17.167 16.817 1.00 0.25
	ATOM	24 HE	ARG S 94	-32.370 17.873 11.238 1.00 0.29
	ATOM	25 1HH1	ARG S 94	-35.352 15.145 10.968 1.00 0.36
	ATOM	26 2HH1	ARG S 94	-35.565 16.510 12.008 1.00 0.36
30	ATOM	27 1HH2	ARG S 94	-33.433 14.882 9.769 1.00 0.36
	ATOM	28 2HH2	ARG S 94	-32.159 16.050 9.887 1.00 0.36
	ATOM	29 N	ASN S 95	-35.397 19.461 17.721 1.00 -0.52
	ATOM	30 CA	ASN S 95	-36.183 20.166 18.729 1.00 0.22
	ATOM	31 C	ASN S 95	-37.332 19.318 19.219 1.00 0.53
35	ATOM	32 O	ASN S 95	-37.969 18.605 18.430 1.00 -0.50
	ATOM	33 CB	ASN S 95	-36.706 21.522 18.229 1.00 0.00

	ATOM	34	CG	ASN S	95	-36.363	22.606	19.233	1.00	0.68
	ATOM	35	OD1	ASN S	95	-37.231	23.137	19.913	1.00	-0.47
	ATOM	36	ND2	ASN S	95	-35.056	22.909	19.294	1.00	-0.87
	ATOM	37	H	ASN S	95	-35.797	18.657	17.281	1.00	0.25
5	ATOM	38	1HD2	ASN S	95	-34.725	23.610	19.925	1.00	0.34
	ATOM	39	2HD2	ASN S	95	-34.397	22.435	18.709	1.00	0.34
	ATOM	40	N	LEU S	96	-37.598	19.391	20.520	1.00	-0.52
	ATOM	41	CA	LEU S	96	-38.679	18.626	21.134	1.00	0.20
	ATOM	42	C	LEU S	96	-39.965	19.383	20.901	1.00	0.53
10	ATOM	43	O	LEU S	96	-40.388	20.181	21.751	1.00	-0.50
	ATOM	44	CB	LEU S	96	-38.396	18.419	22.630	1.00	0.02
	ATOM	45	CG	LEU S	96	-37.665	17.107	22.956	1.00	0.05
	ATOM	46	CD1	LEU S	96	-38.413	15.848	22.489	1.00	-0.01
	ATOM	47	CD2	LEU S	96	-36.219	17.129	22.436	1.00	-0.01
15	ATOM	48	H	LEU S	96	-37.044	19.987	21.103	1.00	0.25
	ATOM	49	N	THR S	97	-40.588	19.136	19.753	1.00	-0.52
	ATOM	50	CA	THR S	97	-41.840	19.794	19.394	1.00	0.27
	ATOM	51	C	THR S	97	-42.809	18.826	18.759	1.00	0.53
	ATOM	52	O	THR S	97	-42.400	17.929	18.007	1.00	-0.50
20	ATOM	53	CB	THR S	97	-41.572	20.990	18.466	1.00	0.21
	ATOM	54	OG1	THR S	97	-42.795	21.657	18.160	1.00	-0.55
	ATOM	55	CG2	THR S	97	-40.854	20.578	17.171	1.00	0.01
	ATOM	56	H	THR S	97	-40.193	18.480	19.110	1.00	0.25
	ATOM	57	HG1	THR S	97	-42.562	22.479	17.722	1.00	0.31
25	ATOM	58	N	ILE S	98	-44.093	19.003	19.059	1.00	-0.52
	ATOM	59	CA	ILE S	98	-45.140	18.142	18.518	1.00	0.20
	ATOM	60	C	ILE S	98	-46.361	18.894	18.043	1.00	0.53
	ATOM	61	O	ILE S	98	-46.834	19.818	18.721	1.00	-0.50
	ATOM	62	CB	ILE S	98	-45.444	17.014	19.516	1.00	0.03
30	ATOM	63	CG1	ILE S	98	-46.244	15.862	18.888	1.00	0.02
	ATOM	64	CG2	ILE S	98	-46.123	17.547	20.788	1.00	0.00
	ATOM	65	CD1	ILE S	98	-45.346	14.810	18.219	1.00	0.00
	ATOM	66	H	ILE S	98	-44.356	19.747	19.673	1.00	0.25
	ATOM	67	N	VAL S	99	-46.872	18.500	16.880	1.00	-0.52
35	ATOM	68	CA	VAL S	99	-48.051	19.135	16.298	1.00	0.20
	ATOM	69	C	VAL S	99	-49.253	18.226	16.395	1.00	0.53

76

```
      ATOM  70  O   VAL S 99   -49.110 16.994 16.408 1.00 -0.50
      ATOM  71  CB  VAL S 99   -47.698 19.525 14.854 1.00  0.03
      ATOM  72  CG1 VAL S 99   -46.688 20.681 14.780 1.00  0.01
      ATOM  73  CG2 VAL S 99   -47.287 18.331 13.978 1.00  0.01
 5    ATOM  74  H   VAL S 99   -46.441 17.747 16.383 1.00  0.25
      ATOM  75  N   ASP S 100  -50.436 18.829 16.461 1.00 -0.52
      ATOM  76  CA  ASP S 100  -51.684 18.077 16.557 1.00  0.25
      ATOM  77  C   ASP S 100  -51.849 17.392 15.222 1.00  0.53
      ATOM  78  O   ASP S 100  -51.673 16.169 15.115 1.00 -0.50
10    ATOM  79  CB  ASP S 100  -52.858 19.041 16.789 1.00 -0.21
      ATOM  80  CG  ASP S 100  -52.508 20.428 16.287 1.00  0.62
      ATOM  81  OD1 ASP S 100  -52.854 20.755 15.156 1.00 -0.71
      ATOM  82  OD2 ASP S 100  -51.889 21.189 17.023 1.00 -0.71
      ATOM  83  H   ASP S 100  -50.481 19.828 16.445 1.00  0.25
15    ATOM  84  N   SER S 101  -52.187 18.177 14.202 1.00 -0.52
      ATOM  85  CA  SER S 101  -52.382 17.652 12.854 1.00  0.29
      ATOM  86  C   SER S 101  -53.017 16.282 12.846 1.00  0.53
      ATOM  87  O   SER S 101  -52.684 15.439 12.000 1.00 -0.50
      ATOM  88  CB  SER S 101  -51.034 17.621 12.116 1.00  0.19
20    ATOM  89  OG  SER S 101  -51.236 17.656 10.705 1.00 -0.55
      ATOM  90  H   SER S 101  -52.314 19.157 14.356 1.00  0.25
      ATOM  91  HG  SER S 101  -50.419 17.987 10.324 1.00  0.31
      ATOM  92  N   GLY S 102  -53.930 16.058 13.786 1.00 -0.52
      ATOM  93  CA  GLY S 102  -54.626 14.779 13.900 1.00  0.25
25    ATOM  94  C   GLY S 102  -53.788 13.536 13.720 1.00  0.53
      ATOM  95  O   GLY S 102  -54.199 12.596 13.024 1.00 -0.50
      ATOM  96  H   GLY S 102  -54.153 16.782 14.439 1.00  0.25
      ATOM  97  N   LEU S 103  -52.615 13.527 14.347 1.00 -0.52
      ATOM  98  CA  LEU S 103  -51.701 12.392 14.263 1.00  0.20
30    ATOM  99  C   LEU S 103  -51.521 11.844 15.658 1.00  0.53
      ATOM 100  O   LEU S 103  -51.586 12.596 16.643 1.00 -0.50
      ATOM 101  CB  LEU S 103  -50.367 12.833 13.641 1.00  0.02
      ATOM 102  CG  LEU S 103  -49.757 14.089 14.284 1.00  0.05
      ATOM 103  CD1 LEU S 103  -48.873 13.793 15.505 1.00 -0.01
35    ATOM 104  CD2 LEU S 103  -49.015 14.944 13.244 1.00 -0.01
      ATOM 105  H   LEU S 103  -52.343 14.319 14.894 1.00  0.25
```

77

SUBSTITUTE SHEET (RULE 26)

```
      ATOM  106 N   LYS S 104   -51.296 10.536 15.747 1.00 -0.52
      ATOM  107 CA  LYS S 104   -51.102  9.870 17.032 1.00  0.23
      ATOM  108 C   LYS S 104   -49.623  9.824 17.329 1.00  0.53
      ATOM  109 O   LYS S 104   -49.013  8.744 17.326 1.00 -0.50
  5   ATOM  110 CB  LYS S 104   -51.738  8.471 17.005 1.00  0.04
      ATOM  111 CG  LYS S 104   -52.308  8.008 18.355 1.00  0.05
      ATOM  112 CD  LYS S 104   -53.074  6.679 18.249 1.00  0.05
      ATOM  113 CE  LYS S 104   -52.171  5.461 18.503 1.00  0.22
      ATOM  114 NZ  LYS S 104   -52.891  4.233 18.143 1.00 -0.27
 10   ATOM  115 H   LYS S 104   -51.256  9.986 14.913 1.00  0.25
      ATOM  116 1HZ LYS S 104   -53.368  4.364 17.227 1.00  0.31
      ATOM  117 2HZ LYS S 104   -53.600  4.018 18.873 1.00  0.31
      ATOM  118 3HZ LYS S 104   -52.219  3.443 18.071 1.00  0.31
      ATOM  119 N   PHE S 105   -49.043 10.993 17.585 1.00 -0.52
 15   ATOM  120 CA  PHE S 105   -47.619 11.101 17.889 1.00  0.21
      ATOM  121 C   PHE S 105   -46.933 10.882 16.562 1.00  0.53
      ATOM  122 O   PHE S 105   -46.495 11.844 15.914 1.00 -0.50
      ATOM  123 CB  PHE S 105   -47.162 10.024 18.886 1.00  0.04
      ATOM  124 CG  PHE S 105   -45.861 10.412 19.549 1.00  0.01
 20   ATOM  125 CD1 PHE S 105   -44.683  9.692 19.251 1.00 -0.01
      ATOM  126 CD2 PHE S 105   -45.849 11.493 20.457 1.00 -0.01
      ATOM  127 CE1 PHE S 105   -43.474 10.058 19.873 1.00  0.00
      ATOM  128 CE2 PHE S 105   -44.641 11.860 21.078 1.00  0.00
      ATOM  129 CZ  PHE S 105   -43.466 11.139 20.780 1.00  0.00
 25   ATOM  130 H   PHE S 105   -49.592 11.829 17.571 1.00  0.25
      ATOM  131 N   VAL S 106   -46.838  9.619 16.156 1.00 -0.52
      ATOM  132 CA  VAL S 106   -46.200  9.259 14.893 1.00  0.20
      ATOM  133 C   VAL S 106   -44.818  9.859 14.800 1.00  0.53
      ATOM  134 O   VAL S 106   -44.261  9.989 13.699 1.00 -0.50
 30   ATOM  135 CB  VAL S 106   -47.136  9.709 13.760 1.00  0.03
      ATOM  136 CG1 VAL S 106   -46.649  9.261 12.372 1.00  0.01
      ATOM  137 CG2 VAL S 106   -48.612  9.356 14.005 1.00  0.01
      ATOM  138 H   VAL S 106   -47.213  8.889 16.726 1.00  0.25
      ATOM  139 N   ALA S 107   -44.263 10.225 15.951 1.00 -0.52
 35   ATOM  140 CA  ALA S 107   -42.930 10.820 16.013 1.00  0.22
      ATOM  141 C   ALA S 107   -42.034  9.846 16.740 1.00  0.53
```

78

```
     ATOM  142 O   ALA S 107   -41.035 10.247 17.354 1.00 -0.50
     ATOM  143 CB  ALA S 107   -42.939 12.156 16.772 1.00  0.03
     ATOM  144 H   ALA S 107   -44.766 10.093 16.805 1.00  0.25
     ATOM  145 N   TYR S 108   -42.388  8.565 16.671 1.00 -0.52
  5  ATOM  146 CA  TYR S 108   -41.616  7.513 17.325 1.00  0.25
     ATOM  147 C   TYR S 108   -40.181  7.445 16.861 1.00  0.53
     ATOM  148 O   TYR S 108   -39.320  6.888 17.557 1.00 -0.50
     ATOM  149 CB  TYR S 108   -42.269  6.142 17.090 1.00  0.02
     ATOM  150 CG  TYR S 108   -43.761  6.173 17.332 1.00  0.00
 10  ATOM  151 CD1 TYR S 108   -44.625  6.208 16.220 1.00 -0.04
     ATOM  152 CD2 TYR S 108   -44.248  6.166 18.656 1.00 -0.04
     ATOM  153 CE1 TYR S 108   -46.012  6.237 16.436 1.00  0.10
     ATOM  154 CE2 TYR S 108   -45.636  6.196 18.871 1.00  0.10
     ATOM  155 CZ  TYR S 108   -46.500  6.231 17.759 1.00 -0.12
 15  ATOM  156 OH  TYR S 108   -47.863  6.259 17.970 1.00 -0.37
     ATOM  157 H   TYR S 108   -43.207  8.308 16.159 1.00  0.25
     ATOM  158 HH  TYR S 108   -48.199  7.127 17.791 1.00  0.34
     ATOM  159 N   LYS S 109   -39.921  8.011 15.685 1.00 -0.52
     ATOM  160 CA  LYS S 109   -38.579  8.021 15.112 1.00  0.23
 20  ATOM  161 C   LYS S 109   -37.724  8.976 15.910 1.00  0.53
     ATOM  162 O   LYS S 109   -36.497  8.811 15.985 1.00 -0.50
     ATOM  163 CB  LYS S 109   -38.641  8.396 13.622 1.00  0.04
     ATOM  164 CG  LYS S 109   -39.200  9.801 13.345 1.00  0.05
     ATOM  165 CD  LYS S 109   -40.553  9.764 12.617 1.00  0.05
 25  ATOM  166 CE  LYS S 109   -41.148 11.167 12.416 1.00  0.22
     ATOM  167 NZ  LYS S 109   -42.394 11.066 11.645 1.00 -0.27
     ATOM  168 H   LYS S 109   -40.662  8.444 15.173 1.00  0.25
     ATOM  169 1HZ LYS S 109   -42.761 12.020 11.449 1.00  0.31
     ATOM  170 2HZ LYS S 109   -43.099 10.531 12.191 1.00  0.31
 30  ATOM  171 3HZ LYS S 109   -42.209 10.576 10.746 1.00  0.31
     ATOM  172 N   ALA S 110   -38.368  9.974 16.509 1.00 -0.52
     ATOM  173 CA  ALA S 110   -37.671 10.972 17.314 1.00  0.22
     ATOM  174 C   ALA S 110   -37.673 10.482 18.742 1.00  0.53
     ATOM  175 O   ALA S 110   -36.724 10.741 19.497 1.00 -0.50
 35  ATOM  176 CB  ALA S 110   -38.368 12.341 17.251 1.00  0.03
     ATOM  177 H   ALA S 110   -39.360 10.050 16.409 1.00  0.25
```

79

```
        ATOM  178 N   PHE S 111    -38.736  9.775 19.114 1.00 -0.52
        ATOM  179 CA  PHE S 111    -38.873  9.238 20.465 1.00  0.21
        ATOM  180 C   PHE S 111    -37.731  8.259 20.599 1.00  0.53
        ATOM  181 O   PHE S 111    -37.123  8.144 21.673 1.00 -0.50
   5    ATOM  182 CB  PHE S 111    -40.207  8.499 20.656 1.00  0.04
        ATOM  183 CG  PHE S 111    -40.461  8.200 22.115 1.00  0.01
        ATOM  184 CD1 PHE S 111    -41.035  9.191 22.942 1.00 -0.01
        ATOM  185 CD2 PHE S 111    -40.116  6.930 22.626 1.00 -0.01
        ATOM  186 CE1 PHE S 111    -41.269  8.906 24.301 1.00  0.00
  10    ATOM  187 CE2 PHE S 111    -40.349  6.645 23.983 1.00  0.00
        ATOM  188 CZ  PHE S 111    -40.924  7.636 24.807 1.00  0.00
        ATOM  189 H   PHE S 111    -39.467  9.602 18.455 1.00  0.25
        ATOM  190 N   LEU S 112    -37.439  7.552 19.511 1.00 -0.52
        ATOM  191 CA  LEU S 112    -36.360  6.568 19.494 1.00  0.20
  15    ATOM  192 C   LEU S 112    -35.074  7.293 19.811 1.00  0.53
        ATOM  193 O   LEU S 112    -34.249  6.798 20.594 1.00 -0.50
        ATOM  194 CB  LEU S 112    -36.305  5.868 18.127 1.00  0.02
        ATOM  195 CG  LEU S 112    -35.374  4.646 18.082 1.00  0.05
        ATOM  196 CD1 LEU S 112    -36.074  3.321 18.421 1.00 -0.01
  20    ATOM  197 CD2 LEU S 112    -34.628  4.563 16.740 1.00 -0.01
        ATOM  198 H   LEU S 112    -37.970  7.692 18.675 1.00  0.25
        ATOM  199 N   LYS S 113    -34.900  8.464 19.205 1.00 -0.52
        ATOM  200 CA  LYS S 113    -33.705  9.275 19.417 1.00  0.23
        ATOM  201 C   LYS S 113    -33.633  9.650 20.878 1.00  0.53
  25    ATOM  202 O   LYS S 113    -32.578  9.508 21.513 1.00 -0.50
        ATOM  203 CB  LYS S 113    -33.728 10.505 18.496 1.00  0.04
        ATOM  204 CG  LYS S 113    -33.318 10.217 17.043 1.00  0.05
        ATOM  205 CD  LYS S 113    -33.954 11.198 16.045 1.00  0.05
        ATOM  206 CE  LYS S 113    -33.790 10.739 14.587 1.00  0.22
  30    ATOM  207 NZ  LYS S 113    -34.498  9.467 14.390 1.00 -0.27
        ATOM  208 H   LYS S 113    -35.605  8.807 18.585 1.00  0.25
        ATOM  209 1HZ LYS S 113    -35.239  9.365 15.113 1.00  0.31
        ATOM  210 2HZ LYS S 113    -33.826  8.678 14.472 1.00  0.31
        ATOM  211 3HZ LYS S 113    -34.933  9.453 13.446 1.00  0.31
  35    ATOM  212 N   ASN S 114    -34.754 10.128 21.412 1.00 -0.52
        ATOM  213 CA  ASN S 114    -34.832 10.531 22.813 1.00  0.22
```

80

```
        ATOM   214 C    ASN S 114    -34.508  9.379 23.733 1.00  0.53
        ATOM   215 O    ASN S 114    -33.878  9.570 24.784 1.00 -0.50
        ATOM   216 CB   ASN S 114    -36.198 11.131 23.180 1.00  0.00
        ATOM   217 CG   ASN S 114    -36.349 12.495 22.535 1.00  0.68
   5    ATOM   218 OD1  ASN S 114    -37.101 12.669 21.585 1.00 -0.47
        ATOM   219 ND2  ASN S 114    -35.597 13.457 23.097 1.00 -0.87
        ATOM   220 H    ASN S 114    -35.572 10.217 20.844 1.00  0.25
        ATOM   221 1HD2 ASN S 114    -35.623 14.393 22.746 1.00  0.34
        ATOM   222 2HD2 ASN S 114    -35.002 13.248 23.873 1.00  0.34
  10    ATOM   223 N    SER S 115    -34.937  8.182 23.342 1.00 -0.52
        ATOM   224 CA   SER S 115    -34.696  6.977 24.131 1.00  0.29
        ATOM   225 C    SER S 115    -33.240  6.580 24.160 1.00  0.53
        ATOM   226 O    SER S 115    -32.755  6.037 25.165 1.00 -0.50
        ATOM   227 CB   SER S 115    -35.553  5.825 23.584 1.00  0.19
  15    ATOM   228 OG   SER S 115    -36.939  6.156 23.655 1.00 -0.55
        ATOM   229 H    SER S 115    -35.440  8.096 22.482 1.00  0.25
        ATOM   230 HG   SER S 115    -37.081  6.859 23.017 1.00  0.31
        ATOM   231 N    ASN S 116    -32.540  6.850 23.062 1.00 -0.52
        ATOM   232 CA   ASN S 116    -31.121  6.522 22.949 1.00  0.22
  20    ATOM   233 C    ASN S 116    -30.264  7.559 23.632 1.00  0.53
        ATOM   234 O    ASN S 116    -29.329  7.216 24.372 1.00 -0.50
        ATOM   235 CB   ASN S 116    -30.671  6.343 21.490 1.00  0.00
        ATOM   236 CG   ASN S 116    -30.988  4.935 21.025 1.00  0.68
        ATOM   237 OD1  ASN S 116    -30.139  4.053 21.046 1.00 -0.47
  25    ATOM   238 ND2  ASN S 116    -32.252  4.764 20.603 1.00 -0.87
        ATOM   239 H    ASN S 116    -32.991  7.290 22.286 1.00  0.25
        ATOM   240 1HD2 ASN S 116    -32.564  3.872 20.275 1.00  0.34
        ATOM   241 2HD2 ASN S 116    -32.898  5.528 20.611 1.00  0.34
        ATOM   242 N    LEU S 117    -30.578  8.828 23.387 1.00 -0.52
  30    ATOM   243 CA   LEU S 117    -29.835  9.937 23.980 1.00  0.23
        ATOM   244 C    LEU S 117    -30.840 10.862 24.645 1.00  0.50
        ATOM   245 O    LEU S 117    -31.725 11.354 23.951 1.00 -0.25
        ATOM   246 CB   LEU S 117    -29.015 10.660 22.900 1.00  0.02
        ATOM   247 CG   LEU S 117    -27.751  9.905 22.458 1.00  0.05
  35    ATOM   248 CD1  LEU S 117    -27.875  9.246 21.075 1.00 -0.01
        ATOM   249 CD2  LEU S 117    -26.506 10.802 22.546 1.00 -0.01
```

81

SUBSTITUTE SHEET (RULE 26)

ATOM   250 OXT LEU S 117   -30.723 11.077 25.849 1.00 -0.25

ATOM   251 H   LEU S 117   -31.344   9.038 22.780 1.00 0.25

END

*Principal residues are bolded.

82

Appendix 3. Geometry of the p75^{NTR} binding site for neurotrophins in PDB format.*

REMARK	1	Second CRD of p75^{NTR}, bound to NGF.						
REMARK	2							
ATOM	1	N	CYS R	39	-32.488	-11.161	6.915	1.00 0.00
ATOM	2	CA	CYS R	39	-33.024	-9.817	7.111	1.00 0.00
ATOM	3	C	CYS R	39	-33.595	-9.148	5.878	1.00 0.00
ATOM	4	O	CYS R	39	-34.221	-8.095	5.967	1.00 0.00
ATOM	5	CB	CYS R	39	-31.991	-8.907	7.780	1.00 0.00
ATOM	6	SG	CYS R	39	-30.272	-9.354	7.401	1.00 0.00
ATOM	7	1H	CYS R	39	-31.698	-11.178	6.287	1.00 0.00
ATOM	8	2H	CYS R	39	-32.170	-11.586	7.775	1.00 0.00
ATOM	9	3H	CYS R	39	-33.166	-11.799	6.523	1.00 0.00
ATOM	10	N	LEU R	40	-33.398	-9.779	4.707	1.00 0.00
ATOM	11	CA	LEU R	40	-34.095	-9.260	3.530	1.00 0.00
ATOM	12	C	LEU R	40	-35.322	-10.097	3.220	1.00 0.00
ATOM	13	O	LEU R	40	-36.442	-9.632	3.041	1.00 0.00
ATOM	14	CB	LEU R	40	-33.148	-9.230	2.327	1.00 0.00
ATOM	15	CG	LEU R	40	-31.880	-8.404	2.561	1.00 0.00
ATOM	16	CD1	LEU R	40	-30.862	-8.604	1.438	1.00 0.00
ATOM	17	CD2	LEU R	40	-32.184	-6.924	2.806	1.00 0.00
ATOM	18	H	LEU R	40	-32.867	-10.625	4.675	1.00 0.00
ATOM	19	N	ASP R	41	-35.034	-11.407	3.188	1.00 0.00
ATOM	20	CA	ASP R	41	-36.070	-12.408	2.947	1.00 0.00
ATOM	21	C	ASP R	41	-35.822	-13.609	3.848	1.00 0.00
ATOM	22	O	ASP R	41	-34.792	-13.673	4.525	1.00 0.00
ATOM	23	CB	ASP R	41	-36.054	-12.772	1.449	1.00 0.00
ATOM	24	CG	ASP R	41	-37.195	-13.703	1.074	1.00 0.00
ATOM	25	OD1	ASP R	41	-38.299	-13.520	1.568	1.00 0.00
ATOM	26	OD2	ASP R	41	-36.979	-14.633	0.314	1.00 0.00
ATOM	27	H	ASP R	41	-34.111	-11.739	3.385	1.00 0.00
ATOM	28	N	SER R	42	-36.757	-14.563	3.825	1.00 0.00
ATOM	29	CA	SER R	42	-36.565	-15.812	4.545	1.00 0.00
ATOM	30	C	SER R	42	-35.305	-16.572	4.150	1.00 0.00
ATOM	31	O	SER R	42	-34.755	-17.350	4.918	1.00 0.00

ATOM	32	CB	SER	R	42	-37.816	-16.678	4.398	1.00 0.00
ATOM	33	OG	SER	R	42	-38.988	-15.930	4.780	1.00 0.00
ATOM	34	H	SER	R	42	-37.497	-14.449	3.168	1.00 0.00
ATOM	35	HG	SER	R	42	-39.404	-15.604	3.984	1.00 0.00
ATOM	36	N	VAL	R	43	-34.794	-16.284	2.940	1.00 0.00
ATOM	37	CA	VAL	R	43	-33.503	-16.883	2.574	1.00 0.00
ATOM	38	C	VAL	R	43	-32.270	-16.339	3.305	1.00 0.00
ATOM	39	O	VAL	R	43	-31.128	-16.743	3.081	1.00 0.00
ATOM	40	CB	VAL	R	43	-33.300	-16.823	1.054	1.00 0.00
ATOM	41	CG1	VAL	R	43	-34.389	-17.623	0.337	1.00 0.00
ATOM	42	CG2	VAL	R	43	-33.208	-15.383	0.537	1.00 0.00
ATOM	43	H	VAL	R	43	-35.321	-15.679	2.336	1.00 0.00
ATOM	44	N	THR	R	44	-32.539	-15.360	4.166	1.00 0.00
ATOM	45	CA	THR	R	44	-31.443	-14.732	4.879	1.00 0.00
ATOM	46	C	THR	R	44	-31.701	-14.680	6.367	1.00 0.00
ATOM	47	O	THR	R	44	-32.659	-14.063	6.830	1.00 0.00
ATOM	48	CB	THR	R	44	-31.171	-13.339	4.300	1.00 0.00
ATOM	49	OG1	THR	R	44	-32.382	-12.578	4.130	1.00 0.00
ATOM	50	CG2	THR	R	44	-30.430	-13.431	2.962	1.00 0.00
ATOM	51	H	THR	R	44	-33.481	-15.090	4.359	1.00 0.00
ATOM	52	HG1	THR	R	44	-33.031	-12.981	4.718	1.00 0.00
ATOM	53	N	PHE	R	45	-30.805	-15.368	7.080	1.00 0.00
ATOM	54	CA	PHE	R	45	-30.829	-15.256	8.526	1.00 0.00
ATOM	55	C	PHE	R	45	-30.085	-13.996	8.932	1.00 0.00
ATOM	56	O	PHE	R	45	-29.293	-13.430	8.175	1.00 0.00
ATOM	57	CB	PHE	R	45	-30.243	-16.531	9.157	1.00 0.00
ATOM	58	CG	PHE	R	45	-30.514	-16.587	10.647	1.00 0.00
ATOM	59	CD1	PHE	R	45	-31.844	-16.581	11.126	1.00 0.00
ATOM	60	CD2	PHE	R	45	-29.423	-16.628	11.539	1.00 0.00
ATOM	61	CE1	PHE	R	45	-32.085	-16.592	12.512	1.00 0.00
ATOM	62	CE2	PHE	R	45	-29.661	-16.637	12.927	1.00 0.00
ATOM	63	CZ	PHE	R	45	-30.989	-16.611	13.400	1.00 0.00
ATOM	64	H	PHE	R	45	-30.025	-15.788	6.623	1.00 0.00
ATOM	65	N	SER	R	46	-30.382	-13.575	10.161	1.00 0.00
ATOM	66	CA	SER	R	46	-29.961	-12.259	10.626	1.00 0.00
ATOM	67	C	SER	R	46	-28.732	-12.274	11.517	1.00 0.00

84

	ATOM	68	O	SER R	46	-28.497	-11.407	12.346	1.00	0.00
	ATOM	69	CB	SER R	46	-31.156	-11.630	11.337	1.00	0.00
	ATOM	70	OG	SER R	46	-31.890	-12.664	12.026	1.00	0.00
	ATOM	71	H	SER R	46	-31.046	-14.080	10.714	1.00	0.00
5	ATOM	72	HG	SER R	46	-32.811	-12.512	11.820	1.00	0.00
	ATOM	73	N	ASP R	47	-27.906	-13.314	11.317	1.00	0.00
	ATOM	74	CA	ASP R	47	-26.772	-13.543	12.226	1.00	0.00
	ATOM	75	C	ASP R	47	-25.567	-12.610	12.077	1.00	0.00
	ATOM	76	O	ASP R	47	-24.410	-13.027	12.086	1.00	0.00
10	ATOM	77	CB	ASP R	47	-26.337	-15.025	12.168	1.00	0.00
	ATOM	78	CG	ASP R	47	-25.807	-15.429	10.794	1.00	0.00
	ATOM	79	OD1	ASP R	47	-26.456	-15.180	9.790	1.00	0.00
	ATOM	80	OD2	ASP R	47	-24.712	-15.961	10.694	1.00	0.00
	ATOM	81	H	ASP R	47	-28.048	-13.919	10.531	1.00	0.00
15	ATOM	82	N	VAL R	48	-25.857	-11.312	11.875	1.00	0.00
	ATOM	83	CA	VAL R	48	-24.733	-10.395	11.691	1.00	0.00
	ATOM	84	C	VAL R	48	-24.130	-9.906	13.003	1.00	0.00
	ATOM	85	O	VAL R	48	-22.914	-9.763	13.131	1.00	0.00
	ATOM	86	CB	VAL R	48	-25.108	-9.258	10.720	1.00	0.00
20	ATOM	87	CG1	VAL R	48	-26.299	-8.421	11.194	1.00	0.00
	ATOM	88	CG2	VAL R	48	-23.886	-8.416	10.349	1.00	0.00
	ATOM	89	H	VAL R	48	-26.767	-10.954	12.073	1.00	0.00
	ATOM	90	N	VAL R	49	-25.034	-9.713	13.984	1.00	0.00
	ATOM	91	CA	VAL R	49	-24.767	-9.685	15.431	1.00	0.00
25	ATOM	92	C	VAL R	49	-23.506	-9.045	16.022	1.00	0.00
	ATOM	93	O	VAL R	49	-23.103	-9.361	17.142	1.00	0.00
	ATOM	94	CB	VAL R	49	-25.003	-11.080	16.043	1.00	0.00
	ATOM	95	CG1	VAL R	49	-26.440	-11.541	15.783	1.00	0.00
	ATOM	96	CG2	VAL R	49	-23.973	-12.125	15.594	1.00	0.00
30	ATOM	97	H	VAL R	49	-25.987	-9.707	13.681	1.00	0.00
	ATOM	98	N	SER R	50	-22.912	-8.118	15.261	1.00	0.00
	ATOM	99	CA	SER R	50	-21.729	-7.376	15.719	1.00	0.00
	ATOM	100	C	SER R	50	-21.546	-6.123	14.873	1.00	0.00
	ATOM	101	O	SER R	50	-21.505	-4.977	15.336	1.00	0.00
35	ATOM	102	CB	SER R	50	-20.431	-8.205	15.623	1.00	0.00
	ATOM	103	OG	SER R	50	-20.525	-9.489	16.273	1.00	0.00

85

```
      ATOM   104 H   SER R  50   -23.312 -7.897 14.372 1.00 0.00
      ATOM   105 HG  SER R  50   -21.302 -9.403 16.827 1.00 0.00
      ATOM   106 N   ALA R  51   -21.454 -6.446 13.572 1.00 0.00
      ATOM   107 CA  ALA R  51   -21.546 -5.403 12.562 1.00 0.00
  5   ATOM   108 C   ALA R  51   -23.013 -5.196 12.263 1.00 0.00
      ATOM   109 O   ALA R  51   -23.862 -5.866 12.848 1.00 0.00
      ATOM   110 CB  ALA R  51   -20.808 -5.825 11.288 1.00 0.00
      ATOM   111 H   ALA R  51   -21.633 -7.392 13.330 1.00 0.00
      ATOM   112 N   THR R  52   -23.266 -4.259 11.348 1.00 0.00
 10   ATOM   113 CA  THR R  52   -24.606 -3.698 11.228 1.00 0.00
      ATOM   114 C   THR R  52   -25.679 -4.557 10.579 1.00 0.00
      ATOM   115 O   THR R  52   -26.564 -5.091 11.239 1.00 0.00
      ATOM   116 CB  THR R  52   -24.481 -2.344 10.532 1.00 0.00
      ATOM   117 OG1 THR R  52   -23.205 -1.766 10.845 1.00 0.00
 15   ATOM   118 CG2 THR R  52   -25.624 -1.389 10.891 1.00 0.00
      ATOM   119 H   THR R  52   -22.533 -3.835 10.820 1.00 0.00
      ATOM   120 HG1 THR R  52   -23.136 -0.977 10.314 1.00 0.00
      ATOM   121 N   GLU R  53   -25.602 -4.625  9.241 1.00 0.00
      ATOM   122 CA  GLU R  53   -26.765 -5.151  8.526 1.00 0.00
 20   ATOM   123 C   GLU R  53   -26.656 -6.149  7.362 1.00 0.00
      ATOM   124 O   GLU R  53   -27.702 -6.492  6.808 1.00 0.00
      ATOM   125 CB  GLU R  53   -27.678 -3.966  8.146 1.00 0.00
      ATOM   126 CG  GLU R  53   -27.452 -3.289  6.779 1.00 0.00
      ATOM   127 CD  GLU R  53   -25.983 -3.036  6.488 1.00 0.00
 25   ATOM   128 OE1 GLU R  53   -25.530 -3.408  5.413 1.00 0.00
      ATOM   129 OE2 GLU R  53   -25.284 -2.484  7.329 1.00 0.00
      ATOM   130 H   GLU R  53   -24.901 -4.146  8.704 1.00 0.00
      ATOM   131 N   PRO R  54   -25.448 -6.634  6.953 1.00 0.00
      ATOM   132 CA  PRO R  54   -25.503 -7.661  5.912 1.00 0.00
 30   ATOM   133 C   PRO R  54   -26.227 -8.929  6.351 1.00 0.00
      ATOM   134 O   PRO R  54   -26.254 -9.343  7.509 1.00 0.00
      ATOM   135 CB  PRO R  54   -24.032 -7.892  5.550 1.00 0.00
      ATOM   136 CG  PRO R  54   -23.286 -6.653  6.033 1.00 0.00
      ATOM   137 CD  PRO R  54   -24.070 -6.275  7.278 1.00 0.00
 35   ATOM   138 N   CYS R  55   -26.841 -9.564  5.355 1.00 0.00
      ATOM   139 CA  CYS R  55   -27.561 -10.782 5.715 1.00 0.00
```

86

	ATOM	140	C	CYS R	55	-26.758	-12.020	5.403	1.00 0.00
	ATOM	141	O	CYS R	55	-25.722	-11.942	4.747	1.00 0.00
	ATOM	142	CB	CYS R	55	-28.884	-10.816	4.980	1.00 0.00
	ATOM	143	SG	CYS R	55	-29.966	-9.423	5.373	1.00 0.00
5	ATOM	144	H	CYS R	55	-26.798	-9.206	4.422	1.00 0.00
	ATOM	145	N	LYS R	56	-27.264	-13.165	5.871	1.00 0.00
	ATOM	146	CA	LYS R	56	-26.589	-14.362	5.398	1.00 0.00
	ATOM	147	C	LYS R	56	-27.549	-15.386	4.837	1.00 0.00
	ATOM	148	O	LYS R	56	-28.519	-15.789	5.477	1.00 0.00
10	ATOM	149	CB	LYS R	56	-25.714	-14.916	6.522	1.00 0.00
	ATOM	150	CG	LYS R	56	-24.805	-16.085	6.153	1.00 0.00
	ATOM	151	CD	LYS R	56	-23.591	-16.147	7.077	1.00 0.00
	ATOM	152	CE	LYS R	56	-23.022	-17.552	7.202	1.00 0.00
	ATOM	153	NZ	LYS R	56	-23.951	-18.331	8.015	1.00 0.00
15	ATOM	154	H	LYS R	56	-28.051	-13.262	6.482	1.00 0.00
	ATOM	155	1HZ	LYS R	56	-23.881	-18.006	8.995	1.00 0.00
	ATOM	156	2HZ	LYS R	56	-23.728	-19.338	7.946	1.00 0.00
	ATOM	157	3HZ	LYS R	56	-24.928	-18.196	7.691	1.00 0.00
	ATOM	158	N	PRO R	57	-27.236	-15.830	3.598	1.00 0.00
20	ATOM	159	CA	PRO R	57	-27.952	-16.989	3.057	1.00 0.00
	ATOM	160	C	PRO R	57	-27.718	-18.237	3.898	1.00 0.00
	ATOM	161	O	PRO R	57	-26.590	-18.524	4.312	1.00 0.00
	ATOM	162	CB	PRO R	57	-27.397	-17.079	1.631	1.00 0.00
	ATOM	163	CG	PRO R	57	-26.018	-16.418	1.682	1.00 0.00
25	ATOM	164	CD	PRO R	57	-26.218	-15.301	2.698	1.00 0.00
	ATOM	165	N	CYS R	58	-28.842	-18.939	4.129	1.00 0.00
	ATOM	166	CA	CYS R	58	-28.833	-20.145	4.956	1.00 0.00
	ATOM	167	C	CYS R	58	-28.246	-21.406	4.309	1.00 0.00
	ATOM	168	O	CYS R	58	-27.067	-21.414	3.958	1.00 0.00
30	ATOM	169	CB	CYS R	58	-30.219	-20.336	5.550	1.00 0.00
	ATOM	170	SG	CYS R	58	-31.446	-20.570	4.242	1.00 0.00
	ATOM	171	H	CYS R	58	-29.694	-18.544	3.776	1.00 0.00
	ATOM	172	N	THR R	59	-29.040	-22.485	4.171	1.00 0.00
	ATOM	173	CA	THR R	59	-28.405	-23.777	3.884	1.00 0.00
35	ATOM	174	C	THR R	59	-29.331	-24.758	3.170	1.00 0.00
	ATOM	175	O	THR R	59	-30.560	-24.647	3.205	1.00 0.00

87

	ATOM	176	CB	THR	R	59	-27.872	-24.385	5.190	1.00	0.00
	ATOM	177	OG1	THR	R	59	-27.853	-23.393	6.235	1.00	0.00
	ATOM	178	CG2	THR	R	59	-26.489	-25.021	5.023	1.00	0.00
	ATOM	179	H	THR	R	59	-30.024	-22.480	4.346	1.00	0.00
5	ATOM	180	HG1	THR	R	59	-27.610	-23.881	7.025	1.00	0.00
	ATOM	181	N	GLU	R	60	-28.701	-25.728	2.496	1.00	0.00
	ATOM	182	CA	GLU	R	60	-29.419	-26.674	1.647	1.00	0.00
	ATOM	183	C	GLU	R	60	-30.161	-27.753	2.390	1.00	0.00
	ATOM	184	O	GLU	R	60	-29.788	-28.927	2.459	1.00	0.00
10	ATOM	185	CB	GLU	R	60	-28.473	-27.229	0.578	1.00	0.00
	ATOM	186	CG	GLU	R	60	-28.436	-26.362	-0.692	1.00	0.00
	ATOM	187	CD	GLU	R	60	-28.332	-24.886	-0.343	1.00	0.00
	ATOM	188	OE1	GLU	R	60	-29.269	-24.151	-0.619	1.00	0.00
	ATOM	189	OE2	GLU	R	60	-27.340	-24.471	0.243	1.00	0.00
15	ATOM	190	H	GLU	R	60	-27.701	-25.728	2.526	1.00	0.00
	ATOM	191	N	CYS	R	61	-31.270	-27.273	2.945	1.00	0.00
	ATOM	192	CA	CYS	R	61	-32.170	-28.156	3.661	1.00	0.00
	ATOM	193	C	CYS	R	61	-33.085	-28.944	2.755	1.00	0.00
	ATOM	194	O	CYS	R	61	-34.299	-28.751	2.709	1.00	0.00
20	ATOM	195	CB	CYS	R	61	-32.910	-27.347	4.714	1.00	0.00
	ATOM	196	SG	CYS	R	61	-31.740	-26.942	6.031	1.00	0.00
	ATOM	197	H	CYS	R	61	-31.509	-26.320	2.772	1.00	0.00
	ATOM	198	N	VAL	R	62	-32.425	-29.827	1.999	1.00	0.00
	ATOM	199	CA	VAL	R	62	-33.134	-30.711	1.091	1.00	0.00
25	ATOM	200	C	VAL	R	62	-32.620	-32.122	1.268	1.00	0.00
	ATOM	201	O	VAL	R	62	-31.507	-32.351	1.744	1.00	0.00
	ATOM	202	CB	VAL	R	62	-32.966	-30.257	-0.371	1.00	0.00
	ATOM	203	CG1	VAL	R	62	-33.771	-28.988	-0.662	1.00	0.00
	ATOM	204	CG2	VAL	R	62	-31.491	-30.099	-0.762	1.00	0.00
30	ATOM	205	H	VAL	R	62	-31.439	-29.935	2.116	1.00	0.00
	ATOM	206	N	GLY	R	63	-33.482	-33.057	0.831	1.00	0.00
	ATOM	207	CA	GLY	R	63	-33.115	-34.472	0.773	1.00	0.00
	ATOM	208	C	GLY	R	63	-32.332	-34.987	1.965	1.00	0.00
	ATOM	209	O	GLY	R	63	-32.817	-35.076	3.086	1.00	0.00
35	ATOM	210	H	GLY	R	63	-34.346	-32.742	0.449	1.00	0.00
	ATOM	211	N	LEU	R	64	-31.064	-35.302	1.662	1.00	0.00

	ATOM	212	CA	LEU R 64	-30.174	-35.897	2.660	1.00	0.00
	ATOM	213	C	LEU R 64	-29.939	-35.063	3.905	1.00	0.00
	ATOM	214	O	LEU R 64	-29.748	-35.602	4.993	1.00	0.00
	ATOM	215	CB	LEU R 64	-28.818	-36.268	2.047	1.00	0.00
5	ATOM	216	CG	LEU R 64	-28.759	-37.594	1.273	1.00	0.00
	ATOM	217	CD1	LEU R 64	-29.223	-38.770	2.135	1.00	0.00
	ATOM	218	CD2	LEU R 64	-29.458	-37.548	-0.089	1.00	0.00
	ATOM	219	H	LEU R 64	-30.789	-35.155	0.715	1.00	0.00
	ATOM	220	N	GLN R 65	-29.920	-33.749	3.667	1.00	0.00
10	ATOM	221	CA	GLN R 65	-29.848	-32.806	4.767	1.00	0.00
	ATOM	222	C	GLN R 65	-31.138	-32.025	4.898	1.00	0.00
	ATOM	223	O	GLN R 65	-31.327	-30.896	4.444	1.00	0.00
	ATOM	224	CB	GLN R 65	-28.607	-31.923	4.628	1.00	0.00
	ATOM	225	CG	GLN R 65	-27.300	-32.698	4.852	1.00	0.00
15	ATOM	226	CD	GLN R 65	-27.227	-33.242	6.271	1.00	0.00
	ATOM	227	OE1	GLN R 65	-28.016	-32.916	7.148	1.00	0.00
	ATOM	228	NE2	GLN R 65	-26.211	-34.066	6.484	1.00	0.00
	ATOM	229	H	GLN R 65	-30.093	-33.389	2.753	1.00	0.00
	ATOM	230	1HE2	GLN R 65	-26.039	-34.449	7.390	1.00	0.00
20	ATOM	231	2HE2	GLN R 65	-25.596	-34.408	5.773	1.00	0.00
	ATOM	232	N	SER R 66	-32.061	-32.731	5.554	1.00	0.00
	ATOM	233	CA	SER R 66	-33.390	-32.190	5.816	1.00	0.00
	ATOM	234	C	SER R 66	-33.405	-31.182	6.954	1.00	0.00
	ATOM	235	O	SER R 66	-32.729	-31.340	7.966	1.00	0.00
25	ATOM	236	CB	SER R 66	-34.355	-33.332	6.140	1.00	0.00
	ATOM	237	OG	SER R 66	-34.545	-34.205	5.013	1.00	0.00
	ATOM	238	H	SER R 66	-31.773	-33.614	5.922	1.00	0.00
	ATOM	239	HG	SER R 66	-33.695	-34.243	4.566	1.00	0.00
	ATOM	240	N	MET R 67	-34.238	-30.147	6.731	1.00	0.00
30	ATOM	241	CA	MET R 67	-34.452	-29.049	7.683	1.00	0.00
	ATOM	242	C	MET R 67	-34.580	-29.454	9.146	1.00	0.00
	ATOM	243	O	MET R 67	-35.591	-30.030	9.547	1.00	0.00
	ATOM	244	CB	MET R 67	-35.701	-28.290	7.216	1.00	0.00
	ATOM	245	CG	MET R 67	-36.123	-27.081	8.053	1.00	0.00
35	ATOM	246	SD	MET R 67	-37.648	-26.329	7.454	1.00	0.00
	ATOM	247	CE	MET R 67	-37.010	-25.683	5.898	1.00	0.00

89

ATOM	248	H	MET R	67	-34.671	-30.083	5.833	1.00 0.00
ATOM	249	N	SER R	68	-33.535	-29.137	9.905	1.00 0.00
ATOM	250	CA	SER R	68	-33.655	-29.183	11.360	1.00 0.00
ATOM	251	C	SER R	68	-34.023	-27.827	11.919	1.00 0.00
ATOM	252	O	SER R	68	-34.862	-27.691	12.800	1.00 0.00
ATOM	253	CB	SER R	68	-32.358	-29.637	12.009	1.00 0.00
ATOM	254	OG	SER R	68	-31.643	-30.509	11.115	1.00 0.00
ATOM	255	H	SER R	68	-32.761	-28.695	9.455	1.00 0.00
ATOM	256	HG	SER R	68	-31.558	-30.009	10.294	1.00 0.00
ATOM	257	N	ALA R	69	-33.375	-26.830	11.302	1.00 0.00
ATOM	258	CA	ALA R	69	-33.917	-25.487	11.420	1.00 0.00
ATOM	259	C	ALA R	69	-34.131	-24.964	10.022	1.00 0.00
ATOM	260	O	ALA R	69	-33.406	-25.351	9.101	1.00 0.00
ATOM	261	CB	ALA R	69	-32.949	-24.567	12.163	1.00 0.00
ATOM	262	H	ALA R	69	-32.643	-27.065	10.660	1.00 0.00
ATOM	263	N	PRO R	70	-35.166	-24.103	9.901	1.00 0.00
ATOM	264	CA	PRO R	70	-35.349	-23.341	8.665	1.00 0.00
ATOM	265	C	PRO R	70	-34.275	-22.271	8.587	1.00 0.00
ATOM	266	O	PRO R	70	-33.227	-22.350	9.229	1.00 0.00
ATOM	267	CB	PRO R	70	-36.770	-22.793	8.852	1.00 0.00
ATOM	268	CG	PRO R	70	-36.928	-22.604	10.359	1.00 0.00
ATOM	269	CD	PRO R	70	-36.166	-23.793	10.921	1.00 0.00
ATOM	270	N	CYS R	71	-34.550	-21.233	7.785	1.00 0.00
ATOM	271	CA	CYS R	71	-33.601	-20.119	7.809	1.00 0.00
ATOM	272	C	CYS R	71	-33.970	-19.007	8.772	1.00 0.00
ATOM	273	O	CYS R	71	-33.266	-18.019	8.957	1.00 0.00
ATOM	274	CB	CYS R	71	-33.418	-19.571	6.407	1.00 0.00
ATOM	275	SG	CYS R	71	-33.225	-20.894	5.186	1.00 0.00
ATOM	276	H	CYS R	71	-35.393	-21.195	7.252	1.00 0.00
ATOM	277	N	VAL R	72	-35.153	-19.212	9.378	1.00 0.00
ATOM	278	CA	VAL R	72	-35.518	-18.365	10.505	1.00 0.00
ATOM	279	C	VAL R	72	-35.220	-19.134	11.781	1.00 0.00
ATOM	280	O	VAL R	72	-34.442	-20.088	11.731	1.00 0.00
ATOM	281	CB	VAL R	72	-36.968	-17.871	10.369	1.00 0.00
ATOM	282	CG1	VAL R	72	-37.035	-16.768	9.311	1.00 0.00
ATOM	283	CG2	VAL R	72	-37.963	-18.992	10.064	1.00 0.00

90

```
        ATOM  284 H   VAL R 72   -35.684 -20.042  9.226 1.00 0.00
        ATOM  285 N   GLU R 73   -35.790 -18.668 12.904 1.00 0.00
        ATOM  286 CA  GLU R 73   -35.488 -19.248 14.217 1.00 0.00
        ATOM  287 C   GLU R 73   -34.000 -19.471 14.515 1.00 0.00
  5     ATOM  288 O   GLU R 73   -33.279 -18.511 14.794 1.00 0.00
        ATOM  289 CB  GLU R 73   -36.399 -20.461 14.483 1.00 0.00
        ATOM  290 CG  GLU R 73   -37.842 -20.111 14.899 1.00 0.00
        ATOM  291 CD  GLU R 73   -38.628 -19.399 13.805 1.00 0.00
        ATOM  292 OE1 GLU R 73   -39.196 -20.066 12.948 1.00 0.00
  10    ATOM  293 OE2 GLU R 73   -38.693 -18.173 13.816 1.00 0.00
        ATOM  294 H   GLU R 73   -36.613 -18.100 12.819 1.00 0.00
        ATOM  295 N   ALA R 74   -33.549 -20.733 14.428 1.00 0.00
        ATOM  296 CA  ALA R 74   -32.139 -20.969 14.723 1.00 0.00
        ATOM  297 C   ALA R 74   -31.209 -20.464 13.628 1.00 0.00
  15    ATOM  298 O   ALA R 74   -31.627 -19.858 12.643 1.00 0.00
        ATOM  299 CB  ALA R 74   -31.896 -22.456 14.994 1.00 0.00
        ATOM  300 H   ALA R 74   -34.142 -21.443 14.054 1.00 0.00
        ATOM  301 N   ASP R 75   -29.901 -20.717 13.841 1.00 0.00
        ATOM  302 CA  ASP R 75   -28.988 -20.165 12.838 1.00 0.00
  20    ATOM  303 C   ASP R 75   -28.978 -20.946 11.540 1.00 0.00
        ATOM  304 O   ASP R 75   -28.907 -22.175 11.568 1.00 0.00
        ATOM  305 CB  ASP R 75   -27.570 -19.881 13.412 1.00 0.00
        ATOM  306 CG  ASP R 75   -26.502 -20.949 13.148 1.00 0.00
        ATOM  307 OD1 ASP R 75   -25.764 -20.841 12.170 1.00 0.00
  25    ATOM  308 OD2 ASP R 75   -26.375 -21.893 13.918 1.00 0.00
        ATOM  309 H   ASP R 75   -29.610 -21.308 14.596 1.00 0.00
        ATOM  310 N   ASP R 76   -29.031 -20.167 10.438 1.00 0.00
        ATOM  311 CA  ASP R 76   -28.563 -20.650  9.133 1.00 0.00
        ATOM  312 C   ASP R 76   -28.887 -22.099  8.799 1.00 0.00
  30    ATOM  313 O   ASP R 76   -28.004 -22.960  8.851 1.00 0.00
        ATOM  314 CB  ASP R 76   -27.048 -20.433  9.048 1.00 0.00
        ATOM  315 CG  ASP R 76   -26.651 -19.628  7.832 1.00 0.00
        ATOM  316 OD1 ASP R 76   -26.280 -20.197  6.821 1.00 0.00
        ATOM  317 OD2 ASP R 76   -26.657 -18.412  7.895 1.00 0.00
  35    ATOM  318 H   ASP R 76   -29.310 -19.218 10.546 1.00 0.00
        ATOM  319 N   ALA R 77   -30.181 -22.342  8.504 1.00 0.00
```

91

SUBSTITUTE SHEET (RULE 26)

```
      ATOM   320 CA  ALA R 77    -30.727 -23.675  8.210 1.00 0.00
      ATOM   321 C   ALA R 77    -29.903 -24.882  8.622 1.00 0.00
      ATOM   322 O   ALA R 77    -28.947 -25.313  7.977 1.00 0.00
      ATOM   323 CB  ALA R 77    -31.146 -23.786  6.745 1.00 0.00
   5  ATOM   324 H   ALA R 77    -30.762 -21.532  8.486 1.00 0.00
      ATOM   325 N   VAL R 78    -30.293 -25.370  9.804 1.00 0.00
      ATOM   326 CA  VAL R 78    -29.473 -26.437 10.365 1.00 0.00
      ATOM   327 C   VAL R 78    -29.674 -27.730  9.608 1.00 0.00
      ATOM   328 O   VAL R 78    -30.689 -28.419  9.719 1.00 0.00
  10  ATOM   329 CB  VAL R 78    -29.705 -26.621 11.875 1.00 0.00
      ATOM   330 CG1 VAL R 78    -28.824 -27.731 12.461 1.00 0.00
      ATOM   331 CG2 VAL R 78    -29.474 -25.311 12.630 1.00 0.00
      ATOM   332 H   VAL R 78    -31.196 -25.121 10.147 1.00 0.00
      ATOM   333 N   CYS R 79    -28.632 -28.038  8.838 1.00 0.00
  15  ATOM   334 CA  CYS R 79    -28.713 -29.247  8.033 1.00 0.00
      ATOM   335 C   CYS R 79    -27.339 -29.828  7.920 1.00 0.00
      ATOM   336 O   CYS R 79    -26.525 -29.376  7.119 1.00 0.00
      ATOM   337 CB  CYS R 79    -29.320 -28.928  6.669 1.00 0.00
      ATOM   338 SG  CYS R 79    -31.114 -28.721  6.825 1.00 0.00
  20  ATOM   339 H   CYS R 79    -27.953 -27.324  8.640 1.00 0.00
      ATOM   340 N   ARG R 80    -27.136 -30.778  8.851 1.00 0.00
      ATOM   341 CA  ARG R 80    -25.874 -31.473  9.118 1.00 0.00
      ATOM   342 C   ARG R 80    -26.145 -32.410 10.286 1.00 0.00
      ATOM   343 O   ARG R 80    -27.174 -32.258 10.947 1.00 0.00
  25  ATOM   344 CB  ARG R 80    -24.794 -30.457  9.480 1.00 0.00
      ATOM   345 CG  ARG R 80    -23.510 -30.612  8.671 1.00 0.00
      ATOM   346 CD  ARG R 80    -23.609 -30.483  7.144 1.00 0.00
      ATOM   347 NE  ARG R 80    -22.248 -30.464  6.602 1.00 0.00
      ATOM   348 CZ  ARG R 80    -21.752 -29.350  6.025 1.00 0.00
  30  ATOM   349 NH1 ARG R 80    -20.446 -29.201  5.899 1.00 0.00
      ATOM   350 NH2 ARG R 80    -22.565 -28.390  5.605 1.00 0.00
      ATOM   351 H   ARG R 80    -27.930 -31.029  9.408 1.00 0.00
      ATOM   352 HE  ARG R 80    -21.632 -31.222  6.850 1.00 0.00
      ATOM   353 1HH1 ARG R 80   -20.066 -28.349  5.510 1.00 0.00
  35  ATOM   354 2HH1 ARG R 80   -19.803 -29.904  6.220 1.00 0.00
      ATOM   355 1HH2 ARG R 80   -22.163 -27.510  5.312 1.00 0.00
```

92

	ATOM	356	2HH2	ARG	R	80	-23.555	-28.546	5.585	1.00	0.00
	ATOM	357	N	CYS	R	81	-25.254	-33.378	10.546	1.00	0.00
	ATOM	358	CA	CYS	R	81	-25.630	-34.302	11.618	1.00	0.00
	ATOM	359	C	CYS	R	81	-24.657	-34.425	12.779	1.00	0.00
5	ATOM	360	O	CYS	R	81	-23.437	-34.482	12.654	1.00	0.00
	ATOM	361	CB	CYS	R	81	-25.971	-35.691	11.060	1.00	0.00
	ATOM	362	SG	CYS	R	81	-27.286	-35.685	9.805	1.00	0.00
	ATOM	363	H	CYS	R	81	-24.383	-33.437	10.057	1.00	0.00
	ATOM	364	N	ALA	R	82	-25.276	-34.521	13.965	1.00	0.00
10	ATOM	365	CA	ALA	R	82	-24.515	-34.749	15.194	1.00	0.00
	ATOM	366	C	ALA	R	82	-25.304	-35.664	16.121	1.00	0.00
	ATOM	367	O	ALA	R	82	-26.298	-36.259	15.706	1.00	0.00
	ATOM	368	CB	ALA	R	82	-24.220	-33.410	15.880	1.00	0.00
	ATOM	369	H	ALA	R	82	-26.275	-34.483	13.959	1.00	0.00
15	ATOM	370	N	TYR	R	83	-24.873	-35.700	17.401	1.00	0.00
	ATOM	371	CA	TYR	R	83	-25.613	-36.307	18.519	1.00	0.00
	ATOM	372	C	TYR	R	83	-25.565	-37.827	18.584	1.00	0.00
	ATOM	373	O	TYR	R	83	-24.974	-38.412	19.487	1.00	0.00
	ATOM	374	CB	TYR	R	83	-27.078	-35.829	18.634	1.00	0.00
20	ATOM	375	CG	TYR	R	83	-27.226	-34.328	18.781	1.00	0.00
	ATOM	376	CD1	TYR	R	83	-26.962	-33.725	20.028	1.00	0.00
	ATOM	377	CD2	TYR	R	83	-27.670	-33.574	17.674	1.00	0.00
	ATOM	378	CE1	TYR	R	83	-27.210	-32.351	20.189	1.00	0.00
	ATOM	379	CE2	TYR	R	83	-27.914	-32.198	17.834	1.00	0.00
25	ATOM	380	CZ	TYR	R	83	-27.710	-31.608	19.099	1.00	0.00
	ATOM	381	OH	TYR	R	83	-28.024	-30.273	19.294	1.00	0.00
	ATOM	382	H	TYR	R	83	-23.940	-35.374	17.555	1.00	0.00
	ATOM	383	HH	TYR	R	83	-28.217	-29.854	18.456	1.00	0.00
	ATOM	384	N	GLY	R	84	-26.236	-38.425	17.591	1.00	0.00
30	ATOM	385	CA	GLY	R	84	-26.228	-39.880	17.476	1.00	0.00
	ATOM	386	C	GLY	R	84	-25.429	-40.269	16.256	1.00	0.00
	ATOM	387	O	GLY	R	84	-24.379	-40.900	16.321	1.00	0.00
	ATOM	388	H	GLY	R	84	-26.647	-37.841	16.890	1.00	0.00
	ATOM	389	N	TYR	R	85	-25.951	-39.784	15.120	1.00	0.00
35	ATOM	390	CA	TYR	R	85	-25.110	-39.752	13.923	1.00	0.00
	ATOM	391	C	TYR	R	85	-24.142	-38.590	13.997	1.00	0.00

93

	ATOM	392	O	TYR R 85	-24.434 -37.463 13.597 1.00 0.00
	ATOM	393	CB	TYR R 85	-25.941 -39.668 12.637 1.00 0.00
	ATOM	394	CG	TYR R 85	-26.885 -40.843 12.509 1.00 0.00
	ATOM	395	CD1	TYR R 85	-26.367 -42.140 12.304 1.00 0.00
5	ATOM	396	CD2	TYR R 85	-28.271 -40.602 12.591 1.00 0.00
	ATOM	397	CE1	TYR R 85	-27.258 -43.221 12.185 1.00 0.00
	ATOM	398	CE2	TYR R 85	-29.161 -41.681 12.467 1.00 0.00
	ATOM	399	CZ	TYR R 85	-28.645 -42.978 12.269 1.00 0.00
	ATOM	400	OH	TYR R 85	-29.528 -44.039 12.161 1.00 0.00
10	ATOM	401	H	TYR R 85	-26.801 -39.267 15.189 1.00 0.00
	ATOM	402	HH	TYR R 85	-30.392 -43.682 11.979 1.00 0.00
	ATOM	403	N	TYR R 86	-23.001 -38.941 14.593 1.00 0.00
	ATOM	404	CA	TYR R 86	-21.996 -37.958 14.983 1.00 0.00
	ATOM	405	C	TYR R 86	-21.418 -37.177 13.824 1.00 0.00
15	ATOM	406	O	TYR R 86	-21.126 -35.992 13.937 1.00 0.00
	ATOM	407	CB	TYR R 86	-20.809 -38.602 15.710 1.00 0.00
	ATOM	408	CG	TYR R 86	-21.207 -39.697 16.673 1.00 0.00
	ATOM	409	CD1	TYR R 86	-20.850 -41.023 16.352 1.00 0.00
	ATOM	410	CD2	TYR R 86	-21.890 -39.374 17.863 1.00 0.00
20	ATOM	411	CE1	TYR R 86	-21.141 -42.050 17.264 1.00 0.00
	ATOM	412	CE2	TYR R 86	-22.184 -40.403 18.774 1.00 0.00
	ATOM	413	CZ	TYR R 86	-21.785 -41.722 18.473 1.00 0.00
	ATOM	414	OH	TYR R 86	-22.023 -42.711 19.413 1.00 0.00
	ATOM	415	H	TYR R 86	-22.958 -39.890 14.897 1.00 0.00
25	ATOM	416	HH	TYR R 86	-21.495 -43.480 19.212 1.00 0.00
	ATOM	417	N	GLN R 87	-21.218 -37.946 12.732 1.00 0.00
	ATOM	418	CA	GLN R 87	-20.570 -37.470 11.510 1.00 0.00
	ATOM	419	C	GLN R 87	-19.097 -37.109 11.556 1.00 0.00
	ATOM	420	O	GLN R 87	-18.514 -36.712 12.563 1.00 0.00
30	ATOM	421	CB	GLN R 87	-21.334 -36.316 10.855 1.00 0.00
	ATOM	422	CG	GLN R 87	-22.628 -36.720 10.170 1.00 0.00
	ATOM	423	CD	GLN R 87	-22.807 -35.859 8.937 1.00 0.00
	ATOM	424	OE1	GLN R 87	-23.553 -34.880 8.908 1.00 0.00
	ATOM	425	NE2	GLN R 87	-22.130 -36.305 7.879 1.00 0.00
35	ATOM	426	H	GLN R 87	-21.584 -38.879 12.734 1.00 0.00
	ATOM	427	1HE2	GLN R 87	-22.399 -35.962 6.979 1.00 0.00

94

	ATOM	428	2HE2	GLN	R	87	-21.431	-37.016	7.960	1.00	0.00
	ATOM	429	N	ASP	R	88	-18.536	-37.210	10.345	1.00	0.00
	ATOM	430	CA	ASP	R	88	-17.727	-36.069	9.929	1.00	0.00
	ATOM	431	C	ASP	R	88	-18.634	-35.318	8.978	1.00	0.00
5	ATOM	432	O	ASP	R	88	-19.200	-35.901	8.064	1.00	0.00
	ATOM	433	CB	ASP	R	88	-16.408	-36.490	9.269	1.00	0.00
	ATOM	434	CG	ASP	R	88	-15.384	-35.376	9.431	1.00	0.00
	ATOM	435	OD1	ASP	R	88	-14.915	-34.822	8.442	1.00	0.00
	ATOM	436	OD2	ASP	R	88	-15.051	-35.032	10.560	1.00	0.00
10	ATOM	437	H	ASP	R	88	-19.040	-37.751	9.666	1.00	0.00
	ATOM	438	N	GLU	R	89	-18.883	-34.048	9.301	1.00	0.00
	ATOM	439	CA	GLU	R	89	-20.163	-33.427	8.949	1.00	0.00
	ATOM	440	C	GLU	R	89	-20.666	-33.353	7.500	1.00	0.00
	ATOM	441	O	GLU	R	89	-21.862	-33.159	7.271	1.00	0.00
15	ATOM	442	CB	GLU	R	89	-20.252	-32.098	9.722	1.00	0.00
	ATOM	443	CG	GLU	R	89	-19.934	-30.765	9.024	1.00	0.00
	ATOM	444	CD	GLU	R	89	-18.588	-30.734	8.336	1.00	0.00
	ATOM	445	OE1	GLU	R	89	-18.494	-31.092	7.174	1.00	0.00
	ATOM	446	OE2	GLU	R	89	-17.616	-30.321	8.940	1.00	0.00
20	ATOM	447	H	GLU	R	89	-18.289	-33.640	9.988	1.00	0.00
	ATOM	448	N	THR	R	90	-19.709	-33.499	6.555	1.00	0.00
	ATOM	449	CA	THR	R	90	-19.933	-32.941	5.217	1.00	0.00
	ATOM	450	C	THR	R	90	-21.285	-33.118	4.552	1.00	0.00
	ATOM	451	O	THR	R	90	-21.938	-34.160	4.600	1.00	0.00
25	ATOM	452	CB	THR	R	90	-18.810	-33.347	4.255	1.00	0.00
	ATOM	453	OG1	THR	R	90	-17.674	-33.836	4.984	1.00	0.00
	ATOM	454	CG2	THR	R	90	-18.392	-32.204	3.324	1.00	0.00
	ATOM	455	H	THR	R	90	-18.784	-33.648	6.889	1.00	0.00
	ATOM	456	HG1	THR	R	90	-17.327	-33.064	5.444	1.00	0.00
30	ATOM	457	N	THR	R	91	-21.647	-32.017	3.895	1.00	0.00
	ATOM	458	CA	THR	R	91	-22.860	-31.897	3.097	1.00	0.00
	ATOM	459	C	THR	R	91	-23.258	-33.149	2.323	1.00	0.00
	ATOM	460	O	THR	R	91	-22.484	-33.676	1.526	1.00	0.00
	ATOM	461	CB	THR	R	91	-22.647	-30.720	2.141	1.00	0.00
35	ATOM	462	OG1	THR	R	91	-21.666	-29.793	2.666	1.00	0.00
	ATOM	463	CG2	THR	R	91	-23.964	-30.007	1.827	1.00	0.00

95

```
        ATOM  464 H   THR R 91    -20.984 -31.271  3.860 1.00 0.00
        ATOM  465 HG1 THR R 91    -20.894 -29.846  2.096 1.00 0.00
        ATOM  466 N   GLY R 92    -24.499 -33.584  2.577 1.00 0.00
        ATOM  467 CA  GLY R 92    -24.978 -34.710  1.781 1.00 0.00
   5    ATOM  468 C   GLY R 92    -24.860 -36.093  2.409 1.00 0.00
        ATOM  469 O   GLY R 92    -25.335 -37.085  1.850 1.00 0.00
        ATOM  470 H   GLY R 92    -25.022 -33.210  3.337 1.00 0.00
        ATOM  471 N   ARG R 93    -24.236 -36.138  3.595 1.00 0.00
        ATOM  472 CA  ARG R 93    -24.173 -37.427  4.280 1.00 0.00
  10    ATOM  473 C   ARG R 93    -24.418 -37.314  5.777 1.00 0.00
        ATOM  474 O   ARG R 93    -24.453 -36.210  6.315 1.00 0.00
        ATOM  475 CB  ARG R 93    -22.867 -38.152  3.925 1.00 0.00
        ATOM  476 CG  ARG R 93    -21.604 -37.313  4.120 1.00 0.00
        ATOM  477 CD  ARG R 93    -20.324 -38.083  3.779 1.00 0.00
  15    ATOM  478 NE  ARG R 93    -19.135 -37.298  4.115 1.00 0.00
        ATOM  479 CZ  ARG R 93    -18.683 -37.255  5.391 1.00 0.00
        ATOM  480 NH1 ARG R 93    -17.741 -36.386  5.728 1.00 0.00
        ATOM  481 NH2 ARG R 93    -19.200 -38.034  6.329 1.00 0.00
        ATOM  482 H   ARG R 93    -23.801 -35.328  3.987 1.00 0.00
  20    ATOM  483 HE  ARG R 93    -18.726 -36.705  3.421 1.00 0.00
        ATOM  484 1HH1 ARG R 93   -17.400 -36.385  6.666 1.00 0.00
        ATOM  485 2HH1 ARG R 93   -17.378 -35.697  5.095 1.00 0.00
        ATOM  486 1HH2 ARG R 93   -18.999 -37.871  7.294 1.00 0.00
        ATOM  487 2HH2 ARG R 93   -19.832 -38.785  6.135 1.00 0.00
  25    ATOM  488 N   CYS R 94    -24.653 -38.506  6.371 1.00 0.00
        ATOM  489 CA  CYS R 94    -24.768 -38.726  7.818 1.00 0.00
        ATOM  490 C   CYS R 94    -24.488 -40.182  8.172 1.00 0.00
        ATOM  491 O   CYS R 94    -25.041 -41.119  7.594 1.00 0.00
        ATOM  492 CB  CYS R 94    -26.138 -38.358  8.397 1.00 0.00
  30    ATOM  493 SG  CYS R 94    -26.692 -36.659  8.083 1.00 0.00
        ATOM  494 H   CYS R 94    -24.611 -39.336  5.816 1.00 0.00
        ATOM  495 N   GLU R 95    -23.572 -40.320  9.142 1.00 0.00
        ATOM  496 CA  GLU R 95    -22.945 -41.588  9.514 1.00 0.00
        ATOM  497 C   GLU R 95    -22.224 -41.383 10.836 1.00 0.00
  35    ATOM  498 O   GLU R 95    -22.258 -40.278 11.382 1.00 0.00
        ATOM  499 CB  GLU R 95    -21.981 -42.075  8.412 1.00 0.00
```

	ATOM	500	CG	GLU R 95	-20.721	-41.229	8.154	1.00 0.00
	ATOM	501	CD	GLU R 95	-21.085	-39.811	7.761	1.00 0.00
	ATOM	502	OE1	GLU R 95	-21.467	-39.570	6.627	1.00 0.00
	ATOM	503	OE2	GLU R 95	-20.997	-38.922	8.591	1.00 0.00
5	ATOM	504	H	GLU R 95	-23.203	-39.480	9.540	1.00 0.00
	ATOM	505	N	ALA R 96	-21.599	-42.462	11.332	1.00 0.00
	ATOM	506	CA	ALA R 96	-20.851	-42.305	12.578	1.00 0.00
	ATOM	507	C	ALA R 96	-19.527	-41.574	12.413	1.00 0.00
	ATOM	508	O	ALA R 96	-18.742	-41.952	11.544	1.00 0.00
10	ATOM	509	CB	ALA R 96	-20.605	-43.668	13.231	1.00 0.00
	ATOM	510	OXT	ALA R 96	-19.293	-40.619	13.151	1.00 0.00
	ATOM	511	H	ALA R 96	-21.711	-43.344	10.871	1.00 0.00
	END							

15   REMARK 1 Second CRD of p75^{NTR}, bound to BDNF.

REMARK 2

	ATOM	1	N	CYS R 39	-28.731	-23.425	17.186	1.00 0.00
	ATOM	2	CA	CYS R 39	-29.491	-22.215	17.484	1.00 0.00
	ATOM	3	C	CYS R 39	-30.988	-22.434	17.523	1.00 0.00
20	ATOM	4	O	CYS R 39	-31.773	-21.495	17.660	1.00 0.00
	ATOM	5	CB	CYS R 39	-29.203	-21.102	16.474	1.00 0.00
	ATOM	6	SG	CYS R 39	-27.698	-21.312	15.471	1.00 0.00
	ATOM	7	1H	CYS R 39	-27.735	-23.264	17.148	1.00 0.00
	ATOM	8	2H	CYS R 39	-28.868	-24.153	17.874	1.00 0.00
25	ATOM	9	3H	CYS R 39	-28.982	-23.835	16.298	1.00 0.00
	ATOM	10	N	LEU R 40	-31.381	-23.704	17.336	1.00 0.00
	ATOM	11	CA	LEU R 40	-32.802	-24.005	17.397	1.00 0.00
	ATOM	12	C	LEU R 40	-33.098	-24.788	18.662	1.00 0.00
	ATOM	13	O	LEU R 40	-32.371	-24.712	19.645	1.00 0.00
30	ATOM	14	CB	LEU R 40	-33.224	-24.736	16.114	1.00 0.00
	ATOM	15	CG	LEU R 40	-33.141	-23.868	14.854	1.00 0.00
	ATOM	16	CD1	LEU R 40	-33.498	-24.664	13.599	1.00 0.00
	ATOM	17	CD2	LEU R 40	-33.987	-22.598	14.968	1.00 0.00
	ATOM	18	H	LEU R 40	-30.734	-24.467	17.314	1.00 0.00
35	ATOM	19	N	ASP R 41	-34.194	-25.545	18.604	1.00 0.00
	ATOM	20	CA	ASP R 41	-34.394	-26.559	19.630	1.00 0.00

97

	ATOM	21	C	ASP R	41	-33.510	-27.762	19.326	1.00	0.00
	ATOM	22	O	ASP R	41	-32.569	-27.678	18.542	1.00	0.00
	ATOM	23	CB	ASP R	41	-35.888	-26.923	19.676	1.00	0.00
	ATOM	24	CG	ASP R	41	-36.282	-27.631	18.391	1.00	0.00
5	ATOM	25	OD1	ASP R	41	-36.462	-28.842	18.426	1.00	0.00
	ATOM	26	OD2	ASP R	41	-36.364	-26.975	17.359	1.00	0.00
	ATOM	27	H	ASP R	41	-34.766	-25.640	17.790	1.00	0.00
	ATOM	28	N	SER R	42	-33.860	-28.892	19.945	1.00	0.00
	ATOM	29	CA	SER R	42	-33.192	-30.156	19.648	1.00	0.00
10	ATOM	30	C	SER R	42	-32.956	-30.499	18.173	1.00	0.00
	ATOM	31	O	SER R	42	-31.967	-31.144	17.816	1.00	0.00
	ATOM	32	CB	SER R	42	-33.975	-31.256	20.359	1.00	0.00
	ATOM	33	OG	SER R	42	-34.507	-30.738	21.597	1.00	0.00
	ATOM	34	H	SER R	42	-34.638	-28.916	20.568	1.00	0.00
15	ATOM	35	HG	SER R	42	-35.328	-31.194	21.757	1.00	0.00
	ATOM	36	N	VAL R	43	-33.884	-30.042	17.310	1.00	0.00
	ATOM	37	CA	VAL R	43	-33.712	-30.372	15.895	1.00	0.00
	ATOM	38	C	VAL R	43	-32.454	-29.826	15.235	1.00	0.00
	ATOM	39	O	VAL R	43	-31.932	-30.402	14.281	1.00	0.00
20	ATOM	40	CB	VAL R	43	-34.955	-30.058	15.044	1.00	0.00
	ATOM	41	CG1	VAL R	43	-36.186	-30.773	15.604	1.00	0.00
	ATOM	42	CG2	VAL R	43	-35.182	-28.560	14.824	1.00	0.00
	ATOM	43	H	VAL R	43	-34.615	-29.433	17.633	1.00	0.00
	ATOM	44	N	THR R	44	-31.938	-28.722	15.786	1.00	0.00
25	ATOM	45	CA	THR R	44	-30.651	-28.248	15.283	1.00	0.00
	ATOM	46	C	THR R	44	-29.869	-27.538	16.372	1.00	0.00
	ATOM	47	O	THR R	44	-30.165	-26.391	16.716	1.00	0.00
	ATOM	48	CB	THR R	44	-30.833	-27.333	14.062	1.00	0.00
	ATOM	49	OG1	THR R	44	-31.913	-27.770	13.215	1.00	0.00
30	ATOM	50	CG2	THR R	44	-29.538	-27.231	13.256	1.00	0.00
	ATOM	51	H	THR R	44	-32.435	-28.226	16.507	1.00	0.00
	ATOM	52	HG1	THR R	44	-31.927	-28.725	13.271	1.00	0.00
	ATOM	53	N	PHE R	45	-28.911	-28.291	16.916	1.00	0.00
	ATOM	54	CA	PHE R	45	-28.186	-27.770	18.069	1.00	0.00
35	ATOM	55	C	PHE R	45	-26.993	-26.926	17.656	1.00	0.00
	ATOM	56	O	PHE R	45	-26.806	-26.646	16.478	1.00	0.00

98

	ATOM	57	CB	PHE R 45	-27.822	-28.924	19.006	1.00	0.00
	ATOM	58	CG	PHE R 45	-26.899	-29.937	18.362	1.00	0.00
	ATOM	59	CD1	PHE R 45	-27.449	-31.094	17.770	1.00	0.00
	ATOM	60	CD2	PHE R 45	-25.503	-29.718	18.376	1.00	0.00
5	ATOM	61	CE1	PHE R 45	-26.592	-32.040	17.179	1.00	0.00
	ATOM	62	CE2	PHE R 45	-24.646	-30.663	17.785	1.00	0.00
	ATOM	63	CZ	PHE R 45	-25.200	-31.813	17.186	1.00	0.00
	ATOM	64	H	PHE R 45	-28.575	-29.099	16.440	1.00	0.00
	ATOM	65	N	SER R 46	-26.169	-26.504	18.621	1.00	0.00
10	ATOM	66	CA	SER R 46	-25.321	-25.406	18.156	1.00	0.00
	ATOM	67	C	SER R 46	-23.805	-25.596	18.062	1.00	0.00
	ATOM	68	O	SER R 46	-23.139	-25.015	17.205	1.00	0.00
	ATOM	69	CB	SER R 46	-25.722	-24.118	18.887	1.00	0.00
	ATOM	70	OG	SER R 46	-27.050	-24.244	19.441	1.00	0.00
15	ATOM	71	H	SER R 46	-26.281	-26.700	19.596	1.00	0.00
	ATOM	72	HG	SER R 46	-26.881	-24.590	20.319	1.00	0.00
	ATOM	73	N	ASP R 47	-23.284	-26.424	18.982	1.00	0.00
	ATOM	74	CA	ASP R 47	-21.847	-26.704	19.149	1.00	0.00
	ATOM	75	C	ASP R 47	-20.914	-25.513	19.394	1.00	0.00
20	ATOM	76	O	ASP R 47	-19.707	-25.533	19.159	1.00	0.00
	ATOM	77	CB	ASP R 47	-21.313	-27.830	18.204	1.00	0.00
	ATOM	78	CG	ASP R 47	-20.687	-27.453	16.853	1.00	0.00
	ATOM	79	OD1	ASP R 47	-20.787	-28.220	15.898	1.00	0.00
	ATOM	80	OD2	ASP R 47	-20.046	-26.421	16.716	1.00	0.00
25	ATOM	81	H	ASP R 47	-23.930	-26.730	19.679	1.00	0.00
	ATOM	82	N	VAL R 48	-21.525	-24.456	19.953	1.00	0.00
	ATOM	83	CA	VAL R 48	-20.791	-23.190	20.089	1.00	0.00
	ATOM	84	C	VAL R 48	-19.752	-23.030	21.212	1.00	0.00
	ATOM	85	O	VAL R 48	-19.796	-22.163	22.083	1.00	0.00
30	ATOM	86	CB	VAL R 48	-21.762	-22.000	20.041	1.00	0.00
	ATOM	87	CG1	VAL R 48	-22.331	-21.847	18.628	1.00	0.00
	ATOM	88	CG2	VAL R 48	-22.865	-22.095	21.103	1.00	0.00
	ATOM	89	H	VAL R 48	-22.434	-24.585	20.351	1.00	0.00
	ATOM	90	N	VAL R 49	-18.722	-23.884	21.116	1.00	0.00
35	ATOM	91	CA	VAL R 49	-17.548	-23.718	21.974	1.00	0.00
	ATOM	92	C	VAL R 49	-16.827	-22.386	21.754	1.00	0.00

99

```
      ATOM   93 O   VAL R 49    -16.199 -21.808 22.647 1.00 0.00
      ATOM   94 CB  VAL R 49    -16.621 -24.942 21.815 1.00 0.00
      ATOM   95 CG1 VAL R 49    -16.113 -25.126 20.379 1.00 0.00
      ATOM   96 CG2 VAL R 49    -15.490 -24.948 22.848 1.00 0.00
  5   ATOM   97 H   VAL R 49    -18.738 -24.575 20.398 1.00 0.00
      ATOM   98 N   SER R 50    -16.984 -21.895 20.512 1.00 0.00
      ATOM   99 CA  SER R 50    -16.545 -20.542 20.170 1.00 0.00
      ATOM  100 C   SER R 50    -17.478 -20.015 19.099 1.00 0.00
      ATOM  101 O   SER R 50    -18.142 -20.822 18.450 1.00 0.00
 10   ATOM  102 CB  SER R 50    -15.104 -20.582 19.665 1.00 0.00
      ATOM  103 OG  SER R 50    -14.388 -21.603 20.381 1.00 0.00
      ATOM  104 H   SER R 50    -17.472 -22.447 19.837 1.00 0.00
      ATOM  105 HG  SER R 50    -14.702 -21.503 21.280 1.00 0.00
      ATOM  106 N   ALA R 51    -17.535 -18.689 18.939 1.00 0.00
 15   ATOM  107 CA  ALA R 51    -18.444 -18.111 17.945 1.00 0.00
      ATOM  108 C   ALA R 51    -18.009 -18.327 16.502 1.00 0.00
      ATOM  109 O   ALA R 51    -17.384 -17.480 15.860 1.00 0.00
      ATOM  110 CB  ALA R 51    -18.633 -16.614 18.202 1.00 0.00
      ATOM  111 H   ALA R 51    -16.914 -18.119 19.470 1.00 0.00
 20   ATOM  112 N   THR R 52    -18.362 -19.542 16.034 1.00 0.00
      ATOM  113 CA  THR R 52    -17.855 -20.040 14.756 1.00 0.00
      ATOM  114 C   THR R 52    -18.740 -21.103 14.084 1.00 0.00
      ATOM  115 O   THR R 52    -18.814 -22.264 14.488 1.00 0.00
      ATOM  116 CB  THR R 52    -16.422 -20.581 14.935 1.00 0.00
 25   ATOM  117 OG1 THR R 52    -15.633 -19.712 15.770 1.00 0.00
      ATOM  118 CG2 THR R 52    -15.723 -20.802 13.589 1.00 0.00
      ATOM  119 H   THR R 52    -18.809 -20.200 16.644 1.00 0.00
      ATOM  120 HG1 THR R 52    -15.985 -18.832 15.634 1.00 0.00
      ATOM  121 N   GLU R 53    -19.349 -20.674 12.968 1.00 0.00
 30   ATOM  122 CA  GLU R 53    -20.398 -19.674 13.115 1.00 0.00
      ATOM  123 C   GLU R 53    -21.732 -20.164 13.692 1.00 0.00
      ATOM  124 O   GLU R 53    -22.195 -19.586 14.668 1.00 0.00
      ATOM  125 CB  GLU R 53    -20.639 -18.835 11.840 1.00 0.00
      ATOM  126 CG  GLU R 53    -19.550 -18.814 10.755 1.00 0.00
 35   ATOM  127 CD  GLU R 53    -19.530 -20.110  9.955 1.00 0.00
      ATOM  128 OE1 GLU R 53    -20.581 -20.583  9.522 1.00 0.00
```

100

	ATOM	129	OE2 GLU R 53	-18.455	-20.666	9.758	1.00 0.00
	ATOM	130	H GLU R 53	-19.314	-21.243	12.150	1.00 0.00
	ATOM	131	N PRO R 54	-22.382	-21.186	13.062	1.00 0.00
	ATOM	132	CA PRO R 54	-23.801	-21.374	13.363	1.00 0.00
5	ATOM	133	C PRO R 54	-24.087	-22.600	14.224	1.00 0.00
	ATOM	134	O PRO R 54	-23.206	-23.245	14.790	1.00 0.00
	ATOM	135	CB PRO R 54	-24.322	-21.543	11.933	1.00 0.00
	ATOM	136	CG PRO R 54	-23.279	-22.449	11.267	1.00 0.00
	ATOM	137	CD PRO R 54	-21.973	-22.056	11.958	1.00 0.00
10	ATOM	138	N CYS R 55	-25.389	-22.945	14.169	1.00 0.00
	ATOM	139	CA CYS R 55	-25.953	-24.243	14.552	1.00 0.00
	ATOM	140	C CYS R 55	-25.269	-25.446	13.903	1.00 0.00
	ATOM	141	O CYS R 55	-24.242	-25.300	13.245	1.00 0.00
	ATOM	142	CB CYS R 55	-27.451	-24.242	14.222	1.00 0.00
15	ATOM	143	SG CYS R 55	-28.150	-22.588	13.922	1.00 0.00
	ATOM	144	H CYS R 55	-26.029	-22.260	13.834	1.00 0.00
	ATOM	145	N LYS R 56	-25.873	-26.628	14.098	1.00 0.00
	ATOM	146	CA LYS R 56	-25.241	-27.917	13.821	1.00 0.00
	ATOM	147	C LYS R 56	-26.256	-29.045	13.957	1.00 0.00
20	ATOM	148	O LYS R 56	-26.703	-29.417	15.037	1.00 0.00
	ATOM	149	CB LYS R 56	-24.073	-28.150	14.789	1.00 0.00
	ATOM	150	CG LYS R 56	-23.350	-29.501	14.702	1.00 0.00
	ATOM	151	CD LYS R 56	-22.658	-29.801	13.373	1.00 0.00
	ATOM	152	CE LYS R 56	-21.673	-30.966	13.503	1.00 0.00
25	ATOM	153	NZ LYS R 56	-20.454	-30.524	14.191	1.00 0.00
	ATOM	154	H LYS R 56	-26.725	-26.673	14.623	1.00 0.00
	ATOM	155	1HZ LYS R 56	-19.887	-31.370	14.402	1.00 0.00
	ATOM	156	2HZ LYS R 56	-20.632	-30.000	15.073	1.00 0.00
	ATOM	157	3HZ LYS R 56	-19.886	-29.946	13.544	1.00 0.00
30	ATOM	158	N PRO R 57	-26.633	-29.599	12.787	1.00 0.00
	ATOM	159	CA PRO R 57	-27.416	-30.837	12.811	1.00 0.00
	ATOM	160	C PRO R 57	-26.644	-31.966	13.476	1.00 0.00
	ATOM	161	O PRO R 57	-25.420	-31.911	13.609	1.00 0.00
	ATOM	162	CB PRO R 57	-27.665	-31.109	11.323	1.00 0.00
35	ATOM	163	CG PRO R 57	-27.447	-29.776	10.607	1.00 0.00

101

	ATOM	164	CD	PRO	R	57	-26.356	-29.119	11.441	1.00	0.00
	ATOM	165	N	CYS	R	58	-27.418	-32.994	13.860	1.00	0.00
	ATOM	166	CA	CYS	R	58	-26.761	-34.217	14.319	1.00	0.00
	ATOM	167	C	CYS	R	58	-26.309	-35.070	13.141	1.00	0.00
5	ATOM	168	O	CYS	R	58	-26.576	-34.743	11.987	1.00	0.00
	ATOM	169	CB	CYS	R	58	-27.709	-34.963	15.259	1.00	0.00
	ATOM	170	SG	CYS	R	58	-27.015	-36.478	15.973	1.00	0.00
	ATOM	171	H	CYS	R	58	-28.408	-32.886	13.776	1.00	0.00
	ATOM	172	N	THR	R	59	-25.623	-36.173	13.459	1.00	0.00
10	ATOM	173	CA	THR	R	59	-25.066	-37.074	12.445	1.00	0.00
	ATOM	174	C	THR	R	59	-26.048	-38.160	11.949	1.00	0.00
	ATOM	175	O	THR	R	59	-27.196	-38.234	12.397	1.00	0.00
	ATOM	176	CB	THR	R	59	-23.767	-37.636	13.055	1.00	0.00
	ATOM	177	OG1	THR	R	59	-23.270	-36.723	14.052	1.00	0.00
15	ATOM	178	CG2	THR	R	59	-22.667	-37.924	12.029	1.00	0.00
	ATOM	179	H	THR	R	59	-25.398	-36.368	14.415	1.00	0.00
	ATOM	180	HG1	THR	R	59	-22.729	-37.252	14.644	1.00	0.00
	ATOM	181	N	GLU	R	60	-25.578	-38.985	10.999	1.00	0.00
	ATOM	182	CA	GLU	R	60	-26.467	-40.006	10.445	1.00	0.00
20	ATOM	183	C	GLU	R	60	-26.899	-41.149	11.355	1.00	0.00
	ATOM	184	O	GLU	R	60	-26.152	-42.083	11.672	1.00	0.00
	ATOM	185	CB	GLU	R	60	-25.943	-40.541	9.111	1.00	0.00
	ATOM	186	CG	GLU	R	60	-27.011	-40.494	8.010	1.00	0.00
	ATOM	187	CD	GLU	R	60	-28.263	-41.228	8.450	1.00	0.00
25	ATOM	188	OE1	GLU	R	60	-28.349	-42.428	8.253	1.00	0.00
	ATOM	189	OE2	GLU	R	60	-29.161	-40.605	9.003	1.00	0.00
	ATOM	190	H	GLU	R	60	-24.642	-38.859	10.693	1.00	0.00
	ATOM	191	N	CYS	R	61	-28.169	-41.001	11.750	1.00	0.00
	ATOM	192	CA	CYS	R	61	-28.775	-41.881	12.742	1.00	0.00
30	ATOM	193	C	CYS	R	61	-29.712	-42.937	12.185	1.00	0.00
	ATOM	194	O	CYS	R	61	-30.148	-43.845	12.890	1.00	0.00
	ATOM	195	CB	CYS	R	61	-29.564	-41.086	13.782	1.00	0.00
	ATOM	196	SG	CYS	R	61	-28.791	-39.568	14.416	1.00	0.00
	ATOM	197	H	CYS	R	61	-28.690	-40.307	11.255	1.00	0.00
35	ATOM	198	N	VAL	R	62	-30.069	-42.806	10.908	1.00	0.00
	ATOM	199	CA	VAL	R	62	-31.084	-43.768	10.496	1.00	0.00

102

```
        ATOM  200 C   VAL R 62   -30.571 -44.884  9.598 1.00 0.00
        ATOM  201 O   VAL R 62   -30.480 -46.055  9.964 1.00 0.00
        ATOM  202 CB  VAL R 62   -32.301 -43.050  9.878 1.00 0.00
        ATOM  203 CG1 VAL R 62   -33.489 -44.005  9.713 1.00 0.00
   5    ATOM  204 CG2 VAL R 62   -32.705 -41.812 10.685 1.00 0.00
        ATOM  205 H   VAL R 62   -29.584 -42.202 10.268 1.00 0.00
        ATOM  206 N   GLY R 63   -30.336 -44.466  8.349 1.00 0.00
        ATOM  207 CA  GLY R 63   -30.443 -45.442  7.270 1.00 0.00
        ATOM  208 C   GLY R 63   -29.148 -45.809  6.584 1.00 0.00
  10    ATOM  209 O   GLY R 63   -29.004 -46.882  6.009 1.00 0.00
        ATOM  210 H   GLY R 63   -30.082 -43.508  8.197 1.00 0.00
        ATOM  211 N   LEU R 64   -28.206 -44.867  6.628 1.00 0.00
        ATOM  212 CA  LEU R 64   -26.859 -45.283  6.260 1.00 0.00
        ATOM  213 C   LEU R 64   -26.145 -45.795  7.489 1.00 0.00
  15    ATOM  214 O   LEU R 64   -25.525 -46.855  7.545 1.00 0.00
        ATOM  215 CB  LEU R 64   -26.088 -44.113  5.644 1.00 0.00
        ATOM  216 CG  LEU R 64   -26.754 -43.525  4.397 1.00 0.00
        ATOM  217 CD1 LEU R 64   -26.073 -42.229  3.958 1.00 0.00
        ATOM  218 CD2 LEU R 64   -26.848 -44.540  3.255 1.00 0.00
  20    ATOM  219 H   LEU R 64   -28.391 -43.992  7.076 1.00 0.00
        ATOM  220 N   GLN R 65   -26.262 -44.951  8.515 1.00 0.00
        ATOM  221 CA  GLN R 65   -25.639 -45.245  9.796 1.00 0.00
        ATOM  222 C   GLN R 65   -26.708 -45.080 10.851 1.00 0.00
        ATOM  223 O   GLN R 65   -27.738 -44.460 10.612 1.00 0.00
  25    ATOM  224 CB  GLN R 65   -24.456 -44.300 10.006 1.00 0.00
        ATOM  225 CG  GLN R 65   -23.336 -44.444  8.965 1.00 0.00
        ATOM  226 CD  GLN R 65   -22.421 -45.624  9.253 1.00 0.00
        ATOM  227 OE1 GLN R 65   -21.315 -45.443  9.762 1.00 0.00
        ATOM  228 NE2 GLN R 65   -22.857 -46.816  8.833 1.00 0.00
  30    ATOM  229 H   GLN R 65   -26.850 -44.141  8.449 1.00 0.00
        ATOM  230 1HE2 GLN R 65  -22.292 -47.635  8.846 1.00 0.00
        ATOM  231 2HE2 GLN R 65  -23.800 -46.898  8.500 1.00 0.00
        ATOM  232 N   SER R 66   -26.473 -45.715 12.001 1.00 0.00
        ATOM  233 CA  SER R 66   -27.657 -45.886 12.838 1.00 0.00
  35    ATOM  234 C   SER R 66   -27.604 -45.224 14.204 1.00 0.00
        ATOM  235 O   SER R 66   -26.542 -44.815 14.682 1.00 0.00
```

103

```
        ATOM   236 CB  SER R 66    -28.013 -47.373 12.884 1.00 0.00
        ATOM   237 OG  SER R 66    -27.869 -47.927 11.565 1.00 0.00
        ATOM   238 H   SER R 66    -25.586 -46.141 12.173 1.00 0.00
        ATOM   239 HG  SER R 66    -28.474 -47.423 11.013 1.00 0.00
   5    ATOM   240 N   MET R 67    -28.808 -45.110 14.779 1.00 0.00
        ATOM   241 CA  MET R 67    -29.048 -44.257 15.939 1.00 0.00
        ATOM   242 C   MET R 67    -28.294 -44.575 17.212 1.00 0.00
        ATOM   243 O   MET R 67    -28.404 -45.649 17.800 1.00 0.00
        ATOM   244 CB  MET R 67    -30.556 -44.203 16.197 1.00 0.00
  10    ATOM   245 CG  MET R 67    -31.008 -42.933 16.916 1.00 0.00
        ATOM   246 SD  MET R 67    -32.793 -42.833 17.123 1.00 0.00
        ATOM   247 CE  MET R 67    -33.244 -42.903 15.380 1.00 0.00
        ATOM   248 H   MET R 67    -29.573 -45.360 14.189 1.00 0.00
        ATOM   249 N   SER R 68    -27.557 -43.553 17.633 1.00 0.00
  15    ATOM   250 CA  SER R 68    -26.992 -43.620 18.977 1.00 0.00
        ATOM   251 C   SER R 68    -27.868 -42.986 20.035 1.00 0.00
        ATOM   252 O   SER R 68    -27.813 -43.326 21.215 1.00 0.00
        ATOM   253 CB  SER R 68    -25.615 -42.989 18.978 1.00 0.00
        ATOM   254 OG  SER R 68    -25.029 -43.228 17.693 1.00 0.00
  20    ATOM   255 H   SER R 68    -27.423 -42.756 17.044 1.00 0.00
        ATOM   256 HG  SER R 68    -24.083 -43.177 17.834 1.00 0.00
        ATOM   257 N   ALA R 69    -28.706 -42.060 19.521 1.00 0.00
        ATOM   258 CA  ALA R 69    -29.837 -41.437 20.214 1.00 0.00
        ATOM   259 C   ALA R 69    -30.311 -40.307 19.312 1.00 0.00
  25    ATOM   260 O   ALA R 69    -29.592 -39.924 18.387 1.00 0.00
        ATOM   261 CB  ALA R 69    -29.406 -40.835 21.565 1.00 0.00
        ATOM   262 H   ALA R 69    -28.493 -41.701 18.610 1.00 0.00
        ATOM   263 N   PRO R 70    -31.506 -39.724 19.607 1.00 0.00
        ATOM   264 CA  PRO R 70    -31.722 -38.322 19.207 1.00 0.00
  30    ATOM   265 C   PRO R 70    -30.580 -37.436 19.699 1.00 0.00
        ATOM   266 O   PRO R 70    -29.722 -37.895 20.456 1.00 0.00
        ATOM   267 CB  PRO R 70    -33.063 -37.990 19.869 1.00 0.00
        ATOM   268 CG  PRO R 70    -33.779 -39.331 20.022 1.00 0.00
        ATOM   269 CD  PRO R 70    -32.637 -40.289 20.334 1.00 0.00
  35    ATOM   270 N   CYS R 71    -30.549 -36.191 19.227 1.00 0.00
        ATOM   271 CA  CYS R 71    -29.381 -35.417 19.642 1.00 0.00
```

104

	ATOM	272	C	CYS R	71	-29.730	-34.124	20.337	1.00	0.00
	ATOM	273	O	CYS R	71	-30.848	-33.618	20.262	1.00	0.00
	ATOM	274	CB	CYS R	71	-28.418	-35.200	18.474	1.00	0.00
	ATOM	275	SG	CYS R	71	-27.801	-36.785	17.835	1.00	0.00
5	ATOM	276	H	CYS R	71	-31.299	-35.781	18.711	1.00	0.00
	ATOM	277	N	VAL R	72	-28.733	-33.641	21.079	1.00	0.00
	ATOM	278	CA	VAL R	72	-28.793	-32.337	21.739	1.00	0.00
	ATOM	279	C	VAL R	72	-27.441	-31.695	21.515	1.00	0.00
	ATOM	280	O	VAL R	72	-26.587	-32.323	20.897	1.00	0.00
10	ATOM	281	CB	VAL R	72	-29.087	-32.477	23.244	1.00	0.00
	ATOM	282	CG1	VAL R	72	-30.554	-32.827	23.502	1.00	0.00
	ATOM	283	CG2	VAL R	72	-28.125	-33.455	23.932	1.00	0.00
	ATOM	284	H	VAL R	72	-27.860	-34.132	21.089	1.00	0.00
	ATOM	285	N	GLU R	73	-27.282	-30.465	22.038	1.00	0.00
15	ATOM	286	CA	GLU R	73	-25.992	-29.787	21.908	1.00	0.00
	ATOM	287	C	GLU R	73	-24.848	-30.522	22.569	1.00	0.00
	ATOM	288	O	GLU R	73	-24.610	-30.447	23.773	1.00	0.00
	ATOM	289	CB	GLU R	73	-26.073	-28.328	22.365	1.00	0.00
	ATOM	290	CG	GLU R	73	-24.825	-27.556	21.923	1.00	0.00
20	ATOM	291	CD	GLU R	73	-24.974	-26.067	22.159	1.00	0.00
	ATOM	292	OE1	GLU R	73	-25.947	-25.478	21.698	1.00	0.00
	ATOM	293	OE2	GLU R	73	-24.103	-25.484	22.793	1.00	0.00
	ATOM	294	H	GLU R	73	-28.030	-30.065	22.564	1.00	0.00
	ATOM	295	N	ALA R	74	-24.183	-31.276	21.690	1.00	0.00
25	ATOM	296	CA	ALA R	74	-22.982	-32.030	22.006	1.00	0.00
	ATOM	297	C	ALA R	74	-22.211	-32.099	20.717	1.00	0.00
	ATOM	298	O	ALA R	74	-22.796	-32.213	19.640	1.00	0.00
	ATOM	299	CB	ALA R	74	-23.328	-33.451	22.455	1.00	0.00
	ATOM	300	H	ALA R	74	-24.600	-31.329	20.777	1.00	0.00
30	ATOM	301	N	ASP R	75	-20.889	-31.945	20.853	1.00	0.00
	ATOM	302	CA	ASP R	75	-20.105	-31.837	19.633	1.00	0.00
	ATOM	303	C	ASP R	75	-20.167	-33.101	18.799	1.00	0.00
	ATOM	304	O	ASP R	75	-20.254	-34.213	19.326	1.00	0.00
	ATOM	305	CB	ASP R	75	-18.676	-31.418	19.976	1.00	0.00
35	ATOM	306	CG	ASP R	75	-18.194	-30.327	19.038	1.00	0.00
	ATOM	307	OD1	ASP R	75	-17.534	-29.398	19.470	1.00	0.00

105

	ATOM	308	OD2	ASP R	75	-18.410	-30.388	17.841	1.00	0.00
	ATOM	309	H	ASP R	75	-20.452	-31.968	21.747	1.00	0.00
	ATOM	310	N	ASP R	76	-20.194	-32.858	17.466	1.00	0.00
	ATOM	311	CA	ASP R	76	-20.556	-33.842	16.433	1.00	0.00
5	ATOM	312	C	ASP R	76	-21.294	-35.063	16.965	1.00	0.00
	ATOM	313	O	ASP R	76	-20.725	-36.140	17.153	1.00	0.00
	ATOM	314	CB	ASP R	76	-19.324	-34.222	15.591	1.00	0.00
	ATOM	315	CG	ASP R	76	-18.850	-33.033	14.765	1.00	0.00
	ATOM	316	OD1	ASP R	76	-18.213	-32.134	15.285	1.00	0.00
10	ATOM	317	OD2	ASP R	76	-19.132	-32.953	13.580	1.00	0.00
	ATOM	318	H	ASP R	76	-19.875	-31.943	17.215	1.00	0.00
	ATOM	319	N	ALA R	77	-22.571	-34.806	17.303	1.00	0.00
	ATOM	320	CA	ALA R	77	-23.290	-35.694	18.218	1.00	0.00
	ATOM	321	C	ALA R	77	-23.531	-37.073	17.651	1.00	0.00
15	ATOM	322	O	ALA R	77	-23.725	-37.259	16.456	1.00	0.00
	ATOM	323	CB	ALA R	77	-24.619	-35.075	18.644	1.00	0.00
	ATOM	324	H	ALA R	77	-23.001	-34.012	16.881	1.00	0.00
	ATOM	325	N	VAL R	78	-23.455	-38.052	18.556	1.00	0.00
	ATOM	326	CA	VAL R	78	-22.704	-39.281	18.232	1.00	0.00
20	ATOM	327	C	VAL R	78	-23.295	-40.388	17.344	1.00	0.00
	ATOM	328	O	VAL R	78	-23.041	-41.583	17.543	1.00	0.00
	ATOM	329	CB	VAL R	78	-22.160	-39.877	19.542	1.00	0.00
	ATOM	330	CG1	VAL R	78	-21.189	-38.911	20.224	1.00	0.00
	ATOM	331	CG2	VAL R	78	-23.287	-40.288	20.497	1.00	0.00
25	ATOM	332	H	VAL R	78	-23.598	-37.743	19.493	1.00	0.00
	ATOM	333	N	CYS R	79	-24.111	-40.011	16.349	1.00	0.00
	ATOM	334	CA	CYS R	79	-24.667	-41.058	15.490	1.00	0.00
	ATOM	335	C	CYS R	79	-23.639	-41.706	14.569	1.00	0.00
	ATOM	336	O	CYS R	79	-23.161	-41.097	13.611	1.00	0.00
30	ATOM	337	CB	CYS R	79	-25.854	-40.535	14.695	1.00	0.00
	ATOM	338	SG	CYS R	79	-27.265	-40.010	15.706	1.00	0.00
	ATOM	339	H	CYS R	79	-24.146	-39.049	16.105	1.00	0.00
	ATOM	340	N	ARG R	80	-23.326	-42.955	14.966	1.00	0.00
	ATOM	341	CA	ARG R	80	-22.220	-43.688	14.354	1.00	0.00
35	ATOM	342	C	ARG R	80	-22.617	-45.027	13.739	1.00	0.00
	ATOM	343	O	ARG R	80	-22.898	-45.120	12.547	1.00	0.00

106

	ATOM	344	CB	ARG R 80	-21.047	-43.866	15.333	1.00	0.00
	ATOM	345	CG	ARG R 80	-19.958	-42.787	15.285	1.00	0.00
	ATOM	346	CD	ARG R 80	-19.283	-42.600	13.916	1.00	0.00
	ATOM	347	NE	ARG R 80	-18.739	-43.844	13.361	1.00	0.00
5	ATOM	348	CZ	ARG R 80	-19.343	-44.423	12.298	1.00	0.00
	ATOM	349	NH1	ARG R 80	-18.915	-45.588	11.814	1.00	0.00
	ATOM	350	NH2	ARG R 80	-20.397	-43.844	11.740	1.00	0.00
	ATOM	351	H	ARG R 80	-23.849	-43.366	15.715	1.00	0.00
	ATOM	352	HE	ARG R 80	-17.952	-44.277	13.804	1.00	0.00
10	ATOM	353	1HH1	ARG R 80	-19.409	-46.064	11.082	1.00	0.00
	ATOM	354	2HH1	ARG R 80	-18.080	-46.022	12.174	1.00	0.00
	ATOM	355	1HH2	ARG R 80	-20.880	-44.269	10.976	1.00	0.00
	ATOM	356	2HH2	ARG R 80	-20.749	-42.984	12.102	1.00	0.00
	ATOM	357	N	CYS R 81	-22.630	-46.086	14.566	1.00	0.00
15	ATOM	358	CA	CYS R 81	-22.946	-47.400	14.002	1.00	0.00
	ATOM	359	C	CYS R 81	-23.527	-48.331	15.049	1.00	0.00
	ATOM	360	O	CYS R 81	-22.830	-49.080	15.728	1.00	0.00
	ATOM	361	CB	CYS R 81	-21.732	-48.025	13.284	1.00	0.00
	ATOM	362	SG	CYS R 81	-22.046	-48.494	11.547	1.00	0.00
20	ATOM	363	H	CYS R 81	-22.342	-45.997	15.517	1.00	0.00
	ATOM	364	N	ALA R 82	-24.869	-48.212	15.160	1.00	0.00
	ATOM	365	CA	ALA R 82	-25.712	-49.047	16.033	1.00	0.00
	ATOM	366	C	ALA R 82	-25.041	-49.677	17.246	1.00	0.00
	ATOM	367	O	ALA R 82	-24.801	-50.881	17.310	1.00	0.00
25	ATOM	368	CB	ALA R 82	-26.390	-50.148	15.212	1.00	0.00
	ATOM	369	H	ALA R 82	-25.322	-47.577	14.537	1.00	0.00
	ATOM	370	N	TYR R 83	-24.697	-48.786	18.189	1.00	0.00
	ATOM	371	CA	TYR R 83	-23.809	-49.240	19.256	1.00	0.00
	ATOM	372	C	TYR R 83	-24.319	-50.384	20.116	1.00	0.00
30	ATOM	373	O	TYR R 83	-25.492	-50.522	20.451	1.00	0.00
	ATOM	374	CB	TYR R 83	-23.268	-48.059	20.087	1.00	0.00
	ATOM	375	CG	TYR R 83	-24.247	-47.511	21.108	1.00	0.00
	ATOM	376	CD1	TYR R 83	-25.207	-46.556	20.715	1.00	0.00
	ATOM	377	CD2	TYR R 83	-24.147	-47.951	22.445	1.00	0.00
35	ATOM	378	CE1	TYR R 83	-26.058	-46.003	21.688	1.00	0.00
	ATOM	379	CE2	TYR R 83	-25.001	-47.400	23.417	1.00	0.00

```
       ATOM   380  CZ  TYR R  83     -25.937 -46.419 23.031 1.00  0.00
       ATOM   381  OH  TYR R  83     -26.753 -45.849 23.995 1.00  0.00
       ATOM   382  H   TYR R  83     -25.061 -47.858 18.145 1.00  0.00
       ATOM   383  HH  TYR R  83     -27.139 -45.055 23.619 1.00  0.00
   5   ATOM   384  N   GLY R  84     -23.359 -51.236 20.478 1.00  0.00
       ATOM   385  CA  GLY R  84     -23.783 -52.411 21.232 1.00  0.00
       ATOM   386  C   GLY R  84     -23.284 -53.694 20.609 1.00  0.00
       ATOM   387  O   GLY R  84     -23.189 -54.732 21.259 1.00  0.00
       ATOM   388  H   GLY R  84     -22.420 -51.099 20.167 1.00  0.00
  10   ATOM   389  N   TYR R  85     -22.925 -53.551 19.317 1.00  0.00
       ATOM   390  CA  TYR R  85     -21.764 -54.346 18.941 1.00  0.00
       ATOM   391  C   TYR R  85     -20.520 -53.484 19.090 1.00  0.00
       ATOM   392  O   TYR R  85     -20.632 -52.266 19.248 1.00  0.00
       ATOM   393  CB  TYR R  85     -21.930 -54.959 17.539 1.00  0.00
  15   ATOM   394  CG  TYR R  85     -21.890 -53.946 16.413 1.00  0.00
       ATOM   395  CD1 TYR R  85     -23.084 -53.333 15.975 1.00  0.00
       ATOM   396  CD2 TYR R  85     -20.649 -53.671 15.805 1.00  0.00
       ATOM   397  CE1 TYR R  85     -23.042 -52.477 14.860 1.00  0.00
       ATOM   398  CE2 TYR R  85     -20.609 -52.814 14.697 1.00  0.00
  20   ATOM   399  CZ  TYR R  85     -21.808 -52.257 14.215 1.00  0.00
       ATOM   400  OH  TYR R  85     -21.760 -51.493 13.062 1.00  0.00
       ATOM   401  H   TYR R  85     -23.172 -52.734 18.790 1.00  0.00
       ATOM   402  HH  TYR R  85     -20.964 -51.753 12.596 1.00  0.00
       ATOM   403  N   TYR R  86     -19.354 -54.143 19.022 1.00  0.00
  25   ATOM   404  CA  TYR R  86     -18.070 -53.498 19.330 1.00  0.00
       ATOM   405  C   TYR R  86     -17.547 -52.466 18.319 1.00  0.00
       ATOM   406  O   TYR R  86     -16.457 -52.635 17.784 1.00  0.00
       ATOM   407  CB  TYR R  86     -17.072 -54.652 19.552 1.00  0.00
       ATOM   408  CG  TYR R  86     -15.786 -54.368 20.316 1.00  0.00
  30   ATOM   409  CD1 TYR R  86     -15.322 -53.061 20.597 1.00  0.00
       ATOM   410  CD2 TYR R  86     -15.053 -55.502 20.719 1.00  0.00
       ATOM   411  CE1 TYR R  86     -14.087 -52.896 21.255 1.00  0.00
       ATOM   412  CE2 TYR R  86     -13.825 -55.340 21.380 1.00  0.00
       ATOM   413  CZ  TYR R  86     -13.346 -54.040 21.627 1.00  0.00
  35   ATOM   414  OH  TYR R  86     -12.110 -53.911 22.244 1.00  0.00
       ATOM   415  H   TYR R  86     -19.425 -55.102 18.757 1.00  0.00
```

108

	ATOM	416	HH	TYR	R	86	-11.829	-53.003	22.149	1.00	0.00
	ATOM	417	N	GLN	R	87	-18.334	-51.399	18.081	1.00	0.00
	ATOM	418	CA	GLN	R	87	-17.800	-50.310	17.258	1.00	0.00
	ATOM	419	C	GLN	R	87	-17.117	-49.255	18.112	1.00	0.00
5	ATOM	420	O	GLN	R	87	-17.704	-48.681	19.022	1.00	0.00
	ATOM	421	CB	GLN	R	87	-18.910	-49.706	16.371	1.00	0.00
	ATOM	422	CG	GLN	R	87	-18.725	-48.273	15.812	1.00	0.00
	ATOM	423	CD	GLN	R	87	-17.729	-48.089	14.663	1.00	0.00
	ATOM	424	OE1	GLN	R	87	-17.701	-47.027	14.040	1.00	0.00
10	ATOM	425	NE2	GLN	R	87	-16.936	-49.120	14.374	1.00	0.00
	ATOM	426	H	GLN	R	87	-19.143	-51.256	18.647	1.00	0.00
	ATOM	427	1HE2	GLN	R	87	-16.239	-49.104	13.659	1.00	0.00
	ATOM	428	2HE2	GLN	R	87	-16.869	-50.003	14.846	1.00	0.00
	ATOM	429	N	ASP	R	88	-15.845	-49.028	17.759	1.00	0.00
15	ATOM	430	CA	ASP	R	88	-15.041	-48.001	18.429	1.00	0.00
	ATOM	431	C	ASP	R	88	-14.442	-47.101	17.361	1.00	0.00
	ATOM	432	O	ASP	R	88	-14.123	-47.592	16.276	1.00	0.00
	ATOM	433	CB	ASP	R	88	-13.968	-48.725	19.273	1.00	0.00
	ATOM	434	CG	ASP	R	88	-12.942	-47.819	19.953	1.00	0.00
20	ATOM	435	OD1	ASP	R	88	-11.758	-48.104	19.876	1.00	0.00
	ATOM	436	OD2	ASP	R	88	-13.294	-46.831	20.580	1.00	0.00
	ATOM	437	H	ASP	R	88	-15.429	-49.592	17.039	1.00	0.00
	ATOM	438	N	GLU	R	89	-14.306	-45.805	17.710	1.00	0.00
	ATOM	439	CA	GLU	R	89	-13.680	-44.795	16.839	1.00	0.00
25	ATOM	440	C	GLU	R	89	-14.515	-44.403	15.614	1.00	0.00
	ATOM	441	O	GLU	R	89	-15.309	-43.460	15.616	1.00	0.00
	ATOM	442	CB	GLU	R	89	-12.257	-45.283	16.493	1.00	0.00
	ATOM	443	CG	GLU	R	89	-11.293	-44.524	15.571	1.00	0.00
	ATOM	444	CD	GLU	R	89	-10.219	-45.518	15.145	1.00	0.00
30	ATOM	445	OE1	GLU	R	89	-9.962	-45.681	13.957	1.00	0.00
	ATOM	446	OE2	GLU	R	89	-9.644	-46.177	15.998	1.00	0.00
	ATOM	447	H	GLU	R	89	-14.511	-45.638	18.676	1.00	0.00
	ATOM	448	N	THR	R	90	-14.293	-45.184	14.553	1.00	0.00
	ATOM	449	CA	THR	R	90	-14.096	-44.591	13.232	1.00	0.00
35	ATOM	450	C	THR	R	90	-15.313	-44.151	12.444	1.00	0.00
	ATOM	451	O	THR	R	90	-16.239	-44.933	12.212	1.00	0.00

109

	ATOM	452	CB	THR	R	90	-13.307	-45.598	12.397	1.00	0.00
	ATOM	453	OG1	THR	R	90	-12.719	-46.613	13.229	1.00	0.00
	ATOM	454	CG2	THR	R	90	-12.269	-44.936	11.490	1.00	0.00
	ATOM	455	H	THR	R	90	-14.031	-46.141	14.672	1.00	0.00
5	ATOM	456	HG1	THR	R	90	-11.932	-46.206	13.613	1.00	0.00
	ATOM	457	N	THR	R	91	-15.264	-42.906	11.946	1.00	0.00
	ATOM	458	CA	THR	R	91	-16.086	-42.598	10.774	1.00	0.00
	ATOM	459	C	THR	R	91	-15.551	-43.214	9.474	1.00	0.00
	ATOM	460	O	THR	R	91	-15.041	-42.576	8.553	1.00	0.00
10	ATOM	461	CB	THR	R	91	-16.263	-41.089	10.611	1.00	0.00
	ATOM	462	OG1	THR	R	91	-15.526	-40.320	11.595	1.00	0.00
	ATOM	463	CG2	THR	R	91	-17.753	-40.737	10.608	1.00	0.00
	ATOM	464	H	THR	R	91	-14.546	-42.271	12.218	1.00	0.00
	ATOM	465	HG1	THR	R	91	-16.170	-40.159	12.292	1.00	0.00
15	ATOM	466	N	GLY	R	92	-15.638	-44.548	9.437	1.00	0.00
	ATOM	467	CA	GLY	R	92	-14.952	-45.240	8.341	1.00	0.00
	ATOM	468	C	GLY	R	92	-14.947	-46.747	8.485	1.00	0.00
	ATOM	469	O	GLY	R	92	-15.038	-47.506	7.517	1.00	0.00
	ATOM	470	H	GLY	R	92	-16.190	-45.008	10.134	1.00	0.00
20	ATOM	471	N	ARG	R	93	-14.906	-47.132	9.766	1.00	0.00
	ATOM	472	CA	ARG	R	93	-15.165	-48.526	10.101	1.00	0.00
	ATOM	473	C	ARG	R	93	-16.597	-48.659	10.561	1.00	0.00
	ATOM	474	O	ARG	R	93	-17.179	-47.725	11.108	1.00	0.00
	ATOM	475	CB	ARG	R	93	-14.257	-49.027	11.231	1.00	0.00
25	ATOM	476	CG	ARG	R	93	-12.866	-49.498	10.801	1.00	0.00
	ATOM	477	CD	ARG	R	93	-12.088	-50.205	11.924	1.00	0.00
	ATOM	478	NE	ARG	R	93	-11.530	-49.278	12.906	1.00	0.00
	ATOM	479	CZ	ARG	R	93	-11.885	-49.270	14.210	1.00	0.00
	ATOM	480	NH1	ARG	R	93	-11.321	-48.407	15.046	1.00	0.00
30	ATOM	481	NH2	ARG	R	93	-12.806	-50.108	14.666	1.00	0.00
	ATOM	482	H	ARG	R	93	-14.866	-46.429	10.469	1.00	0.00
	ATOM	483	HE	ARG	R	93	-10.826	-48.644	12.583	1.00	0.00
	ATOM	484	1HH1| ARG	R	93	-11.678	-48.273	15.969	1.00	0.00
	ATOM	485	2HH1| ARG	R	93	-10.552	-47.825	14.774	1.00	0.00
35	ATOM	486	1HH2| ARG	R	93	-13.112	-50.146	15.616	1.00	0.00
	ATOM	487	2HH2| ARG	R	93	-13.266	-50.761	14.058	1.00	0.00

110

```
       ATOM   488 N   CYS R  94    -17.121 -49.864 10.349 1.00 0.00
       ATOM   489 CA  CYS R  94    -18.327 -50.307 11.053 1.00 0.00
       ATOM   490 C   CYS R  94    -18.187 -51.790 11.280 1.00 0.00
       ATOM   491 O   CYS R  94    -18.340 -52.598 10.361 1.00 0.00
    5  ATOM   492 CB  CYS R  94    -19.611 -50.063 10.264 1.00 0.00
       ATOM   493 SG  CYS R  94    -20.314 -48.399 10.429 1.00 0.00
       ATOM   494 H   CYS R  94    -16.640 -50.508  9.754 1.00 0.00
       ATOM   495 N   GLU R  95    -17.798 -52.106 12.524 1.00 0.00
       ATOM   496 CA  GLU R  95    -17.382 -53.477 12.826 1.00 0.00
   10  ATOM   497 C   GLU R  95    -18.334 -54.564 12.388 1.00 0.00
       ATOM   498 O   GLU R  95    -19.545 -54.380 12.270 1.00 0.00
       ATOM   499 CB  GLU R  95    -17.063 -53.650 14.313 1.00 0.00
       ATOM   500 CG  GLU R  95    -15.587 -53.436 14.658 1.00 0.00
       ATOM   501 CD  GLU R  95    -15.185 -51.998 14.416 1.00 0.00
   15  ATOM   502 OE1 GLU R  95    -14.757 -51.672 13.318 1.00 0.00
       ATOM   503 OE2 GLU R  95    -15.280 -51.193 15.328 1.00 0.00
       ATOM   504 H   GLU R  95    -17.570 -51.381 13.172 1.00 0.00
       ATOM   505 N   ALA R  96    -17.715 -55.723 12.129 1.00 0.00
       ATOM   506 CA  ALA R  96    -18.517 -56.877 11.727 1.00 0.00
   20  ATOM   507 C   ALA R  96    -18.962 -57.733 12.900 1.00 0.00
       ATOM   508 O   ALA R  96    -20.158 -57.994 13.010 1.00 0.00
       ATOM   509 CB  ALA R  96    -17.748 -57.740 10.723 1.00 0.00
       ATOM   510 OXT ALA R  96    -18.116 -58.127 13.704 1.00 0.00
       ATOM   511 H   ALA R  96    -16.728 -55.754 12.290 1.00 0.00
   25  END
```

---

*Principal residues are bolded.

111

Appendix 4. The Fortran-77 source code of the VBMC algorithm.*

```
       SUBROUTINE MONTE(XMIN,N,S0)
    C*
5   C*      Variable Basis Monte Carlo simulated annealing:
    C*      XMIN - initial configurational variables and
    C*            final variables for subsequent local energy
    C*            refinement.
    C*      N - the number of configurational variables.
10  C*      S0 - initial energy.
    C*      FUN - potential energy function.
    C*
       IMPLICIT REAL*8(A-H,O-Z)
       DIMENSION XX(250),X(250),XMIN(1)
15     DIMENSION Y(500,250),C(250,250),E(250),V(250,250)
       IYES=0
       ITEST=0
       READ(5,1)N1,N4,N5,NG1,ITE,IPR1,N33
       IF(N1.EQ.0)RETURN
20     WRITE(6,3000)ITE,S0
       TT=ITE
    3000 FORMAT(/10X,'INITIAL TEMPERATURE',I7,
       1    '  INITIAL ENERGY ',F15.6/)
       PR1=IPR1
25     PR2=PR1*2.D0
       WRITE(6,210)PR1,PR1
    210 FORMAT(' RANDOM TORSIONAL INCREMENT -'
       2    ,F5.2,' TO +',F5.2,' GRAD')
       WRITE(6,302)
30  302 FORMAT(10X,'*VARIABLE BASIS MC SIMULATED ANNEALING*'/)
    C*      Boltzmann factor.
       T=-1./(0.001987*TT)
    C    *** TEMPERATURE T=ITE ***
       1 FORMAT(15I5)
35     N1=N*N1
       N3=N
```

112

```
        K=N
C*      Cooling schedule.
        DT=(ITE-120)/(N5*N3)
        NG=NG1
5       IF(NG.EQ.0)NG=1
C*      Initial set of random number generator.
        CALL SRAND(NG)
        WRITE(6,2)N1,N3,N4,N5,NG
      2 FORMAT(/5X,'MONTE-CARLO PARAMETERS:'/
10     *5X,'BLIND CUT',I10/
       *5X,'BYPASS',I10/
       *5X,'FREQUENCY OF CONTROL OUTPUT',I10/
       *5X,'LENGTH OF ANNEALING REGION',I10/
       *5X,'INITIAL SET OF THE RANDOM GENERATOR ',I10/)
15      IBEGIN=0
        MNCARL=0
        LQ=0
        I7=0
        L1=0
20      EMIN=1.D37
        S3=0.
        S4=0.
C*      Initial set of basis of independent variables.
        DO 88 I=1,N
25      DO 88 J=1,N
        V(I,J)=0.D0
        IF(I.EQ.J)V(I,J)=1.D0
     88 CONTINUE
        DO 2005 I=1,N
30   2005 X(I)=XMIN(I)
    264 S1=0.
        S2=0.
        L=0
C*      Method Monte Carlo.
35      IYES=0
        KG=0
```

113

```
          L2=0
          I=0
       26 I=I+1
C*        Random choice of a variable to move.
5         H=RAND()
          IK=IDINT(H*N)+1
          RA=RAND()
          D=RA*PR2-PR1
C*        Variable Basis Markov chain: move along basis vectors.
10        DO 513 II=1,N
      513 XX(II)=X(II)+V(II,IK)*D
          CALL FUN(N,XX,SS)
C*        SS - potential energy of the configuration XX.
          S=SS-S0
15        BI=S*T
          IF(BI.GT.50.D0) GOTO 263
C*        CALCULATION OF TRANSITION PROBABILITY
          IF(BI.LT.-50.D0) GOTO 262
          B=DEXP(BI)
20        W7=B/(B+1.D0)
C*        DOES TRANSITION TAKE PLACE ?
          Z=RAND()
          IF(W7-Z)262,263,263
C*        ** NO **
25    262 CONTINUE
          GOTO 274
C*        ** YES ! **
      263 S0=SS
          IYES=IYES+1
30        DO 1314 II=1,N
     1314 X(II)=XX(II)
C*        Blind cut off
      274 IF(IBEGIN.EQ.1) GOTO 266
          MNCARL=MNCARL+1
35        IF(MNCARL-N1)26,1264,265
     1264 WRITE(6,1265)MNCARL,S0
```

114

```
      1265 FORMAT('Initial point has been cut off',I10,1PD17.9)
      C*     Cut off upon criteria.
           GOTO 264
       265 S1=S1+S0
           S2=S2+S0*S0
           L=L+1
           IF(L.NE.20*N) GOTO 26
           L=0
           SR1=S1/I
           DISP1=S2/I-SR1**2
           IF(DABS(SR1-S0)-DSQRT(DISP1))270,270,271
       271 ITEST=0
           GOTO 272
       270 ITEST=ITEST+1
       272 YES=(1.D2*IYES)/I
           WRITE(6,268)I,S0,SR1,DISP1,ITEST,YES
       268 FORMAT('Cut off',I8,3D14.7,I3,2PF7.1)
           IF(I.GE.50000)GOTO 267
           IF(ITEST-3) 26,267,267
       267 IBEGIN=1
           WRITE(6,1265)MNCARL,S0
           WRITE(6,269)
       269 FORMAT(//45X,'Equilibrium has been reached '/)
           GOTO 264
      C*     N3 - parameter of bypassing.
      C*     DT - cooling schedule.
       266 L=L+1
           IF(TT.LE.120.D0)GOTO 3333
      C*     Slow cooling.
           TT=TT-DT
      C*     Boltzmann factor.
           T=-1.D0/(1.987D-3*TT)
           IF(L.LT.N3)GOTO 26
           L=0
           KG=KG+1
      C*      Accumulating N33 sequential points of the Markov chain.
```

115

```
         DO 1992 J=1,N
     1992 Y(KG,J)=X(J)
         L1=L1+1
         L2=L2+1
5        IF(S0.GE.EMIN)GOTO 1957
         EMIN=S0
         DO 1961 IJ=1,N
     1961 XMIN(IJ)=X(IJ)
         LQ=LQ+1
10       WRITE(6,100)LQ,I,EMIN,TT,(XMIN(J),J=1,N)
     100  FORMAT(/' LQ',2I7,D17.9,F7.1/(1X,10F12.3))
     447  FORMAT(/' CR',2I7,D17.9,F7.1/(1X,10F12.3))
     1957 IF(KG.LT.N33)GOTO 45
C*       Computing covariant matrix of the distribution of
15  C*       the N33 accumulated points in the configurational
C*       space.
         KG=0
         DO 71 II=1,K
         YYY=0.0
20       DO 82 J=1,N33
      82 YYY=YYY+Y(J,II)
         YYY=YYY/N
         DO 54 J=1,N33
      54 Y(J,II)=Y(J,II)-YYY
25    71 CONTINUE
         DO 710 II=1,K      ...
         DO 710 J=1,K
         S=0.0
         DO 711 LL=1,N33
30   711 S=S+Y(LL,II)*Y(LL,J)
     710 C(II,J)=S
C*       Covariant matrix is ready.
C*       Roration of basis V:
         CALL SDIAG2(250,K,C,E,V)
35    45 IF(L2.LT.N4) GOTO 26
```

116

```
           L2=0
           YES=(1.D2*IYES)/I
           WRITE(6,72)I,L1,EMIN,S0,TT,YES
        72 FORMAT(' CO',2I10,2D15.6,F7.1,2PF7.1)
5          IF(L1.LT.N5) GOTO 26
        3333 WRITE(6,1111)
        1111 FORMAT(//10X,'END OF MONTE CARLO STAGE')
           RETURN
           END
10         SUBROUTINE SDIAG2(M,N,A,D,X)
        C*
        C*      Diagonalization of symmetric matrix A (NxN).
        C*      Results: D - eigenvalues; X - eigenvectors.
        C*
15         IMPLICIT REAL*8(A-H,O-Z)
           DIMENSION A(M,M),D(M),X(M,M)
           DIMENSION E(250)
           EPS=1.0D-14
           TOL=1.0D-30
20         IF(N.EQ.1)GOTO 400
           DO 10 I=1,N
           DO 10 J=1,I
        10 X(I,J)=A(I,J)
           DO 150 NI=2,N
25         II=N+2-NI
           DO 150 I=II,II
           L=I-2
           H=.0D0
           G=X(I,I-1)
30         IF(L)140,140,20
        20 DO 30 K=1,L
        30 H=H+X(I,K)**2
           S=H+G*G
           IF(S.GE.TOL)GOTO 50
35         H=.0D0
           GOTO 140
```

117

```
50 IF(H)140,140,60
60 L=L+1
   F=G
   G=DSQRT(S)
   IF(F)75,75,70
70 G=-G
75 H=S-F*G
   X(I,I-1)=F-G
   F=.0D0
   DO 110 J=1,L
   X(J,I)=X(I,J)/H
   S=.0D0
   DO 80 K=1,J
80 S=S+X(J,K)*X(I,K)
   J1=J+1
   IF(J1.GT.L)GOTO 100
   DO 90 K=J1,L
90 S=S+X(K,J)*X(I,K)
100 E(J)=S/H
110 F=F+S*X(J,I)
   F=F/(H+H)
   DO 120 J=1,L
120 E(J)=E(J)-F*X(I,J)
   DO 130 J=1,L
   F=X(I,J)
   S=E(J)
   DO 130 K=1,J
130 X(J,K)=X(J,K)-F*E(K)-X(I,K)*S
140 D(I)=H
150 E(I-1)=G
160 D(1)=X(1,1)
   X(1,1)=1.D0
   DO 220 I=2,N
   L=I-1
   IF(D(I))200,200,170
170 DO 190 J=1,L
```

```
         S=.0D0
         DO 180 K=1,L
     180 S=S+X(I,K)*X(K,J)
         DO 190 K=1,L
 5   190 X(K,J)=X(K,J)-S*X(K,I)
     200 D(I)=X(I,I)
         X(I,I)=1.D0
     210 DO 220 J=1,L
         X(I,J)=.0D0
10   220 X(J,I)=.0D0
         B=.0D0
         F=.0D0
         E(N)=.0D0
         DO 340 L=1,N
15       H=EPS*(DABS(D(L))+DABS(E(L)))
         IF(H.LE.B)GOTO 235
         B=H
     235 DO 240 J=L,N
         IF(DABS(E(J)).LE.B)GOTO 250
20   240 CONTINUE
     250 IF(J.EQ.L)GOTO 340
     260 P=(D(L+1)-D(L))*.5D0/E(L)
         R=DSQRT(P*P+1.D0)
         IF(P)270,280,280
25   270 P=P-R
         GOTO 290
     280 P=P+R
     290 H=D(L)-E(L)/P
         DO 300 I=L,N
30   300 D(I)=D(I)-H
         F=F+H
         P=D(J)
         C=1.D0
         S=0.D0
35       J1=J-1
         DO 330 NI=L,J1
```

119

```
           II=L+J1-NI
           DO 330 I=II,II
           G=C*E(I)
           H=C*P
    5      IF(DABS(P).LT.DABS(E(I)))GOTO 310
           C=E(I)/P
           R=DSQRT(C*C+1.D0)
           E(I+1)=S*P*R
           S=C/R
   10      C=1.D0/R
           GOTO 320
       310 C=P/E(I)
           R=DSQRT(C*C+1.D0)
           E(I+1)=S*E(I)*R
   15      S=1.D0/R
           C=C/R
       320 P=C*D(I)-S*G
           D(I+1)=H+S*(C*G+S*D(I))
           DO 330 K=1,N
   20      H=X(K,I+1)
           X(K,I+1)=X(K,I)*S+H*C
       330 X(K,I)=X(K,I)*C-H*S
           E(L)=S*P
           D(L)=C*P
   25      IF(DABS(E(L)).GT.B)GOTO 260
       340 D(L)=D(L)+F
           NI=N-1
       350 DO 380 I=1,NI
           K=I
   30      P=D(I)
           J1=I+1
           DO 360 J=J1,N
           IF(D(J).GE.P)GOTO 360
           K=J
   35      P=D(J)
       360 CONTINUE
```

```
        IF(K.EQ.I)GOTO 380
        D(K)=D(I)
        D(I)=P
        DO 370 J=1,N
5       P=X(J,I)
        X(J,I)=X(J,K)
370 X(J,K)=P
380 CONTINUE
        RETURN
10 400 D(1)=A(1,1)
        X(1,1)=1.D0
        RETURN
        END
```

15

*The essential places of the VBMC algorithm (different from conventional Monte Carlo technique) are bolded.

20

25

30

35

121

REFERENCES

Allen, M.P., and D.J.Tildesley. 1987. Computer Simulation of Liquids. Claredon Press: Oxford.

Baldwin, A.N., and E.M. Shooter. 1994. *J.Biol.Chem.* 269:11456-11461.

5   Baldwin, A.N., and E.M. Shooter. 1995. *J.Biol.Chem.* 270:4594-4602.

Banner, D.W., A. D'Arcy, W. Janes, R. Gentz, H.-J. Schoenfeld, C. Broger, H. Loetscher, and W. Lesslauer. 1993. *Cell* 73:431-445.

Barbacid, M. 1993. *Oncogene* 8:2033-2042.

Barbacid, M. 1994. *J.Neurobiol.* 25:1386-1403.

10   Barde, Y.-A. 1989. *Neuron* 2:1525-1534.

Barker, P.A., and E.M.Shooter. 1994. *Neuron* 13:203-215.

Baumann, U.; Wu, S.; Flaherty, K.M.; McKay, D.B. 1993. *EMBO J.* 12: 3357-3364.

Ben Ari, Y.; Represa, A. 1990. *TINS* 13: 312-318.

Benedetti, M., A. Levi, and M.V. Chao. 1993. *Proc. Natl. Acad. Sci. U.S.A.* 90:7859-7863.

15   Berkemeier, L., J. Winslow, D. Kaplan, K. Nicolics, D. Goeddel, and A. Rosenthal. 1991. *Neuron* 7:857-866.

Bothwell, M.A. 1991. *Cell* 65:915-918.

Bothwell, M.A., Shooter, E.M. 1977. *J. Biol. Chem.* 23: 8532-8536.

Bradshaw, R.A., J. Murray-Rust, C.F. Ibáñez, N.Q. McDonald, R. Lapatto, and T.L. Blundell.

20   1994. *Protein Science* 3:1901-1913.

Brooks, B.R., R.E. Bruccoleri, B.D. Olason, D.J. States, S. Swaminathan, and M. Karplus. 1983. *J. Comput. Chem.* 4:187-217.

Brooks III, C.L., and D.A. Case, 1993. *Chem. Rev.* 93: 2487-2502.

Brünger, A.T. 1988. *J. Mol. Biol.* 203:803-816.

25   Burton, L.E., C.H. Schmelzer, E. Szönyi, C. Yedinak, and A. Gorrell. 1992. *J. Neurochem.* 59:1937-1945.

Burton, G., C. Schmelzer, M. Sadic, F. Hefti, and J. Treanor. 1995. *Soc. Neurosci. Abs.* 21:1061.

Carter, B.D., C. Kaltschmidt, B. Kaltschmidt, N. Offenhäuser, R. Böhm-Matthaei, P. A.

30   Baeuerle, and Y.-A. Barde. 1996. *Science* 272:542-545.

Cassacia-Bonnefil, P., B.D. Carter, R.T. Dobrowsky, and M.V. Chao. 1996. *Nature* 383:716-719.

Chang, G., W.C. Guida, and W.C. Still. 1989. *J. Am. Chem. Soc.* 111:4379-4386.

Chao, M.V. 1992a. *Cell* 68:995-997.

35   Chao, M.V. 1992b. *Neuron* 9:583-593.

Chao, M. 1994. *J. Neurobiol.* 25:1373-1385.

Chao, M.V., and B.L. Hempstead. 1995. *Trends Neurosci.* 18:321-326.

Clackson, T., and J.A. Wells. 1995. *Science* 267:383-386.

Clary, D.O., and L.F. Reichardt. 1994. *Proc. Natl. Acad. Sci. U.S.A.* 91:11133-11137.

5   Davies, A.M. 1994. *J. Neurobiol.* 25:1334-1348.

Dobrowsky, R., M.H. Werner, A.M. Castellino, M.V. Chao, and Y.A. Hannun. 1994. *Science* 265:1596-1599.

Drinkwater, C.C., P.A. Barker, U. Suter, and E.M. Shooter. 1993. *J. Biol. Chem.* 268:23202-23207.

10   Escandon, E., L.E. Burton, E. Szonyi, and K.J. Nikolics. 1993. *Neurosci. Res.* 34:601-613.

Frade, J.M., A. Rodrigues-Tébar, Y.-A. Barde. 1996. *Nature* 383:166-168.

Gibson, K.D., and H.A Scheraga. 1988. In *Structure and Expression: Vol. 1. From Proteins to Ribosomes*; Sarma, M.H., Sarma, R.H., Eds.; Adenine Press: Guilderland, NY, pp. 67-94.

Gidas, B. 1985. *J. Stat. Phys.* 39: 73-131.

15   Glass, D.; Nye, S.; Hantzopoulos, P.; Macchi, M.; Squinto, S.; Goldfarb, M.; Yancopoulos, G. 1991. *Cell* 66: 405-413.

Gotz, R.; Koster, R.; Winkler, C.; Raulf, F.; Lottspeich, F.; Schard, M.; Thoenen, H. 1994. *Nature* 372: 266-269.

Gregory, D.S., A.C.R. Martin, J.C. Cheetham, and A.R. Rees. 1993. *Protein Engineering*

20   6:29-35.

Gunningham, G.W.; Meijer, P.H.E. 1976. *J. Comp. Phys.* 20: 50-63.

Hallböök, F., C.F. Ibáñez, and H. Persson. 1991. *Neuron* 6:845-858.

Hefti, F.H. 1986. *J. Neurosci.* 6:2155-2162.

Hefti, F.H., and Weiner, W.J. 1986. *Annals of Neurology* 20:275-281.

25   Heldin, C.H., A. Ernlund, C. Rorsman, and L. Rönnstrand. 1989. *J. Biol. Chem.* 264:8905-8912.

Hempstead, B.L., D. Martin-Zanca, D.L. Kaplan, L.F. Parada, and M.V. Chao. 1991. *Nature* 350:678-683.

Herrmann, J.L., D.G. Menter, J. Hamada, D. Marchetti, M. Nakajima, and G.L. Nicolson.

30   1993. *Mol. Biol.* 4:1205-1216.

Hobza, P., H.L. Selzle, and E.W. Schlag. 1994. *J. Am. Chem. Soc.* 116:3500-3506.

Hodes, Z.I., G. Némethy, and H.A. Scheraga. 1979. *Biopolymers* 18:1565-1610.

Hohn, A.; Leibrock, J.; Bailey, K.; Barde, Y.-A. 1990. *Nature* 344: 339-341.

Hopfinger, A.J. 1973. Conformational Properties of Macromolecules. Academic Press, New

35   York-London. pp. 70-85.

123

Hunter, C.A., and J.K.M. Sanders. 1990. *J. Am. Chem. Soc.* 112:5525-5534.

Hunter, C.A., J. Singh, and J.M. Thornton. 1991. *J. Mol. Biol.* 218:837-846.

Ibáñez, C.F., T. Ebendal, and H. Persson. 1991. *EMBO J.* 10:2105-2110.

Ibáñez, C.F., T. Ebendal, G. Barbany, J. Murray-Rust, T.L. Blundell, and H. Persson. 1992.

Cell 69:329-341.

Ibáñez, C.F., L. Ilag, J. Murray-Rust, and H. Persson. 1993. *EMBO J.* 12:2281-2293.

Ibáñez, C.F. 1994. *J. Neurobiol.* 25:1349-1361.

Ibáñez, C.F. 1995. *Trends Biotech.* 13:217-227.

Ilag, L.L., P. Lönnerberg, H. Persson, and C.F. Ibáñez. 1994. *J. Biol. Chem.*

269:19941-19946.

IUPAC-IUB Commission on Biochemical Nomenclature. 1970. *Biochemistry* 9:3471-3479.

Jing, S.Q., P. Tapley, and M. Barbacid. 1992. *Neuron* 9:1067-1079.

Johnson, D., A. Lanahan, C.R. Buck, A. Sehgal, C. Morgan, E. Mercer, M. Bothwell, and M.

Chao. 1986. *Cell* 47:545-554.

Judson, R.S.; Jaeger, E.P.; Treasurywala, A.M. 1994. *J. Mol. Struct. (Theochem)* 308:

191-206.

Kahle, P., L.E. Burton, C.H. Schmelzer, and C. Hertel. 1992. *J. Biol. Chem.*

267:22707-22710.

Kaplan, D.R.; Hempstead, B.L.; Martin-Zanca, D.; Chao, M.V.; Parada, L.F. 1991. *Science*

252: 554-558.

Kaplan, D.R., and R.M. Stephens. 1994. *J. Neurobiol.* 25:1404-1417.

Kincaid, R.H.; Scheraga, H.A. 1982. *J. Comput. Chem.* 3: 525-547.

Kirkpatrick, S., C.D. Gelatt, Jr., and M.P. Vecchi. 1983. *Science* 220:671-680.

Klein, R.; Jing, S.; Nanduri, V.; O'Rourke, E.; Barbacid, M. 1991. *Cell* 65: 189-197.

Klein, R.; Lamballe, F.; Bryant, S.; Barbacid, M. 1992. *Neuron* 8: 947-956.

Kobe, B., and J. Deisenhofer. 1993. *Nature* 366:751-756.

Kobe, B., and J. Deisenhofer. 1994. *Trends Biochem. Sci.* 19:415-421.

Kobe, B., and J. Deisenhofer. 1995. *Nature* 374:183-186.

Korsching, S. 1993. *J. Neurosci.* 13:2739-2748.

Krüttgen, A., J.V. Heymach, P. Kahle, and E.M. Shooter. 1996. *Soc. Neurosci. Abs.* 22:557.

Kullander, K., and T. Ebendal. 1994. *J. Neurosci. Res.* 39:195-210.

Kullander, K., and T. Ebendal. 1996. *Soc. Neurosci. Abs.* 22:557.

Kushner, H.J. 1987. *SIAM J. Appl. Math.* 47: 169-185.

Lai, K.-O., D.J. Glass, D. Geis, G.D. Yancopoulos, and N.Y. Ip. 1996. *J. Neurosci. Res.*

46:618-629.

124

Lamballe, F.; Klein, R.; Barbacid, M. 1991. *Cell* 66: 967-970.

Landreth, G.E., and E.M. Shooter. 1980. *Proc. Natl. Acad. Sci. U.S.A.* 77: 4751-4755.

Large, T.H., G. Weskamp, J.C. Helder, M.J. Radeke, T.P. Misko, E.M. Shooter, and L.F. Reichardt. 1989. *Neuron* 2:1123-1134.

5   Leibrock, J.; Lottspeich, A.H.; Hohn, A.; Hofer, M.; Hengerer, B.; Masiakowski, P.; Thoenen, H.; Barde, Y.-A. 1989. *Nature* 341: 149-152.

Lelj, F.; Grimaldi, P.; Cristianziano, P.L. 1991. *Biopolymers* 31: 663-670.

Leven, G.R.; Mendel, L.M. 1993. *TINS* 16: 353-359.

Levi-Montalcini, R. 1987. *EMBO J.* 6:1145-1154.

10   Li, Z.; Scheraga, H.A. 1988. *J. Mol. Struct. (Theochem)* 179: 333-352.

Livnah, O., E.A. Stura, D.L. Johnson, S.A. Middleton, L. S. Mulcahy, N.C. Wrighton, W.J. Dower, L.K. Jolliffe, and I.A. Wilson. 1996. *Science* 273:464-471.

Loeb, D.M.; Maragos, J.; Martin-Zanca, D.; Chao, M.V.; Parada, L.F.; Greene, L.A. 1991. *Cell* 66: 961-966.

15   Luo, Y., and K.E. Neet. 1992. *J. Biol. Chem.* 267:12275-12283.

MacDonald, J.I.S., and S.O. Meakin. 1996. *Mol. Cell. Neurosci.* 7:371-390.

Mahadeo, D., L. Kaplan, M.V. Chao, and B.L. Hempstead. 1994. *J. Biol. Chem.* 269:6884-6891.

Maisopierre, P.C.; Belluscio, L.S.S.; Squinto, S.; Ip, N.Y.; Furth, M.E.; Lindsay, R.M.;

20   Yancopoulos, G.D. 1990. *Science* 247: 1446-1451.

Maness, L.M., A.J. Kastin, J.T. Weber, W.A. Banks, B.S. Beckman, and J.E. Zadina. 1994. *Neurosci. Biobehav. Rev.* 18:143-159.

Marchetti, D., McQuillan, D.J., W.C. Spohn, D.D. Carson, and G.L. Nicolson. 1996. *Cancer Res.* 56:2856-2863.

25   Matsumoto, K., R.K. Wada, J.M. Yamashiro, D.R. Kaplan, and C.J. Thiele. 1995. *Cancer Res.* 55:1798-1806.

McDonald, N.Q., R. Lapatto, J. Murray-Rust, J. Gunning, A. Wlodawer, and T.L. Blundell. 1991. *Nature* 354:411-414.

McKee, A.C.; Kosik, K.S.; Kowal, N.W. 1991. *Ann. Neurol.* 30: 156.

30   McMahon, S.B.; Bennett, D.L.H.; Priestley, J.V.; Shelton, D.L. 1995. *Nature Med.* 1: 774-780.

Meakin, S.O., and E.M. Shooter. 1992. *Trends Neurosci.* 15:323-331.

Merrell, R., M.W. Pulliam, L. Randono, L.F. Boyd, R.A. Bradshaw, and L. Glaser. 1975. *Proc. Natl. Acad. Sci. U.S.A.* 72:4270-4274.

Metropolis, N.; Rosenbluth, A.W.; Rosenbluth, M.N.; Teller, A.H.; Teller, E. 1953. *J. Chem.*

35   *Phys.* 21: 1087-1092.

125

Moore, J.B., and E.M. Shooter. 1975. *Neurobiology* 5:369-381.

Morgan *et al.* 1989. In Annual Reports in Medicinal Chemistry. Ed.: Vinick, F.J. Academic Press, San Diego, CA, pp. 243-252.

Nayeem, A.; Vila, J.; Scheraga, H.A. 1991. *J. Comput. Chem.* 12: 594-605.

5   Nilges, M., G.M. Clore, and A.M. Gronenborn. 1988. *FEBS Lett.* 229:317-324.

Paine, G.H.; Scheraga, H.A. 1985. *Biopolymers* 24: 1391-1436.

Pérez, P., P.M. Coll, B.L. Hempstead, D. Martin-Zanca, and M.V. Chao. 1995. *Mol. Cell. Neurosci.* 6:97-105.

Persson, H., and C.F. Ibáñez. 1993. *Curr. Opin. Neurol. Neurosurg.* 6:11-18.

10   Piela, L.; Kostrowicki, J.; Scheraga, H.A. 1989. *J. Phys. Chem.* 93: 3339-3346.

Piela, L.; Olszewski, K.A.; Pillardy, J. 1994. *J. Mol. Struct. (Theochem)* 308: 229-239.

Ponnuswamy, P.K., and P. Manavalan. 1976. *J. Theor. Biol.* 60:481-486.

Purves, D. 1988. Body and Brain. A Trophic Theory of Neural Connectors. Cambridge, MA: Harvard University Press, pp. 1-1231.

15   Radeke, M.J., T.P. Misko, C. Hsu, L.A. Herzenberg, and E.M. Shooter. 1987. *Nature* 325:593-597.

Radziejewski, C., and R.C. Robinson. 1993. Biochemistry 32:13350-13356.

Radziejewski, C.; Robinson, R. C.; DiStefano, P.S.; Taylor, J.W. 1992. *Biochemistry* 31: 4431-4436.

20   Raj, N.; Morley, S.D.; Jackson, D.E. 1994. *J. Mol. Struct. (Theochem)* 308: 175-190.

Rao, M.; Pangali, C.; Berne, B.J. 1979. *Mol. Phys.* 37: 1773-1798.

Rashid, K.; van der Zee, C.E.E.M.; Ross, G.M.; Chapman, C.A.; Stanisz, J.; Riopelle, R.J.; Racine, R.J.; Fahnestock, M. 1995. *Proc. Natl. Acad. Sci. U.S.A.* 92: 9495-9499.

Ripoll, D.R.; Scheraga, H.A. 1988. *Biopolymers* 27: 283-1303.

25   Robinson, R.C., C. Radziejewski, D.I. Stuart, and E.Y. Jones. 1995. *Biochemistry* 34:4139-4146.

Rodrigues-Tébar, A., G. Dechant, and Y.-A. Barde. 1990. *Neuron* 4:487-492.

Rodrigues-Tébar, A., G. Dechant, R. Gotz, and Y.-A. Barde. 1992. *EMBO J.* 11:917-922.

Rosenthal, A.; Goeddel, D.V.; Nguyen, T.; Lewis, M.; Shih, A.; Laramee, G.R.; Nikolics, K.;
30   Winslow, J.W. 1990. *Neuron* 4: 767-773.

Ross, A.H., M.-C. Daou, C. A. McKinnon, P.J. Condon, M.B. Lachyankar, R.M. Stephens, D.R. Kaplan, and D.E. Wolf. 1996. *J. Cell Biol.* 132:945-953.

Ross, G.M., I.L. Shamovsky, G. Lawrance, M. Solc, S.M. Dostaler, S.L. Jimmo, D.F. Weaver, and R.J. Riopelle. 1997. *Nature Med.* 3:872-878.

35   Rossky, P. J. ; Doll, J. D. ; Friedman, H. L. 1978. *J. Chem. Phys.* 69: 4628-4633.

126

Rovelli, G.; Heller, R.A.; Canossa, M.; Shooter, E.M. 1993. *Proc. Natl. Acad. Sci. USA* 90: 8717-8721.

Ryckaert, J.-P., Ciccotti, G.; Berendsen, H.J.C. 1977. *J. Comput. Phys.* 23:327-341.

Rydén, M., J. Murray-Rust, D. Glass, L.L. Ilag, M. Trupp, G.D. Yancopoulos, N.Q. McDonald, and C.F. Ibáñez. 1995. *EMBO J.* 14:1979-1990.

Rydén, M., and C.F. Ibáñez, C.F. 1996. *J. Biol. Chem.* 271:5623-5627.

Schauer, M., and E.R. Bernstein. 1985. *J. Chem. Phys.* 82:3722-3727.

Schechter, A.L., and M.A. Bothwell. 1981. *Cell* 24:867-874.

Scheraga, H.A. 1989. *Prog. Clin. Biol. Res.* 289: 3-18.

Scheraga, H.A. 1994. *Pol. J. Chem.* 68: 889-891.

Schmelzer, C.H., L.E. Burton, W.-P. Chan, E. Martin, C. Gorman, E. Canova-Davis, V.T. Ling, M.B. Sliwkowski, G. McCray, J.A. Briggs, T.H. Nguyen, and G. Polastri. 1992. *J. Neurochem.* 59:1675-1683.

Schneider, R., E. Schneider-Scherzer, M. Thumher, B. Auer, and M. Schweiger. 1988. *EMBO J.* 7:4151-4156.

Schneider, R., and M. Schweiger. 1991. *Oncogene* 6:1807-1811.

Shamovsky, I.L.; Yarovskaya, I.Yu.; Khrapova, N.G.; Burlakova, E.B. 1992. *J. Mol. Struct. (Theochem)* 253: 149-159.

Shamovsky, I.L., G.M. Ross, R.J. Riopelle, and D.F. Weaver. 1996. *J. Am. Chem. Soc.* 118:9743-9749.

Shih, A., G.R. Laramee, C.H. Schmelzer, L.E. Burton, and J.W. Winslow. 1994. *J. Biol. Chem.* 269:27679-27686.

Simon, I.; Nemethy, G.; Scheraga, H.A. 1978. *Macromolecules* 11: 797-804.

Snider, W.D., and E.M. Johnson. 1989. *Ann. Neurol.* 26:489-506.

Snow, M.E. 1992. *J. Comput. Chem.* 13: 579-584.

Soppet, D.; Escandon, E.; Maragos, J.; Middlemas, D.S.; Reid, S.W.; Blair, J.; Burton, L.E.; Stanton, B.; Kaplan, D.R.; Hunter, T.; Nikolics, K.; Parada, L.F. 1991. *Cell* 65: 895-903.

Squinto, S.P.; Stitt, T.N.; Aldrich, T.H.; Davis, S.; Bianco, S.M.; Radziejewski, C.; Glass, D.J.; Masiakowski, P.; Furth, M.E.; Valenzuela, D.M.; DiStefano, P.S.; Yancopoulos, G.D. 1991. *Cell* 65: 885-893.

Suter, U., C. Angst, C.-L. Tien, C.C. Drinkwater, R.M. Lindsay, and E.M. Shooter. 1992. *J. Neurosci.* 12:306-318.

Sutter, A., R.J. Riopelle, R.M. Harris-Warrick, and E.M. Shooter. 1979. *J. Biol. Chem.* 254:5972-5982.

Szentpsly, L.V.; Shamovsky, I.L.; Nefedova, V.V.; Zubkus, V.E. 1994. *J. Mol. Struct.*

127

(Theochem) 308: 125-140.

Taylor, R.A.V., J.F. Kerrigan, F.M. Longo, M. deBoisblanc, and W.C. Mobley. 1991. *Soc. Neurosci. Abs.* 17: 712.

Thoenen, H. 1991. *Trends Neurosci.* 14: 165-170.

5   Treanor, J.J.S., C. Schmelzer, B. Knusel, J.W. Winslow, D.L. Shelton, F. Hefti, K. Nikolics, and L.E. Burton. 1995. *J. Biol. Chem.* 270: 23104-23110.

Ullrich, A., and J. Schlessinger. 1990. *Cell* 61: 203-212.

Urfer, R., P. Tsoulfas, D. Soppet, E. Escandón, L.F. Parada, and L.G. Presta. 1994. *EMBO J.* 13:5896-5909.

10   Urfer, R., P. Tsoulfas, L. O'Connell, D.L. Shelton, L.F. Parada, and L.G. Presta. 1995. *EMBO J.* 14:2795-2805.

Vale, R.D.; Shooter, E.M. 1985. *Methods Enzymol.* 109: 21-39.

Vanderbilt, D., and S.G. Louie. 1984. *J. Comput. Phys.* 56:259-271.

Van der Zee, C.E.E., G.M. Ross, R.J. Riopelle, and T. Hagg. 1996. *Science* 274: 1729-1732.

15   Villani, V.; Tamburro, A.M. 1994. *J. Mol. Struct. (Theochem)* 308: 141-157.

Warme, P.K., and R.S. Morgan. 1978. *J. Mol. Biol.* 118: 289-304.

Washiyama, K., Y. Muragaki, L.B. Rorke, V.M.-Y.Lee, S.C. Feinstein, M.J. Radeke, D. Blumberg, D.R. Kaplan, and J.Q. Trojanowski. 1996. *Amer. J. Path.* 148:929-940.

Weiner, S.J., P.A. Kollman, D.A. Case, U.C. Singh, C. Ghio, G. Alagona, S. Profeta Jr., and

20   P.Weiner. 1984. *J.Am.Chem.Soc.* 106:765-784.

Weskamp, G.; Reichardt, L.F. 1991. *Neuron* 6: 649-663.

Wilson, C., and S. Doniach. 1989. *Proteins* 6:193-209.

Wilson, S.R., W. Cui, J.W. Moscowitz, and K.E. Schmidt. 1988. *Tetrahedron Lett.* 29:4373-4376.

25   Windisch, J.M., B. Auer, R. Marksteiner, M.E. Lang, and R. Schneider. 1995a. *FEBS Lett.* 374:125-129.

Windisch, J.M., R. Marksteiner, and R. Schneider. 1995b. *J. Biol. Chem.* 270: 28133-28138.

Windisch, J.M., R. Marksteiner, M.E. Lang, B. Auer, and R. Schneider. 1995c. *Biochemistry* 34:11256-11263.

30   Wolf, D.E., C.A. McKinnon, M.-C. Daou, R.M. Stephens, D.R. Kaplan, and A.H. Ross. 1995. *J. Biol. Chem.* 270:2133-2138.

Woo, S.B., D.E. Timm, and K.E. Neet. 1995. *J. Biol. Chem.* 270:6278-6285.

Woo, S.B., and K.E. Neet. 1996. *J. Biol. Chem.* 271:24433-24441.

Woolf, C.J.; Doubell, T.A. 1994. *Current Opinions in Neurobiol.* 4: 525-534.

35   Yan, H., and M.V. Chao. 1991. *J. Biol. Chem.* 266:12099-12104.

128

Yoder, M.D.; Keen, N.T.; Jurnak, F. 1993. *Science* 260: 1503-1507.

WHAT IS CLAIMED IS:

1.   A variable basis Monte-Carlo (VBMC) simulated annealing method for identifying an optimal structure in a molecular system, comprising:

(a)   providing a Markov chain with an initial basis set of N configurational variables which define a structure for said molecular system;

(b)   translating the N configurational variables simultaneously along a basis vector to produce a new structure for the molecular system, wherein magnitude of translation is randomly chosen within a preselected range;

(c)   calculating potential energy of the new structure of the molecular system;

(d)   deciding whether to accept or reject the new structure using an effective temperature dependent transition function, and if the new structure is accepted, replacing the current structure with the accepted structure;

(e)   repeating steps (b) to (d), each repetition having a new basis vector, for a preselected first number of repetitions at a preselected upper temperature; then

(f)   decreasing temperature according to a preselected cooling schedule;

(g)   repeating steps (b) to (d) and (f), each repetition having a new basis vector, for a preselected second number of repetitions; then

(h)   storing current structure of the molecular system;

(I)   repeating steps (g) and (h) until a preselected number of stored structures have been accumulated; then

(j)   rotating the basis set of configurational variables according to an effective distribution of the accumulated structures so that basis vectors are directed along low-energy valleys of a potential energy hypersurface thereby accelerating conformational motions and structural transitions of the molecular system, and erasing accumulated structures from steps (h) and (I);

(k)   repeating steps (I) and (j) until, after an effective third number of repetitions, a preselected lower temperature limit is reached, thereby producing an unrefined global minimum structure; and

(l)   refining the global energy minimum structure so that at least one local minimum on the potential energy hypersurface is identified.

2.   The method of claim 1, wherein the basis vector is chosen randomly within said preselected range.

3.   The method of claim 1, wherein the basis vector is chosen deterministically within said

130

preselected range.

4.   The method of claim 1 wherein the preselected second number of repetitions is N or a multiple thereof.

5

5.   The method of claim 1 wherein the preselected second number of repetitions is at least about 2N.

6.   The method of claim 1 wherein the refining step is non-linear minimization.

10

7.   The method of claim 6, wherein the refining step is gradient descent minimization.

8.   The method of claim 6, wherein the refining step is conjugate gradient minimization.

15   9.   The method of claim 6, wherein the refining step is a quasi-Newton minimization method.

10.   The method of claim 9, wherein the quasi-Newton method is Newton -Raphson method.

20

11.   The method of claim 6, wherein the refining step is Marquardt method.

12.   The method of claim 6, wherein the refining step is a variable metric method.

25   13.   The method of claim 6, wherein the refining step is Powell method.

14.   The method of claim 1 wherein said molecular system is at least one peptide domain comprising amino acid residues, each amino acid residue comprising a main chain having α-carbon atoms, carbonyl carbon atoms and nitrogen atoms, said basis set of configurational

30   variables comprising torsional angles (ψ_i) between said α-carbon atoms and neighbouring carbonyl carbon atoms, and torsional angles (ϕ_i) between said α-carbon atoms and neighbouring nitrogen atoms.

15.   The method of claim 14 wherein torsional angles describing planar portions of said

35   peptide domains are held constant.

131

16.   The method of claim 14 wherein said effective temperature dependent transition

function for screening a new state x_{i+1} derived from a previous state x_i is given by:

$$W(x_i \Rightarrow x_{i+1}) = 1/[1 + \exp(\Delta E_i /kT)]$$

where ΔE_i is the difference between conformational energies of the states x_{i+1} and x_i, k is the

Boltzmann constant and T is absolute temperature.

17.   The method of claim 14 wherein said effective temperature dependent transition

function for screening a new state x_{i+1} derived from a previous state x_i is given by:

$$W(x_i \Rightarrow x_{i+1}) = 1, \qquad\qquad\qquad \text{if } E(x_{i+1}) \leq E(W(x_i))$$

$$= \exp(-\Delta E_i /kT), \quad \text{if } E(x_{i+1}) \geq E(W(x_i))$$

where ΔE_i is the difference between conformational energies of the states x_{i+1} and x_i, k is the

Boltzmann constant and T is absolute temperature.

18.   The method of claims 14, 15, 16 or 17 wherein said preselected upper temperature is

about $1000^\circ K$.

19.   The method of claim 18 wherein said preselected lower temperature is about $120^\circ K$.

20.   A method of identifying structures of a peptide domain of a neurotrophin to bind with a

binding site of a receptor, comprising;

        a)   providing a plurality of neurotrophin analogues wherein at least one

neurotrophin analogue binds said receptor;

        b)   identifying an optimal or near-optimal structure for respective peptide domains

of the neurotrophin analogues that bind said receptor by applying a preselected number of the

variable basis Monte-Carlo (VBMC) annealing simulations according to claim 1 to each of the

respective peptide domains to identify minimum or near-minimum energy structures for said

peptide domains; and

        c)   comparing said minimum or near-minimum energy structures to identify

common structural features shared by neurotrophin analogues exhibiting receptor mediated

activity.

21.   The method according to claim 20 wherein said common structural features are

absent from neurotrophin analogues that do not exhibit receptor-mediated activity.

22.   A method of identifying structures of a domain of a ligand to bind with a binding site of

132

a receptor, comprising;

       a)   providing a plurality of ligand analogues wherein at least one ligand analogue binds said receptor;

       b)   identifying an optimal or near-optimal structure for respective domains of the ligand analogues that bind said receptor by applying a preselected number of the variable basis Monte-Carlo (VBMC) annealing simulations according to claim 1 to each of the respective domains to identify minimum or near-minimum energy structures for said domains; and

       c)   comparing said minimum or near-minimum energy structures to identify common structural features shared by ligands exhibiting receptor mediated activity.

23.   The method according to claim 22 wherein said common structural features are absent from ligand analogues that do not exhibit receptor-mediated activity.

24.   The method according to claim 20 wherein said neurotrophin is NGF, and said receptor is TrkA.

25.   The method according to claim 20 wherein said neurotrophin is brain-derived neurotrophic factor (BDNF), neurotrophin-3 (NT-3), or neurotrophin-4 (NT-4), and said receptor is TrkB.

26.   The method according to claim 20 wherein said neurotrophin is neurotrophin-3 (NT-3) and said receptor is TrkC.

27.   The method according to claim 20 wherein said receptor is the common neurotrophin receptor $p75^{NTR}$.

28.   A ligand for binding with TrkA, wherein TrkA comprises a leucine rich motif (LRM) comprising amino acid residues 93 to 117, wherein coordinates of the residues of said LRM are given in Appendix 1, said LRM having five binding areas, area A comprising amino acid residue Phe^{105tA} capable of hydrophobic interaction, area B comprising amino acid residues Phe^{111tA}, Phe^{113tA}, and Thr^{114tA} capable of hydrophobic interaction, area C comprising amino acid residues Asp^{109tA} and His^{112tA} capable of ionic interaction, area D comprising amino acid residue Lys^{100tA} capable of ionic interaction, and area E comprising Asn^{95tA} to Ile^{98tA} capable of multiple parallel β-strand type hydrogen bonding, the ligand comprising;

       at least three moieties each comprising effective atomic elements having spatial

133

occupancy, relative atomic position, bond type and charge to define a three dimensional conformation of said ligand so that a first moiety can bind with a first binding area, a second moiety can bind with a second binding area, and a third moiety can bind with a third binding area.

5

29.   The ligand according to claim 28 wherein the first moiety can hydrophobically bond with binding area A, the second moiety can ionically bind with binding area C, and the third moiety can ionically bind with binding area D.

10   30.   The ligand according to claim 29 comprising a fourth moiety effectively spaced with respect to the other moieties so it can hydrophobically bond with binding area B.

31.   The ligand according to claim 29 comprising a fourth moiety effectively spaced with respect to the other moieties so it can hydrogen bond with binding area E.

15

32.   The ligand according to claim 29 wherein the first moiety is capable of hydrophobic bonding to Phe^{105tA} in binding area A, the second moiety is positively charged and present in an effective position in said ligand to ionically interact with Asp^{109tA} and His^{112tA} in binding area C, and the third moiety is negatively charged and present in an effective position in said

20   ligand to ionically interact with Lys^{100tA} in binding area D.

33.   The ligand according to claim 32 wherein the moiety hydrophobically bonded to Phe^{105tA} in binding area A is Trp, wherein the positively charged moiety which ionically interacts with Asp^{109tA} and His^{112tA} in binding area C is Arg and Lys, and wherein the negatively

25   charged moiety which ionically interacts with Lys^{100tA} in binding area D is Asp.

34.   The ligand according to claim 32 wherein said first, second and third moieties are amino acids or isosteres thereof.

30   35.   The ligand according to claim 30 wherein said fourth moiety is an amino acid or isostere thereof.

36.   The ligand according to claim 31 wherein said fourth moiety is an amino acid or isostere thereof.

35

37.   A method of designing a ligand to bind with a LRM of TrkA, comprising:

134

providing a template of said LRM of TrkA, said LRM comprising amino acid residue

sequence 93 to 117 inclusive, said amino acid residues having spatial Cartesian coordinates

given in Appendix 1 wherein said binding area A comprises Phe^{105tA} capable of hydrophobic

bonding, binding area B comprises Phe^{111tA}, Phe^{113tA}, Thr^{114tA} capable of hydrophobic bonding,

5   binding area C comprises Asp^{109tA} and His^{112tA} capable of ionic interaction, binding area D

comprises Lys^{100tA} capable of ionic interaction, and binding area E comprises Asn^{95tA} to Ile^{98tA}

capable of hydrogen bonding; and

computationally evolving a ligand using an effective algorithm so that said evolved

ligand comprises at least three effective moieties located relative to each other in the ligand

10   so that a first moiety can bind with a first of said five binding areas, a second moiety can bind

with a second of said five binding areas, and a third moiety can bind with a third of said

binding areas.

38.   The method according to claim 37 including the step of generating said ligand under a

15   constraint that the evolved ligand comprises said first effective moiety spatially located to

hydrophobically bind with binding area A, said second moiety spatially located to ionically

interact with binding area C, and said third moiety spatially located to ionically interact with ·

binding area D.

20   39.   The method according to claim 37 including the step of generating said ligand under a

constraint that the evolved ligand comprises an effective moiety spatially located to

hydrophobically interact with binding area B.

40.   The method according to claim 37 including the step of generating said ligand under a

25   constraint that the evolved ligand comprises an effective moiety spatially located to hydrogen

bond with binding area E.

41.   A ligand for binding with TrkB, wherein TrkB comprises a leucine-rich motif (LRM)

comprising amino acid residues 93 to 117, the coordinates of the residues of said LRM given

30   in Appendix 2, said LRM having five binding areas, binding area F comprising amino acid

residue Asp^{100tB} capable of ionic interaction, binding area G comprising amino acid residue

Lys^{109tB} capable of ionic interaction, binding area H comprising amino acid residue Lys^{113tB}

capable of ionic interaction, binding area I comprising amino acid residue Arg^{94tB} capable of

ionic interaction, and binding area K comprising amino acid residue Lys^{104tB} capable of

35   hydrogen bonding or ionic interaction, the ligand comprising:

at least three moieties each comprising effective atomic elements having spatial

135

occupancy, relative atomic position, bond type and charge to define a three dimensional conformation of said ligand so that a first moiety can bind with a first binding area, a second moiety can bind with a second binding area, and a third moiety can bind with a third binding area.

5

42.   The ligand according to claim 41 wherein one of said at least three moieties can ionically bind with binding area F, another of said at least three moieties can ionically bind with binding area G, and another of said at least three moieties can form a hydrogen bond or ionically bind with binding area K.

10

43.   The ligand according to claim 42 wherein said ligand includes a fourth moiety effectively spaced relative to said at least three moieties so that it can ionically bind with binding area H.

15

44.   The ligand according to claim 42 wherein said ligand includes a fourth moiety effectively spaced relative to said at least three moieties so that it can ionically bind with binding area I.

45.   The ligand according to claim 41 wherein the first moiety is positively charged and

20   present in an effective position in said ligand to ionically bind to Asp^{100tB} in binding area F, the second moiety is negatively charged and present in an effective position in said ligand to ionically interact with Lys^{109tB} in binding area G, and the third moiety is neutral or negatively charged and capable of hydrogen bonding or ionically bonding to Lys^{104tB} in binding area K.

25   46.   The ligand according to claim 45 wherein a fourth moiety is negatively charged and present in an effective position in said ligand to ionically bind to Lys^{113tB} in binding area H, and wherein a fifth moiety is negatively charged and present in an effective position in said ligand to ionically bind to Arg^{94tB} in binding area I.

30   47.   The ligand according to claim 46 wherein the positively charged moiety ionically bonded to Asp^{100tB} in binding area F is Arg, wherein the charged moiety which ionically interacts with Lys^{109tB} in binding area G is Glu and Lys, and wherein the negatively charged moiety ionically bonded with Lys^{113tB} in binding area H is Asp.

35   48.   The ligand according to claim 47 wherein the negatively charged amino acid residue ionically bonded to Arg^{94tB} in binding area I is Glu.

136

49.   The ligand according to claim 45 wherein the neutral or negatively charged moiety capable of hydrogen bonding or ionically bonding to Lys^{104tB} in binding area K is Thr.

50.   The ligand according to claim 45 wherein said first, second and third moieties are amino acids or isosteres thereof.

51.   The ligand according to claim 46 wherein said fourth and fifth moieties are amino acids or isosteres thereof.

52.   A method of designing a ligand to bind with TrkB, wherein TrkB comprises a leucine-rich motif (LRM) comprising amino acid residues 93 to 117, the coordinates of the residues of said LRM given in Appendix 2, said LRM having five binding areas, binding area F comprising amino acid residue Asp^{100tB} capable of ionic interaction, binding area G comprising amino acid residue Lys^{109tB} capable of ionic interaction, binding area H comprising amino acid residue Lys^{113tB} capable of ionic interaction, binding area I comprising amino acid residue Arg^{94tB} capable of ionic interaction, and binding area K comprising amino acid residue Lys^{104tB} capable of hydrogen bonding or ionic interaction, the method comprising:
        computationally evolving a ligand using an effective algorithm so that said evolved ligand comprises at least three effective moieties located relative to each other in the ligand so that a first moiety can bind with a first of said five binding areas, a second moiety can bind with a second of said five binding areas, and a third moiety can bind with a third of said binding areas.

53.   A ligand for binding with the common neurotrophin receptor $p75^{NTR}$, wherein $p75^{NTR}$ comprises a binding site including amino acid residues Cys^{39p} to Cys^{94p} inclusive, said residues of said binding site having spatial coordinates given in Appendix 3, said binding site having three binding areas including binding loop 2A comprising region Cys^{39p} to Cys^{58p} capable of attractive electrostatic interaction, binding loop 2B comprising region Cys^{58p} to Cys^{79p} capable of attractive electrostatic interaction, and binding loop 3A comprising region Cys^{79p} to Cys^{94p} capable of attractive electrostatic interaction, the ligand comprising;
        at least two moieties each comprising effective atomic elements having spatial occupancy, relative atomic position, bond type and charge to define a three dimensional conformation of said ligand so that a first moiety can bind with a first binding area, and a second moiety can bind with a second binding area.

54.   The ligand according to claim 53 wherein said ligand is an agonist, and wherein one

137

SUBSTITUTE SHEET (RULE 26)

of said at least two moieties binds to loop 2B.

55.   The ligand according to claim 53 further comprising a third moiety wherein said first moiety can bind to loop 2A, said second moiety can bind to loop 2B and said third moiety can bind to loop 3A.

56.   The ligand according to claim 53 wherein said first moiety binds to any two of Asp^{47p}, Lys^{56p} and Glu^{53p}.

57.   The ligand according to claim 53 wherein said binding loop 2A includes amino acid residues Asp^{47p} and Lys^{56p} and said first moiety ionically binds to said residues Asp^{47p} and Lys^{56p}.

58.   The ligand according to claim 53 wherein said binding loop 2B includes amino acid residues Asp^{75p} and Asp^{76p} and said second moiety ionically binds to said residues Asp^{75p} and Asp^{76p}.

59.   The ligand according to claim 55 wherein said binding loop 3A includes amino acid residues Asp^{88p} and Glu^{89p} and said third moiety ionically binds to said residues Asp^{88p} and Glu^{89p}.

60.   The ligand according to claim 55 wherein said third moiety binds to any two of Asp^{88p}, Glu^{89p} and Arg^{80p}.

61.   A method of designing a ligand for binding with the common neurotrophin receptor p75^{NTR}, wherein p75^{NTR} comprises a binding site including amino acid residues Cys^{39p} to Cys^{94p} inclusive, said residues of said binding site having spatial coordinates given in Appendix 3, said binding site having three binding areas including binding loop 2A comprising region Cys^{39p} to Cys^{58p} capable of attractive electrostatic interaction, binding loop 2B comprising region Cys^{58p} to Cys^{79p} capable of attractive electrostatic interaction, and binding loop 3A comprising region Cys^{79p} to Cys^{94p} capable of attractive electrostatic interaction, the method comprising;

        computationally evolving a ligand using an effective algorithm so that said evolved ligand comprises at least two effective moieties located relative to each other in the ligand so that a first moiety can bind to a first of said three loops and a second moiety can bind to a second loop of said three loops.

138

62.   A method of identifying a ligand to bind with a leucine rich motif (LRM) of TrkA, comprising:

    providing a three dimensional conformation for said LRM, said LRM comprising amino acid residue sequence 93 to 117 inclusive, said amino acid residues having spatial Cartesian

5   coordinates given in Appendix 1, said LRM having five binding areas, area A comprising amino acid residue Phe^{105tA} capable of hydrophobic interaction, area B comprising amino acid residues Phe^{111tA}, Phe^{113tA}, and Thr^{114tA} capable of hydrophobic interaction, area C comprising amino acid residues Asp^{109tA} and His^{112tA} capable of ionic interaction, area D comprising amino acid residue Lys^{100tA} capable of ionic interaction, and area E comprising Asn^{95tA} to Ile^{98tA}

10   capable of multiple parallel β-strand type hydrogen bonding;

    providing a data base containing molecules coded for spatial occupancy, relative atomic position, bond type and/or charge; and

    screening said data base to select those molecules comprising moieties having a three dimensional conformation and effective charge that can bind with at least three of said

15   five binding areas.

63.   A method of identifying a ligand to bind with a leucine rich motif (LRM) of TrkB, comprising:

    providing a three dimensional conformation for said LRM, said LRM comprising amino

20   acid residues 93 to 117, the coordinates of the residues of said LRM given in Appendix 2, said LRM having five binding areas, binding area F comprising amino acid residue Asp^{100tB} capable of ionic interaction, binding area G comprising amino acid residue Lys^{109tB} capable of ionic interaction, binding area H comprising amino acid residue Lys^{113tB} capable of ionic interaction, binding area I comprising amino acid residue Arg^{94tB} capable of ionic interaction,

25   and binding area K comprising amino acid residue Lys^{104tB} capable of hydrogen bonding or ionic interaction;

    providing a data base containing molecules coded for spatial occupancy, relative atomic position, bond type and/or charge; and

    screening said data base to select those molecules comprising moieties having a

30   three dimensional conformation and effective charge that can bind with at least three of said five binding areas.

64.   A method of identifying a ligand to bind with common neurotrophin receptor p75^{NTR}, comprising:

35   providing a three dimensional conformation for the common neurotrophin receptor p75^{NTR}, wherein p75^{NTR} comprises a binding site including amino acid residues Cys^{39p} to

139

Cys^{94p} inclusive, said residues of said binding site having spatial coordinates given in Appendix 3, said binding site having three binding areas including binding loop 2A comprising region Cys^{39p} to Cys^{58p} capable of attractive electrostatic interaction, binding loop 2B comprising region Cys^{58p} to Cys^{79p} capable of attractive electrostatic interaction, and binding

5   loop 3A comprising region Cys^{79p} to Cys^{94p} capable of attractive electrostatic interaction;

           providing a data base containing molecules coded for spatial occupancy, relative atomic position, bond type and/or charge; and

           screening said data base to select those molecules comprising moieties that can bind with at least two of said three binding loops.

10

15

140

First monomer: amino terminus

	1				5					10					15	
hNGF	S	S	S	H	P	I	F	H	R	G	E	F	S	V	C ...
mNGF	S	S	T	H	P	V	F	H	M	G	E	F	S	V	C ...
mNGFΔ3-9	-	-	-	-	-	-	-	S	S	G	E	F	S	V	C ...
hNGF-H4D	S	S	S	D	P	I	F	H	R	G	E	F	S	V	C ...
mNGFΔ1-8	-	-	-	-	-	-	-	-	M	G	E	F	S	V	C ...
BDNF	-	-	H	S	D	P	A	R	R	G	E	L	S	V	C ...

Second monomer: carboxyl terminus

				112'					118'	
hNGF	... C	V	C	V	L	S	R	K	A	V	R
mNGF	... C	V	C	V	L	S	R	K	A	T	R
mNGFΔ3-9	... C	V	C	V	L	S	R	K	A	T	R
hNGF-H4D	... C	V	C	V	L	S	R	K	A	V	R
mNGFΔ1-8	... C	V	C	V	L	S	R	K	A	T	R
BDNF	... C	V	C	T	L	T	I	K	R	G	R

Figure 1
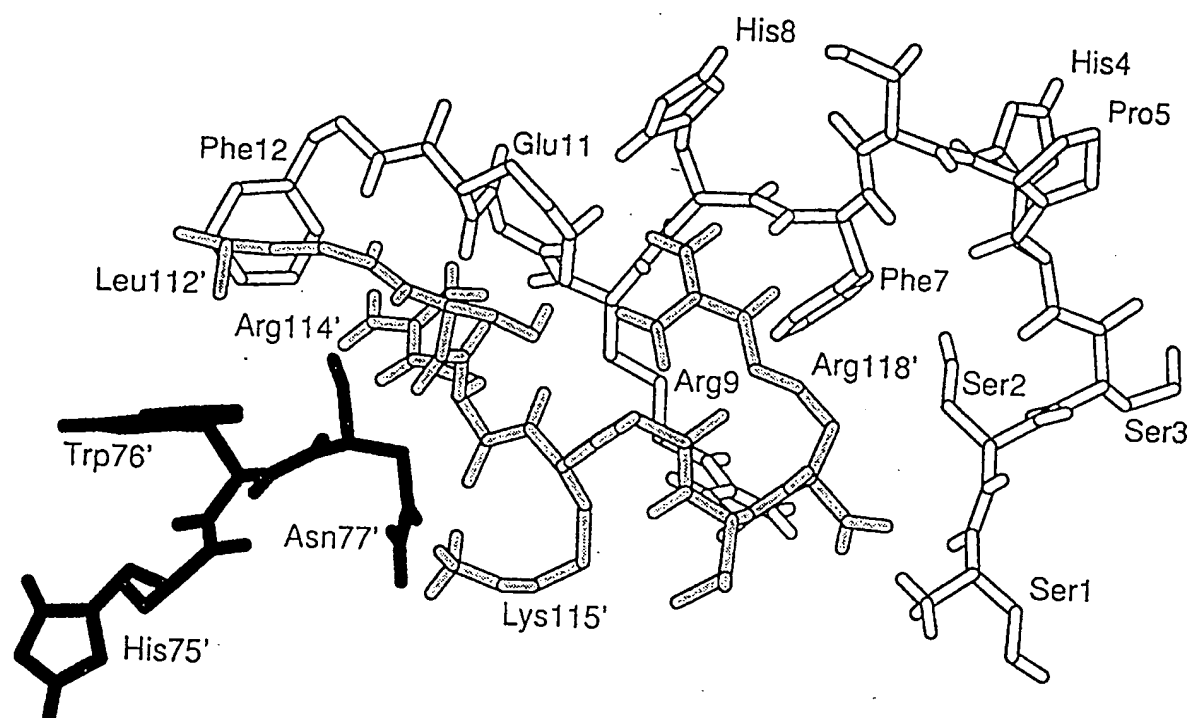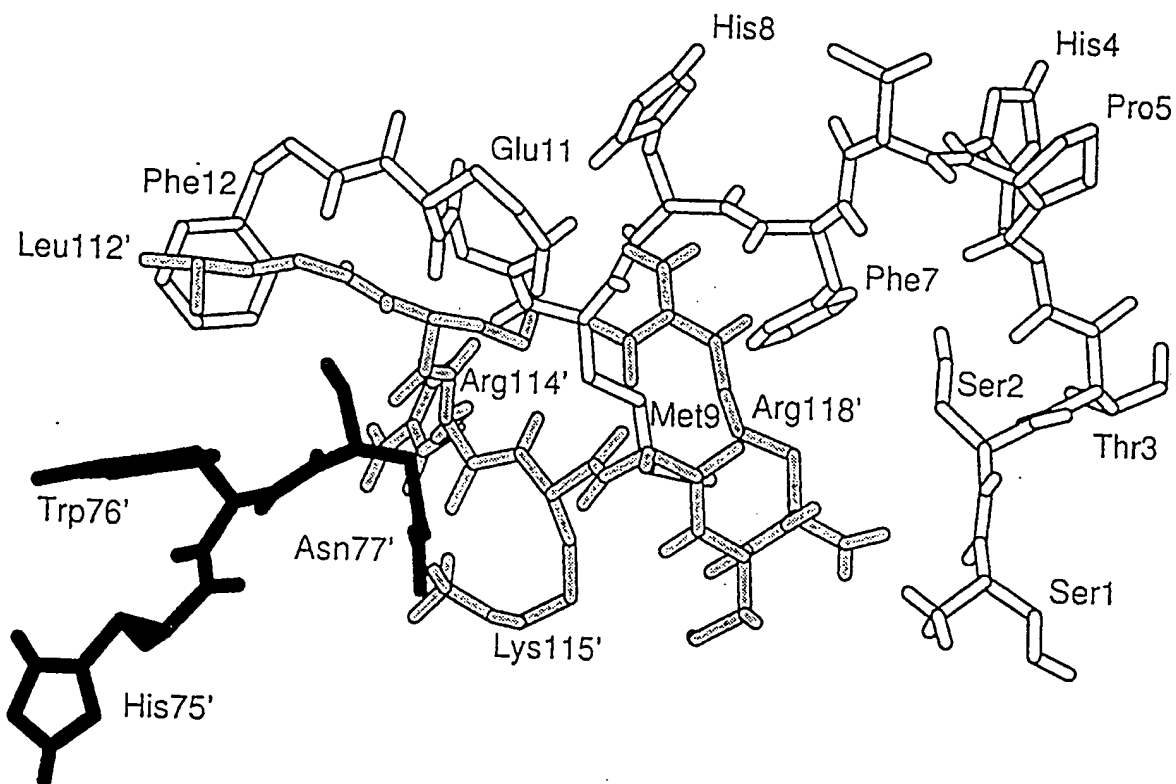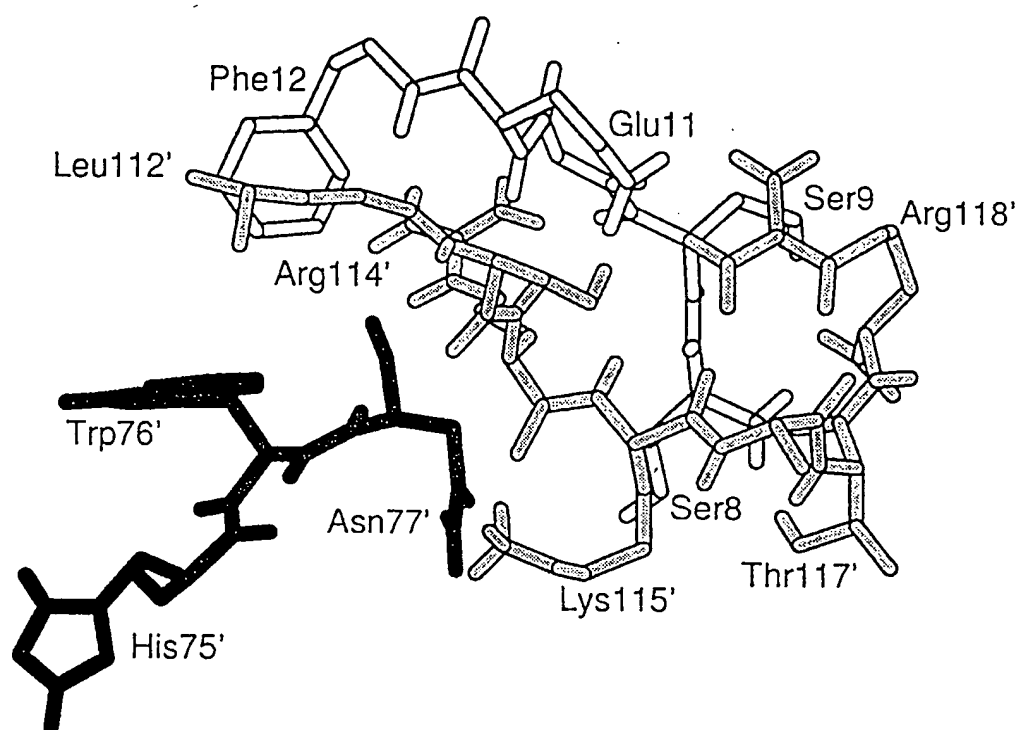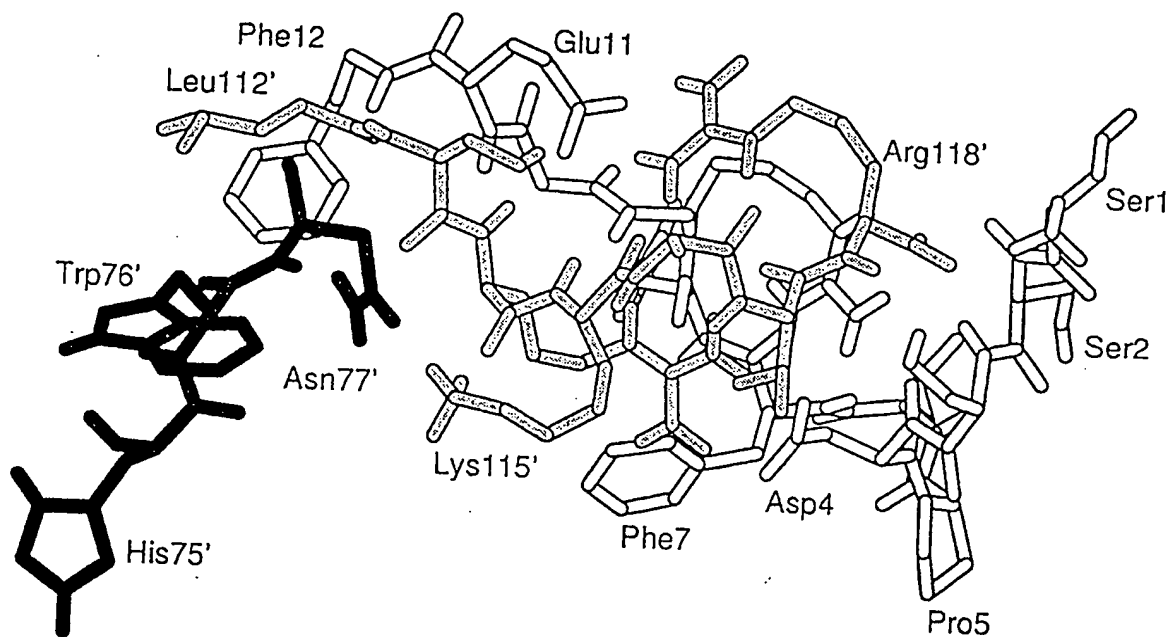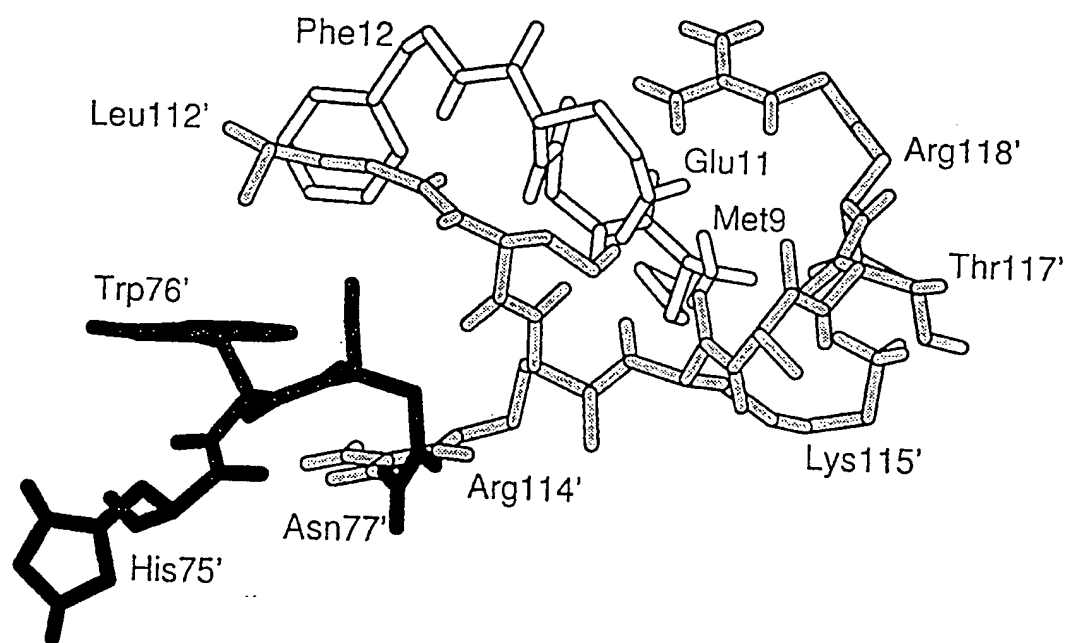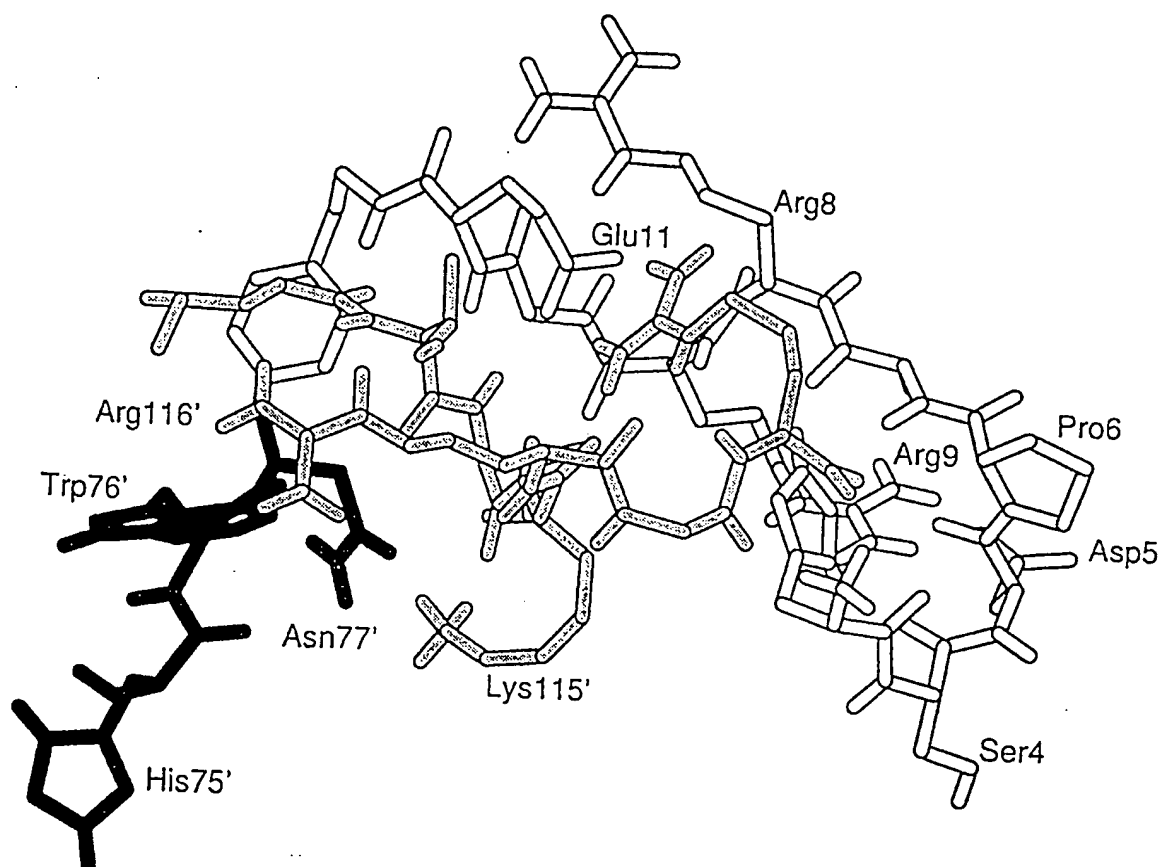
Figure 2

Figure 3

Figure 4

Figure 5

Figure 6

Figure 7

8/29
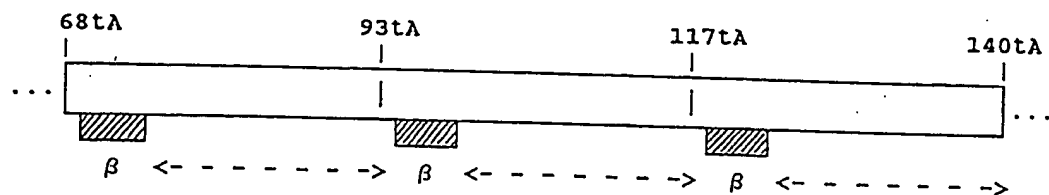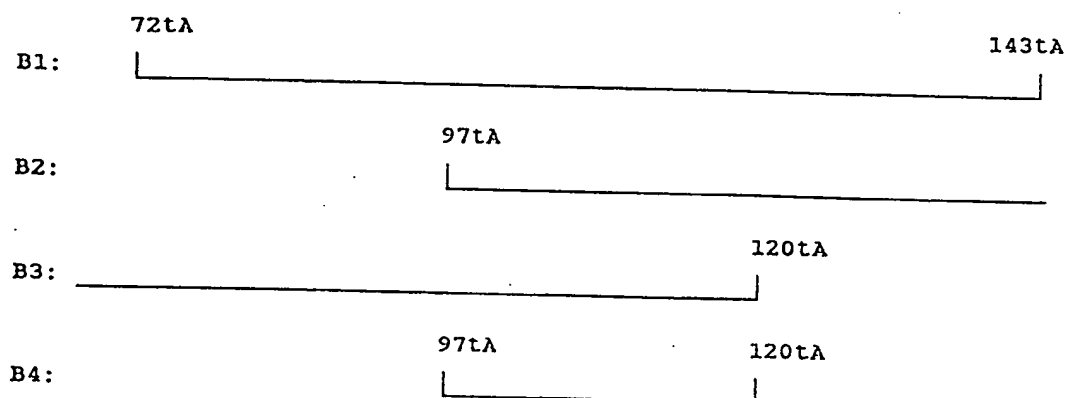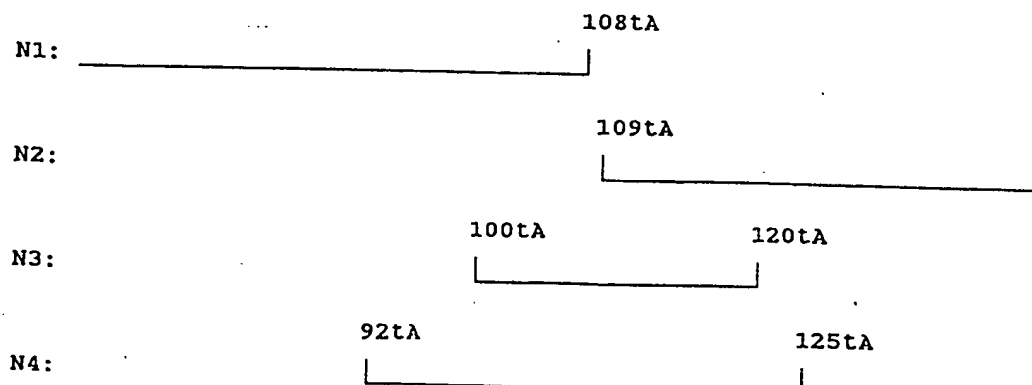
Figure 8

First monomer: amino terminus

	1				5					10					15				
hNGF	S	S	S	H	P	I	F	H	R	G	E	F	S	V	C	D	...
mNGF	S	S	T	H	P	V	F	H	M	G	E	F	S	V	C	D	...
mNGFΔ3-9	-	-	-	-	-	-	S	S	S	G	E	F	S	V	C	D	...
hNGF:NT-4/5	S	S	S	H	P	I	F	H	R	G	E	F	S	V	C	D	...

Second monomer: carboxyl terminus

	75'							110'				115'						118'
hNGF	... K	H	W	N	...	C	V	C	V	L	S	R	K	A	V	R
mNGF	... K	H	W	N	...	C	V	C	V	L	S	R	K	A	T	R
mNGFΔ3-9	... K	H	W	N	...	C	V	C	V	L	S	R	K	A	T	R
hNGF:NT-4/5	... R	H	W	V	...	C	V	C	T	L	L	S	R	T	G	R
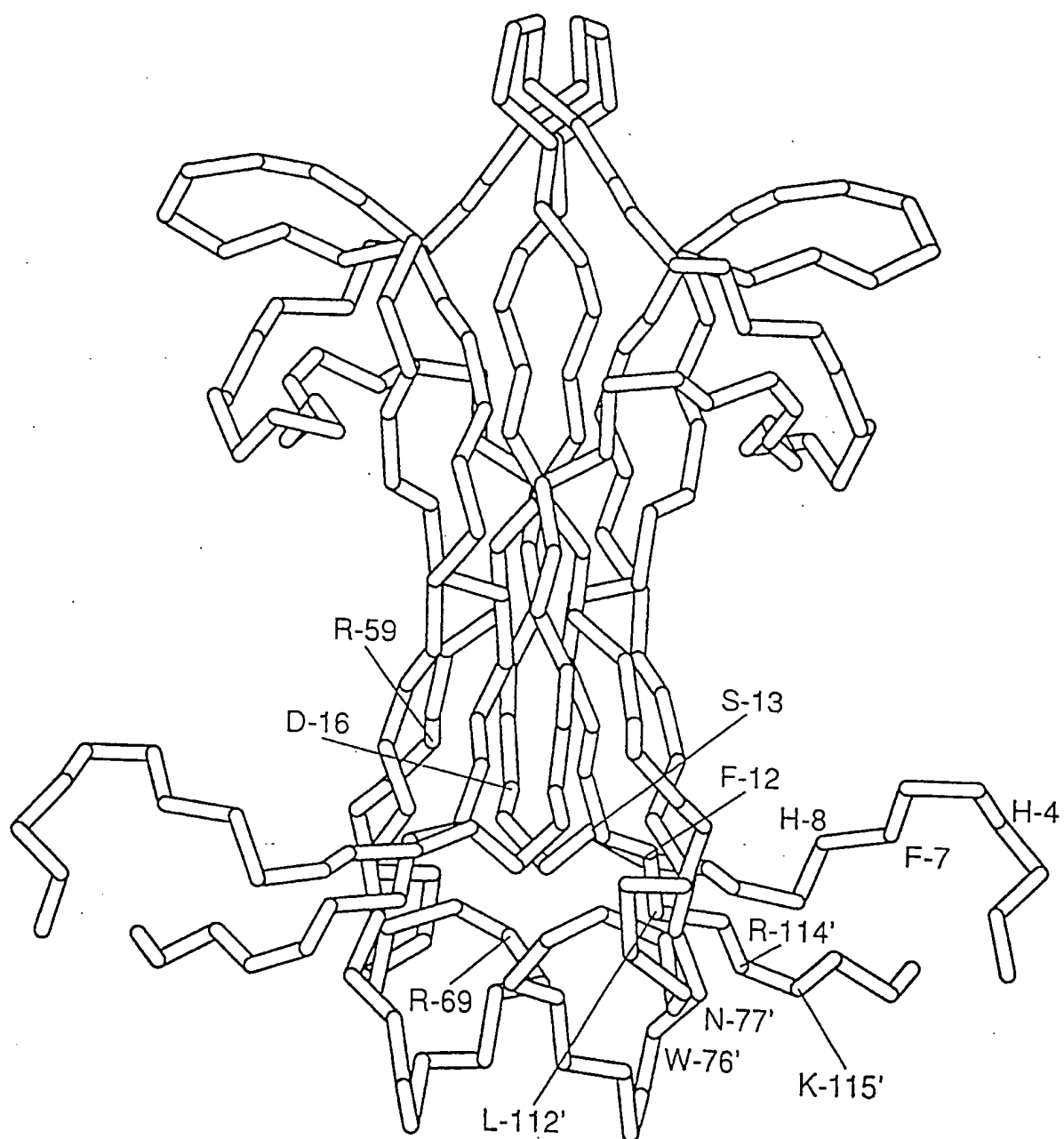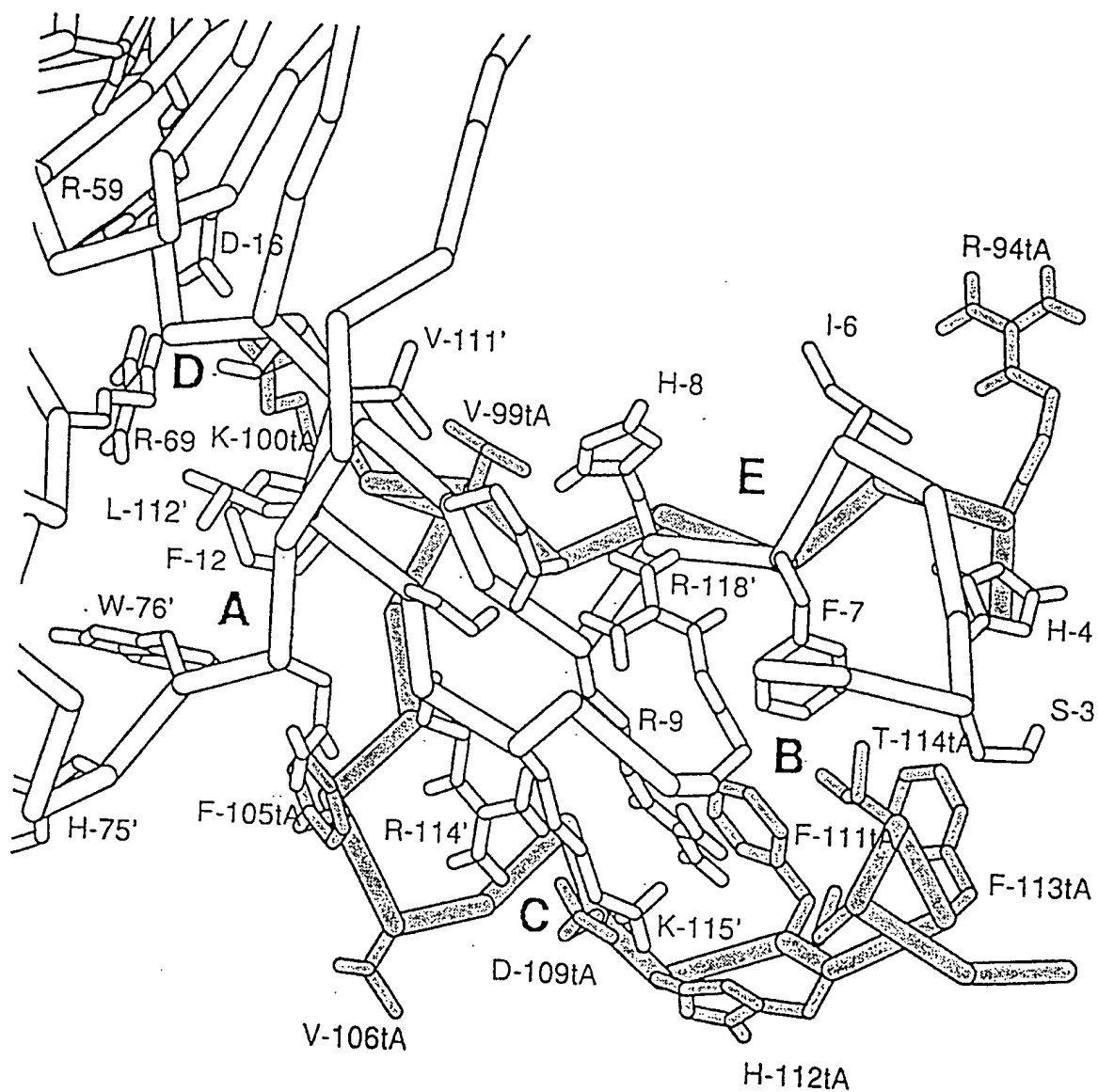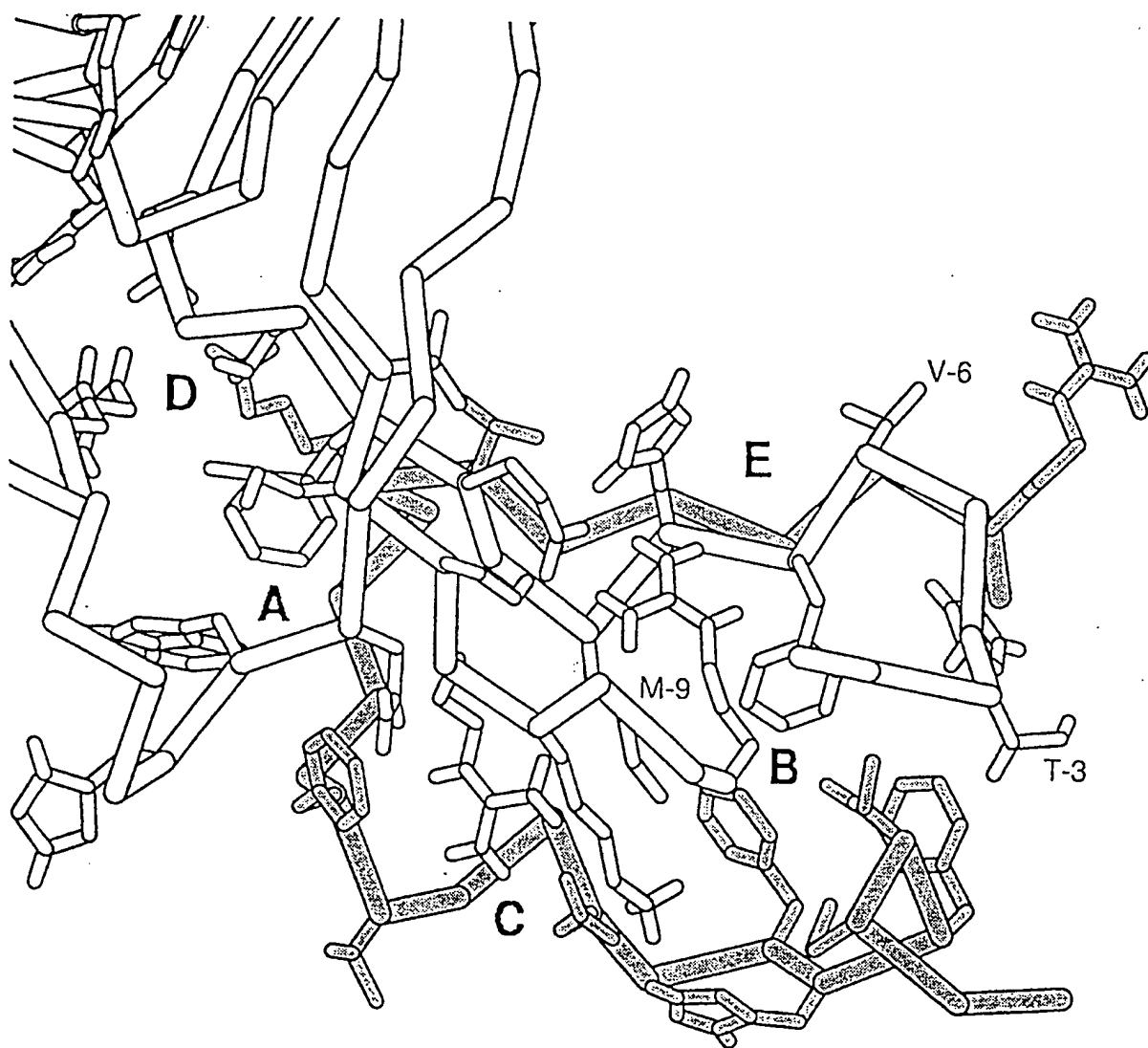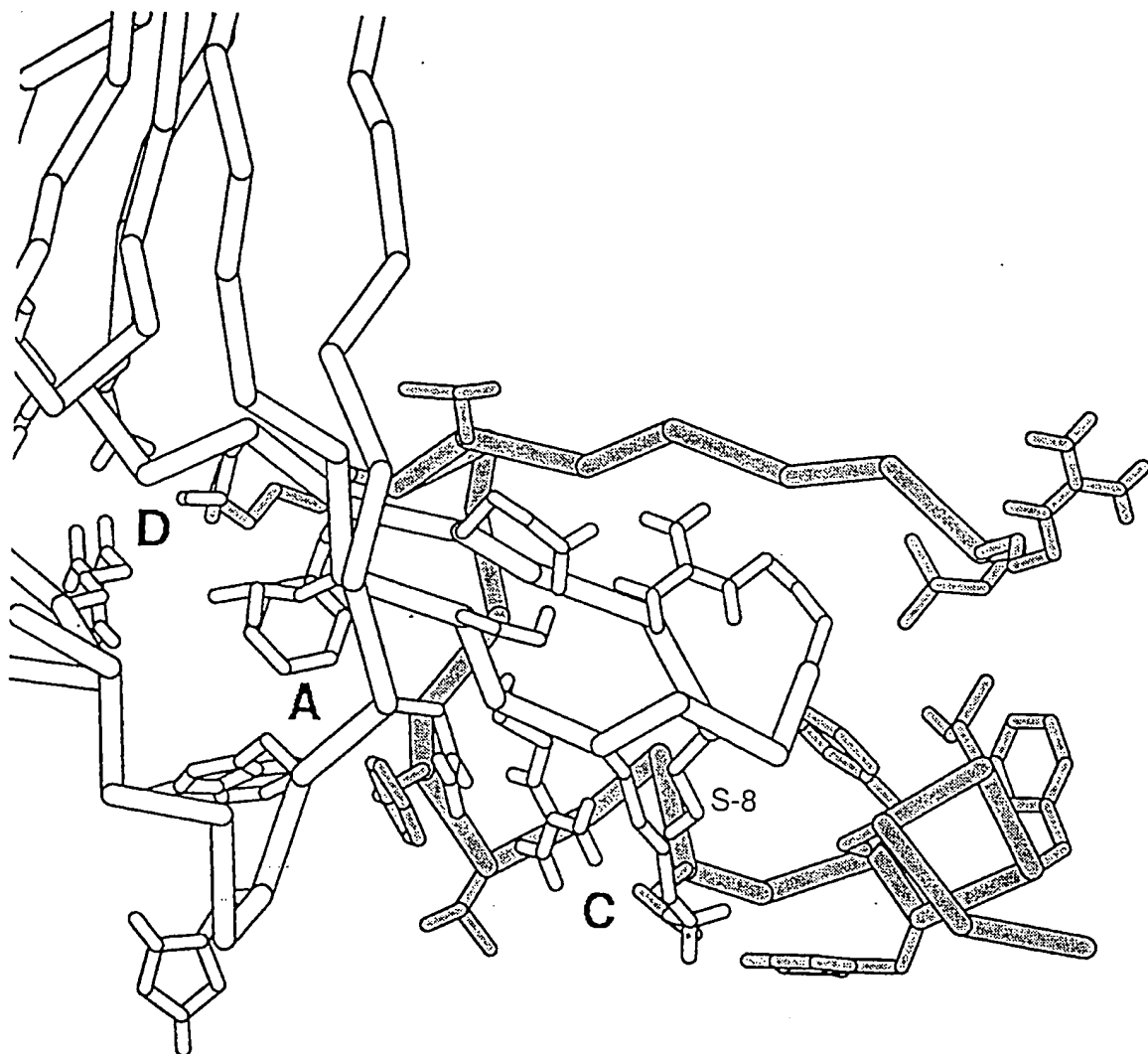
Figure 9
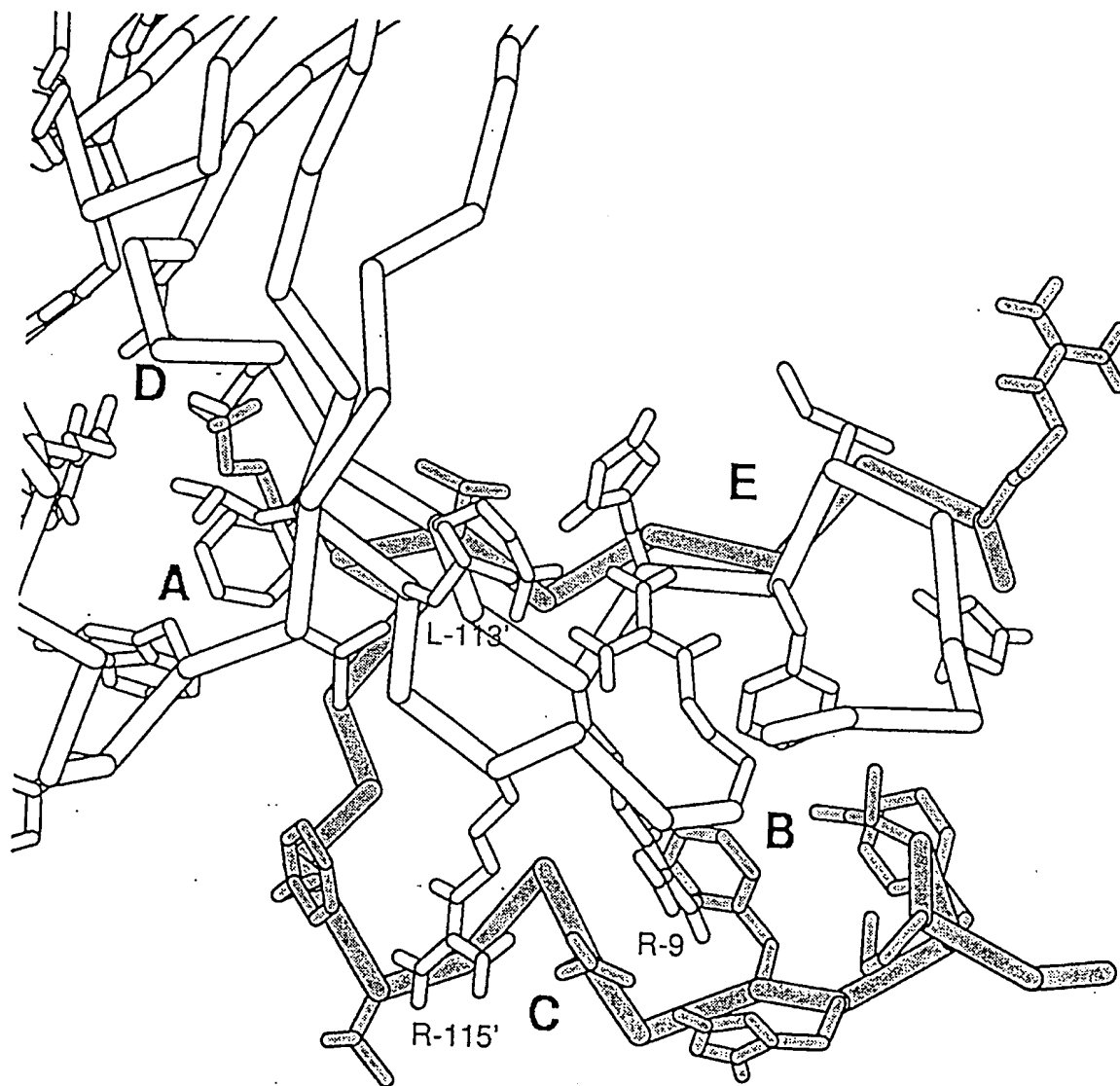
Figure 10a

Figure 10b
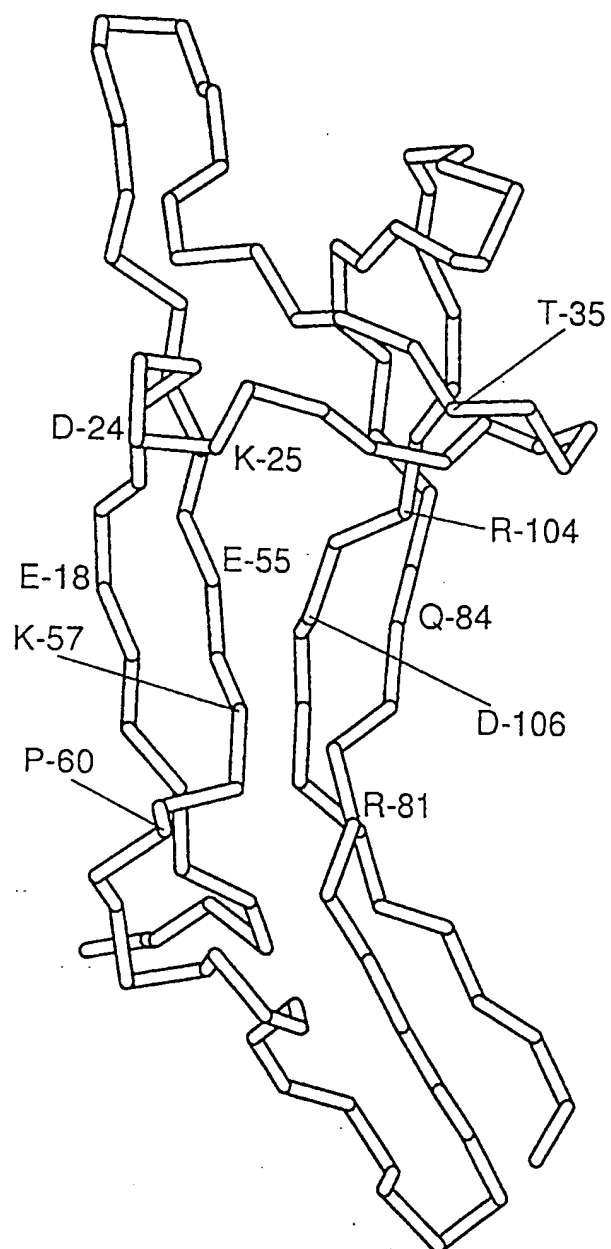
Figure 10c
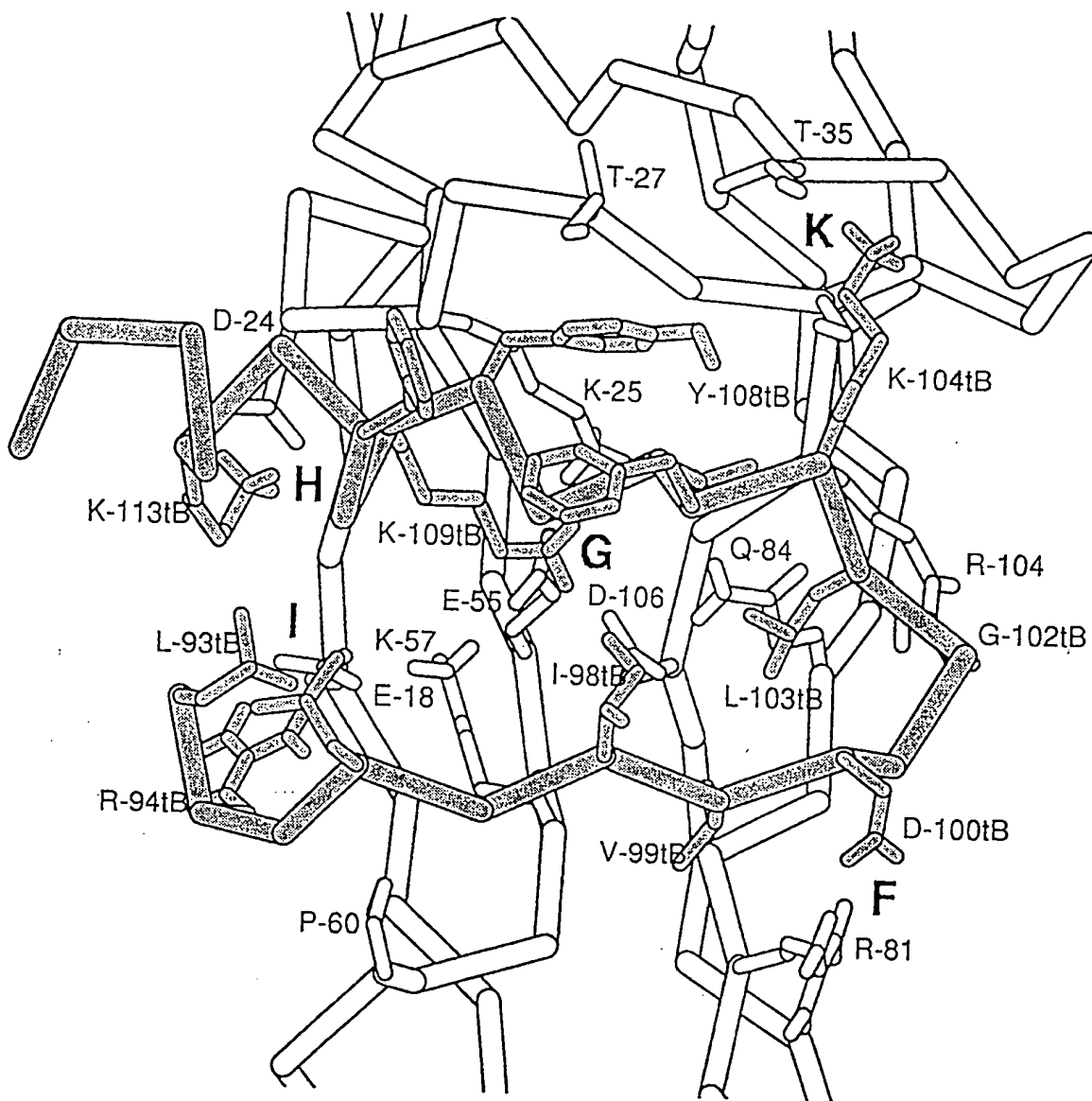
Figure 10d

Figure 10e
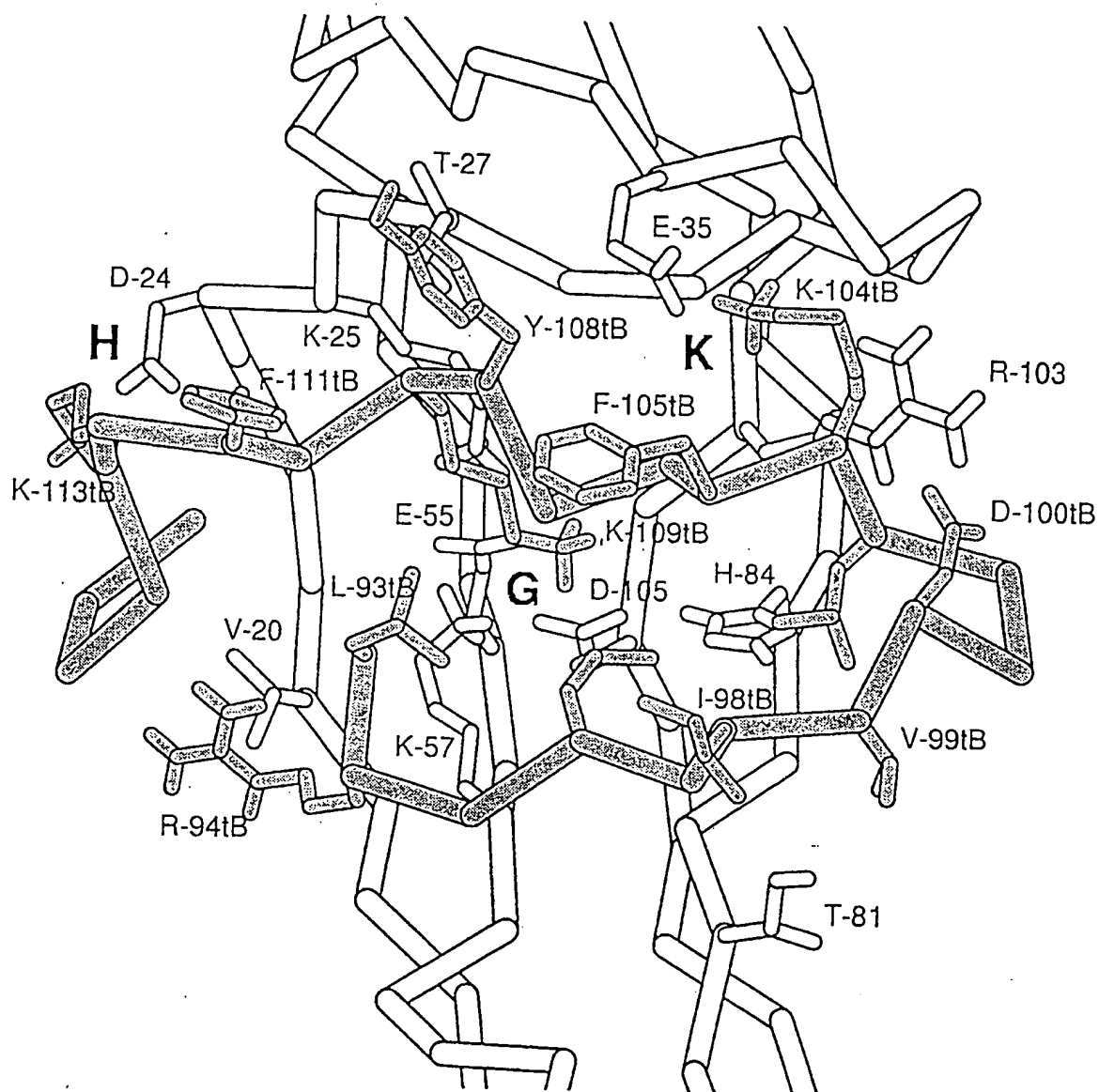
Figure 11a
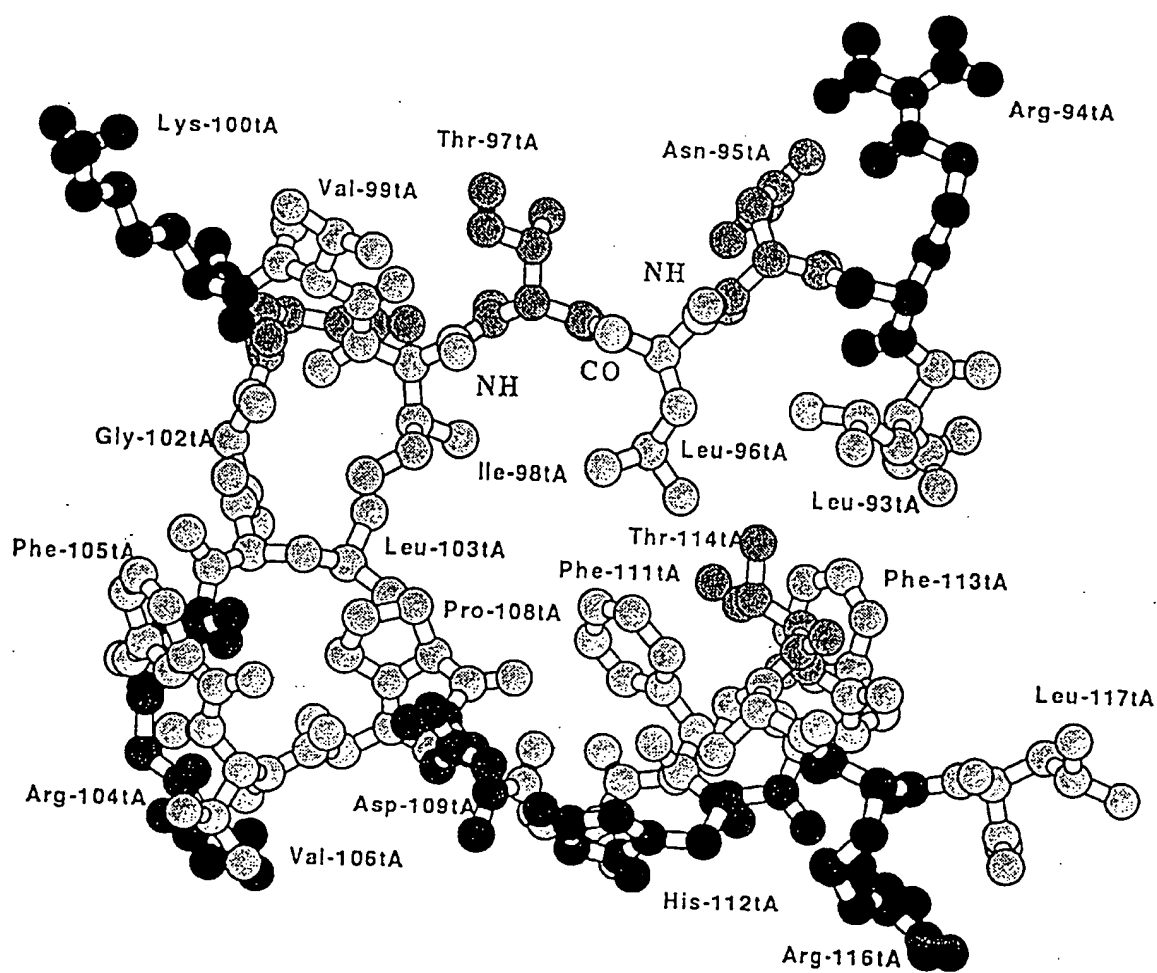
Figure 11b

Figure 11c

Figure 12

Amino terminus

	1				5					10					15	
hNGF sequence	S	S	S	H	P	I	F	H	R	G	E	F	S	V	C	D...
Conserved in NGF	-	-	X̲	-	X̲	X	-	X	X	X̲	X̲	X	X̲	X̲	X̲	X̲
Determine structure	-	-	X	-	X	X	-	X	X	X	X	X	X	X	X	X
Interact with LRM	-	-	-	-	X	X	X	-	-	-	X	-	X	-	-	X
LRM binding sites			E		B	E		E			E		D		D	D

Carboxyl terminus

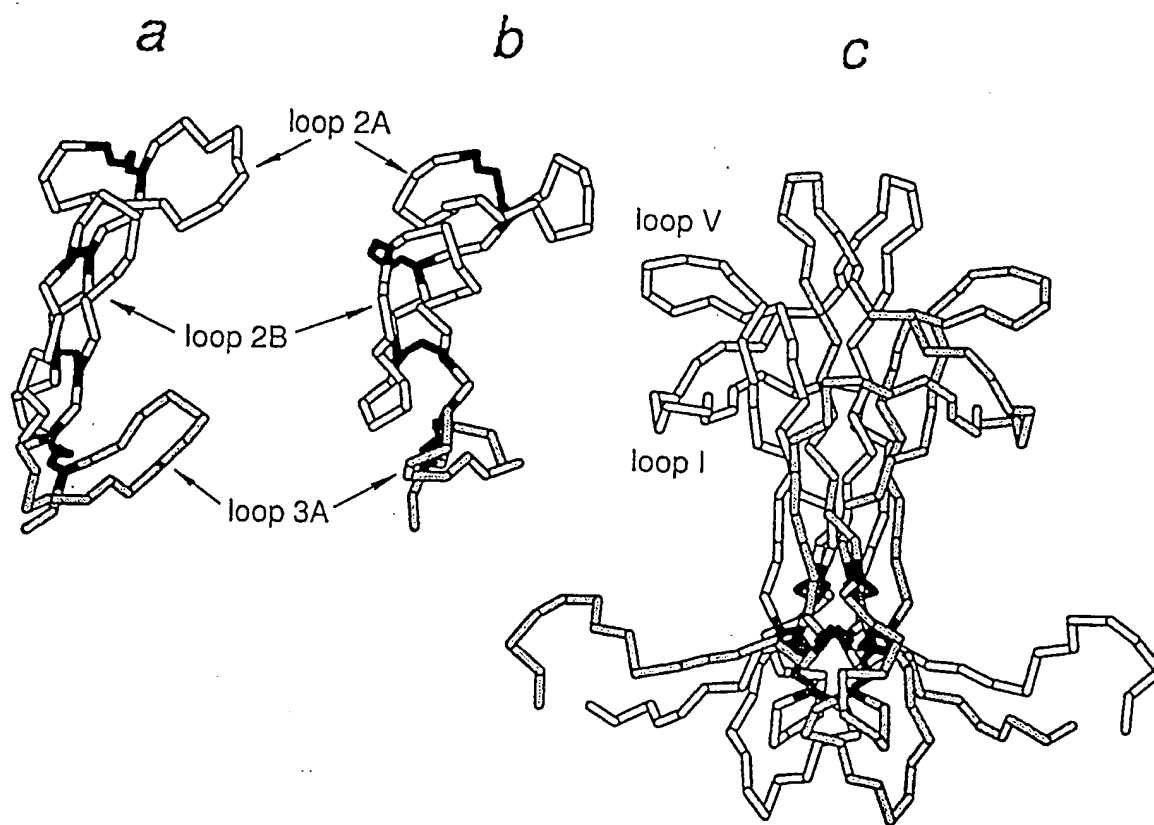|		75'							110'				115'			
hNGF sequence	...K	H	W	N	....	C	V	C	V	L	S	R	K	A	V	R
Conserved in NGF	-	X̲	X̲	-		X̲	X̲	X̲	X̲	X	X	X̲	-	-	-	X
Determine structure	-	X	X	-		X	X	X	X	X	X	X	-	-	-	X
Interact with LRM	-	-	X	-		-	-	-	-	-	-	X	X	-	-	-
LRM binding sites			A									C	C			

Figure 13

Figure 14

Figure 15

Figure 16

Second Cysteine-Rich Domain

```
p75ᴺᵀᴿ(h)   39    C L D S V T F S D V V S A T E P C K P C T
p75ᴺᵀᴿ(r)   39    C L D N V T F S D V V S A T E P C K P C T
p75ᴺᵀᴿ(c)   40    C L D S V T Y S D T V S A T E P C K P C T
p55ᵀᴺᶠᴿ     41    C - E S G S F T A S E N H L R H C L S C S


p75ᴺᵀᴿ(h)   60    E C V G L Q S M S A - - P C V E A D D A V C
p75ᴺᵀᴿ(r)   60    E C L G L Q S M S A - - P C V E A D D A V C
p75ᴺᵀᴿ(c)   61    Q C V G L H S M S A - - P C V E S D D A V C
p55ᵀᴺᶠᴿ     61    K C R K E M G Q V E I S S C T V D R D T V C
```

Third Cysteine-Rich Domain

```
p75ᴺᵀᴿ(h)   80    R C A Y G Y Y Q D E - - - T T G R C E A
p75ᴺᵀᴿ(r)   80    R C A Y G Y Y Q D E - - - E T G H C E A
p75ᴺᵀᴿ(c)   81    R C A Y G Y F Q D E - - - L S G S C K E
p55ᵀᴺᶠᴿ     83    G C R K N Q Y R H Y W S E N L F Q C F N
```
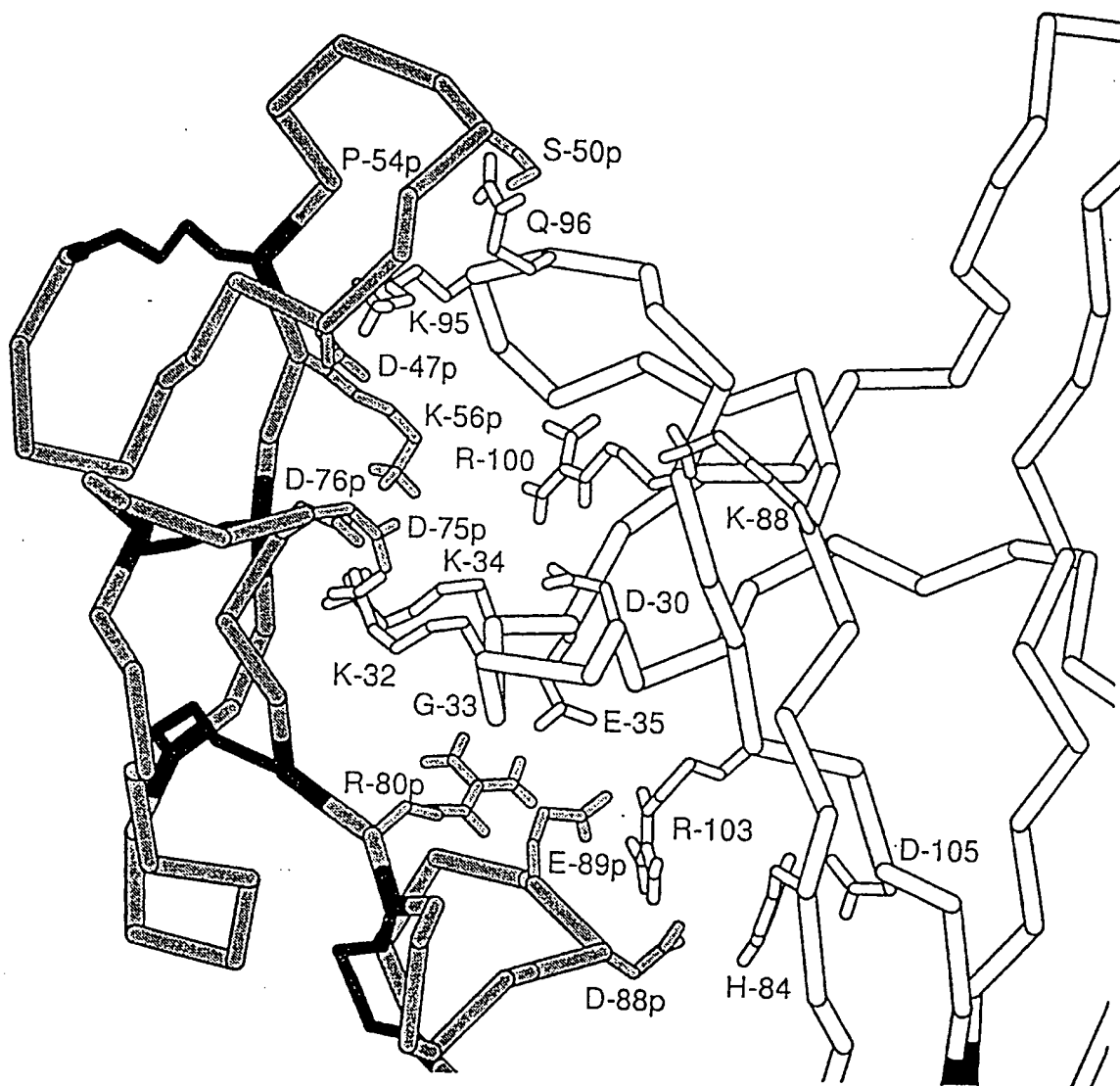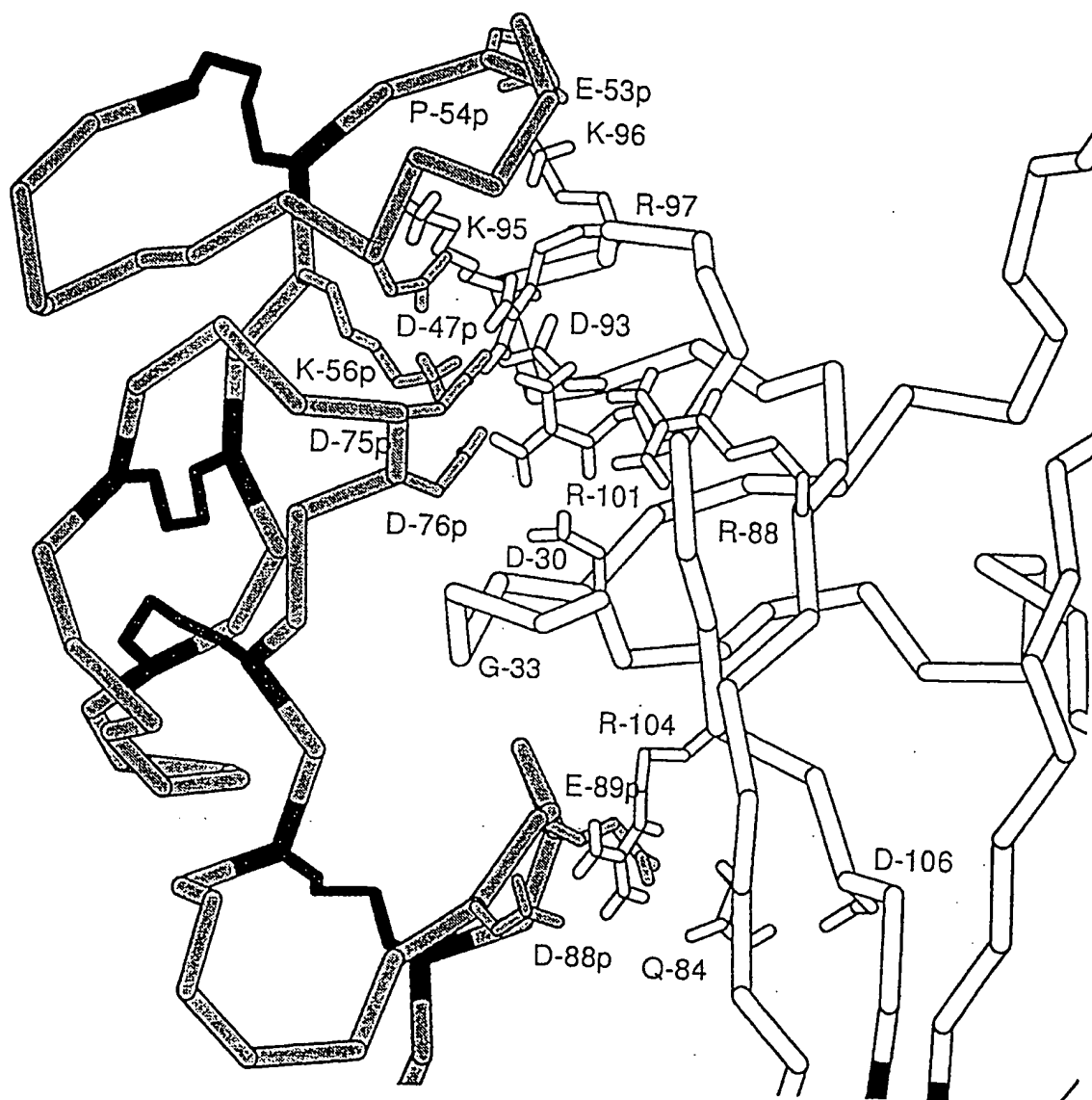
Figure 17

Figure 18a

Figure 18b
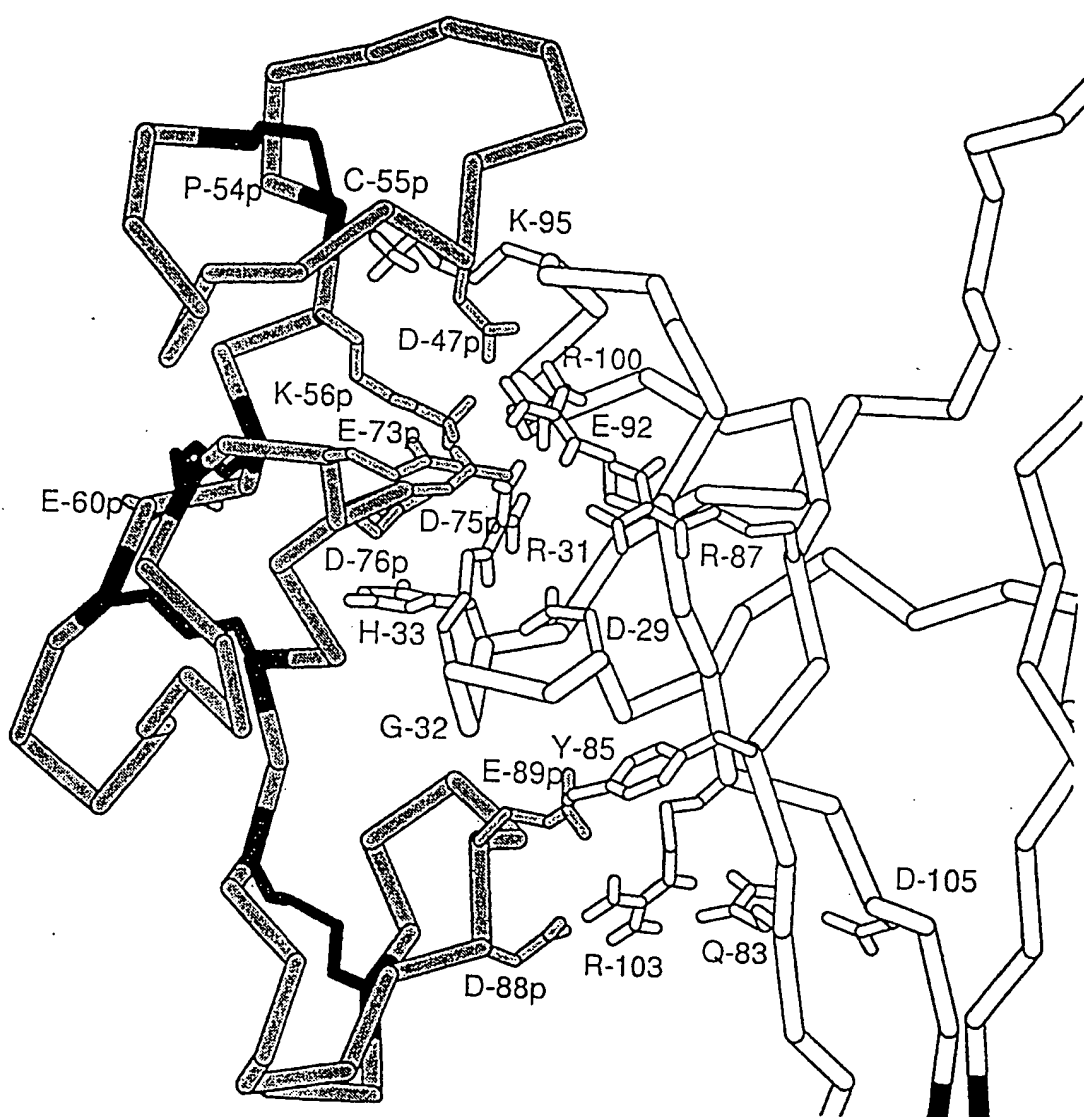
Figure 18c

Figure 18d